CLCA:

CHLORIDE CHANNEL OR MODULATOR?

Submitted to the College of Graduate Studies and Research of the University of Saskatchewan for partial completion of the Doctor of Philosophy degree in the Department of Veterinary Biomedical Sciences, pertaining to Physiology and Biochemistry in the Western College of Veterinary Medicine at the University of Saskatchewan

by

Matthew Eric Loewen D.V.M.

PERMISSION TO USE

In agreement with the outlines set out by the College of Graduate Studies and Research at the University of Saskatchewan, I allow the University of Saskatchewan Libraries to make this thesis available to all interested parties. Also in accordance with the College of Graduate Studies and Research, I allow this thesis to be copied "in any manner, in whole or in part, for scholarly purposes". This thesis may not, however, be reproduced or used in any manner for financial gain without my written consent. Any scholarly use of this thesis, in part or in whole, must acknowledge both myself and the University of Saskatchewan.

Any requests for copying or using this thesis, in any form or capacity, should be made to:

Head of the Department of Veterinary Biomedical Sciences
Western College of Veterinary Medicine
University of Saskatchewan
Saskatoon, Saskatchewan
S7N 5B4

ABSTRACT

A CLCA protein (CL for chloride channel and CA for calcium activated) cloned from porcine ileum RNA was expressed and characterized. The regulatory behavior, inhibitor sensitivity, and functional properties of chloride conductance associated with the expression of pCLCA1 cDNA were investigated in non-epithelial NIH/3T3 fibroblasts and in an epithelial Caco-2 cell line. These properties were also investigated in freshly isolated retinal pigment epithelial (RPE) cells and in primary cultures of these cells which express an endogenous cCLCA1. In NIH/3T3 fibroblasts, the chloride efflux induced by pCLCA1 was directly activated by calcium. A and C kinase agonists were without effect. The electrogenic nature of chloride efflux was confirmed by detection of outwardly rectified chloride currents. Selected anion channel blockers inhibited both the pCLCA1 agonist-induced current and chloride efflux. The inhibitors also reduced Ussing chamber short circuit current and chloride efflux from primary RPE cultures. However, these same agents did not inhibit chloride efflux in fibroblasts expressing the cystic fibrosis transmembrane regulator (CFTR) conductive chloride channel. The expression of pCLCA1 increased cAMP/A kinase-dependent chloride ion release from fibroblasts and Caco-2 cells expressing CFTR. These pleiotropic effects of CLCA protein expression suggested that the protein may regulate the activity of chloride conductance, rather than functioning as a primary ion transporter. This putative regulatory behavior was further investigated in Caco-2 cells. The rate of $^{36}Cl^-$ efflux and the amplitude of currents in patch clamp studies after activation of A kinase or intracellular Ca^{2+} mobilization was significantly increased in freshly passaged Caco-2 cells expressing pCLCA1. However, $^{36}Cl^-$ efflux and short circuit Ussing chamber

studies in polarized Caco-2 cells provided evidence that both endogenous and pCLCA1-dependent Ca^{2+}-sensitive chloride conductance were lost from 14 day post-passage cells. cAMP-dependent chloride conductance continued to be modulated by pCLCA1 expression in differentiated 14 day post-passage Caco-2 cells, demonstrating the retention of pCLCA1 effects in these mature cells. We conclude that pCLCA1 expression enhances the sensitivity of endogenous chloride channels to both natural agonists, $Ca^{2+}$and cAMP, but that it lacks inherent Ca^{2+}-dependent chloride channel activity.

ACKNOWLEDGMENTS

I would first like to thank my supervisor, Dr. George W. Forsyth, for his supervision and guidance, for patiently teaching me so much and for endless support throughout my Ph.D. program in Department of Veterinary Biomedical Sciences. (Formerly the Department of Veterinary Physiological Sciences)

I would also like to thank my advisory committee members Drs. Donald L. Hamilton, Greg D. Appleyard, Gillian D. Muir for their guidance during the course of this work. Dr. Sherif E. Gabriel also provided critical training in his laboratory at the University of North Carolina. Thanks to Darlene Hall for her invaluable technical assistance. I also acknowledge support from the Western College of Veterinary Medicine Interprovincial Fellowship Fund for my salary.

Additonal thanks should go to the external examiner, Dr. Calvin U. Cotton from Case Western Reserve University, School of Medicine in Cleveland, Ohio, USA.

I also owe a great deal to a number of people who made the completion of this project a much more enriching task then it would have otherwise been:

To Dr. Don L. Hamilton for introducing me to the science of physiology and comparative medicine (How many nephrons in a rat?).

To L.K. Bekar and Dr. Wolfgang Walz (both true academics), in the Department of Physiology in the College of Medicine, for full use and help with their electrophysiological equipment over the years.

To Dr. Paul Lee for stimulating scientific conversation as well providing excellent food from his Mandarin Restaurant.

To S.N. Schneider for his friendship in the trenches over the years.

To Dr. Greg D. Appleyard for use of his lab and intellectual conversations on diagnostic approaches to infectious disease.

To Dr. G. M. Hammond who has always given me something else to worry about over these years.

To Dr. M.A.L. Hansford for loving life.

Finally to my parents, Dr. P.C. Loewen, Dr. L.C. Loewen, sister Dr. M.C. Loewen, and the rest of the family for their everlasting encouragement and support in all my activities.

DEDICATION

I dedicate this thesis to my parents.

Peter C. Loewen Ph.D. Tier 1, Canada Research Chair in Protein Chemistry and

Linda C. Loewen M.D. FRCPC

who have consistently supported scientific inquiry

TABLE OF CONTENTS

LIST OF TABLES

LIST OF FIGURES

LIST OF ABBREVIATINS

α- PC .....α -phenylcinnamate
AHR.....airway hyperresponsiveness
ASL.....airway surface liquid
ATP.....adenosine-5'-triphosphate
BAPTA-AM.....2-bis (2 aminophenoxy)ethane-N,N,N',N'-tetraacetic acid-acetoxymethyl ester
Best.....bestrophin gene
BK channels.....large-conductance Ca 2+-activated K+ channels
BMD.....Best's vitelliform macular dystrophy
CaCC.....calcium regulated chloride channel
CaMKII.....calcium calmodulin kinase II
cAMP.....adenosine-3'-5'cyclic monophosphate
cAMP.....3',5'-adenosine monophosphate
cDNA.....cloned reverse transcribed gene product
CF.....cystic fibrosis
CFTR.....cystic fibrosis transmembrane regulator
cGMP.....guanosine monophosphate
ClC.....chloride channel
CLCA.....Cl for chloride channel, CA for calcium-activated, putative gene family
CMV.....cytomegalovirus
CPT-cAMP.....8-(4-Chlorophenylthio)-3',5'-cyclicAMP
cRNA.....RNA produced from cDNA
d.p.c .....days post conception
DIDS.....4,4'-diisothiocyanostilbene-2,2'-disulfonic acid
DMEM.....Dulbecco's Modified Eagle's Medium
DMSO.....dimethylsulfoxide
DNA.....deoxyribonucleic acid
DPC.....diphenylamine carboxylate
DTT.....dithiothreitol
EDTA.....ethylenediaminetetraacetic acid
EGTA.....ethylene glycol-bis(2-aminoethylether)-N,N,N',N'-tetraacetic acid
ELISA.....enzyme-linked immunosorbent assay
ENac.....epithelial sodium channel
EOG.....electrooculogram
Erev.....equilibrium potential (ie electrical reversal potential)
ERG.....electroretinogram
ERK.....extracellular signal-regulated kinase
EST.....expressed sequence tags
FAK.....focal adhesion kinase
FBS.....fetal bovine serum
FITC.....fluorescein isothiocyanate
GI.....gastrointestinal
GMA.....glycolmethacrylate

Grb.....growth factor receptor-bound protein
HEK.....human embryonic kidney
HEPES.....N-2-hydroxyethylpiperazine-N'-2-ethanesulphonate
HGF.....hepatocyte growth factor
I/V.....current/voltage
IBMX.....3-isobutyl-1-methylxanthine
IgG.....immunoglobulin class M
IgG.....immunoglobulin class G
IL.....interlukin
INF.....interferon
Ins(3,4,5,6)P4.....D-myoinositol-3,4,5,6-tetrakisphosphate
Isc.....short circuit current
KATP.....ATP-inhibited potassium channel
kDa.....kiloDalton, Dalton = (1.657 x10-24 g)
KN-93.....N-(2-hydroxyethyl)-N-methyl-4-methoxybenzenesulfonamide
Kv.....voltage activated potassium channel
MAPK.....mitogen-activated protein kinase pathways
MIDAS.....metal ion-dependent adhesion site
mRNA.....messenger ribonucleic acid
Na+/K+ ATPase.....sodium/potassium adenosine triphosphatase
NFA.....niflumic acid
NIH.....National Institutes of Health
NO.....nitric oxide
NPPB.....5-nitro-2-(3-phenylpropylamino)benzoate
OpAmp.....operational amplifier
ORCC.....outwardly rectifying chloride channel
ORF.....open reading frame
OVA.....ovalbumin
PAGE.....polyacrylamide gel electrophoesis
PBS.....phosphate-buffered saline
PCR.....polymerase chain reaction
PD.....potential difference
PI3K.....phosphatidylinositol-3-kinase
PKA.....protein kinase A, cAMP-dependent protein kinase
PKC.....protein kinase C
PKG.....cGMP-dependent protein kinase
PMA.....phorbol-12-myristoyl-13-acetate
pS.....picoSiemen
Pyk2.....proline-rich tyrosine kinase
RNA.....ribonucleic acid
RPE.....retinal pigment epithelium
RT.....reverse transcriptase
SCID.....severe combined immunodeficiency
SDL.....specificity-determining loop
SDS..... …….sodiumdodecylsulphate
SITS.....4-acetamido-4'-isothiocyanostilbene-2,2'-disulfonate

SNARE.....soluble N-ethylmaleimide-sensitive factor attachment protein
SOS.....Son of Sevenless
TBS.....Tris-buffered saline
TES.....N-tris(hydroxymethyl)methyl-2-aminoethanesulfonic acid
Th1.....type 1 helper T
Th2.....type 2 helper T
Tris.....Tris[hydroxymethyl]aminomethane
V.....Voltage or Volts
VMD.....Bestrophin gene
VWA.....von Willebrand's Factor Domain A

Chapter 1. LITERATURE REVIEW

1.1. Introduction

Despite nearly a decade of research, the understanding of the contributions of the CLCA (Cl for chloride channel, CA for calcium-activated) gene family members to chordate biochemical, physiological and pathological processes remains incomplete and unclear. The uncertainty about some unifying basis for the molecular function of the CLCA proteins arises at least partly from reports of a diverse array of apparently unrelated processes that have been associated with the expression of various CLCA protein isoforms. Some proposed CLCA roles appear to be in direct conflict. CLCA is reported to be central to tumor metastasis, but also appears to have an important role in tumor suppressor activity (Gruber and Pauli 1999c; Abdel-Ghany, Cheng et al. 2001; Elble and Pauli 2001; Abdel-Ghany, Cheng et al. 2002; Abdel-Ghany, Cheng et al. 2003). In other cases the disease processes involving altered CLCA expression seem unrelated. CLCA proteins are major regulators of mucus production in the asthmatic airway, ion transport in the airway of cystic fibrosis patients, vascular smooth muscle tone affecting hypertension and erectile dysfunction, and of ion transport associated with retinal function that is disrupted in the pathology of Best's vitelliform macular dystrophy (Anderson and Welsh 1991; Nakanishi, Morita et al. 2001; Greenwood, Miller et al. 2002; Hoshino, Morita et al. 2002; Toda, Tulic et al. 2002; Hauber, Manoukian et al. 2003; Karkanis, DeYoung et al. 2003). By first describing the basic

biophysical properties associated with expression of isoforms of the CLCA family and then the pathophysiology of the implicated disease processes, we hope to provide the reader with a thread of logic to bind the apparently diverse functions of the proteins produced by the CLCA gene family. First the cloning of the CLCA family will be surveyed, followed by predictions that have been made for protein structure, and function. Then what is currently known about the normal physiology of CLCA isoforms, their connections to disease conditions, and possible beneficial effects of pharmacological modulation of CLCA protein function will be explored.

1.2. Cloning of the CLCA Gene Family

The CLCA gene family members are named for the species source from which they were cloned, and numbered in chronological order of cloning within each species. This unfortunate situation creates a need to present the history behind the cloning of the CLCA gene family in order to clarify why series numbers within each species do not correlate with functional attributes of the expressed proteins. The historical perspective also gives insight into why the proteins have been named for, and viewed by some to possess, chloride channel activity. Figure 1.1 gives the phylogenetic relationship between these published clones.

Secretory epithelial cell layers are known to possess a number of ion channels that are able to direct the flow of ions to produce net fluid movement into the lumen of tissues such as the GI tract and the trachea. Conductive chloride channels, located on

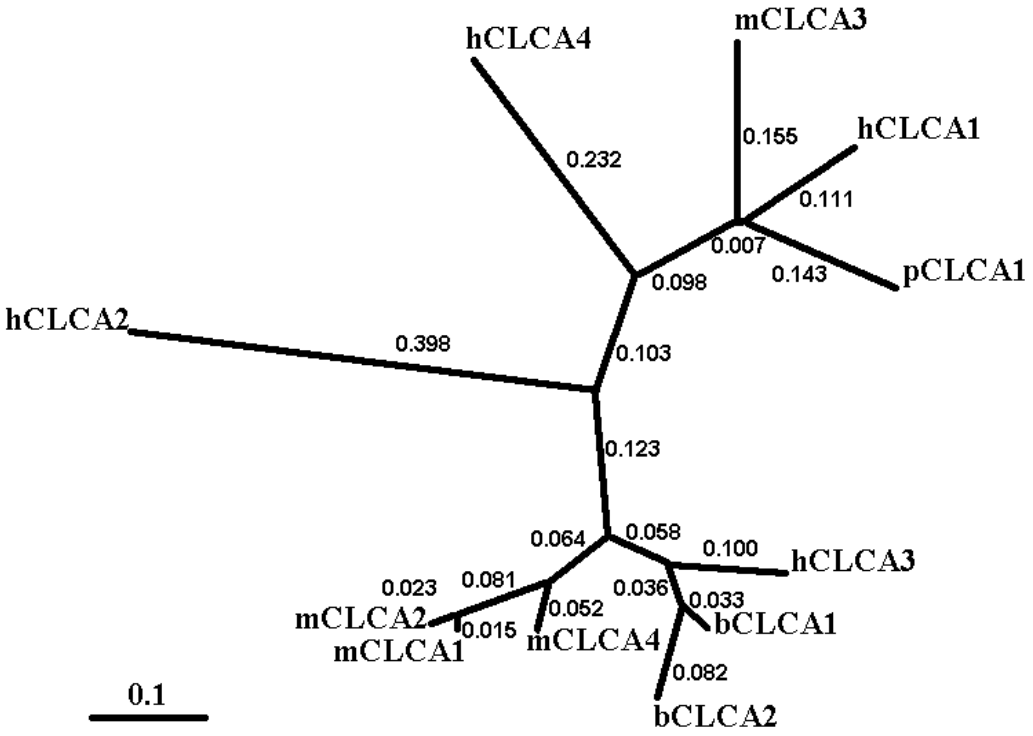

Figure 1.1. Phylogenetic tree of the published clones of the CLCA gene family. Tree developed using Clustalw followed by Phylip Software. The scale is substitution per site expressed as a percent using nucleic acid sequence. Each arm is labeled accordingly.

the apical membrane of these secretory cells are of special interest. Regulation of chloride conductance channels by intracellular second messengers is the primary level of control for epithelial fluid secretion. Increases in intracellular calcium ion concentration are known to activate chloride conductance, so there has been significant interest in identifying the protein(s) responsible for the conductive movement of chloride across the apical membrane of secretory epithelial cells. The cloning of the first CLCA cDNA sequence (bCLCA1) was reported in 1995 (Cunningham, Awayda et al. 1995). The clone was obtained by screening a gene expression library with a polyclonal antibody generated to a 36-38 kDa reduced protein purified from bovine tracheal epithelium. This antigenic peptide lacked intrinsic chloride channel properties in a lipid bilayer (Ran, Fuller et al. 1992; Cunningham, Awayda et al. 1995). This non-conducting protein was thought to be a subunit of a larger 140 kDa protein. Purification of this 140 kDa protein under non-reducing conditions and reconstitution into planar lipid bilayers, caused the appearance of an anion channel whose activity was increased by activation of Ca^{2+} /calmodulin-dependent protein kinase. It was hypothesized at that time that the original purified protein of 140 kDa was a homotetramer of identical 38 kDa subunits, linked together by disulfide bonds which could be reduced to produce a 64 kDa dimer and 38 kDa monomers. This clone was originally termed CaCC, but is now called bCLCA1 (Cunningham, Awayda et al. 1995; Fuller and Benos 2000b; Pauli, Abdel-Ghany et al. 2000; Fuller, Ji et al. 2001).

The second CLCA sequence (bCLCA2) was reported in 1997 (Elble, Widom et al. 1997). Like bCLCA1, bCLCA2 was obtained by screening a gene expression library with antibody. However, the monoclonal antibody used in this case had no connection

to inhibition of anion conductance. This antibody was generated to identify an adhesion-receptor/ligand pair that mediated binding of lung-metastatic melanoma cells to lung matrix-modulated bovine aortic endothelial cells (Zhu, Cheng et al. 1991; Zhu and Pauli 1991; Zhu, Cheng et al. 1992; Zhu and Pauli 1993; Elble, Widom et al. 1997). The monoclonal antibody used in screening an expression library was shown to inhibit this specific adhesion to endothelial cells (Zhu, Cheng et al. 1992). Expression of a clone identified in this screening produced a protein with properties that have been described as the lung endothelial cell adhesion molecule-1 (Lu ECAM-1) (Elble, Widom et al. 1997). Lu ECAM-1 is now termed bCLCA2 (Fuller and Benos 2000b; Pauli, Abdel-Ghany et al. 2000).

Two other cDNA clones with significant identity to bCLCA1 and 2 were reported in 1998 from screening a human gene library and a mouse lung cDNA library.

The human orthologue hCLCA1 was cloned using the open reading frame (ORF) sequence of the bCLCA2 cDNA as a probe in a human genomic library. A PCR-based genomic walking and cloning strategy was employed to fill the gaps between isolated genomic clones and to obtain the full sequence and the putative promoter region of the gene (Gruber, Elble et al. 1998). The human CLCA1 gene was found to encompass 31902 bp and is located on chromosome 1p22-p31. A total of 15 exons ranging from 90 to 604 bp in size are interspersed with 14 introns of 170 to 5651 bp (Gruber, Elble et al. 1998). The start codon was found on the second exon. A promoter region containing a TATA box precedes the predicted site of transcriptional initiation by 22 nucleotides (Gruber, Elble et al. 1998). The promoter region has a high GC content and there are numerous other potential binding sites for transciptional regulators

in this area. A second consensus TATA box was also found to be located 950 bp upstream of the first exon (Gruber, Elble et al. 1998). Mutation analysis of these putative transcriptional start sites has not been reported, so it is difficult to speculate on the individual importance of each. The hCLCA1 sequence was found independently in 1999 using a Human Genome Sciences Expressed Sequence Tags (EST) database, screened with the bCLCA1 sequence. The group coined it HCaCC1, which is really hCLCA1 (Agnel, Vermat et al. 1999). Primers have been generated to amplify the 2745 bp ORF of hCLCA1 to obtain full length cDNA for functional expression.

Similarly, mCLCA1 was cloned from a mouse lung cDNA library using a bCLCA2 probe (Gandhi, Elble et al. 1998). Concurrently, an independent group found mCLCA1 in a EST database using bovine bCLCA1 sequence (Romio, Musante et al. 1999). This group localized the mCLCA1 to chromosome 3 at the H2-H3 band. Because CLCA genes are numbered as they are cloned, it should be noted that mCLCA1 is not the human orthologue of hCLCA1 (Figure 1.1) even though they contain a considerable degree of sequence identity and their expressed forms may have many similar biophysical properties.

The sequences of a large number of CLCA isoforms were published in 1999. mCLCA2 was cloned from mouse mammary gland in a suppression subtractive hybridization on the involuting mammary gland (Lee, Ha et al. 1999). The human orthologue hCLCA2 was cloned from a human lung using a bCLCA1 cDNA probe (Gruber, Schreur et al. 1999). As with mCLCA2, hCLCA2 was expressed at relatively high levels in the mammary gland. hCLCA2 was also found independently at the same time and called hCaCC3 (Agnel, Vermat et al. 1999). This same group also

concurrently found what they called HCaCC2 now called hCLCA4 by matching an EST database to bovine bCLCA1 sequence (Agnel, Vermat et al. 1999).

Around the same time Gruber and Pauli reported the cloning of hCLCA3, the first fully secreted CLCA protein. hCLCA3 was cloned from human spleen cDNA and was found to be a secreted protein in several tissues (Gruber and Pauli 1999b).

Finally, Gob-5 or mCLCA3, which is the closest mouse orthologue to hCLCA1, was cloned from mouse gut cDNA (Komiya, Tanigawa et al. 1999). mCLCA3 and mCLCA1 co-localize on mouse chromosome 3 H2 - H3 (Romio, Musante et al. 1999; Leverkoehne and Gruber 2000).

In the human, hCLCA1, hCLCA2 and hCLCA3 are clustered on the short arm of chromosome 1 (1p22 -31)(Gruber and Pauli 1999a). This close clustering was unexpected given the low sequence identity (~ 60%) between the three CLCA isoforms (Gruber and Pauli 1999a). Recently, analysis of the human genome has shown hCLCA2, hCLCA1, hCLCA4 and hCLCA3 are lined up consecutively in the same orientation, encompassing 232 kB, with no other genes interspersed (Gruber, Elble et al. 2002). An area 1617 bp upstream of the first intron codes for 24 different transcription factor binding sites, of unknown function significance. Gene clustering is often used as a mechanism for controlling temporal gene expression by internal intron or bidirectional promoters (Keegan, Haerry et al. 1997; Zhang, Ding et al. 2003). However, any regulatory or functional significance of the CLCA gene clustering is not known.

In 2000 the full length sequence of the porcine CLCA clone (pCLCA1) was published (Gaspar, Racette et al. 2000). Unlike the other cloning strategies, pCLCA1 was cloned using a monoclonal antibody which inhibited chloride channel conductance.

The antibody was developed against porcine ileal brush border vesicle protein, and the monoclonal antibody selected for inhibition of chloride conductance in the vesicles (Gabriel and Forsyth 1991; Gabriel, Racette et al. 1992). The inhibitory antibody was then used to screen a gene expression library. Although the 3' fragment of pCLCA1 was cloned in 1994, sequencing and expression of the full-length clone was only completed and published in 2000. A high regional GC content and associated secondary structure contributed to difficulties in cloning and sequencing the pCLCA1 cDNA. The antibody selection strategy employed to identify this isoform provided a strong functional link to chloride conductance.

Reports of a calcium-activated chloride conductance in smooth muscle (Nelson, Conway et al. 1997; Hirakawa, Gericke et al. 1999) stimulated a search for CLCA proteins in this tissue. A recent addition to the CLCA family (mCLCA4) was cloned from mouse smooth muscle cell total RNA by RT-PCR using degenerate primers to bCLCA2 (Elble, Ji et al. 2002). It should be noted that mCLCA4 is not the orthologue to hCLCA4 (see Figure 1.1.)

Small segments of CLCA cDNA from other species have also been cloned. A portion of a rat orthologue rCLCA1 has been cloned from rat pancreas cDNA (Thevenod, Roussa et al. 2003). A partial canine CLCA, cCLCA1 cloned from dog retinal pigment epithelium with primers specific for the porcine pCLCA1 has also been reported, and expression levels investigated (Loewen, Smith et al. 2003).

A hCLCA5 has been reported recently (Abdel-Ghany, Cheng et al. 2003). However, little information on its sequence or cloning is currently available.

1.3 Tissue Expression

1.3.1. Human Orthologues

1.3.1.1. hCLCA1

Expression of hCLCA1 *in vivo* is mainly found in mucus secreting cells of large and small intestine (Gruber, Elble et al. 1998). A study using Northern blots found the largest expression in the small intestine, appendix and colon. Lower expression levels were found in the uterus, stomach, testis and kidney (Agnel, Vermat et al. 1999). However, another extensive study was only able to find expression in the small intestine and colon (Gruber, Elble et al. 1998). This same study, using highly stringent *in situ* hybridization conditions, identified specific cell types which expressed hCLCA1. Strong expression was detected in the cytosol of a subset of enterocytes scattered throughout the intestinal lining in the jejunum, ileum and colon. The majority of the mRNA signal was in cells at the base of the crypts. The goblet cells were most prominently stained. Expression in the small intestine and colon were also demonstrated by Northern blot and RT-PCR (Gruber, Elble et al. 1998). However, more recent reports have found induction of hCLCA1 expression in the airways under pathophysiological conditions (Hoshino, Morita et al. 2002) (Hauber, Manoukian et al. 2003).

1.3.1.2. hCLCA2

The human orthologue hCLCA2 is expressed at highest levels in the trachea and mammary gland on Northern blotting under physiological conditions (Gruber, Schreur et al. 1999). It has also been found in nasal epithelium (Mall, Gonska et al. 2003). Strong expression is also found in most basal cells in stratified epithelia (Connon, Yamasaki et al. 2004). Although isolated from a lung cDNA library, hCLCA2 was not

detected in the lung by Northern blot hybridization. However, in the same study a weak RT-PCR signal for hCLCA2 was obtained from lung. But, the strongest signal was found in the trachea and mammary gland (Gruber, Schreur et al. 1999). Expression of hCLCA2 in mammary gland and trachea was confirmed independently by Northern blot (Agnel, Vermat et al. 1999). They were not able to find expression by Northern blot in the lung. However they detected expression in the testis, prostate and uterus, which had not been identified as showing mRNA expression in the first study by the same group (Agnel, Vermat et al. 1999). The hCLCA2 orthologue was also found to be highly expressed in a nonmalignant transformed human mammary epithelial cell line MCF10A using both Northern blot and RT-PCR. However, hCLCA2 expression in tumorigenic cell lines MDA-MB-231, MDA-MD-468 and MCF7 was not detected by Northern blot. These findings were in agreement with an *in situ* hybridization staining of acini and small in normal mammary tissue, but there was an absence of staining in breast cancer samples (Gruber, Schreur et al. 1999).

1.3.1.3. hCLCA3

The third human orthologue, hCLCA3, was originally cloned from spleen. The full length mRNA is expressed in the lung, trachea, mammary gland and thymus (Gruber and Pauli 1999b). Its presence has also been reported in nasal epithelium (Mall, Gonska et al. 2003).

1.3.1.4. hCLCA4

Unlike the other human orthologues, hCLCA4 has a very high expression in neural tissue (Agnel, Vermat et al. 1999). On Northern blot analysis the amygdala, caudate nucleaus, cerebral cortex, frontal lobe, hippocampus, medulla oblongata,

occipital lobe, putamen, substantia nigra, temporal lobe, thalamus, acumbens expressed hCLCA4. Interestingly, the cerebellum and spinal cord did not show any evidence of hCLCA4 expression. The strongest signal from hCLCA4 came from the colon, with twice the signal intensity of that found in neural tissue. Expression was also found in the bladder, uterus, prostate, stomach, testis, salivary gland, mammary gland, small intestine, appendix and trachea (Agnel, Vermat et al. 1999).

1.3.2. Murine Orthologues

1.3.2.1. mCLCA1

The strongest expression of mCLCA1 was detected in the lung, aorta, spleen and bone marrow using real-time RT-PCR quantitation normalized against expression of elongation factor 1a (Leverkoehne, Horstmeier et al. 2002). High levels have also been reported in the kidney and skin by Romio et al. (Romio, Musante et al. 1999). Lower levels were detected in the esophagus, stomach, duodenum, jejunum, ileum, cecum, proximal colon, distal colon, rectum, pancreas, liver, gall bladder, parotid, nasal turbinate, trachea, heart, thymus, spleen, lymph nodes, kidney, urinary bladder, ovaries, uterus, testes, epididymis, penis, vesicular gland, adrenal gland, eye, tail skin, juvenile mammary gland, skeletal muscle, cerebral cortex, brain stem, medulla oblongata and cerebellum and throughout gestation in the placenta. Expression was undetectable in the prostate and the pregnant, lactating and involuting mammary gland. However, an independent study did find mCLCA1 expression in virgin, pregnant and lactating gland (Elble and Pauli 2001). Both studies shared the conclusion that mCLCA1 expression was lost during mammary gland involution (Elble and Pauli 2001; Leverkoehne, Horstmeier et al. 2002). In the developing fetus, mCLCA1 expression was not detected

until 10 days post-conception (d.p.c). The expression of mCLCA1 increases in the fetal liver from 10 d.p.c to 13.5 d.p.c. Similarly, the kidney increased its expression from day 13.5 to day 18. Both the intestine and lung showed an increase in expression over gestation increasing from day 10 to day 13.5, however this increase dropped on day 18 in both tissues (Leverkoehne, Horstmeier et al. 2002). This dynamic change in mCLCA1 expression over gestation points to a yet to be defined role of mCLCA1 in cell maturation and differentiation.

Unfortunately many of the earlier studies using *in situ* hybridization probes to localize expression of mCLCA1 mRNA did not take into account the existence of mCLCA2 (Gruber, Gandhi et al. 1998). However, the majority of the signal in Northern analysis and *in situ* hybridization staining of the spleen, lymphoid nodes and lung was most likely mCLCA1. It is also interesting to note that mCLCA1 is the only CLCA to be found in the cerebellum and brainstem (Leverkoehne, Horstmeier et al. 2002). This significantly differs from hCLCA4, which had extensive expression in other areas of the nervous system (Agnel, Vermat et al. 1999). Additionally, mCLCA2 in the same study was undetectable in cerebellum and brainstem (Gruber, Gandhi et al. 1998). These preliminary observations about temporal and tissue-specific expression patterns within the same physiological system could be broad hints of diverse roles of CLCA proteins in tissue development and functional differentiation.

Given the importance of a calcium-activated chloride conductance in renal epithelium, it was to be expected that a number of small CLCA segments with a high sequence identity to mCLCA1 and mCLCA2 would be available for cloning from a mouse inner medullary collecting tubule cell line (Boese, Glanville et al. 2000).

Subsequent RT-PCR of the mouse nephron found mCLCA1 in the glomeruli and thick ascending limb, but not in the proximal tubule and cortical collecting duct (Boese, Glanville et al. 2000). Interestingly, a study using a non-specific mCLCA1/ mCLCA2 probe only identified CLCA in the tubular epithelial cells and found no signal in the glomeruli. The proximal tubule had the most intense staining with weaker staining in the loop of Henle and distal tubuli. The collecting duct was negative (Gruber, Gandhi et al. 1998). This difference is likely due to a specificity of the probe and primers used in the studies and a difference in the actual orthologue expressed at different areas within the kidney. Once again the differences may be evidence for distinct physiological roles of each CLCA orthologue.

1.3.2.2. mCLCA2

The strongest mCLCA2 expression was detected in the mammary gland (Lee, Ha et al. 1999; Elble and Pauli 2001; Leverkoehne, Horstmeier et al. 2002). High expression was reported from pregnancy to involution as determined in two studies by RT-PCR (Elble and Pauli 2001; Leverkoehne, Horstmeier et al. 2002). However, an original study using Northern blot analysis only found mCLCA2 expression in the involuting stage (Lee, Ha et al. 1999). This difference may have arisen from differences in the stringency of the blot and the large expression at involution. *In situ* hybridization in normal murine mammary tissue with a probe which would detect both mCLCA1 and mCLCA2 found staining in both alveolar and ductal epithelial cells (Gruber, Gandhi et al. 1998). Lower mCLCA2 levels were detected in the esophagus, stomach, duodenum, jejunum, ileum, cecum, proximal colon, distal colon, rectum, pancreas, liver, gall bladder, parotid, nasal turbinate, trachea, lung, heart, thoracic and abdominal aorta,

thymus, spleen, lymph nodes, kidney, urinary bladder, ovaries, uterus, testes, epididymis, penis, vesicular gland, adrenal gland, eye, tail skin, juvenile mammary gland, skeletal muscle, cerebral cortex, medulla oblongata (Leverkoehne, Horstmeier et al. 2002). mCLCA2 was undetectable in the brainstem, cerebellum and prostate. In a real time quantitative RT-PCR, study the mammary gland seemed to express purely mCLCA2. This was the only tissue screen that had absolutely no mCLCA1 signal (Leverkoehne, Horstmeier et al. 2002). However, a study directly looking at mCLCA1 and mCLCA2 expression patterns did find mCLCA1 at all stages except at the time of involution (Elble and Pauli 2001). mCLCA2 was detected in both the placenta and fetus. Like mCLCA1, mCLCA2 fetal expression was dynamic. At 8.5 d.p.c. the developing fetus had only mCLCA2 (Elble and Pauli 2001; Leverkoehne, Horstmeier et al. 2002). The mCLCA2 became undetectable a day later, and only mCLCA1 was expressed at 12.5 d.p.c (Elble and Pauli 2001; Leverkoehne, Horstmeier et al. 2002). Low levels of mCLCA2 mRNA were detected again in various tissues at 13.5 days and increased gradually until they exceeded mCLCA1 expression by 19 d.p.c.. Unlike mCLCA1, mCLCA2 is undetectable in the fetal liver (Leverkoehne, Horstmeier et al. 2002). However, the dynamic interplay between these two isoforms of the CLCA gene family would once again suggest that they are involved in different physiological roles. It is interesting to note that the highest expression of mCLCA2 seems to be in those tissues with the high rate of cell division and cell death (Elble and Pauli 2001). A possible connection to cell cycle control or an apoptotic role for mCLCA2 could be considered for these tissues.

1.3.2.3. mCLCA3

Expression of mCLCA3 is primarily in mucus secreting cells (Komiya, Tanigawa et al. 1999; Leverkoehne and Gruber 2002). It was originally cloned from, and found to have highest expression in the crypt of the large intestine (Komiya, Tanigawa et al. 1999). An extensive immunohistochemical study was undertaken for mCLCA3 showing exclusive expression in the digestive, respiratory tracts and uterus (Leverkoehne and Gruber 2002). The mCLCA3 antigen was not found in the gallbladder, kidney, pancreas, sublingual salivary glands, oviduct, mammary gland or prostate (Leverkoehne and Gruber 2002). Concurrent staining for mucin and immunohistochemical localization of mCLCA3 antigen clearly indicated that mCLCA3 was expressed only in the mucin-producing cells. But, not all mucin-producing cells demonstrated mCLCA3 expression. In the respiratory tract, high expression was seen in the trachea and major bronchi of single or clustered goblet cells. Staining was also found in the limited submucosal glands of the mouse in the upper trachea. All ciliated epithelial cells were negative. Similar results were found in the uterine goblet cells and the mucinous cells of the uterine gland stained positive for mucin and mCLCA3.

In the stomach, the parietal and chief cells were negative, but the surface mucus cells were positive. All goblet cells stained positive for mCLCA3 expression in the duodenum, jejunum, and ileum. A dynamic expression pattern was seen in the crypt goblet cells in both the large and small intestine, with expression only in approximately the upper two-thirds of the crypt, whereas weak, or no, staining was observed in the basal third (Leverkoehne and Gruber 2002). The physiological importance of this distribution pattern for gastrointestinal mCLCA3 has not been determined, but it may be

significant that difference in expression correlate with the crypt-villus axis. Staining was not found in those cells which migrate to the crypts and undergo apoptosis but was seen in those that migrate to the luminal apex of the villus and are sloughed off (Leverkoehne and Gruber 2002). CLCA proteins have been promoted as proapoptotic (Elble and Pauli 2001), but it is the cell group directed toward apoptotic removal at the base of the crypts that loses mCLCA3 expression. However, mCLCA2 and mCLCA1 expression may increase as mCLCA3 levels decline, and play some role in apoptosis at the base of the crypts. Although mCLCA1 and 2 expression has been identified in the crypts, their histological localization within the GI crypts has not been determined (Gruber, Gandhi et al. 1998). It is also interesting to note the detection of CLCA1 and possibly CLCA2 by *in situ* hybridization in the ciliated tracheal epithelial cells, which are not associated with mucus secretion (Gruber, Gandhi et al. 1998). These findings support an emerging pattern where in each CLCA family member could perform discrete physiologic functions as cells mature and differentiate within the same tissue.

The development of a good antibody allowed intracellular localization of the mCLCA3 antigen (Leverkoehne and Gruber 2002). In simple paraffin embedded tissue sections the cytosol was stained positive with a diffuse granular pattern. Goblet cells often had an intensely stained apical membrane. A similar staining pattern was found in glycolmethacrylate (GMA)-embedded histological preparations that permit better access of the antibody to the tissue. However, obvious labeling was noted around the mucin granules. This result led to an immune transmission electron microscopy study using gold-labeled secondary antibodies which associated mCLCA3 with the peripheral membrane of mucin granules in positively staining cells. No labeling was found in the

center of the granule, cytosol, nucleus, other organelles or along the basolateral membrane of goblet cells (Leverkoehne and Gruber 2002) . These studies suggest a connection of mCLCA3 to mucin production.

1.3.2.4. mCLCA4

Cloned from smooth muscle, mCLCA4 was detected in the gastrointestinal tract, uterus, lung and heart in a multiple cDNA array using gene-specific primers. A large component of mCLCA4 cDNA expression was detected by RT-PCR in the smooth muscle of the dissected tunic muscularis of the bladder and stomach (Elble and Pauli 2001). *In situ* hybridization with a mCLCA4-specific probe was performed to determine cell-specific expression in these mixed organs. However, the degree of specificity of the probe used to detect mCLCA4 in this study was not clear, as it spanned a combination of 3' ORF (from mCLCA4 base 2670) to an unspecified position in the 3'- untranslated region. The ability of the probe to distinguish mCLCA4 mRNA from mCLCA1 and 2 was not determined. This probe produced a very strong signal in the pulmonary vein, aorta, and atrioventricular bundle with a much lower level in cardiac muscle, coronary artery and endothelium. In the lung, both the bronchioles and blood vessels were labeled. In the gastrointestinal tract, labeling was associated more with the mucosa than the muscularis tunica. This mucosal labeling was most intense towards the villus tip (Elble, Ji et al. 2002). It should be noted that this is the first CLCA with a reported increase in expression towards the villus tip. mCLCA1 and possibly 2 are thought to be primarily expressed in the crypt (Gruber, Gandhi et al. 1998). mCLCA3 is associated with upper cypt and mid-shaft of the villus (Leverkoehne and Gruber 2002). Again we see differing expression patterns of each isoform within a tissue that associate with

major differences in cell physiology. Adipose and connective tissue were consistently negative (Elble and Pauli 2001).

1.3.3. Bovine Orthologues

1.3.3.1. bCLCA1

The bCLCA1 orthologue is primarily expressed on the brush border of ciliated tracheal epithelial cells (Elble, Widom et al. 1997). This is the tissue from which it was originally cloned (Cunningham, Awayda et al. 1995). This expression site is similar to that reported for mCLCA1/2 (Gruber, Gandhi et al. 1998). The expression in other tissue is not currently known.

1.3.3.2. bCLCA2

The bCLCA2 orthologue is primarily thought of as a luminal membrane protein of the venular endothelia of the lungs and the spleen. However, antibodies to bCLCA2 located a strong antigen signal in endothelia of small to medium size venules as well as in the respiratory epithelial of the bronchi and trachea (Elble, Widom et al. 1997). The antigen of bronchial epithelium was deemed to be mainly on intracellular vesicles. The expression in the tracheal epithelium was predominately in the apical plasma membrane. However, due to the lack of information on the other bovine CLCA isoforms it is likely that several orthologues may have been cross-reacting with the screening antibody. The antibody reaction in the tracheal epithelium is most likely with bCLCA1 and that in the vesicular bodies is more likely to be a yet un-cloned bCLCA.

1.3.4. Porcine Orthologues

1.3.4.1. pCLCA1

Original studies using the IgM monoclonal antibody used to clone pCLCA1 had distinct staining on the enterocyte border of the villi. Labeling intensity was distributed over the mucosal surface, with the most intense staining observed in the mid to upper crypt region (Racette, Gabriel et al. 1996). When pCLCA1 cDNA sequence became available a CLCA mRNA was identified by *in situ* hybridization in the ileal mucosa. But, a more diffuse staining was found in the crypt-villus axis. In the trachea pCLCA1 mRNA expression was localized to surface epithelium and the underlying submucosal glands. The most intense staining was found in a subset of the submucosal glands (Gaspar, Racette et al. 2000). These tissues were also positive for pCLCA1 expression when tested by RT-PCR. pCLCA1 expression was not detected in the colon. RT-PCR identified pCLCA1 mRNA in the parotid, sublingual and submandibular salivary glands (Gaspar, Racette et al. 2000). Other tissues which are known to express a variety of chloride channels including the exocrine pancreas, cardiac and skeletal muscle, liver and kidney did not reveal any pCLCA1 mRNA (Gaspar, Racette et al. 2000).

1.3.5. Canine Orthologue

1.3.5.1 cCLCA1

Antibodies generated against pCLCA1 were used to stain canine retinal pigment epithelial cells (Loewen, Smith et al. 2003). Intense staining was seen in the basolateral membrane of the epithelium, which is really the apical secretory side. The Muller cells, which are reported to maintain appropriate extracellular environment for retinal

neurons, also showed significant cCLCA1 expression. (Loewen, Grahn et al., unpublished data)

1.3.6. Rat Orthologue

1.3.6.1 rCLCA1

Antibodies generated to rCLCA1 reacted extensively in the pancreas. On cellular localization most of the staining was associated with the zymogen granules (Thevenod, Roussa et al. 2003). Interestingly, a independent study was unable to detect expression of hCLCA1, the closest orthologue to the rCLCA1 or hCLCA2 in a pancreatic duct adenocarcinoma cell line with calcium-activated chloride conductance (Fong, Argent et al. 2003). This negative finding is consistent with observations by others that CLCA expression does not always correlate with the presence of calcium-activated chloride currents (Loewen, Bekar et al. unpublished observations, 2004). It is also in agreement with the loss of expression of CLCA products in carcinoma cell lines (Elble and Pauli 2001).

1.4. CLCA Structure

1.4.1. Human Orthologues

1.4.1.1. hCLCA1

hCLCA1 It is predicted that the cDNA for the hCLCA1 gene encodes a 914 amino acid protein with a calculated molecular weight of 100.9 kDa (Gruber, Elble et al. 1998). Four putative transmembrane domains have been proposed for the intact protein based on major hydrophobic regions, combined with a predicted helical sequence. A signal sequence is present in the first 20 amino acids with a predicted signal sequence cleavage site at amino acids 20 or 21. The predicted sequence motifs in

the protein include 9 potential sites for asparagine-linked glycosylation, 13 consensus sites for PKC phosphorylation and 3 consensus sites for phosphorylation by Ca^{2+}/calmodulin-dependent kinase II. No PKA or tyrosine phosphorylation consensus sequences were found (Gruber, Elble et al. 1998).

In vitro translation of the human CLCA1 resulted in a 100 kDa product that increased in size to 125 kDa in the presence of canine pancreatic microsomes, indicating extensive glycosylation.

Structure modeling predictions for the protein are complicated by post-translational processing that can include proteolytic cleavage. Some insight into the structure has been obtained by inserting an antigenic epitope into various regions in the amino acid sequence. However, several of the tagged constructs were resistant to normal processing by proteases, indicating that the cleavage may be conformationally dependent. This was not entirely unexpected, as the majority of the cleavage sites were consensus sequences for monobasic proteases which are significantly affected by protein confirmation (Schwartz and Devi 1986; Devi 1991). Insertion of the c-myc epitope (EQKLISEEDL) between aa366/367 or 492/493 resulted in a 90 kDa polypeptide, but little or no full length 125 kDa product. These locations for the epitope apparently interfered with the ability of the smaller cleaved ~ 40 kDa product to interact with the larger 90 kDa subunit. In contrast, varying ratios of both 125 kDa and 90 kDa were produced when the epitope was placed at aa27/28 and aa593/594. It was difficult to determine whether the 125 kDa product in the last two epitope placements was due to subunit association or uncleaved polypeptide because the ~ 40 kDa fragment could not

be detected. These difficulties were illustrated with an epitope placed at 877/879 to identify the ~ 40 kDa product that only produced a 125 kDa product.

These disruptions of protein processing by epitope insertion indicate the importance of relatively small inserted amino acid segments to overall protein structure. Possible effects of structural changes on membrane topology may also be a significant concern when considering the predictions of membrane association and topology produced by surface biotinylation and fluorescent labeling studies.

After cell surface biotinylation, immunoprecipitation and streptavidin probing, the N terminal epitopes inserted after amino acids 90 or 125 immunoprecipitated with 37, 39 and 41 kDa product. This would indicate that all three of these fragments are inserted into the apical membrane. These smaller polypeptides are thought to be the glycosylated products from proteolytic processing at one of two monobasic cleavage sites, either 660/661 and 718/719. Results from the c-myc epitope insertion experiments produced a model with an extracellular N and C terminus, and four transmembrane domains. The 37 to 41 kDa amino terminal cleaved product is assumed to be entirely extracellular (Gruber, Schreur et al. 1999; Pauli, Abdel-Ghany et al. 2000). However, possible effects of disruption of structure and processing caused by c-myc epitope insertion should not be ignored when considering the validity of this model.

It should be noted that a significantly different model for hCLCA1 structure and relationship to the membrane has been predicted (Whittaker and Hynes 2002). Using SMART predictions based on sequence homology to other proteins they suggest that the CLCA family members consist of a central (extracellular) VWA domain and a single transmembrane domain near the C terminus. The significant disparity between the

alternate models arises from predictions about the folding and topography of the amino-terminal half of the protein. The alternatives suggest that this region of the protein contains either two helical transmembrane domains (TM1 and TM2), or it is entirely extracellular, folded with secondary and tertiary structure appropriate to form a VWA domain.

The VWA domains are recognized for involvement in protein-protein interactions. There is direct evidence from two independent systems for the interaction of CLCA proteins with other protein species. Functional effects of hetero-oligomeric CLCA interactions have been demonstrated for cell binding and mitogenic signaling via integrins (Abdel-Ghany, Cheng et al. 2001; Abdel-Ghany, Cheng et al. 2002; Abdel-Ghany, Cheng et al. 2003), and for ion channel modulation via the β_1-subunit of the large conductance potassium channel (Greenwood, Miller et al. 2002). There is also indirect evidence for modulatory effects of CLCA expression on chloride conductance, suggesting that some chloride conductance channels may function as hetero-oligomeric structures. The literature contains precedents for VWA domain involvement in ion channel subunit interactions. In the case of voltage-gated calcium channels, the pore-forming α1 subunit is modulated by the α2δ VWA domain-containing subunit complex to alter the properties of the channel (Hobom, Dai et al. 2000; Whittaker and Hynes 2002). In addition to involvement in straightforward protein-protein interactions, some VWA domains contain an internal structural element called a metal-ion dependent adhesion site or MIDAS domain. These domains are composed of non-contiguous amino acid sequence that can be organized into a complete cation binding structure through normal VWA folding. Magnesium and calcium binding to MIDAS domains,

and participation of the bound cations in stabilizing protein-protein interactions has been demonstrated. Several predicted CLCA structures contain amino acid sequence meeting the requirements for VWA folding and MIDAS function (Whittaker and Hynes 2002). Calcium binding within the MIDAS domain in CLCA proteins could participate in a signaling response to alter the conductivity of a chloride ion channel. These observations could be the basis for an attractive hypothesis connecting CLCA proteins to the assembly and regulation of chloride channels. However, the MIDAS domain is normally composed of extracellular polypeptide structure, while effects of Ca^{2+} ionophores on chloride conductance associated with CLCA expression imply that changes in intracellular Ca^{2+} concentration are the basis for physiological regulation of this chloride conductance. In addition, in spite of excellent amino acid sequence homologies, there has been no direct evidence for VWA domain formation and function in CLCA proteins (see Figure 1.2).

1.4.1.2. hCLCA2

The hCLCA2 orthologue is predicted to form a 943 amino acid polypeptide (Gruber, Schreur et al. 1999). It contains a canonical signal sequence with a predicted signal peptidase cleavage site between amino acids 31 and 32. The predicted size of the full-length protein is a 104 kDa. This is confirmed by a primary translation product of 105 kDa from an *in vitro* translation assay. Glycosylation of the product using microsomal membranes increased the size to 120 kDa. As with other orthologues, the translated product appears to undergo proteolytic processing. Placement of a c-myc epitope with the N terminus or the C terminus allowed probing of the size of products

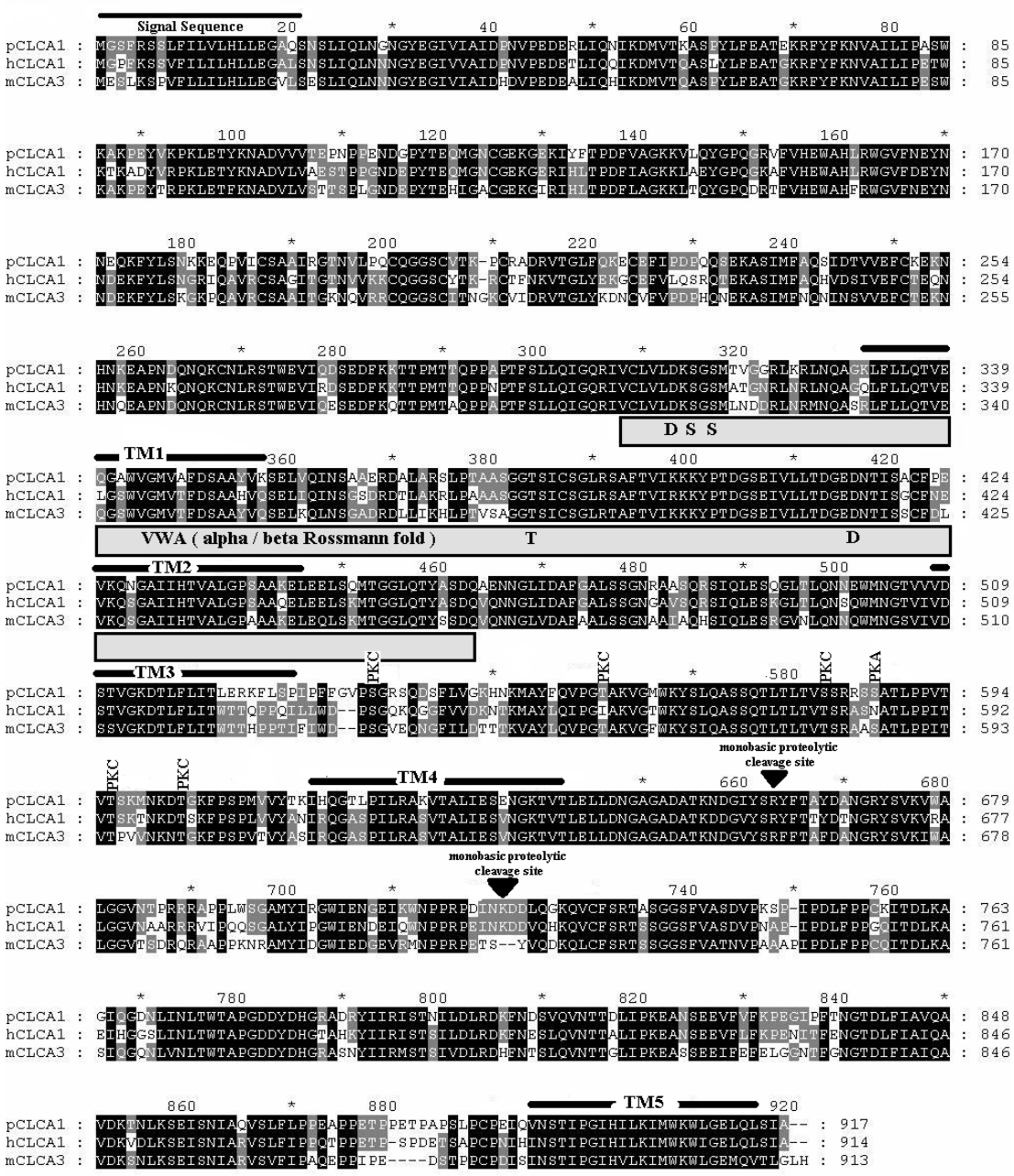

Figure1.2. Alignment of the closest mammalian orthologues mCLCA3 (gob-5) and hCLCA1 with pCLCA1. The amino acid sequence identity for pCLCA1:hCLCA1 was 78 %, pCLCA1:mCLCA3 was 73 % and hCLCA1:mCLCA3 was 75 % as determined by Clustalw software. The VWA domain and the major transmembrane domains predicted by Gruber et al. are outlined. Phosphorylation consensus sequences on the major cytoplasmic loop are identified

present in whole cell lysate. The N-terminal tag was found on an 86 kDa protein and a 34 kDa protein was identified when the tag was situated near the C terminus. It is presumed that the cleavage occurs at the monobasic proteolytic 673/674 cleavage site.

Deglycosylation of these products resulted in a size reduction that would correspond with 4 glycosylation sites on the 86 kDa subunit and one on the smaller 34 kDa fragment. Asn to Gln mutation abolished glycosylation sites and resulted in a ~ 2 kDa size change. Mutants made at N terminal N150Q indicating an extracellular N terminus, and the N522Q substitution indicated an extracellular loop between predicted transmembrane domains 2 and 3. A N822Q mutation indicated an extracellular loop in the smaller cleaved product between transmembrane domains 4 and 5.

A protein protection assay digesting all internal loops resulted in a 30 kDa product thought to be the N terminus plus transmembrane domain 1. The digest also produced an 18 kDa product that was thought to consist of transmembrane domains 2 and 3 and the first extracellular loop, and a 21 kDa product resulting in the final two transmembrane domains and the extracellular loop. This gave the interpreted 5 transmembrane domain structure of hCLCA2. It should also be noted that the two units were detected in surface-biotinylated, nonpermeablized HEK-293 cells, suggesting that both the larger and the smaller subunits are expressed on the cell surface. In this model the internal loops contained seven PKC phosphorylation sites. However, there were no consensus sites for Ca^{2+}/calmodulin protein kinase II or cAMP-dependent protein kinase (Gruber, Schreur et al. 1999). HCLCA2 as well as several other CLCA proteins contain a β_4 integrin binding domain (Abdel-Ghany, Cheng et al. 2003). The significance of this is discussed later.

1.4.1.3. hCLCA3

Initial analysis of the hCLCA3 gene readily revealed a very different structural product for this member of the family (Gruber and Pauli 1999b). hCLCA3 has a high degree of identity to the CLCA consensus sequence, but, unlike the other members of the gene family, it contains two open reading frames (ORF). Both these reading frames terminate early, producing significantly smaller products than other family members. The ORF1 on the 3.6 kb gene product codes for a 262 amino acid polypeptide containing the N terminus and the signal sequence of a standard CLCA protein. The second ORF codes for amino acids corresponding to positions 266 to 461 in an intact CLCA protein. Together, the two ORFs code for approximately the first 1/3 of the full length CLCA protein. Analysis of this sequence predicts that ORF1 lacks potential transmembrane domains. ORF2 does not have a signal sequence, but codes for two hydrophobic domains with significant sequence identity to the first two transmembrane domains of other CLCA family members. *In vivo* transcription and translation in a TNT T7 coupled reticulocyte lysate system produced 30 and 22 kDa products corresponding to calculated size for ORF1 and ORF2 respectively. *In vitro* glycosylation increased the weight of the 30 kDa protein to 37 kDa and did not change the 22 kDa protein. It is thought that the increase in size was due to carbohydrate addition to three consensus sites for N-linked glycosylation observed in its amino acid sequence. However, a tagged ORF1 peptide was the only product identified in HEK 293 cells transfected with constructs coding for expression of both ORF1 and ORF2. The excreted ORF1 product could also be detected upon immunoblotting the supernatant from transfected cells. It is

also interesting to note that ORF1 translation terminates before the VWA domain is produced, so hCLCA3 is the only CLCA which lacks the potential to form a VWA domain (Gruber and Pauli 1999b).

1.4.1.4. hCLCA4

Unfortunately there is currently no structural data for the hCLCA4 clone.

1.4.2. Mouse Orthologues

1.4.2.1. mCLCA1

The predicted size of 100 kDa correlates with the *in vitro* translated size of 100 kDa for this 902 amino acid protein. A signal sequence was noted at the amino terminus of the protein (Gandhi, Elble et al. 1998). Glycosylation of the translated product with canine microsomes increased the size to approximately 125 kDa. On expression in HEK 293 cells antibodies to the N-terminal end identified products of 130, 125 and 90 kDa. Antibodies that detected a carboxyl-terminal epitope identified a triplet of bands ranging in size from 32 to 38 kDa. It was suggested that the alternate glycoforms of 125 and 130 kDa, are postranslationally processed into the 90 and 38/32 kDa components. A general 4 transmembrane domain structure was proposed for this gene, leaving the C terminus without a transmembrane domain.

1.4.2.2. mCLCA2.

Little or no structural data is available on mCLCA2. Its closest orthologue is thought to be hCLCA2. It has been reported without accompanying data that mCLCA2 yields similar processed products as those observed for mCLCA1 when expressed in HEK293 cells (Elble and Pauli 2001).

1.4.2.3. mCLCA3

The mCLCA3 cDNA coded for a 100 kDa protein in an *in vitro* translation assay. The product increased in size to approximately 110 kDa after glycosylation with microsomal membranes (Leverkoehne and Gruber 2002). After microsomal protease treatment, only a 35 kDa product was detected, which, in the proposed model, would correlate with the N terminus being extracellular. A 90 kDa product was identified using these same antibodies as a probe in HEK293 and COS-7 cells transiently transfected with mCLCA3. These antibodies also identified a 90 kDa product in both the large and small intestine, with the expression being more intense in the small intestine. Interestingly, a 45 kDa product was also detected in the large, but not in the small intestine (Leverkoehne and Gruber 2002). This enterocyte product remains unexplained, but is thought to be a fragment of a truncated portion of the amino terminus of the protein with similarities to the secreted 37 kDa amino terminus of hCLCA3. The fragment represents either another isoform within the gut or a cell type specific difference in cleavage of the mCLCA3 protein (Figure 1.2).

1.4.2.4. mCLCA4

To date there is limited information on the structure of mCLCA4. The primary structure contains many similarities to mCLCA1 and 2. It is 909 amino acids in length, with a conserved cleaved amino terminal signal and a second monobasic cleavage site which results in a 90 and 30 to 40 kDa products (Elble, Ji et al. 2002). The primary structure also contains most of the calcium/calmodulin kinase II sites found in mCLCA1 and mCLCA2.

1.4.3. Bovine Orthologues

1.4.3.1 bCLCA1

The primary structure of bCLCA1 is thought to consist of 903 amino acids, giving a predicting product of 100 kDa (Cunningham, Awayda et al. 1995). On motif analysis it is predicted of have 15 protein kinase C acceptor sites, 10 Ca^{2+}/calmodulin-dependent protein kinase sites, and three tyrosine kinase sites. Four transmembrane domains and an amino terminal signal sequence were suggested based on hydropathy plots. *In vitro* translation yielded the predicted 100 kDa product. On glycosylation with canine pancreatic microsomes, the molecular weight shifted to 140 kDa. This correlated with the original 140 kDa purified chloride conducting product. However, it did not reduce to the smaller fragments observed with the purified tracheal product (Ran, Fuller et al. 1992). This was assumed to be due to the lack of monobasic protease cleavage activity in the *in vitro* translation assay, although it was considered possible that the bCLCA1 protein was not the antigen containing the original epitope involved in chloride transport in the trachea. Polyclonal antibodies generated against an N terminal fragment of the bCLCA1 clone recognized a reduced 36/38 kDa bovine tracheal lysate product similar to the antigen identified by the original antibodies that were used to clone bCLCA1 (Ran, Fuller et al. 1992; Cunningham, Awayda et al. 1995). However, these polyclonal antibodies were never used on the *in vitro* translated or the oocyte-expressed clone. It was hypothesized the original purified protein of 140 kDa consisted of four identical 38 kDa subunits linked together by disulfide bonds and only reduced to 64 and 38 kDa due to exceptionally strong disulfide bonding between two of the identical subunits (Ran, Fuller et al. 1992). However, the sequence data and the identification of the 100 kDa unglycosylated form of bCLCA1 indicate that the 38 kDa

protein is a post-translational cleavage product associating with a larger fragment of the original translated protein (Cunningham, Awayda et al. 1995). This model has now been promoted for the other cloned isoforms and orthologues.

1.4.3.2.bCLCA2

The cloned sequence had a predicted hydrophobic amino terminal signal sequence and cleavage site for membrane association. As seen in bCLCA1, a hydropathy plot predicted 4 transmembrane domains. *In vitro* translation resulted in a 101 kDa product without glycosylation and 120 kDa with glycosylation.

Deglycosylation of native bCLCA2 with N-glycosidase F from endothelial cells reduced the apparent size of 38 and 32 kDa polypeptides to 22 kDa, and the 90 kDa band to 77 kDa, giving the predicted deglycosylated size of the processed bCLCA2 clone (Elble, Widom et al. 1997). This is consistent with an original study immunoprecipitating bCLCA2 (Lu-ECAM-1) as a 90 kDa protein using an antibody to N terminal amino acid sequence (Zhu and Pauli 1991). Immunoblot with antibodies to the N terminus of bCLCA2 identified products at 90, 120, and 130 kDa but not at 38 or 32 kDa. Antibodies generated against C terminal sequence identified products of 38, 32, 120 and 130 kDa but not 90 kDa. This demonstrates that the 90 kDa polypeptide has no epitope in common with the 32 or 38 kDa fragments. But the 120 and 130 kDa proteins do share epitopes, indicating that products above 100 kDa can be separated into two non-identical proteins (Elble, Widom et al. 1997). The earlier suggestions of a homo-tetrameric structure for this protein (Ran, Fuller et al. 1992) are not supported by these experimental observations. Similar results were found with expression of

bCLCA2 in human embryonic kidney cells (HEK 293). Immunoblotting detected 120, 90 and 38 kDa products. Interestingly, the 130 and 32 kDa products observed in bovine aortic endothelial cells were not detected. This likely indicates differences in glycosylation between the expression system and the native expression in the endothelial cell (Elble, Widom et al. 1997).

1.4.4 Porcine Orthologues

1.4.4.1 pCLCA1

The full-length pCLCA1 transcript was estimated to be ~ 2.9 kb on Northern blot analysis. The full length cloned sequence contained 3,079 base pairs and a 2,751 base open reading frame which is predicted to encode a 917 amino acid protein with a molecular mass of 100.7 kDa (Gaspar, Racette et al. 2000). Its closest orthologue is hCLCA1, sharing 78% amino acid sequence identity. The areas with the greatest sequence differences between these related genes were in the putative extracellular N terminus between amino acids K181 and S323, and in the proposed cytosolic loop lying between transmembrane domains 3 and 4. The high similarity for amino acid sequence and hydrophobicity between pCLCA1 and the closest human orthologue, hCLCA1, suggested a similar transmembrane topology for the two proteins. Modeling this structure according to the suggestions of Gruber et al. (Gruber, Schreur et al. 1999) would give an extracellular amino terminus followed by four transmembrane domains and a hydrophobic C-terminus (Fig 1.2)(Gaspar, Racette et al. 2000).

The predicted pCLCA1 protein is similar to several other CLCA proteins, containing a signal sequence for membrane targeting, and potential proteolytic cleavage sites which are shared with hCLCA1. There is an amidation cleavage site at residue 140

and two monobasic proteolytic cleavage sites at R662 and another at K720. Both of these monobasic proteolytic cleavage sites would be located in the C- terminal extracellular loop if the predicted structural topology from Fig 1.2 is correct. These multiple sites for potential proteolytic cleavage appear to be significantly dependent on protein conformation for actual post-translational processing. This could account for the multiple sizes of protein (~130, 90 and 60 kDa) detected by Western blotting or immunoprecipitation of brush border vesicles protein with an inhibitory antibody (Gabriel, Racette et al. 1992; Racette, Gabriel et al. 1996). It should be noted that the original antibody that inhibited brush border conductive chloride transport was generated from electro-eluted protein fractions of porcine ileal brush border. Monoclonal antibody selected on the same basis was used for cDNA library screening. The only antigen pool yielding antibody that inhibited chloride conductance was a high molecular weight fraction >110 kDa (Gabriel and Forsyth 1991; Gabriel, Racette et al. 1992). The pCLCA1 orthologue would have avoided proteolytic processing, or lower molecular weight cleavage fragments of pCLCA1 would have had to associate with other proteins to give this molecular mass to the antigen. The extent to which currently available evidence supports varying degrees of proteolytic processing, versus association of processed fragments of pCLCA1, with other unidentified proteins is not clear. Expression of exogenous pCLCA1 in transfected Caco-2 cells produced a ~ 60 kDa product upon Western blotting which was present at much lower levels in control transfected cells. The antibody used for this screening was developed to an amino-terminal peptide (C250- K266) of pCLCA1. It is also possible that the processing of CLCA isoforms may vary with expression in different tissues. As is often mentioned in

the literature, not all isoforms or orthologues in every tissue are processed into the commonest ~ 90 and ~ 35 kDa fragments (Pauli, Abdel-Ghany et al. 2000; Fuller, Ji et al. 2001). This is supported by the evidence that a ~ 60 kDa bCLCA1 fragment and ~ 60 kDa pCLCA1 product were expressed in epithelial cells, as well as a preliminary report of a ~ 60 kDa protein contributing to anion conductance in the rabbit ileum (Peerce, Seifert et al. 1991; Ran, Fuller et al. 1992)

Similar to other CLCA clones, pCLCA amino acid sequence from V307 to Q462 has extensive homology with sequences that form a VWA domain (Figure 1.2). The previously noted incompatibility between an extracellular VWA domain and the predicted four transmembrane domains (Gruber, Schreur et al. 1999) also applies to pCLCA1. Within pCLCA1's putative VWA domain there is a perfect non-contiguous consensus sequence for a MIDAS motif (D-x-S-x-S...T...D) beginning at 313D. hCLCA1 has a similar motif. Loewen et al. have presented evidence for a direct regulatory role of calcium in the modulation of chloride conductance by pCLCA1 (Loewen, Gabriel et al. 2002), but no connection has been made between Ca^{2+} binding to this MIDAS site and the regulation of pCLCA1. However, structural modeling of the pCLCA1 MIDAS domain does reveal appropriate folding (Figure 1.3).

The pCLCA1 sequence contains 14 potential C kinase phosphorylation sites. The most amino terminal four sites lie before the first predicted transmembrane domain. This places them in the extracellular space if predicted transmembrane topology is correct. Four of the C kinase sites found within the predicted cytosolic loop between transmembrane domains 3 and 4 are shared with hCLCA1, while pCLCA1 has a fifth

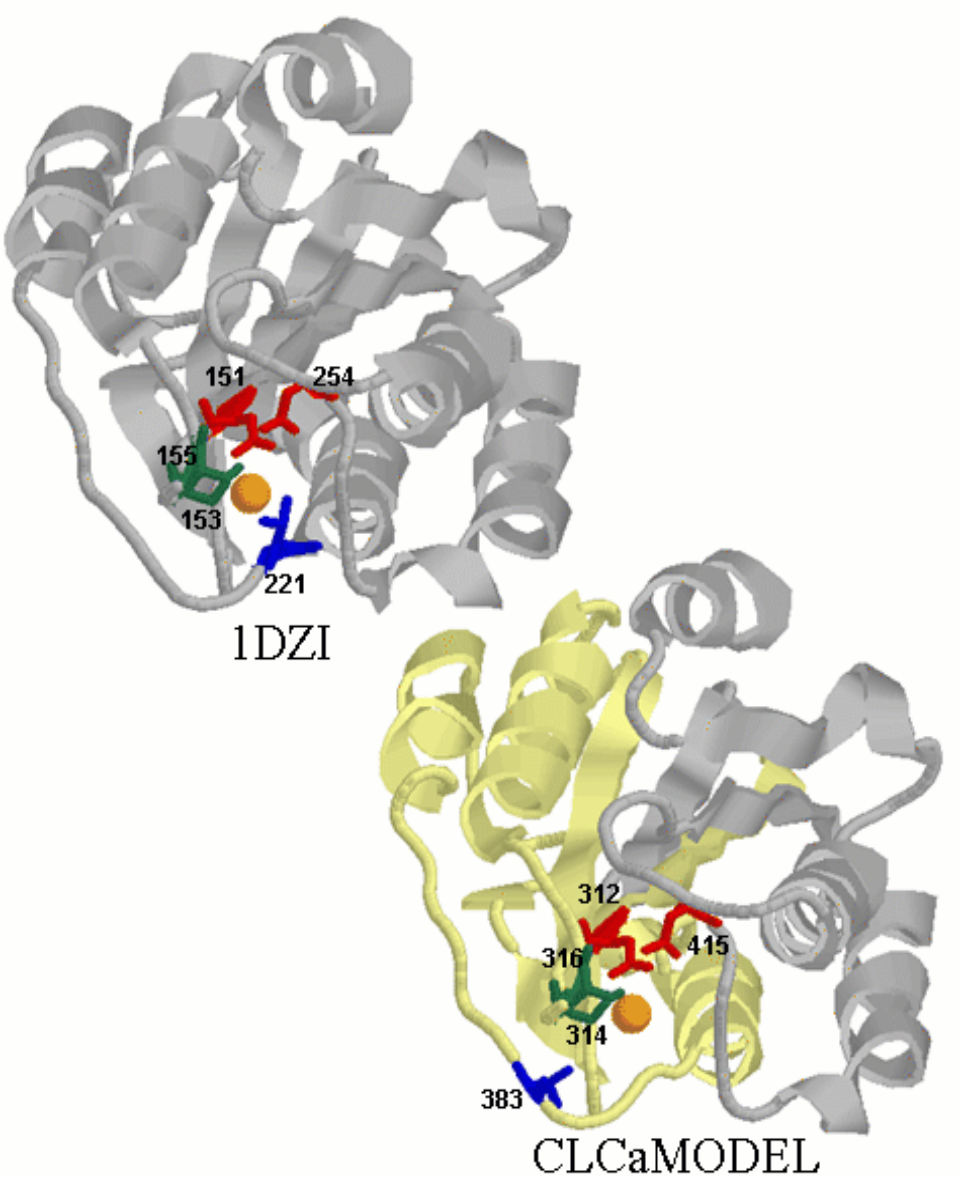

Figure 1.3. Structural modeling of the von Willebrand A MIDAS domain in pCLCA1. Amino acids 310 to 415 of pCLCA1 were aligned with and spliced into the alpha-2 integrin collagen receptor sequence. Clustalw gave a sequence identity of 48 % of the hybrid to the integrin alpha-2 VWA domain. This new hybrid sequence was modeled using Swiss Model to the solved structure of the alpha-2 integrin VWA domain of the I domain designated 1DZI(Emsley, King et al. 1997; Emsley, Knight et al. 2000). Grey is 1DZI template structure/sequence. Yellow is pCLCA1 sequence in model hybrid. Red = Asp, green = Ser, blue = Thr, and the orange ball is the calcium ion. Note the classical Rossmann fold with the open twisted β sheet surrounded by α helices on both sides. Also note the metal ion coordination site at the surface which defines this Rossmann fold as the VWA domain. The pCLCA1 hybrid MIDAS seems to have the appropriate coordinates for ion binding in this model. A weak Thr 383 bond would be expected given interatomic distances in this model.

unique site in this same loop. Also found in this loop is a strong A-kinase site which is unique to pCLCA1 (Gaspar, Racette et al. 2000). Unfortunately, the effects of mutagenesis of this highly phosphorylated loop in the modulation of chloride conductance by CLCA proteins has not been reported

1.5. Functional Expression

1.5.1. Human Orthologues

1.5.1.1. hCLCA1

Initial functional characterization of hCLCA1 involved transient expression in HEK 293 human embryonic kidney cells (Gruber, Elble et al. 1998). Transfection with hCLCA1 increased calcium-activated whole cell currents from 1.57 ± 0.72 pA/ pF in control cells to 11.06 pA/pF in transfected cells, producing a time-independent outwardly rectifying current. This current was said to be "electrically isolated" for chloride, based on the blockage of cation current using large bulky cations. Unfortunately however, the chloride dependence of the current was not determined. These putative chloride currents were reduced by DIDS, DTT, and niflumic acid. However, DIDS is the only one of these inhibitors known to be primarily a blocker of chloride channels. Interestingly, this study presents the only single channel patch clamp study of the CLCA proteins. It was reported that hCLCA1 had a slope conductance of 13.4 pS in cell-attached conformation after the addition of ionomycin in the presence of 1 mM Ca^{2+} (Gruber, Elble et al. 1998). Apparently no difficulties were encountered in this study with the background non-selective and anion currents previously reported in these cells (Ye, Rogers et al. 1996; Zhu, Zhang et al. 1998).

1.5.1.2. hCLCA2

When HEK 293 cells were transiently transfected, hCLC2 produced a calcium-activated, non time-dependent, outwardly rectifying increase in whole cell current. Transfection increased the whole cell current from 1.52 ± 1.83 pA/pF in control to 10.77 ± 3.8 in transfected cells (Gruber, Schreur et al. 1999). Once again, neither the background current in untransfected cells nor the chloride-dependence of the current produced in transfected cells has been explored. However, the "electrically isolated" anion current was blocked by DIDS, DTT, NFA and Tamoxifen (Gruber, Schreur et al. 1999).

1.5.1.3. hCLCA3 and hCLCA4.

There are no current reports of ion transport functional data on hCLCA3 and hCLCA4.

1.5.2. Mouse Orthologues

1.5.2.1. mCLCA1

Two independent groups characterized mCLCA1 concurrently (Gandhi, Elble et al. 1998; Romio, Musante et al. 1999) in different expression models. As reported for the human CLCAs, expression of mCLCA1 in HEK293 cells caused the appearance of a significant calcium-activated chloride current. The current was non time-dependent and outwardly rectifying (Gandhi, Elble et al. 1998). The current increased from 2.05±1.09 pA/pF to10.23 pA/pF upon addition of ionomycin. Background Cl^- currents were apparently insignificant in this study and the anionic dependence of the current was not determined. NFA, DTT and DIDS inhibited the reported chloride current. Romio et al. concurrently cloned and expressed mCLCA1 in Xenopus oocytes (Romio,

Musante et al. 1999). In cRNA injected oocytes, there was a significant increase in oocyte current without calcium activation. At -80 mV, the current in mCLCA1 mRNA-injected oocytes was -398 ± 136 nA compared to -97 ± 12 nA for water-injected oocytes. The current in the mCLCA1-injected oocytes was chloride-dependent, but there was no chloride dependence for the current from water-injected oocytes. The lack of an E_{rev} shift when bath solution was changed to low NaCl indicated that the background current was a combination of both anion and cation currents. Both DIDS and niflumic acid inhibited chloride current in mCLCA1-injected oocytes. However, they also reduced the endogenous current of the water-injected oocytes. Interestingly, the application of a Ca^{2+} ionophore (ionomycin) caused a transient increase in current to 1805 ± 473 nA in mCLCA1-expressing oocytes compared to 1109 ± 389 nA in control oocytes. However, this difference in the stimulated currents between mCLCA1 and mock-injected oocytes was not statistically significant (Romio, Musante et al. 1999). Due to the large background currents it is difficult to determine the calcium-activated dependence of chloride conductance associated with CLCA expression in Xenopus oocytes.

More recent studies have shown enlarged whole cell currents induced by mCLCA1 expression (Britton, Ohya et al. 2002; Greenwood, Miller et al. 2002). Generally mCLCA1 expression in HEK 293 cells resulted in a mildly outwardly rectifing, time independent current. This current was only elicited when 2 mM Ca^{2+} was placed in the pipette. The Ca^{2+}-activated currents did not increase above control values when 500 nM Ca^{2+} was present. The stimulated mCLCA1 current was found to be more permeable to SCN^- than Cl^-, which was more permeable than isethionate (Britton, Ohya

et al. 2002). This is the permeability sequence established by this group for Ca^{2+}-activated chloride channels in smooth muscle from which they cloned mCLCA1 (Britton, Ohya et al. 2002). Unfortunately, the anion dependence of the whole cell current in control HEK 293 cells was not assessed.

The mCLCA1-dependent calcium-stimulated current changed significantly when co-expressed with a potassium channel β-subunit (Greenwood, Miller et al. 2002). This co-expression changed the current from time-independent to time-dependent, as well as increasing the total whole cell conductance. Co-expression also resulted in a greater sensitivity to activation by calcium. Addition of 500 nM Ca^{2+} in the pipette solution could stimulate the anion current in β-subunit mCLCA1 expressing cells. This difference in current and agonist sensitivity was shown by a mammalian two-hybrid system to be the result of a direct interaction between β-subunit and mCLCA1. Unfortunately, the anionic dependence of the current was only assessed through the permeability ratios for SCN^- and Cl^- which were consistent with those found in smooth muscle. Again, as with several other CLCA studies, the background currents were not shown or characterized (Greenwood, Miller et al. 2002).

However, the study by Greenwood et al. was the first report suggesting that a CLCA protein required coexpression with other proteins in order to produce functional chloride channels. It demonstrated that the currents induced on CLCA1 expression could be modified by an accessory subunit, suggesting that CLCA proteins may be part of a channel complex, rather than independently forming a channel.

1.5.2.2. mCLCA2

There is currently no electrophysiological data on mCLCA2. Given that it is the closest murine orthologue to hCLCA2, it may have similar electrophysiological parameters.

1.5.2.3 mCLCA3

The effects of mCLCA3 or Gob 5 expression have been characterized briefly in HEK293 cells (Winpenny, Lavery et al. 2002). mCLCA3 expression increased an outwardly rectifying current without agonist addition. Current densities at +60 mV increased from 59 ± 17 to 230 ± 47 pA/pF. Addition of 10 mM EGTA to the pipette solution significantly decreased these currents (Winpenny, Lavery et al. 2002).

1.5.2.4 mCLCA4

Increasing intracellular calcium by treating with ionomycin or methacholine evoked transient inward currents in mCLCA4-transfected cells held at a controlled undefined voltage (Elble, Ji et al. 2002). This would be consistent with the inward movement of cations or the outward movement of anions. In this case, a strong anionic dependence to the stimulated current was shown by a shift in the current-voltage relationship to the equilibrium potential of chloride when bath solution was switched to low chloride after ionomycin addition. Unlike previously characterized isoforms, the current was found to be non-rectifying. The transient nature of the current was thought to be analogous to the Ca^{2+}-independent inactivation of the smooth muscle Ca^{2+}-activated chloride channel. This inward current was found to be spontaneous, similar to those in smooth muscle cells that are induced by a "calcium spark" and are involved in buffering the membrane potential, relaxation and spontaneous rhythmic contraction of

smooth muscle (Nelson, Cheng et al. 1995) (Jaggar, Porter et al. 2000). Current-voltage relationships in non-transfected cells were not examined, as voltage-clamped inward currents were not seen (Elble, Ji et al. 2002).

1.5.3. Bovine Orthologues

1.5.3.1. bCLCA1

Oocytes transfected with bCLCA1 cRNA had a significantly larger current than water-injected oocytes (Cunningham, Awayda et al. 1995). At a holding potential of -100 mV, the mean current for water-injected oocytes was -96 ± 25 pA and -2052 ± 528 pA in oocytes injected with bCLCA1 mRNA. At +90 mV the currents were 457 ± 209 pA (water-injected) and 8084 ± 1700 pA for bCLCA1 mRNA-injected oocytes. bCLCA1 expression clearly increased an endogenous outwardly-rectifying current. This current was sensitive to DIDS and DTT but insensitive to niflumic acid. Addition of 1 μm ionomycin to oocytes resulted in the activation of endogenous chloride channels which were inhibited by niflumic acid. Unfortunately, data showing the effect of the ionophore on bCLCA1-injected oocytes was not presented or discussed (Cunningham, Awayda et al. 1995).

When bCLCA1 was expressed in COS-7 cells, a non-rectifying, Ca^{2+}-activated, DTT-inhibitable current was produced (Cunningham, Awayda et al. 1995). The bCLCA1 current was unlike that seen with most of the other CLCA family members which produced outwardly rectified currents. However, none of the other family members have been characterized using COS-7 cells. It is interesting to note that the currents induced in the oocytes had a both time-dependent and rectifying quality,

whereas those induced in the COS-7 cells had neither (Cunningham, Awayda et al. 1995). This suggests that bCLCA1 may be working with different cellular components in different cell lines to affect the activity of Ca^{2+}-activated chloride channels.

Lipid bilayers were constructed from oocytes membranes that had been injected with bCLCA1 cRNA (Cunningham, Awayda et al. 1995). Recordings from these vesicles had a unit channel conductance of 21 pS. The open probability increased from 0.41 ± 0.07 to 0.60 ± 0.08 in the presence of Ca^{2+} added only to the side opposite to that where DIDS was added. The channel was inhibited by DIDS and DTT, but insensitive to niflumic acid. The channel had an 8:1 anion to cation selectivity ratio and 3:1 selectivity for iodide over chloride under bionic conditions. The biophysical properties were similar to those found for a purified chloride channel from bovine trachea. Some bilayers in the study did have a Ca^{2+}-activated chloride conductance that was inhibited by niflumic acid. This was said to be the endogenous Ca^{2+}-activated chloride channel of the oocyte. Unfortunately, bilayer studies were not performed on purified bCLCA1 in an artificial bilayer.

Other researchers, using bCLCA1 as a control for mCLCA1 characterization, found that they were able to significantly inhibit bCLCA1-induced current by 78 % with niflumic acid. Subsequent addition of DIDS (100 μM) caused a further 33 % inhibition of the anion current (Romio, Musante et al. 1999). Differences in oocyte preparations may have caused these differences in inhibitor sensitivity.

1.5.4. Porcine Orthologue

1.5.4.1. pCLCA1

Effects of pCLCA1 expression on chloride conductance have been studied extensively in NIH/3T3 cells (Gaspar, Racette et al. 2000; Loewen, Gabriel et al. 2002; Loewen, Smith et al. 2003). pCLCA1 was found to increase a calcium-activated $^{36}Cl^-$ efflux from NIH/3T3 cells. Agonists for calcium-dependent protein kinase (PKC) phorbol-12- myristate-13-acetate (PMA) or cAMP-dependent protein kinase (PKA) forskolin and isobutyl-1-methylxanthine (IBMX) had no effect on conductance. However, application of 10 μm ionomycin significantly increased $^{36}Cl^-$efflux from transfected cells. Inhibition of this effect by the membrane-permeable Ca^{2+} chelator 1,2 bis (2-aminophenoxy) ethane-N,N,N',N'-tetraaceticacid acetooxymethylester (BAPTA-AM), combined with the lack of inhibition by the calcium calmodulin kinase II (CaMKII) inhibitor KN-93, suggested that calcium directly regulates pCLCA1 effects on chloride transport. The pCLCA1 effect on chloride efflux was inhibited by bulky organic anions including 5-nitro-2-(3-phenylpropylamino) benzoate (NPPB), glibenclaminde, diphenylamine carboxylate (DPC) and α-phenylcinnamate (α-PC). Both NPPB and DPC inhibited the calcium-activated chloride conductance at much lower concentrations than were required for inhibition of CFTR. NPPB was effective at a concentration similar to that which was required to inhibit Ca^{2+}-activated chloride conductance in Xenopus oocytes (Loewen, Gabriel et al. 2002).

In a patch clamp study, pCLCA1 increased an endogenous Ca^{2+}-activated chloride conductance, making the current more anion dependent, as determined by a low chloride shift to the anion Nernstian equilibrium potential (Loewen, Gabriel et al.

2002). The current induced by pCLCA1 expression was found to be outwardly rectifying and time-dependent. This time-dependence has not been seen in the characterization of other CLCA proteins, and it might be a result of expression in NIH/3T3 fibroblasts having different member components on which to act. As seen in the $^{36}Cl^-$ efflux, DIDS did not inhibit whole cell chloride current, but NPPB, DPC, and α-PC were inhibitory (Loewen, Gabriel et al. 2002). It should be noted that both DTT and DIDS have been reported to be consistent inhibitors of chloride current activity in previous studies with different CLCA proteins and different expression systems (Cunningham, Awayda et al. 1995; Gandhi, Elble et al. 1998; Gruber, Elble et al. 1998), but were not inhibitory for pCLCA1 in this study.

The study of pCLCA1 expression in an a non-epithelial fibroblast cell line gave some insight to its function as a Ca^{2+}-dependent chloride channel regulator (Loewen, Bekar et al. 2002). In addition, transfection of epithelial Caco-2 human colon carcinoma cell line significantly altered the kinetics of cAMP-activated chloride conductance, possibly through some interaction with CFTR (Loewen, Bekar et al. 2002). The pCLCA1 and PKA-dependent currents were found to be anion-dependent, time-independent and non-rectifying. The effects of pCLCA1 expression on PKA-dependent chloride conductance were evident in both freshly passaged and in differentiated epithelial cells, both of which have endogenous CFTR-mediated chloride conductance. This modulation of chloride conductance by pCLCA1 expression was also seen when CFTR and pCLCA1 were co-expressed in non-epithelial NIH/3T3 fibroblasts (Loewen, Smith et al. 2003).

Expression of pCLCA1 also alters the characteristics of chloride conductance activated by calcium ionophore or PKA agonists in Caco-2 epithelial cells. The Ca^{2+}-dependent $^{36}Cl^-$ efflux effects of pCLCA1 expression stimulated a time-dependent outwardly rectifying current by patch clamp (Loewen, Bekar et al. 2004). However the endogenous Ca^{2+}-activated chloride conductance is only found in freshly passaged Caco-2 cells. As the cells mature, they lose Ca^{2+}-activated chloride conductance. When endogenous Ca^{2+}-activated chloride conductance disappears, the ability of pCLCA1 to activate a Ca^{2+}-dependent chloride conductance is also lost (Loewen, Bekar et al. 2004). This separate line of evidence supports previous observations of the importance of contributions of the endogenous chloride channel activity of the host expression system to the properties of the chloride channels observed upon CLCA-expression.

1.5.5. Rat Orthologue

1.5.5.1 rCLCA1

This CLCA isoform has been identified in rat pancreas. It has not been fully cloned or functionally characterized, but it has been indirectly implicated in bicarbonate transport and vesicle exocytosis in the pancreas.

1.5.6. Canine Orthologue

1.5.6.1. cCLCA1

The cCLCA1-cDNA has been produced from canine retinal pigment epithelium mRNA, but this canine variant has not been fully cloned to permit functional expression. The cloned fragment of the cCLCA1 isoform has a significant degree of

identity to porcine pCLCA1. Its tissue localization suggests that it has a strong association with secretory epithelial cells in the canine retina (Loewen, Smith et al. 2003).

1.6. Pathophysiologic Connections to CLCA Expression

1.6.1. CLCA in Asthma

Orthologues of the CLCA gene family have been shown to be over-expressed and to have a key role in mediating the bronchial allergic asthmatic response, especially the over-production of mucus (Nakanishi, Morita et al. 2001; Hoshino, Morita et al. 2002; Toda, Tulic et al. 2002).

1.6.1.1. Asthma and the Genesis of its Mediators

Bronchial allergic asthma is a serious inflammatory condition of the airways resulting in bronchial narrowing, constriction and CLCA-dependent overproduction of mucus. (Busse and Lemanske 2001; Toda, Tulic et al. 2002). Simplistically, the uncontrolled inflammatory response, which is accompanied by the overexpression of CLCA protein, is thought to occur through a dysregulation between type 1 helper T (Th1) and type 2 helper T (Th2) cell immune responses to disease (Robinson, Hamid et al. 1992; Walker, Bauer et al. 1994; Humbert, Durham et al. 1996; Nakamura, Ghaffar et al. 1999; Busse and Lemanske 2001; Arima, Umeshita-Suyama et al. 2002; El Biaze, Boniface et al. 2003). The Th1-immunological response involving cytokines (interleukin 2 and interferon- γ) is seen as a cell-mediated response and is associated with disease in situations such as infection with *Mycobacterium tuberculosis*, measles

virus, hepatitis A virus or poor hygiene (Strachan 1989; Matricardi, Rosmini et al. 1997; Shirakawa, Enomoto et al. 1997; Mattes and Karmaus 1999; Bremner, Carey et al. 2003). The Th2 disease response involving cytokines (interleukins 4, 5, 6, 9, and 13) is generally thought of as humoral, involving the stimulation of B cells and the production of IgE. The IgE binds to IgE receptors on mast cells, lymphocytes, eosinophils, platelets and macrophages. Binding of allergen to the IgE results in the release of inflammatory mediators from mast cells and activation and potentiation of an inflammatory response (Busse and Lemanske 2001).

Proper priming of the immune system to differing immunological challenges is essential to develop a normal Th1 response. The Th1 response then has a role in modulating the Th2 response. An uncontrolled Th2 response, dominates the disease state of asthma. This association between Th2 cytokine expression response and asthma is demonstrated in Th2 asthma models. Functional blockade of the Th2 cytokine pathways significantly dampens the asthmatic response (Brusselle, Kips et al. 1994; Foster, Hogan et al. 1996).

1.6.1.2. Th2 cytokines mediate CLCA expression

The Th2 response and the associated cytokines appear to be directly linked to CLCA over-expression in the asthmatic patient. A study using subtractive hybridization between a Th2 cytokine IL-9 over-expressing mouse versus a wild-type mouse identified significant over-expression of mCLCA3, the closest murine orthologue to hCLCA1 (Zhou, Dong et al. 2001). Induction of mCLCA3 expression was also found when Th2 cytokines IL-4 and IL-13 were introduced into tracheas of anesthetized mice daily for 10 days (Zhou, Dong et al. 2001). Interestingly, instilled Th1 cytokine

interferon gamma (INF γ) did not induce expression of mCLCA3. Similar results were found using an allergic asthma mouse model of ovalbumin (OVA) sensitization. Induction of mCLCA3 was found in the lung and bronchi in normal mice after OVA challenge (Nakanishi, Morita et al. 2001). Subsequent adenoviral gene transfer with an antisense mCLCA3 construct suppressed the pathology of the allergic asthma through prevention of airway hyperresponsiveness (AHR) and mucus overproduction. When this same model was treated with a sense mCLCA3 mRNA construct there was severe AHR and mucus production (Nakanishi, Morita et al. 2001). *In vitro* over-expression of mCLCA3 or its closest human orthologue hCLCA1 in human mucoepidermoid cells (NCI-H292) resulted in overall increased mucus secretion, as well as over-expression of the major secretory mucin gene of asthma, MUC5AC (Hoshino, Morita et al. 2002). Similar results were found in the asthmatic patient, with an increase in hCLCA1 that correlated with an increase in mucus and IL-9 receptor (Hoshino, Morita et al. 2002) (Toda, Tulic et al. 2002) (Figure 1.4).

Most current asthma treatment is focused on leukocytes and airway smooth muscle hyper-responsiveness. The identification of relationships between the function of hCLCA1 as a chloride channel regulator, and its integral role in mucus production in the asthmatic airway are of considerable interest. This relationship suggests that hCLCA1might be a potential therapeutic target in patients suffering from asthma.

Exposure of human bronchial epithelial cells to Th2 cytokines, interleukins 13 or 4, greatly increases the magnitude and duration of activated calcium-dependent chloride conductance (Danahay, Atherton et al. 2002; Atherton, Jones et al. 2003). This group of cytokines has an overall tendency to switch epithelial transport from net

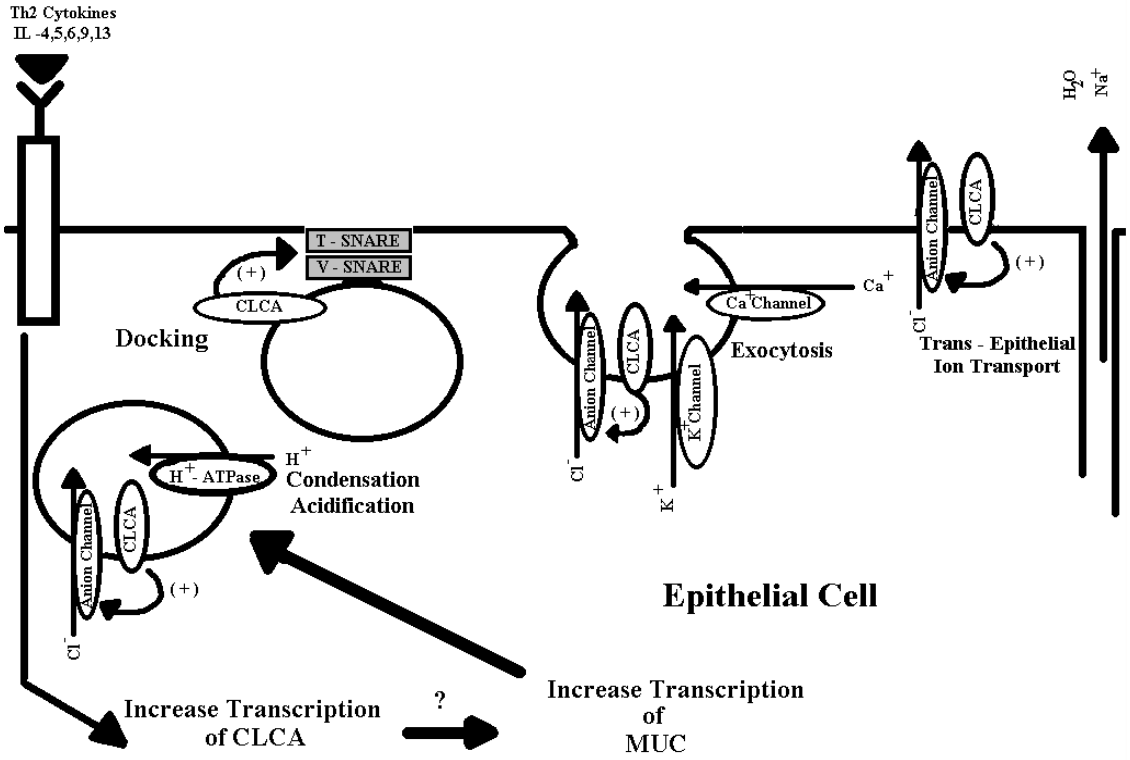

Figure 1.4. Hypothetical roles for CLCA protein in the asthmatic airway. Increased expression of CLCA is presumably cytokine-driven. CLCA could then (1) increase the transcription or translation of MUC genes; (2) Increase the transport of mucin to the plasma membrane by increasing the condensation (packaging process) by acidification of the mucin granule; (3) Take part in the membrane fusing process by interaction with the SNARE apparatus; (4) Facilitate the ion transport component of the exocytosis process. CLCA protein may also have a role in increasing net ion/fluid transport (increasing chloride conductance and decreasing sodium absorption) to the inflamed epithelium to increase mucus transport up the mucociliary ladder.

absorption to a secretory phenotype. This is accomplished by decreasing sodium absorption and increasing apical chloride conductance. It is hypothesized that inflammation may trigger this phenotypic switch as an evolved response to flush particulate and secreted mucus out of the airway. An excellent model for this strategy exists in pseudohypoaldosteronism, where increasing the secretion by decreasing absorption significantly increases the rate of mucociliary clearance (Kerem, Bistritzer et al. 1999; Bistritzer, Kerem et al. 2002; Danahay, Atherton et al. 2002).

A functional increase in calcium-activated chloride conductance has been reported in airway hyper-responsiveness (AHR). The pharmacologic sensitivity of this induced chloride conductance is similar to that reported for CLCA-stimulated conductance (Danahay, Atherton et al. 2002; Atherton, Mesher et al. 2003). There is no direct evidence connecting CLCA induction with the Th2 cytokine-mediated increase in Ca^{2+}-activated chloride conductance, but CLCA could have a dual function to connect and co-ordinate these two events. Increases in epithelial mucus production generate a need to increase the clearance of the mucus through increased local fluid secretion from the epithelium.

If CLCA proteins can modulate Ca^{2+}-activated chloride channels, then an increase in Ca^{2+}-activated chloride conductance should accompany the induction of increased CLCA expression by inflammatory mediators. Linkages between CLCA protein and mucus secretion are less clear. It is obvious from previous studies that inhibiting CLCA expression inhibits mucus production (Nakanishi, Morita et al. 2001). The identification of mCLCA3 expression in mucin granules membranes of the respiratory and gastrointestinal tract implicates this protein in mucin storage or release

(Leverkoehne and Gruber 2002). It was suggested that mCLCA3 is needed for mucin maturation. Negatively charged mucus glycoproteins require strong acidification for mucin condensation in the granules. Granule acidification could occur via a H^+-ATPase with electroneutrality maintained by a parallel CLCA-modulated chloride conductance (Verdugo 1991; Espinosa, Noe et al. 2002; Leverkoehne and Gruber 2002; Thevenod 2002). Potassium release and Ca^{2+} entry into the vesicles may also be important in the condensation process (Espinosa, Noe et al. 2002; Thevenod 2002).

CLCA proteins could also participate in mucus secretion by promoting rehydration of condensed mucins or by connecting mucin granule docking proteins with the proteins of exocytosis. Upon stimulation, the mucin granules dock and fuse with the plasma membrane though a process involving two classes of Ca^{2+}-dependent and independent docking fusion proteins called the soluble N-ethylmaleimide-sensitive factor attachment protein (SNARE). The V-SNARE (synaptobrevin) proteins are on the vesicle and T-SNARE (syntaxin and SNAP-25) proteins on the plasma membrane (McNew, Parlati et al. 2000; Parlati, McNew et al. 2000). Families of V- and T-SNAREs share motifs for binding interactions, allowing appropriate fusion to the correct membrane (Li, Low et al. 2002; Weimbs, Low et al. 2003). SNARE machinery permits fusing granules to form a pore through the cytoplasmic membrane. The mucin is released through this pore upon its rehydration by influx of extracellular solution through the pore, as well as by controlled ionic flux through granule membrane from the cytosol (Thevenod 2002). CLCA protein could mediate the ion transport required for mucin rehydration through the vesicle membrane during exocytosis (Figure 1.4.).

If modulation of chloride conductance by CLCA proteins is involved in mucin secretion, then inhibition of chloride conductance could be an interesting anti-asthma strategy. Zhou et al. have shown that putative inhibitors of the chloride conductance associated with CLCA protein expression can inhibit mucus secretion (Zhou, Shapiro et al. 2002). However, on closer examination, the putative inhibitors were found to inhibit calcium entry into the epithelial cells, independent of a chloride channel blockage effect (Bertrand, Danahay et al. 2003). It was determined that the mechanism for niflumic acid interference with mucin exocytosis involved blocking Ca^{2+} entry, rather than chloride conductance. Calcium ion entry is central to the process of mucin exocytosis, triggering activation of the SNARE complex (Bertrand, Danahay et al. 2003). Unfortunately this finding does not clarify the role for CLCA protein in the regulatory mechanisms for mucin secretion. The answer to this puzzle may lie in a better understanding of the ability of CLCA proteins to modulate chloride channel activity.

1.6.2. CLCA - Role in Cystic Fibrosis

Cystic fibrosis disease affects most if not all secretory epithelial tissues in the body. The fundamental cause of this disease is dysregulation of epithelial ion transport (Matsui, Grubb et al. 1998; Matsui, Davis et al. 2000). CLCA expression in secretory epithelial cells and its function as a modulator of chloride conductance makes it a secondary focal point, after CFTR, in investigating possible compensatory mechanisms for defective epithelial ion transport. (Gaspar, Racette et al. 2000; Loewen, Bekar et al. 2002; Loewen, Gabriel et al. 2002; Loewen, Smith et al. 2003; Loewen, Bekar et al. 2004).

1.6.2.1. CLCA in the Normal Epithelium

In a normal epithelium the electrical driving force for the chloride ion transport that is modulated by CLCA proteins comes from coupling the hydrolysis of ATP to the inward transport of 2 K^+ ions and the outward transport of 3 Na^+ ions by the basolateral $3Na^+/2K^+$ ATPase, (Kirk, Halm et al. 1980; Klaassen and Depont 1994; Lewis 1996). This vectoral cation transport results in an inwardly-directed Na^+ concentration gradient that drives the electroneutral entry of Na^+, K^+ and Cl^- into the cell through the basolaterally-located Na^+-K^+-$2Cl^-$ cotransporter (O'Grady, Musch et al. 1986; O'Grady, Palfrey et al. 1987). The charge separation provided by the stoichiometry of the $3Na^+/2K^+$ ATPase and the basolateral K^+ conductance lowers the resting membrane potential, creating a driving force for chloride to exit the epithelial cell through CLCA-modulated anion conductance channels in the apical membrane (Lewis 1996; Cotton 2000; Loewen, MacDonald et al. 2000; Loewen, Bekar et al. 2002; Loewen, Gabriel et al. 2002; Loewen, Smith et al. 2003; Loewen, Bekar et al. 2004). Sodium follows paracellularly to maintain electrical neutrality, resulting in a secretory epithelium. However, a decrease or loss of the apical chloride conductance can cause sodium to be drawn back into the cell by the electro-chemical gradient created by the $3Na^+/2K^+$ ATPase, making the epithelium absorptive. Chloride then follows the sodium movement across the cell (Willumsen and Boucher 1989; Willumsen, Boucher et al. 1989).

1.6.2.2. CLCA in the Diseased CF Epithelium

The CLCA orthologues have a modulatory role on the normal transepithelial sodium chloride transport which is defective in the genetic disease of cystic fibrosis (Matsui, Grubb et al. 1998; Loewen, MacDonald et al. 2000; Matsui, Davis et al. 2000; Loewen, Bekar et al. 2002; Loewen, Gabriel et al. 2002; Loewen, Smith et al. 2003; Loewen, Bekar et al. 2004). The genetic abnormality in transport is caused by a mutation in the cystic fibrosis conductance regulator (CFTR). CFTR has two major functions relevant to the status of fluid movement across secretory epithelia (Figure 1.5.). It is the major apical chloride transporting channel of epithelium and it down-regulates the activity of the apical absorptive sodium channel in epithelium (ENaC) (Kunzelmann, Kathofer et al. 1995; Stutts, Canessa et al. 1995). The commonest mutation in CFTR causing clinical disease involves the deletion of the codon specifying a phenylalanine residue at position 508 (F508) (Kerem, Rommens et al. 1989; Riordan, Rommens et al. 1989). CFTR molecules lacking residue F508 can function normally, but their transport through the normal maturation pathway of the ER and Golgi is interrupted, and very little F508 CFTR protein is found in the cytoplasmic membrane (Cheng, Gregory et al. 1990). Diminished numbers of CFTR molecules at the apical membrane of secretory tracheal epithelial cells decreases the production of airway surface liquid (ASL), the thin film of fluid covering the luminal aspect of airway epithelial cells (Matsui, Grubb et al. 1998). This lack of CFTR also indirectly increases salt and fluid absorption via the loss of normal negative effects of CFTR on sodium absorption by ENaC. The resulting reductions in the ASL volume (Cotton, Stutts et al. 1987; Matsui, Grubb et al. 1998) increase the viscosity of airway mucus, decrease

mucocilliary clearance, and favor bacterial colonization of the mucosal surface (Lyczak, Cannon et al. 2002; Pier 2002).

It has been suggested that activation of an alternative chloride channel in the apical membrane of CF epithelium could compensate for the lack of CFTR. It is very likely that CLCA would have a modulatory effect on such an alternative channel given its effects on both cAMP and Ca^{2+}-activated chloride conductance (Gruber, Elble et al. 1998; Loewen, Bekar et al. 2002; Loewen, Gabriel et al. 2002; Loewen, Smith et al. 2003; Loewen, Bekar et al. 2004). This situation may occur in the CFTR knockout mouse where up-regulation of a Ca^{2+}-activated chloride channel appears to protect against lung pathology (Snouwaert, Brigman et al. 1992; Grubb, Vick et al. 1994; Gabriel, Makhlina et al. 2000; Thomas, Gabriel et al. 2000; Tarran, Loewen et al. 2002). This Ca^{2+}-activated chloride channel is also found in human CF patients, but it lacks sufficient activity to maintain normal ASL hydration and prevent disease (Boucher, Cheng et al. 1989) (Willumsen and Boucher 1989; Anderson and Welsh 1991). Activation of this channel through purinergic receptors has been explored as a potential therapy for CF patients (Clarke and Boucher 1992; Yerxa, Sabater et al. 2002). However, activation of a Ca^{2+}-dependent chloride conductance does not replace the inhibitory effects of CFTR on ENaC, and persistent sodium absorption continues to contribute to ASL dehydration and potential airway pathology (Cotton, Stutts et al. 1987; Matsui, Grubb et al. 1998). The role of CLCA proteins in cystic fibrosis disease is unclear. Both hCLCA1 and Ca^{2+}-activated chloride conductance have been shown to be increased in the CF airway (Boucher, Cheng et al. 1989; Willumsen and Boucher 1989; Anderson and Welsh 1991; Clarke and Boucher 1992; Hauber, Manoukian et al. 2003).

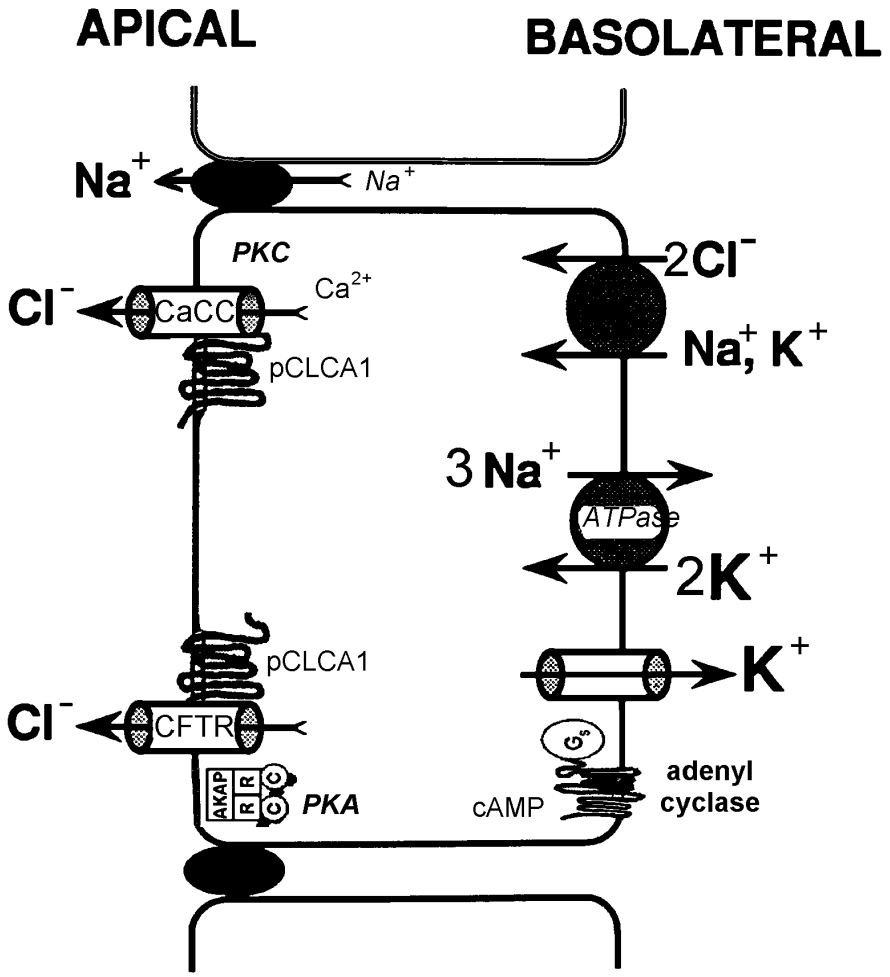

Figure1.5. Possible roles by which a CLCA protein (pCLCA1) could contribute to epithelial ion transport in the CF patient. Modulation of apical chloride conductance by CLCA protein interactions may have beneficial effects on ion transport in the CF patient. Beneficial mechanisms would occur through increasing the activity of CaCC or promoting proper CFTR trafficking.

Enhanced CLCA activity could have beneficial effects by interacting with other proteins to increase apical chloride conductance, and reduce the net absorptive flux, if not actually switching the diseased epithelium to a net secretory state. This could be an effective strategy, as CLCA proteins have been shown to significantly increase both endogenous Ca^{2+}-activated and cAMP-activated chloride conductance (Loewen, Gabriel et al. 2002; Loewen, Bekar et al. 2004) (Figure 1.5).

However, the involvement of hCLCA1 in mucus secretion must be considered when contemplating attempts to upregulate CLCA activity in CF patients. It is even possible that elevations in hCLCA1 expression in CF patients could be detrimental by contributing to mucus over-production and airway obstruction. Parallels have been drawn between elevated levels of hCLCA1 expression in AHR in asthmatic patients and significantly increased hCLCA1 levels associated with the inflammatory processes of CF (Hauber, Manoukian et al. 2003). Agents such as niflumic acid that were thought to inhibit hCLCA1 conductance may be clinically beneficial through reduction of mucus production (Karkanis, DeYoung et al. 2003). Future efforts should be directed toward dissecting out desired effects of CLCA proteins on net fluid secretion from less appropriate stimulation of mucus secretion, since the effects of niflumic acid may not be mediated through inhibition of the chloride conductance of hCLCA1 (Bertrand, Danahay et al. 2003). However, it is also possible that an obligatory linkage between the modulation of chloride conductance by CLCA proteins and stimulatory effects of CLCA proteins on mucus secretion may be so close as to render CLCA useless as therapeutic target.

1.6.3 Oncologic Importance of CLCA

Orthologues of the CLCA gene family have been shown to play two seemingly contradictory roles in cancer metastasis. Within the transformed cell, CLCA functions as a tumor suppressor, likely through its modulation of ion transport. Expression of CLCA protein is usually lost in tumor cell lines (Gruber and Pauli 1999c; Elble and Pauli 2001; Li, Cowell et al. 2004). However, tumor cells which have lost CLCA expression then bind endothelial-expressed CLCA via a novel endothelial CLCA/β_4 tumor cell adhesion which results in intravascular metastatic arrest and a mitogenic signal for intravascular tumor growth followed by tissue invasion(Zhu and Pauli 1991; Zhu, Cheng et al. 1992; Zhu and Pauli 1993; Abdel-Ghany, Cheng et al. 2001; Abdel-Ghany, Cheng et al. 2002; Abdel-Ghany, Cheng et al. 2003).

1.6.3.1. CLCA Tumor Supressor

1.6.3.1.1. CLCA Tumor Suppressor is Lost in Tumorigenic Cell Lines

One piece of evidence that CLCA has tumor suppressor properties is its loss in tumorigenic cell lines (Gruber and Pauli 1999c; Elble and Pauli 2001; Li, Cowell et al. 2004). Two studies from the same group have shown that CLCA2 (mCLCA2 or hCLCA2) expression has a significant impact on *in vivo* and *in vitro* growth of tumor cells (Gruber and Pauli 1999c; Elble and Pauli 2001). An initial study demonstrated non-tumorigenic breast epithelial cells (MCF10 A and MDA-MB-453) expressed hCLCA2. Transformed tumorigenic cells lines (MDA-MB-231, MDA-MB-435, MDA-MB 468 and MCF7) however did not (Gruber and Pauli 1999c). This lack of hCLCA2 expression was not caused by a genomic deletion. PCR amplification confirmed the

presence of the promoter region and the CLCA2 gene in the chromosomal region 1p22 - 31 to which the CLCA gene family has been mapped. This loss of CLCA2 expression in tumorgenic cell lines was due to transcriptional down-regulation of the gene or abnormal RNA processing (Gruber and Pauli 1999c; Li, Cowell et al. 2004). Intron/exon junction information in mCLCA2 transcripts was used to identify PCR products of mCLCA2 cDNA from JC and CSML-0 adenocarcinoma cell lines as splice variants rather than genomic deletions (Elble and Pauli 2001). However, mCLCA1 is also normally expressed in mammary tissue, and mCLCA1 transcripts were not found in these tumor cells, suggesting disrupted expression at the promoter level in the tumor (Elble and Pauli 2001; Li, Cowell et al. 2004).

Cell migration through 8 μm pore polycarbonate membranes of a chemotaxis chamber measures potential cell invasiveness. Reintroducing CLCA2 into these tumorigenic cell lines significantly reduced migratory ability in MDA-MB-435 cells, a line with low migratory ability, but only slightly reduced it in MDA-MB-231 a cell line with high migratory ability. Both transfected cell lines had significantly reduced *in vitro* invasion through a film of Matrigel in a chemotaxis chamber (Gruber and Pauli 1999c). CLCA2 expression did not change growth rate or anchorage-independent growth of these cells in soft and hard agar. Transfection of MDA-MB1-231 cells with a vector expressing mCLCA2 significantly reduced the number of animals with tumors, and reduced tumor size in subcutaneously injected nude mice when compared to control MDA-MB-231 inoculates (Gruber and Pauli 1999c). Similarly, mice receiving intravenous MDA-MB-231 cells transfected with CLCA2 had no tumors or significantly fewer tumors in their lungs when compared with mice receiving MDA-

MB-231 control cells which usually died within 8 weeks. Unfortunately, *in vitro* decreases in invasiveness and migration as indicators of tumor transformation/metastic potential, without changes in growth rate or anchorage-independent growth, do not totally account for the loss of tumorigenicity in this study. An undetermined phenotypic effect of CLCA in relation of cell differentiation still needs to be defined.

Subsequent studies by an independent group confirmed the relationship between loss of hCLCA2 expression and tumorigenicity, and the authors provide titillating evidence that hCLCA2 is the product of the hitherto unidentified 1p31 breast cancer tumor suppressor gene. They identified hypermethylation of the CLCA promoter region to be the major mechanism for loss to expression of CLCA in tumorgenic cells (Li, Cowell et al. 2004).

1.6.3.1.2. CLCA and Cell Cycle Tumor Suppression

The mechanism of CLCA tumor suppressive effects have not been fully worked out. However, there is a growing body of evidence showing that the activity of both anion channels which are modulated by CLCA, and independent cation channels have a significant impact on cell cycle control(Kim, Kang et al. 1999; Wohlrab and Markwardt 1999; Malhi, Irani et al. 2000; Loewen, Bekar et al. 2002; Loewen, Gabriel et al. 2002; Kim, Kang et al. 2003). Blockage of potassium conductance in a variety of cell types results in reduced cellular proliferation and synchronization at G0/G1 of the cell cycle (DeCoursey, Chandy et al. 1984; Nilius and Wohlrab 1992; Woodfork, Wonderlin et al. 1995; Wang, Melkoumian et al. 1998; Wohlrab and Markwardt 1999; Malhi, Irani et al. 2000). Decreasing chloride conductance causes the opposite effect, increasing cell

proliferation and protecting from apoptotic death (Deane and Mannie 1992; Wilson and Chiu 1993; Wohlrab and Markwardt 1999; Kim, Kang et al. 2003). The cell cycle-specific chloride current was found to be highest during G1 and lowest during S phase (Villaz, Cinniger et al. 1995; Ullrich and Sontheimer 1997). If stimulatory effects of CLCA on chloride conductance contribute to these currents, then CLCA expression or activity could be significantly down-regulated in tumorgenic cell lines, and activation of this channel modulator could be a novel strategic approach to suppressing growth of transformed cells (Gruber and Pauli 1999c; Kim, Kang et al. 1999; Elble and Pauli 2001; Kim, Kang et al. 2003).

1.6.3.1.3. CLCA Over-Expression May Affect Cell Cycle

Aberrant cell morphology found with mCLCA2 over-expression has been interpreted as strong supporting evidence for CLCA modulation of cell cycle. The over-expressing cells tended to be larger and multinucleated (Elble and Pauli 2001). It is interesting that previous studies did not reveal this morphology problem, but the level of expression of the mCLCA2 protein may be important. The morphological differences could be a consequence of abnormalities in cell cycle control (Elble and Pauli 2001). If inappropriate amounts or timing of CLCA expression affect chloride channel activity it could disrupt the intricate depolarization and polarization accompanying the cell cycle. Any resulting blockage at one specific point in the cell cycle could cause abnormal morphology. Multinuclear giant cells are associated with the disruption of many cellular pathways leading to arrest at various points in the cell cycle (Murray 1994). However, specific cell cycle studies have not yet been done.

1.6.3.1.4. CLCA Proapoptoic Tumor Supression

CLCA2 could be suppressing tumor growth through proapoptotic effects (Gruber and Pauli 1999c). CLCA2 expression could create a permissive environment or tip the balance towards apoptosis if cells receive the correct signal. This would explain the absence in changes in growth rate or anchorage-independent growth in culture conditions where the cellular environment did not favor apoptosis. This hypothesis was illustrated by a study which found that transfection of the mammary epithelial cell line HC11 with mCLCA2 significantly increased the rate of apoptosis when subjected to serum starvation compared to a control cell (Elble and Pauli 2001). Additionally, if the HC11 cell line which is not normally tumorgenic is selected for resistance to detachment-induced apoptosis (anoikis), mCLCA1 message was lost and mCLCA2 was assumed to be aberrantly spliced and not functional. These cells are then tumorigenic when injected into mice (Elble and Pauli 2001). It was also interesting that cells transfected with mCLCA1 or mCLCA2 and selected by resistance to Zeocin all died within a four-week period (Elble and Pauli 2001). However, this slow growth and death was not found in the original study of stable transfectants selected and maintained with G418 (Gruber and Pauli 1999c). This difference may be due to the distinct mechanisms of the selective drugs. Zeocin is an antibiotic in the bleomycin family. It causes cell death by intercalating into, and cleaving, DNA (Ghosh, Mendoza et al. 2002; Mekid, Tounekti et al. 2003). This type of stress activates the p53 apoptotic pathway and, at higher doses, independent pathways. G418 or Geneticin binds to the 80S ribosome and prevents protein synthesis in eukaryotic cells without directly inducing apoptosis. This means that Zeocin-selected, but not G418-selected cells, are always fighting apoptosis.

Combining this stress with proapoptotic effects of hCLCA2 could account for poor growth and increased apoptosis seen with Zeocin and not G418.

1.6.3.1.5. CLCA's Proapoptotic Mechansim

This information brings up an important question. How do the effects of CLCA protein on anion conduction result in proapoptotic responses? A number of reports have shown that blockage of chloride conductance increases cell proliferation and confers protection from apoptotic death (Gottlieb and Dosanjh 1996; Szabo, Lepple-Wienhues et al. 1998; Wohlrab and Markwardt 1999; Kim, Kang et al. 2003). Generally, there is an influx of calcium in the initial stages of apoptosis which activates both potassium and chloride channels (Orrenius, Zhivotovsky et al. 2003). One possible apoptotic scenario would have increasing potassium conductance hyperpolarizing the cell, increasing the driving force for anion conductance through the already open calcium-activated chloride channel. Then intracellular pH could be lowered by bicarbonate exiting through the anion conducting channel. A reduction in the intracellular pH would increase the activity of caspase 3, cause destruction of DNA and trigger an apoptotic cascade (Segal and Beem 2001). Expression of CLCA could activate anion conductance to stimulate the exit of bicarbonate or chloride, resulting in a larger number of cells entering the apoptosis cascade.

1.6.3.2. CLCA in Metastasis

1.6.3.2.1. CLCA is a Cell Adhesion Molecule for Lung Tumor Metastasis

The bCLCA2 (Lu-ECAM-1) orthologue was originally cloned with an antibody which blocked the adhesion-receptor/ligand pair that mediates binding of lung metastatic melanoma cells to bovine aortic endothelial cells (Zhu, Cheng et al. 1991; Zhu and Pauli 1993; Goetz, el-Sabban et al. 1996; Elble, Widom et al. 1997). The origins of this clone led to the hypothesis that CLCA was the molecular identity of the endothelial adhesion molecule to which spreading hematogenous tumor cells bound, resulting in vascular arrest before tumor growth and invasion. Studies involving human tissue identified hCLCA2 as the human counterpart to the original bCLCA2 (Lu-ECAM-1) clone (Abdel-Ghany, Cheng et al. 2001) Like bCLCA2, hCLCA2 is expressed by endothelial cells from different lung vascular compartments (Zhu and Pauli 1991; Abdel-Ghany, Cheng et al. 2001). This expression was found to be paramount for the establishment and colonization of human breast cancer cell lines (Abdel-Ghany, Cheng et al. 2001).

1.6.3.2.2. CLCA Binds Only Lung Colonizing Tumorigenic Cell Lines *in vitro*.

Only hematogenous lung colonizing tumorigenic cells where able to bind to HEK293-hCLCA2 expressing cell lines (Abdel-Ghany, Cheng et al. 2001). The MDA-MB-231 cell line, which colonizes the lungs of nude mice following intravenous injection, would bind at a 75% efficiency to a hCLCA2 expressing monolayer of HEK 293 cells (Abdel-Ghany, Cheng et al. 2001)

Cell lines such as MBA-MB-435 which only form metastases after orthotopic tumor xenografts and are unable to form metastasis on IV injection, or MCF 7 cell lines which are not tumorigenic only bound at ~ 4 and 7 % respectively to HEK 293 hCLCA2 expressing monolayers (Abdel-Ghany, Cheng et al. 2001). This evidence suggests that hematogenous metastastsis and lung colonization is dependent on the ability of the tumor cell line to bind to CLCA.

1.6.3.2.3. CLCA Binds to β_4 integrin in Tumorigenic Cell Lines

The nature of the ligand in the tumorigenic cell lines that binds to CLCA proteins was determined using hCLCA2-myc constructs expressed in HEK 293 cells. MDA-MB-231 cells were biotinylated, then bound to hCLCA2-myc expressing HEK293 cells. The bound cells were harvested together and immunoprecipitated with anti-myc antibody. Anti-streptavidin-HRP identified a single band of 205 kDa on Western blotting. Subsequent probing with specific antibodies identified the immunoprecipitated band as β_4 integrin, and confirmed that it had indeed co-precipitated with hCLCA2 (Abdel-Ghany, Cheng et al. 2001).

The direct binding of hCLCA2 to β_4 integrin was also demonstrated in a far Western blot of the β_4 integrin cell lysate with myc-hCLCA2 construct and anti-myc antibodies (Abdel-Ghany, Cheng et al. 2001).

1.6.3.2.4 β_4 integrin Expression Correlates With CLCA Binding and Metastasis in Tumorigenic Cell lines

In further studies involving additional cancer cells lines which expressed different levels of β_4 integrin, there was a strong correlation between the level of β_4

integrin expression and the adhesion of HEK 293 cells expressing hCLCA2. A similar correlation was observed *in vivo* between β_4 integrin expression in tumorigenic cell lines, and the number of lung metastases observed in nude mice given the different cells.

Similarly, in syngeneic animals using integrin Kirsten-Ras-transformed Balb/3T3 oncogenic cell line with induced over-expression of β_4 integrin, there was an increase in adhesion of these cells to mCLCA1 as well as an increase in the number of metastatic colonies in the lung found on induction. It should be noted that location of the metastases is consistent with reported sites of mCLCA1 expression in the mouse. This result provides more evidence that β_4 integrin binding to CLCA is important for hematogenous metastasis.

Antibodies to either β_4 integrin or hCLCA2 were able to inhibit binding of the hCLCA2-expressing HEK 293 cells to the MDA-MB-231 cell line. The binding to hCLCA2 expressing cells was found to be specific for β_4 integrin, as antibodies directed to other integrins did not affect binding. Additionally, specific cleavage of β_4 integrin on the cell surface with matrilysin greatly reduced binding. The importance of the interaction between the two proteins in hematogenous metastasis was confirmed by using antibodies to hCLCA2 and β_4 integrin injected concurrently in the nude mouse model. This treatment greatly reduced lung metastases by 84 % and 100 %. The ability of hCLCA2 and β_4 integrin to interact in a far Western blot, as well as inactivation of the binding process with cleavage of β_4 subunit indicates that the associated α_6 integrin subunit, which β_4 usually associates with *in vivo* to bind to laminin, is not needed for this binding interaction process to occur (Abdel-Ghany, Cheng et al. 2001).

1.6.3.2.5. CLCA / β_4 Integrin Binding Not Sufficient for Tumorigenesis in Non-tumorigenic Cell lines

Although CLCA/β_4 integrin binding is need for lung metastasis to occur, there are undefined molecular events which must be in place before tumorigensis can occur (Abdel-Ghany, Cheng et al. 2001). Cell lines which are not tumorigenic and were selected for β_4 expression or transfected with β_4 had increased binding to CLCA but did not result in increased lung colonization (Abdel-Ghany, Cheng et al. 2001).

Specifically, the MDA-MB-435 cell line has a low level of endogenous β_4 integrin expression. When this cell line was transfected to overexpress β_4 integrin, the adhesion of the cells to hCLCA2 was increased compared to the untransfected cells. The adhesion levels in the over-expressing MDA-MB-435 cell line were similar to those in the MDA-MB-435 L2 line which was selected for over expression of β_4 integrin (Abdel-Ghany, Cheng et al. 2001). Interestingly, the over-expression of β_4 integrin in MDA-MB-435 cells increased adhesion to hCLCA2 *in vitro*, but did not cause increased lung colonization. This was unlike the correlative data obtained from metastatic cell lines whose colonizing abilities increase with the level of β_4 integrin. The authors attributed this discrepancy to the over-expressed β_4 integrin interacting with an intrinsic protein that would affect metastasis but not *in vitro* adhesion to hCLCA2 (Abdel-Ghany, Cheng et al. 2001).

. There is additional evidence that overexpression of β_4 integrin may be necessary, but not sufficient for metastasis. This is seen with β_4 integrin over-expression in the metastatically incompetent MDA-MB-468 cell line. This cell line had a relatively normal growth phenotype *in vitro*, and a slow adenomatous growth *in vivo*. Moderate

levels of β_4 expression in this cell line did not correlate with a lack of *in vivo* metastases for these cells. Apparently, β_4 integrin effects on metastasis are somewhat cell-type dependent. In general, β_4 integrin expression leads to lung metatasis only in those cancer cells which have the genotype of over-expression combined with down-regulation of the appropriate genes (Abdel-Ghany, Cheng et al. 2001).

It is possible that over-expressed β_4 integrin in the non-tumorgenic cell line is interacting with an unidentified membrane protein. This suggestion is supported by evidence of β_4 and α_6 integrins co-immunoprecipitating from the metatastic MDA-MB-231 cell line but not in the non-metastatic MDA-MB-435. When this cell line is transfected with, and over-expresses β_4 integrin (MDA-MB-435 β_4) it was found to have an increased adherence to hCLCA2 *in vivo*, but is unable to produce metastatic long colonies. Failure to co-immunoprecipitate β_4 and α_6 integrins may be the result of the β_4 integrin interacting with something other than its normal α_6 counterpart in the MDA-MB-435 β_4 cells. The unidentified protein could then exert a dominant negative effect on metastasis. It appears that the β_4 integrin is needed for binding to endothelium, and that the interactions between the α_6 and β_4 pair are required to promote metastasis (Abdel-Ghany, Cheng et al. 2001). Nonetheless, other groups have found that the β_4 integrin is central to increasing lung metastic performance and cDNA arrays have shown a definitive increase in β_4 integrin with increased metastatic potential (Abdel-Ghany, Cheng et al. 2001; Trusolino, Bertotti et al. 2001).

1.6.3.2.6. CLCA binds to β_4 Integrin Binding Though a Specific Domain

CLCA interaction with the β_4 integrin is mediated through a specific binding domain that favors the association of these proteins. β_4 integrin-binding motifs are present in both the 90 and 35 kDa subunits in most CLCA family members (Abdel-Ghany, Cheng et al. 2003). These binding domains belong to the addressins, which are distinct vascular addresses used by both immune and blood borne cancer cells to colonize specific organs (Ruoslahti and Rajotte 2000). It is believed that cell binding in lung metastatic cancer is particularly mediated through binding of the β_4 integrin to the CLCA addressin (Abdel-Ghany, Cheng et al. 2003).

The binding motifs in the CLCA for the β_4 integrin protein have been identified and functionally demonstrated in both 90 and 35 kDa products of CLCA processing (Abdel-Ghany, Cheng et al. 2003). This was accomplished using a series of polypeptides encompassing the length of both the 90 kDa as well as the 35 kDa product. Antibodies which blocked β_4/CLCA adhesion were used to immunoprecipitate polypeptide fragments containing the potential binding motifs. These polypeptides were then used to coat microtitre plates and the binding of the β_4 integrin/metastatic cell line MDA-MB-231 cell was assessed. These assays generally identified an area which would be in the second extracellular domain of hCLCA2, bCLCA2 and mCLCA1, as defined by the proposed current topographical models (Gandhi, Elble et al. 1998; Gruber, Schreur et al. 1999). A computer-aided motif search found sequences at amino acids 479 to 488 in hCLCA2 which could account for the binding activity occurring in the 90 kDa fragment. A second binding motif was found at amino acids 740 to 749 in the 35 kDa segment (Abdel-Ghany, Cheng et al. 2003). Similar binding domains were

found in bCLCA2 and mCLCA1. F(S/N)R(I/L/V)(S/T)S is the general consensus sequence for the binding (Abdel-Ghany, Cheng et al. 2003). Both the 90 kDa and the 35 kDa motifs bound specifically to the β_4 integrin when expressed and purified, but not to β_1, β_3, fibronectin or BSA in ELISA and "pull-down assays". Adhesion was found to increase with concentration of ligand and was Mn^{2+} but not Mg^{2+} or Ca^{2+}-dependent. These purified binding motifs were also able to bind to lung-metastatic MDA-MB-231 cancer cells. Incubation of tumorigenic cells with purified binding motifs was found to significantly block lung colonization after intravenous injection of these cells into SCID/ beige mice and prevent binding (Abdel-Ghany, Cheng et al. 2003).

The β_4 integrin binding domain in hCLCA2 is not conserved in the hCLCA1 90 kDa segment, but is present in the hCLCA1 35 kDa segment. The sequence disruption in the 90 kDa was caused by the substitution of amino acids G473 A474 for SR resulting in the sequence FGALSS which lacks β_4 integrin binding activity (Abdel-Ghany, Cheng et al. 2003) (Abdel-Ghany, Cheng et al. 2003). Both β_4 integrin binding motifs are disrupted in pCLCA1 and mCLCA3 (Gob-5). The corresponding pCLCA1 90 kDa sequence is identical to that in hCLCA1 (FGALSS) and the 35kDa change is (FSRTAS). The mCLCA3 90 kDa 4 integrin binding domain region is changed to (FAALSS) and the 35kDa sequence is (FSRT(deletion)SS). The lack of conservation of these binding domains among major CLCA orthologues may be an indicator of significant functional divergence within the CLCA protein family (Figure 1.6).

As previously observed, there are two alternative models for the membrane topology of the CLCA proteins. Experimental evidence favors the presence of four

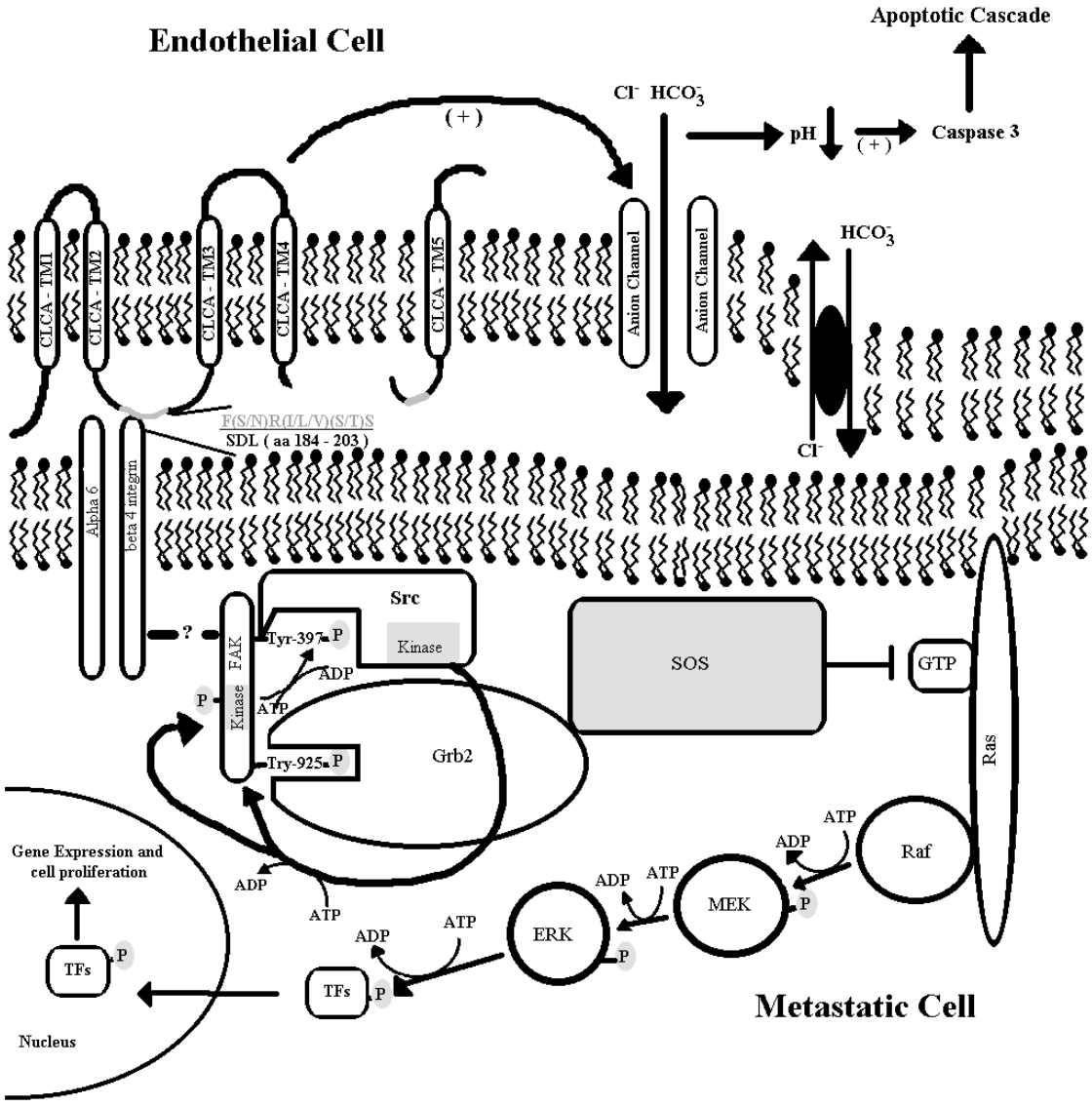

Figure 1.6. Mitogenic signal cascade induced by endothelial CLCA binding to β_4 integrin on metastatic cell. Note the absence of phosphorylation of the β_4 cytoplasmic tail and the dependence on FAK and Src for initiation of the signal transduction cascade. In addition, note the absence of activation of the PI3K pathway

transmembrane domains, where the 90 kDa β_4 binding domain would be located on an extracellular loop between TM2 and TM3. However, theoretical modeling based on integrin structure predicts a large extracellular von Willebrand's Factor A (VWA)-like domain in the hCLCA2 protein. If this VWA folding should occur, the 90 kDa β_4 binding motif would still be extracellular, but now it would be toward the C-terminal end of the folded VWFA domain. Hence the functional data arising from studies of CLCA protein binding to the the β_4 integrin do not resolve the issue of the two conflicting topologies.

1.6.3.2.7. Novel β_4 integrin binding domain binds to CLCA

The binding of CLCA to the β_4 integrin is mediated through a novel CLCA binding domain in the β_4 integrin (Abdel-Ghany, Cheng et al. 2001; Abdel-Ghany, Cheng et al. 2003)

Binding to the specificity-determining loop (SDL) was predicted, as this is a non-conserved loop sequence that has been associated before with ligand binding (Puzon-McLaughlin and Takada 1996; Takagi, Kamata et al. 1997). A short purified fusion protein, of β_4 segments, corresponding to the predicted loop of β_1 and β_3 integrins, found previously to be important in integrin binding, was constructed and tested to determine the binding domain (Takagi, Kamata et al. 1997). An area in the β_4 SDL sequence (amino acids 184-203) bound to CLCA in ELISA and pull-down assays. The same sequence from the β_1 integrin did not bind. The relevance of the binding to hCLCA2 was confirmed by using the synthetic peptide sequence of the β_4 loop to block

metastatic cell line adhesion of CLCA protein (Abdel-Ghany, Cheng et al. 2003) (Figure 1.6).

The binding of the β_4 integrin to laminin-5 has been attributed to a binding site at the N terminus of the SDL loop as determined by point mutations K177A and Q182L (Tsuruta, Hopkinson et al. 2003). However, as described above, the β_4 integrin to CLCA binding appears to involve the C terminal part of the SDL (Abdel-Ghany, Cheng et al. 2003). Hence it is likely that laminin-5 and hCLCA2 interact with different SDL binding motifs. This difference in interaction may explain the difference in the mitogenic pathways activated by β_4 integrin when binding to CLCA or laminin.

1.6.3.2.8. Mitogenic Signaling of CLCA /β4 Integrin Binding

As previously discussed, the binding of β_4 integrin to hCLCA2 is important for cell adhesion in the beginning stages of lung metastasis (Zhu, Cheng et al. 1992; Abdel-Ghany, Cheng et al. 2001). Once adhered, the tumor can either extravasate early, resulting in immediate tissue invasion, or it can undergo extensive intravascular growth. Extensive intravascular growth results in the tumor cells coming to occupy the entire circumference of the vessel lumen. The vessel wall disintegrates and the tumor progresses into the adjacent tissue (Vaage and Harlos 1987; Lapis, Paku et al. 1988) (Vaage and Harlos 1987; Lapis, Paku et al. 1988). It is the β_4 integrin/CLCA binding that provides the mitogenic stimulation important for intravascular growth (Abdel-Ghany, Cheng et al. 2001; Abdel-Ghany, Cheng et al. 2002) (Figure 1.6).

The signal cascade which results in intravascular tumor growth from the β_4 integrin/CLCA binding has been investigated (Abdel-Ghany, Cheng et al. 2002). Possible mitogen signal cascades from the β_4 integrin which have shown activation in

the past are the focal adhesion kinase (FAK), proline-rich tyrosine kinase-2 (Pyk2), and phosphatidylinositol 3 kinase (PI3K)(Schlaepfer, Hauck et al. 1999; Zhao and Guan 2000; Mercurio, Rabinovitz et al. 2001). When β_4-expressing B16-F10 cells are serum deprived and plated onto mCLCA1 coated dishes, only FAK was found to be significantly activated. A direct interaction was found between ligated mCLCA1/β_4 integrin and FAK, as FAK was only co-immunoprecipated with β_4 integrin ligated to mCLCA1. This interaction was dependent on mCLCA1/β_4 integrin ligation. It was assumed that complex formation between FAK and β_4 integrin results in the auto-phosphorylation of FAK (Abdel-Ghany, Cheng et al. 2002) (Figure 1.6).

1.6.3.2.9. A Novel β_4 Mitogenic Signaling Pathway

A model for the role of β_4 integrin in a mitogenic pathway has evolved over the past decade. Initial experiments revealed that laminin or antibody-induced ligation of the α_6 β_4 complex resulted in the Shc associating with a phosphotyrosine-containing β_4 subunit (Figure1.7). The adaptor protein Shc is then phosphorylated, which recruits Grb2 and potentially activates the ras MAP kinase pathway, through the recruitment of SOS (Mainiero, Pepe et al. 1995; Tsuruta, Hopkinson et al. 2003). The binding of Shc to β_4 also activates phosphoinositide-3-OH kinase (PI3K) through a yet undefined mechanism, which in turn activates Akt kinase resulting in phosphorylation of Bad as well as activation of oncogenic transcription factors and cell survival (Shaw, Rabinovitz et al. 1997; Tang, Nie et al. 1999; Gambaletta, Marchetti et al. 2000; Trusolino, Bertotti et al. 2001; Chung, Bachelder et al. 2002). Mutagenic studies of the β_4 cytoplasmic tail show that Shc preferentially bound to tyrosines 1440 and 1456 (Dans, Gagnoux-Palacios et al. 2001). The initial phosphorylation/activation of the β_4 integrin for Shc

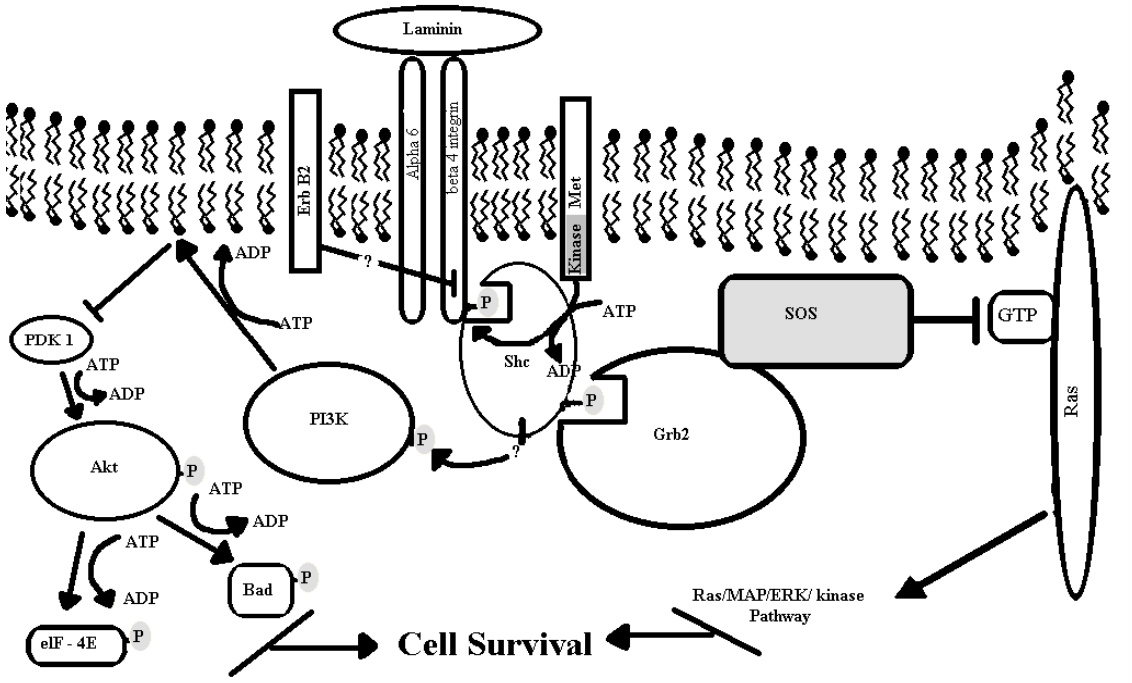

Figure 1.7. Accepted mitogenic signal transduction pathway from β_4 binding to laminin. Note the initial dependents of Met kinase and the direct phosphorylation of the β_4 or the Erb-B2 activation of the cascade. Also note the activation of the PI3 K/Akt pathway for cell survival. Additionally, the presence of Shc and the absence of Src and FAK should be noted in the activation of the Ras-MAP kinase pathway

binding is thought to be mediated in part through the Met tyrosine kinase of the receptor for the hepatocyte growth factor (HGF)(Trusolino, Bertotti et al. 2001). Similarly, the ErbB-2 receptor oncogene was found to mediate its effects through binding with the cytoplasmic tail of the 4 integrin and activation of the PI3K(Gambaletta, Marchetti et al. 2000) (Figure 1.7). Interestingly neither of these oncogenic effects required the extracellular domains of β_4 subunit. Thus, the β_4 subunit is acting more as a modulator of oncogenic signals. The events accompanying the initial phosphorylation during laminin or antibody binding of β_4, and release of its own mitogenic cascade, is still uncertain.

In comparison to the activation pathway described above, the binding of CLCA to the β_4 subunit is thought to initiate a novel signal transduction phosphorylation sequence (Figure 1.6). The CLCA-initiated cascade is described as Met, ErbB-2 independent, and not requiring phosphorylation of the cytoplasmic tail or Shc binding domain of the β_4 subunit for downstream signaling (Abdel-Ghany, Cheng et al. 2002). In additional there is no activation of PI3K (Abdel-Ghany, Cheng et al. 2002)

Instead, the CLCA pathway proceeds from CLCA binding with β_4 integrin to the aggregation of Focal adhesion kinase (FAK) with the β_4 cytoplasmic tail through a yet undetermined mechanism. The close association of FAK with β_4 results in autophosphorylation at tyrosine 397, causing the binding of Src, protein tyrosine kinase which then phosphorylates FAK at tyrosine 925. Phosphorylated FAK binds Grb2 and then recruits SOS, leading to the activation of the Ras-MAP kinase pathway involving extracellular signal-regulated kinase (ERK) (Abdel-Ghany, Cheng et al. 2002). A

similar pathway has been described in astrocytoma cells and the transforming growth factor-β-inducible gene h3 (Kim, Yun et al. 2003).

In addition to FAK, downstream Src kinase and ERK were also found to be activated (Abdel-Ghany, Cheng et al. 2002). ERK reached maximum activation slightly after FAK. However Src was constitutively activated in the tumor cell line. Antibodies which blocked the adhesion of mCLCA1 to β_4 integrin also blocked FAK and ERK activation.

The activation of FAK by the mCLCA1/ β_4 integrin complex was somewhat unique, as this activation was not seen when cells were grown on laminin which binds β_4 integrin. Transfection of the cell line with the dominant negative FAK (FANK) (a non-kinase FAK) blocked activation of ERK. Transfection with the wild type FAK significantly increased ERK activation upon ligation with mCLCA1 (Abdel-Ghany, Cheng et al. 2002).

The FAK-mediated activation of ERK was found to be Src dependent (Abdel-Ghany, Cheng et al. 2002) as the dominate negative FAKY397F did not allow phosphorylation, and reduced complex formation between Src and FAK. Impairing Src binding also impaired Src phosphorylation of FAK for growth factor receptor-bound protein (Grb) binding. Antibodies directed against α-Grb co-immunoprecipitated FAK but not FAKY397F, indicating that the activated Src must bind the autophosphorylated FAK at 397 and phosphorylate Y925 to allow Grb2 binding which then allows activation of ERK (Abdel-Ghany, Cheng et al. 2002).

Briefly, the binding of Grb 2 allows the translocation of Son of Sevenless (SOS) to the membrane to increase the guanine nucleotide exchange of Ras (Rozakis-Adcock,

Fernley et al. 1993; Downward 1996). GTP Ras has increased activity and activates the downstream mitogen-activated protein kinase pathways (MAPK) or Raf/MEK/ERK (Alberola-Ila and Hernandez-Hoyos 2003; Smalley 2003). In the GTP-bound state, Ras interacts with and activates Raf which phosphorylates MEK which in turn phosphorylates ERK which goes on to phosphorylate a number of transcription factors, activating the cell cycle and causing proliferation.

It is interesting to note that both dominant negative cell lines of B16-F10 melanoma cell produced as described above had greatly reduced lung metastatic potential (Abdel-Ghany, Cheng et al. 2002). This is evidence for the importance of CLCA contributions to this pathway of tumor metastasis. In addition, this CLCA-activated pathway may also be important in those metastases that undergo extravasation before growth because the ERK activation can also induce the production of invasive products such as metalloproteinase, and even increase drug resistance (Alberola-Ila and Hernandez-Hoyos 2003).

1.6.3.2.10. Tumor Invasion

Despite the activation of a cellular proliferation cascade there is little invasion into the actual organ until the vessel becomes filled with mammary tumor cells (Vaage and Harlos 1987; Lapis, Paku et al. 1988; Abdel-Ghany, Cheng et al. 2002). There almost seems to be a need to restrict some of the blood supply before tumor invasion occurs through the vasculature. It is also possible that β_4/mCLCA1 interactions may activate an endothelial chloride conductance which, as indicated previously, could tip the endothelial cell wall towards apoptosis cascade. The tumor could invade by first

filling the vessel and restricting blood supply to the endothelium which in turn, becomes slightly hypoxic, dropping the intracellular pH. The β_4/mCLCA1 could then participate in opening a channel to allow chloride entry, electrically balancing the hydrogen ion production and facilitating a rapid drop in intracellular pH (Figure 1.6). This pH drop would activate caspases and the apoptotic cascade (Brenner and Kroemer 2000; Segal and Beem 2001). The endothelial cells will die, and the tumor invades.

1.6.4. Mammary Gland Involution Different CLCA ortholgues are expressed at times times during the cycle of mammary gland development, lactation and involution. Most importantly this dynamic change is central for the the proper involution of the mammary gland.

1.6.4.1. Lactation

During late stages of pregnancy, high levels of estrogen, progesterone, prolactin and growth hormone cause increased growth of stroma, ductal systems, lobules, budding of alveoli and development of secretory characteristics in the cells of the alveoli (Nandi 1958; Neville, McFadden et al. 2002). Although growth promoting, the inhibitory effects of estrogen and progesterone on actual lactation are lost at parturition. The developed mammary tissue is maintained with only the somatic sensory/neuronal hormonal reflex of lactogenic prolactin and oxytocin surges at the time of nursing (Neville, McFadden et al. 2002).

The tissue CLCA isoform expression pattern in the mouse mammary gland quickly switches from mCLCA1 to mCLCA2 expression if this somato-sensory nipple stimulation is not maintained (Lee, Ha et al. 1999; Elble and Pauli 2001; Leverkoehne,

Horstmeier et al. 2002). This change in expression was used as the basis for obtaining the original mCLCA2 clone, which involved a suppressive subtractive process of lactating vs involuting mammary gland (Lee, Ha et al. 1999). Further investigation revealed that mCLCA1 was expressed primarily during lactation and mCLCA2 was expressed during the first stage of involution (Elble and Pauli 2001).

1.6.4.2. Involution

Mammary involution is generally divided into two phases (Lund, Romer et al. 1996). The first phase encompass the first three days after nursing has stopped. This involves the engorgement of the gland with milk which accumulates in the lumen of the ducts, and initial apoptosis of epithelial cells (Lund, Romer et al. 1996). It is believed that the stasis of milk causes distention of the alveoli leading to restricted blood flow from the increased pressure, and mechanical stress that causes a mild hypoxia (Jerry, Dickinson et al. 2002; Stefanon, Colitti et al. 2002). Both reduced mammary blood flow and increased positive alveolar pressure measured in the initial phase are thought to induce apoptosis (Fleet and Peaker 1978). In the initial stage, at a cellular level, there is strong activation of p53 apoptotic pathways and other apopotic factors (Lund, Romer et al. 1996; Jerry, Dickinson et al. 2002).

1.6.4.3. Involution and CLCA

It was found that mCLCA1 expression was lost in stage 1 of involution and mCLCA2 as induced at days 2 and 3 post-weaning. Expression of mCLCA2 then stopped on day 4, the beginning of the second phase of mammary involution, which involves the expression of stromal protease and the beginning of tissue remodeling

(Lund, Romer et al. 1996; Lee, Ha et al. 1999; Elble and Pauli 2001). The role which mCLCA1 and mCLCA2 play in the cycle of mammary development and involution is not fully understood.

The strong correlation between expression of mCLCA2 and the apoptotic intermediate Bax once again connects CLCA proteins to apoptotic tumor-suppressor activity. Studies from both serum-starved HC11 mammary tumor cell line and mammary tissue in the first stage of involution reveal an increase in expression of an apoptotic factor termed Bax (Elble and Pauli 2001; Jerry, Dickinson et al. 2002). The expression of Bax is usually, but not always upregulated by activated p53. Bax, in turn, stimulates the mitochondria to release cytochrome C which activate caspases-8 and -9. More caspase activation follows, causing selective destruction of cellular structure, organelles and genomic DNA (Brenner and Kroemer 2000). Interestingly, the cell line used in this study was p53 independent, indicating multiple apoptotic pathways for the involution phase (Abdel-Ghany, Cheng et al. 2002). The normally oncogenic STAT3 activation and its activation of leucine zipper CCAAT-enhancer binding protein (c/EBP delta) is an example of such multiple pathways in mammary gland apoptosis (Levy and Lee 2002; Kritikou, Sharkey et al. 2003) .

The factors that induce and maintain the apoptotic cascade through the initial phase of involution are not fully known. Many factors are involved and the CLCA proteins could play a role. It has been suggested that mCLCA2 is a constitutively activated form of mCLCA1 specializing in stress response (Elble and Pauli 2001). As previously indicated, factors such as CLCA proteins that activate anion conductance may help to push a cell into apoptosis (Kim, Kang et al. 1999). Participation of anion

conductance in cytoplasmic acidification can be important for the activation of caspases even in the presence of cytochrome c (Segal and Beem 2001).

1.6.4.4. CLCA's Possible Role in Milk Yield

Genetically selecting or pharmacologically manipulating CLCA ability to induce mammary gland apopotosis could have a significant impact on milk yield. During the normal cycle of lactation in the cow there is a gradual decline in mammary cell number occurring through a slight excess in the rate of apoptosis in relation to the production of new cells (Capuco, Wood et al. 2001). A similar situation is seen the goat, but not in the rat, where the decrease in milk yield through lactation is due to a reduced secretory capacity per cell (Knight, Docherty et al. 1984; Knight and Peaker 1984).

Thus, in the cow, an increased rate of cell replacement or decreased apoptosis during lactation may provide a means to increase persistency of lactation. Increasing cell replacement has shown to be a controversial yet economically viable option with the use of bovine somatotropin, which appears to increase the rate of cell renewal in the lactating mammary gland (Capuco, Wood et al. 2001; Baldi, Modina et al. 2002). However, decreasing the rate of apoptosis has not been a significant pharmacological target. Hydrocortisone was shown to inhibit involution, but it did not stop induction of the apoptotic cascade (Lund, Romer et al. 1996).

It is believed that the initial apoptotic cascade is induced locally by milk stasis within the alveoli (Jerry, Dickinson et al. 2002; Stefanon, Colitti et al. 2002). This is evident from the apoptotic changes in milked and non-milked glands on the same animal. It is then possible that part of the decline in lactation in the post-partum animal

may be due to induction of minor apoptosis via small periods of interruption in milk removal (Stefanon, Colitti et al. 2002). Thus, manipulation of CLCA2 function to decrease this minor apopotosis throughout lactation could have a significant impact in the total lactation yield of an animal.

1.6.5. CLCA Vascular Tone and Pathologies Orthologues of the CLCA gene family are expressed in vascular smooth muscle (Britton, Ohya et al. 2002; Elble, Ji et al. 2002; Leverkoehne, Horstmeier et al. 2002). CLCA has been shown to modulate Ca^{2+}-activated chloride conductance as well as interact with the subunits of the Ca^{2+}-activated potassium (BK) channel (Greenwood, Miller et al. 2002; Loewen, Gabriel et al. 2002; Loewen, Bekar et al. 2004). Both Ca^{2+}-activated chloride conductance and postassium conductance control vascular tone making a modulating protein such as CLCA a viable drug target in hypertension and erectile dysfunction.

1.6.5.1. Hypertension

Hypertension or an increased vascular tone in humans is defined as the mean arterial blood pressure being greater than 110 mm Hg. This usually results from the diastolic pressure greater than 90 mm Hg and the systolic pressure greater than 140 mm Hg (WHO 1999; Chobanian, Bakris et al. 2003; Fagard and Van den Enden 2003). Sustained increases in vascular tone can be very detrimental. Increased blood pressure is known contribute to the development of congestive heart failure due to an increased workload on the heart, and small renal hemorrhage causing renal failure. Hypertension

also predisposes to coronary artery disease and stroke (Chobanian, Bakris et al. 2003; Rashid, Leonardi-Bee et al. 2003).

Hypertension can result from, or be modulated through changes to the renin/angiotensin system (Chobanian, Bakris et al. 2003). The regulation of blood pressure begins with the rate of renal clearance of sodium by the glomerulus of the kidney. Renal clearance of sodium determines the amount of chloride presented to the macula densa, which determines the rate of the $Na^+K^+2Cl^-$ co-transporter in the macula densa (Schlatter, Salomonsson et al. 1989). Upon a decrease in the rate of the $Na^+K^+2Cl^-$ co-transporter, the macula densa then signals the juxtaglomerular cells, via a cyclooxygenase-2 inhibited process, to release renin (Greenberg, Lorenz et al. 1993; Cheng, Wang et al. 1999; Breyer and Harris 2001). Renin is converted to angiotensin I and angiotensin II in the lung. Angiotensin II is a vasoactive substance causing vasoconstriction and increased blood pressure through contraction of the smooth muscle of the vasculature, increased glomerular sodium chloride clearance, and increased activity of the $Na^+K^+2Cl^-$ co-transporter. These effects combine to cause a decrease in renin release (Harris and Breyer 2001). The release of aldosterone by angiotensin II also increases blood pressure by volume intake in the distal collecting duct of the kidney, which also increases glomerular sodium chloride clearance and decreases renin release. This system does permit modulation of vascular tone and its malfunction results in hypertension, but the actual etiology of most chronic hypertension is unknown (Watson 2003).

Hypertension is often treated by modulation of the renin-angiotensin system, either by blocking angiotensin receptors or preventing the conversion of renin to

angiotensin to decrease vascular tone (Chobanian, Bakris et al. 2003). An alternative to inhibiting agonists of hypertension would be to modulate vasoconstriction. This might be accomplished through manipulating the interplay of potassium, chloride, as in the case of CLCA, and calcium channels that regulate the membrane potential to determine the influx of calcium into the smooth muscle cell (Jackson 2000).

In smooth muscle, the equilibrium potential for chloride is more positive than the resting membrane potential, while the potassium equilibrium is more negative (Chipperfield and Harper 2000). The net result is that the opening of a chloride channel will result in depolarization of the membrane, whereas activation of a potassium conductance will result in hyperpolarization (Jackson 2000). Negative charges leave the cell upon chloride channel activation, resulting in membrane depolarization from ~ -60 mV to a chloride equilibrium potential of ~ -30 mV. This depolarization results in the activation of L-type calcium channels which permits an influx of Ca^{2+} that causes muscle contraction. Unlike the contraction in skeletal muscle, the majority of the Ca^{2+} for vascular smooth muscle contraction comes from the extracellular compartment after depolarization and activation of L-type Ca^{2+} channels (Nelson, Patlak et al. 1990; Hughes 1995). Simplistically, it is believed that the influx of Ca^{2+} ions binds calmodulin, resulting in a complex which activates myosin light chain kinase (Pfitzer 2001). The resulting phosphorylation of myosin allows myosin/actin cross-bridging and initiates the "ratchet theory" of contraction through the hydrolysis of ATP (Tyska, Dupuis et al. 1999; Kad, Rovner et al. 2003). Then the same Ca^{2+} which activates contraction also activates Ca^{2+}-activated potassium channels resulting in positive cations leaving, hyperpolarization and inactivation of L-type Ca^{2+} channels, stopping

muscle contraction (Nelson, Patlak et al. 1990; Chipperfield and Harper 2000; Jackson 2000).

Thus, an agonist-induced increase in potassium and decrease in chloride channel conductance in smooth muscle will result in muscle relaxation, vasodilation and hypotension. Conversely, an agonist that decreases potassium conductance or increases chloride channel conductance will cause muscle contraction, vasoconstriction and hypertension as is the case for angiotensin or norepinephrine (Figure 1.8.). This can be seen by the inhibition of norephephrine or angiotensin II-induced chloride conductance which significantly reduces smooth muscle contraction (Guibert, Marthan et al. 1997; Wang and Kotlikoff 1997). Given CLCA smooth muscle expression and the effects of CLCA expression on Ca^{2+}-activated chloride currents and molecular interaction with subunits of the BK potassium channel, it is likely that this gene family plays a part in agonist-induced smooth muscle contraction (Britton, Ohya et al. 2002; Elble, Ji et al. 2002).

The molecular mechanism of basal vascular tone is just beginning to be understood. The basal vascular tone is thought to be maintained by "calcium sparks" (Nelson, Cheng et al. 1995; Jaggar, Porter et al. 2000) which originate from a ryanodine-sensitive Ca^{2+} release channel in the sarcoplasmic reticulum (Jaggar, Porter et al. 2000). This Ca^{2+} release is only local and does not cause contraction. But it does result in the activation of the large-conductance Ca^{2+}-activated K^+ (BK) channels. This BK channel is made up of a pore-forming α-subunit and the β1 subunit that regulates its Ca^{2+}-sensitive activity (Amberg, Bonev et al. 2003). The importance of this subunit can be seen in rodent hypertensive models: β1 knockout mice were found to be

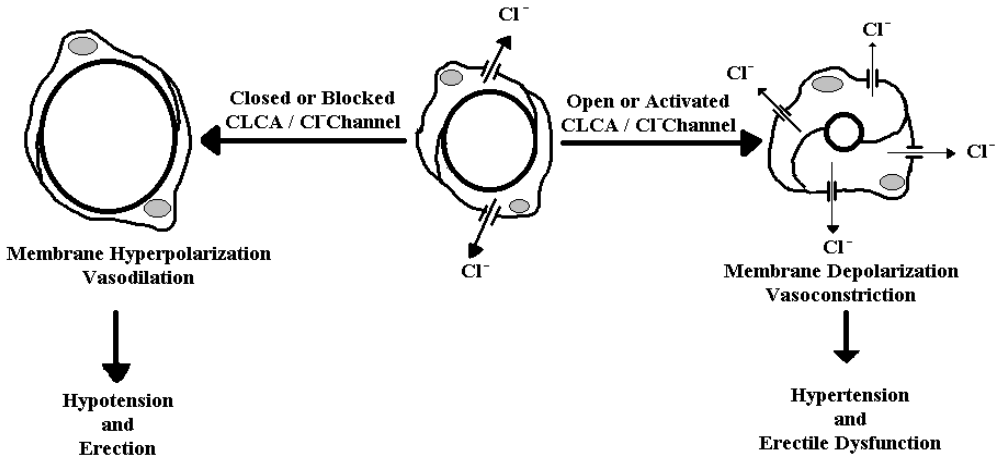

Figure 1.8. Physiological consequences of smooth muscle chloride channel activation or inactivation. Chloride channel activation results in membrane depolarization and smooth muscle contraction, whereas inactivation of chloride channels causes membrane hyperpolarization

hypertensive (Brenner, Perez et al. 2000). The β1 subunit expression was down-regulated in genetically hypertensive rats (Amberg and Santana 2003). In addition, where prolonged exposure to angiotensin II in the rodent model made the rats hypertensive, the rats were also found to down-regulate the β1 subunit (Amberg, Bonev et al. 2003). This down-regulation correlated with *in vivo* whole cell and single channel studies reporting a decrease in the channel sensitivity to Ca^{2+} (Amberg, Bonev et al. 2003).

Recent findings by two independent groups have implicated the CLCA gene family in vascular tone and in calcium sparks (Britton, Ohya et al. 2002; Elble, Ji et al. 2002). Both groups identified the expression of CLCA in the vascular smooth muscle of the mouse. Neither group's clones elicited whole cell recordings that are normally associated with the presence of Ca^{2+}-activated chloride channels of smooth muscle HEK 293 cells. However, mCLCA4 did result in expression of a Ca^{2+}-activated inward current (Elble, Ji et al. 2002). This would be consistent with the outward movement of chloride depolarizing the cell. This current was found to be non-rectifying and time independent. Similarly, the clone of mCLCA1 from murine portal vein was time-independent and only slightly rectifying upon stimulation by Ca^{2+} (Greenwood, Miller et al. 2002). These types of biophysical properties were not seen in smooth muscle cell recordings, which produce time-dependent currents with strong rectification.

However, on cotransfection with the β1 subunit of the BK potassium channel the resulting current became very similar to the smooth muscle recordings (Greenwood, Miller et al. 2002). The effect of β1 subunit on CLCA was found to be a direct protein-protein interaction as determined by a mammalian two hybrid system (Greenwood,

Miller et al. 2002). Unfortunately, they did not determine the effect of cotransfection on the inward-induced current. The inward current, or outward movement of chloride, would likely have been reduced in the dual transfection, given the strong rectification induced by the β1 subunit. In smooth muscle, an interaction of CLCA with β1 subunit would reduce the depolarization of the membrane by suppressing chloride conductance and preventing contraction.

In smooth muscle, the "calcium spark" may occur through the β1 BK subunit interactions that reduce the stimulatory effects of CLCA proteins on chloride conductance. This makes endogenous chloride channels more rectifying, and stops chloride release. In contrast to the "spark", there is larger Ca^{2+} release on agonist addition. At higher Ca^{2+} levels, there is a significantly larger inward current or (movement of chloride out of the cell) in the dual CLCA β 1 transfected cells (Greenwood, Miller et al. 2002). Thus, at lower Ca^{2+} levels during "sparks", the outward flux of chloride may be inhibited by the β1 subunit interactions with a CLCA protein. At higher Ca^{2+} levels this inhibitory effect is lost. Thus, modulation of an endogenous chloride conductance by altering CLCA activity in the smooth muscle cells could have a significant impact on hypertensive subjects.

1.6.5.2. Role of CLCA in Penile Erection

Upon genital arousal, nitric oxide (NO), produced by nitric oxide synthase, is released from the nonadrenergic-noncholinergic nerves as well as from the cavernosal smooth muscles and endothelial cells (Archer 2002). The NO free radical activates guanylate cyclase, producing cyclic guanosine monophosphate (cGMP) in the smooth muscle of the corpus cavernosum. The cGMP activates cGMP-dependent protein kinase

(PKG) which phosphorylates and activates the high conductance Ca^{2+}-sensitive potassium channel ($BKCa^{2+}$), the ATP inhibited KATP and voltage activated Kv channel. The net result is hyperpolarization of the cell membrane and inactivation of Ca^{2+} channels (Archer, Huang et al. 1994; Kubo, Nakaya et al. 1994; Zhao, Wang et al. 1997; Archer 2002). The resulting decrease in intracellular Ca^{2+} causes smooth muscle relaxation and vasodilation. The corpus cavernosum is then flooded with blood, expanding its thick fibrous coat and crimping off the venous drains resulting in sustained tumescence (Archer 2002). The impact of cGMP on vascular Ca^{2+}-activated chloride conductance and the importance of the PKG effects on this process can be seen in the success of the type 5 phosphodiesterase inhibitor Sildenafil (VIAGRA).

Both CLCA and Ca^{2+}-activated chloride conductance are found in penis smooth muscle vasculature (Leverkoehne, Horstmeier et al. 2002; Karkanis, DeYoung et al. 2003) . Injection of inhibitors of CLCA/ Ca^{2+}-activated chloride channels into corpus cavernosum of a rat greatly increased both the pressure/rigidity and time of the penile erection (Karkanis, DeYoung et al. 2003) (Figure 1.8). Patch clamp studies on resting human and rat corpus cavernosum found spontaneous depolarizing inward chloride currents mediated through "Ca^{2+} sparks". These currents were inhibited by a cGMP analogue (Karkanis, DeYoung et al. 2003), indicating that the contracted resting state of the corpus cavernosum is mediated through Ca^{2+}-activated chloride channels. In addition, a non voltage-dependent chloride channel is activated by the α-1 adrenergic agonist phenylephrine, which has been shown to increase intracellular Ca^{2+}. Phenylephrine has also been used to mimic the sympathetic stimulation which causes detumescence at the resolution of the sexual act (Karkanis, DeYoung et al. 2003). Thus,

the Ca^{2+}-activated chloride channel maintains the unstimulated penis flaccid and resolves the erection upon its activation (Figure 1.8).

Given the inhibitory effects of cGMP analogues *in vivo* and the presence of CLCA expression in the corpus cavernosus, it follows that tissue-specific inhibition of the stimulatory effects of CLCA on chloride conductance could provide an alternative pharmacologic target in treating erectile dysfunction. However, tissue-specific inhibition of CLCA may not be a realistic goal unless there are tissue-specific CLCA isoforms involved in controlling smooth muscle tone in the corpus cavernosum. If systemic vasculature and corpus cavernosum CLCA isoforms are identical, then pharmacological modulation of CLCA activity for erectile proposes could cause significant side effects in the form of systemic hypotension. Hence the CLCA proteins are probably not as attractive as the cyclic GMP phosphodiesterase as pharmacologic targets for treating erectile dysfunction.

1.6.6. CLCA Bestrophins and Retinopathy

Bestrophins are proteins named from the disease where they malfunction, Best's vitelliform macular dystrophy. Bestrophins are of particular current interest as candidates for the molecular identity of Ca^{2+}-activated chloride conductance. However, they too may be modulators, or only a single component of a multi-subunit chloride channel. A better understanding of CLCA and Bestrophins may give more insight into this disease and into the molecular identity of the components that make up the Ca^{2+}-activated chloride conductance.

Best's vitelliform macular dystrophy (BMD) is an autosomal dominant inherited disorder of the eye, with juvenile onset. The disease is characterized by a vitelliform ("egg yolk" or "vitelline") macular (discolored spots) lesion easily visible during a fundus examination (Benson, Kolker et al. 1975). The vitelliform lesion is due to deposition of lipofuscin (fatty pigment)-like material within and below the retinal pigment epithelium (Frangieh, Green et al. 1982; Weingeist, Kobrin et al. 1982). This often results in degeneration of the retinal pigment epithelial cells (O'Gorman, Flaherty et al. 1988). However, the most defining clinical feature of the disease is a light peak to dark trough ratio in the electrooculogram (EOG) of less than 1.5, without abnormalities in the electroretinogram (ERG) (Cross and Bard 1974). The EOG measures the late response of the eye to light. It is the result of depolarization of the basal plasma membrane of the retinal pigment epithelium (RPE) (Gallemore, Griff et al. 1988; Gallemore, Steinberg et al. 1989). It is thought that this depolarization is normally caused by a Ca^{2+}-sensitive chloride channel which is activated by some yet undefined signal from the stimulated retina (Gallemore, Griff et al. 1988). The net result of the depolarization is transport of fluid and salt away from the retinal rods and cones and into the choriocapillaris vascular drainage out of the eye.

The general ion and fluid transport mechanism of the RPE is thought to be similar to that in other secretory epithelia, except for a reversal from the normal "apical" and "basal" nomenclature. The Na^+-K^+-ATPase located in the "apical" membrane adjacent to the retinal rod and cone photoreceptors generates a large sodium gradient across the membrane (Tsuboi, Manabe et al. 1986; Tsuboi 1987; Bialek and Miller 1994). This sodium gradient is coupled the uptake of Cl^- and K^+ by the Na^+K^+ $2Cl^-$

cotransporter, also localized mainly to the "apical" membrane. As for other secretory epithelia, intracellular potassium and chloride are maintained at concentrations above their respective equilibrium potentials. The vectoral arrangement of ion transport proteins includes a "basolateral" chloride conductance, permitting net fluid movement from the vitreous to the choroid in an apical to basal direction (Bialek and Miller 1994). The release of Cl^- from the basolateral membrane is generally under the control of Ca^{2+} (Loewen, Smith et al. 2003). The rate of chloride release increases in the light-evoked EOG (Gallemore, Steinberg et al. 1989). Thus, it is natural to speculate that part of the pathology of BMD is a defect in basolateral Ca^{2+}-activated chloride conductance.

The mutation responsible for BMD was found in the gene coding for a 68 kDa protein named bestrophin. This protein has become a new molecular candidate for the Ca^{2+}-activated chloride channel (Petrukhin, Koisti et al. 1998) whose activity may be modulated by CLCA proteins. Overall 79 different mutations have been found in BMD patients (Marmorstein, McLaughlin et al. 2002) (summarized at the VMD2 mutation data base, www.uni-wuerzburg.de/humangenetics/vmd2.html). These include missense, single amino acid deletions, splice site and frameshift mutations (Marquardt, Stohr et al. 1998; Petrukhin, Koisti et al. 1998; Allikmets, Seddon et al. 1999; Bakall, Marknell et al. 1999; Caldwell, Kakuk et al. 1999) (Kramer, White et al. 2000; Lotery, Munier et al. 2000; Palomba, Rozzo et al. 2000; Eksandh, Bakall et al. 2001) (Marchant, Gogat et al. 2001). Bestrophins shares homology with the Caenorhabditis elegans RFP gene family, named for the presence of a conserved RFP amino acid sequence motif which is found in 26 transmembrane proteins with related sequences grouped in worm family eight (Stohr, Marquardt et al. 2002).

Four bestrophin isoforms have been found in humans (Marquardt, Stohr et al. 1998; Petrukhin, Koisti et al. 1998; Tsunenari, Sun et al. 2003). hBest1 or VMD2, the mutated gene in BMD, is expressed in RPE, retina and testes. hBest2 or VMD2L1 protein is found in RPE, colon and testes, hBest3 or VMD2L3 expression was found in skeletal muscle, brain, spinal cord, bone marrow, retina, thymus and testes, hBest4 or VMD2L2 was found predominantly in the colon and weakly in fetal brain, spinal cord, retina, lung, trachea, testes and placenta (Stohr, Marquardt et al. 2002; Tsunenari, Sun et al. 2003). It is interesting that hBest1, hBest2 and hBest4 are highly expressed in the RPE and colon, two tissues with active ion and fluid transport (Tsunenari, Sun et al. 2003). Electrophysiological experiments with expressed Best1 and 2 as well as Caenorhabditis elegans RFP proteins in HEK 293 cells generated chloride currents which increased with increasing intracellular Ca^{2+} concentration (Sun, Tsunenari et al. 2002; Tsunenari, Sun et al. 2003). This correlates with the basolateral localization of hBest1 in the RPE, and supports the possibility that bestrophins are calcium-activated chloride channels (Marmorstein, Marmorstein et al. 2000). However, hBest 1 was unable to produce a detectable chloride current when expressed in Xenopus oocytes (Tsunenari, Sun et al. 2003). Apparently HEK 293 cells contain an accessory subunit that may be required for bestrophin to function. In a subsequent study, Xenopus bestrophin produced a Ca^{2+}-activated chloride current when expressed in HEK 293 cells (Qu, Wei et al. 2003). Introduction of a non-conducting mutation produces a dominate negative effect in wild type oocytes channels (Qu, Wei et al. 2003). It seems likely that Bestrophins may have a significant impact on Ca^{2+}-activated chloride conductance, but that these proteins are not working alone.

The confusion surrounding differing results from different groups using different expression systems may be informative pieces of the Ca^{2+}-activated chloride channel puzzle. A potassium channel β1 subunit modulates a CLCA induced current (Greenwood, Miller et al. 2002). CFTR cAMP induced chloride currents are modulated by CLCA (Loewen, Bekar et al. 2002). Differences in CLCA-dependent whole cell chloride currents are associated with different expression systems (Cunningham, Awayda et al. 1995; Loewen, Bekar et al. 2002; Loewen, Gabriel et al. 2002). Mammalian bestrophin proteins induce large chloride currents upon expression in mammalian but not amphibian cells (Tsunenari, Sun et al. 2003). The amphibian bestrophins have a significant impact on both mammalian and amphibian Ca^{2+}-activated chloride conductance (Qu, Wei et al. 2003). Is a mammalian CLCA protein needed to make mammalian bestrophin work in the amphibian expression system?

The CLCA proteins hCLCA1, mCLCA3 and pCLCA1 are logical candidates to control the activity of bestrophins. Both the CLCA proteins and the bestrophins have been functionally connected to Ca^{2+}-activated chloride conductance, but neither protein seems fully functional without expression in a proper complimentary background. A recent study has demonstrated that CLCA is localized to the basolateral membrane of the RPE (Loewen, Bekar et al. 2004), in the same location as bestrophins, and in the area where Ca^{2+}-activated chloride conductance must function (Gallemore, Steinberg et al. 1989). It is an intriguing possibility that some combination of suitable CLCA and bestrophin proteins may constitute at least a part of the molecular identity of a Ca^{2+}-activated chloride channel.

The combination of the known facts and the speculative points surrounding this puzzle raise the possibility that the molecular components of Ca^{2+}-activated chloride channels have mostly if not entirely been cloned. The varied properties of chloride conductance associated with CLCA expression in different systems argue that these proteins are at best a component; perhaps a regulatory component, of a Ca^{2+}-dependent chloride channel, requiring the presence of other proteins to reconstitute complete chloride conductance activity. Critical co-expression and protein interaction experiments are required to connect the pieces to this puzzle and to define the permutations and combinations of membrane proteins that produce and regulate the activity of Ca^{2+}-dependent chloride conductance.

1.7. Summary

The CLCA gene family, although clustered together on a small portion of the chordate genome, is both structurally and functionally diverse. The functional diversity of this gene family implicates the members in a number of interesting physiological and pathological processes. The underlying question of whether its role in these processes is to function as a chloride channel, or to contribute to modulating the chloride conductance of other proteins has been addressed in the experiments that follow.

Chapter 2. OBJECTIVES

2.1. Specific objectives of the studies presented herein were to:

1) Determine pCLCA1 effects on agonist-induced chloride conductance upon heterologous expression in a non-epithelial cell line with low chloride channel background activity (Chapter 5).
2) Determine pCLCA1 effects on endogenous chloride currents upon heterologous expression in an epithelial cell line (Chapter 6).
3) Explore pCLCA1 contribution to chloride conductance in a tissue with endogenous pCLCA1 expression (Chapter 7).
4) Investigate the role of pCLCA1 in the Ca^{2+}-dependent chloride current in cells that have a natural developmental loss of this agonist response (Chapter 8).

2.2. Overall Objective:

Apical chloride conductance in enterocytes is important in the pathophysiology of neonatal diarrhea. Uncontrolled activation of the apical chloride conductance by bacterial enterotoxins results in dehydration, acidosis, hyperkalemia and death due to cardiac failure. An improved knowledge of the molecular pathophysiology could contribute to a better understanding of neonatal diarrhea and to the implementation of new treatment or prevention strategies. The identification of the major molecular

components of epithelial chloride transport in the apical membrane of ileal enterocytes has been the long term goal of the laboratory originating this particular project.

pCLCA1 was cloned from a ileal gene expression library with antibodies that inhibited apical chloride transport of porcine enterocytes. The protein produced by the cloned gene was studied to determine what effects pCLCA1 might have on chloride conductance, either by its own intrinsic channel properties or by its regulatory effects on other chloride channel proteins.

Chapter 3. HYPOTHESIS

The pCLCA1 protein is able to alter apical epithelial chloride channel activity through some innate ability to form a chloride channel, or to affect the activity of other proteins with intrinsic anion conductance properties.

Chapter 4. GENERAL MATERIALS, METHODS, PROCEDURES AND CONSIDERATIONS

This chapter provides an overview of the theoretical background to the experimental setup used in studying chloride conductance, which is not found within the manuscript chapters. Some equations and details of experimental procedures which are only briefly referenced in the individual manuscript chapters are also found here.

4.1. Patch-Clamp

Whole cell patch clamp was used to measure whole cell electrical current under voltage-clamp conditions. Using a micro-manipulator and microscope, a glass micro-pipette containing a physiological buffer under positive pressure is lowered gently onto the surface of a cell submerged in a physiological buffer. The positive pressure is released and slight negative pressure applied until a gigaohm seal (10^9 Ω) ("gigaseal") is formed between the pipette and the plasma membrane. This membrane to glass seal is highly important for low noise recordings of single channels in the membrane. It is also important when larger negative pressure is applied to disrupt the membrane within the pipette, allowing dialysis of the cell with pipette solution to produce what is described as the "whole cell configuration". The tightness of the gigaseal prevents current leak between the pipette electrode and the reference electrode in the bathing solution. It also prevents the flooding of the cell with solution bathing the cell "the bath solution". The

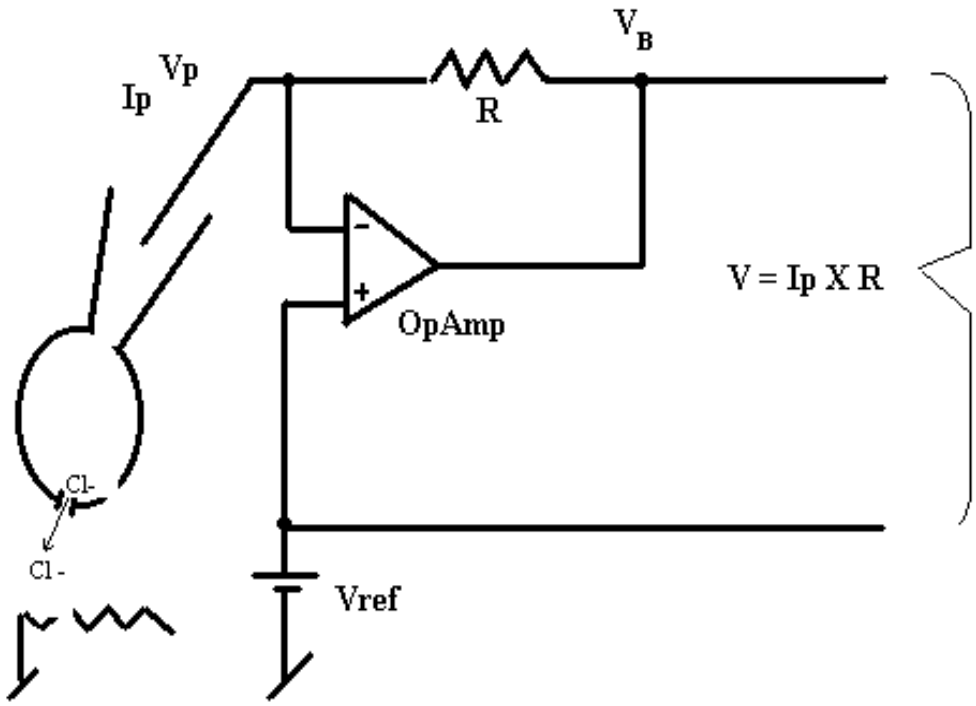

Figure 4.1. Patch Clamp current-to-voltage converter circuit. The op-amp varies the voltage output V_B at a very rapid and precise rate so that Vp = Vref and the voltage clamp is maintained even with a potential drop in Vp due to current measurement. This circuit also allows the measurement of V_B - Vref to determine the Ip. The V_B - Vp measurement is no longer needed as Vp = Vref (Sakmann 1995; Walz 2002).

pipette contents then act as a fluid bridge connecting the headstage amplifier input to the interior of the cell.

Within the headstage of the amplifier, a voltage-to-current converter maintains the voltage clamp of the cell membrane by a constant (Vp) voltage as set by the (Vref) voltage (Figure 1.4).

To determine the membrane current, voltage is passed from a source V_B to the pipette electrode across a resistor of high impedance. The voltage drop across this resistance, as determined by the difference between V_B and Vp, is proportional to the current flow between the pipette and membrane, which then can be used to determine the membrane current (Figure 1.4.).

However, the voltage drop also results in a voltage loss. To maintain a voltage clamp despite a voltage loss, an operation amplifier (OAmp) is used to automatically input voltage (compensate for the voltage loss) generating an opposing current (pipette to V_B if the membrane current is away from the pipette). Thus, the reported membrane current would be the opposite of the opposing current used to maintain pipette voltages and the resulting voltage clamp (Sakmann 1995; Walz 2002).

4.2. Reversal Potentials to Determine Anion Dependence of Current

The ionic nature of the whole cell current is assessed by the change in the equilibrium potential or E_{rev} (the membrane voltage at which no current flows) resulting from a lowering or increasing bath or pipette ion concentration. An E_{rev} movement towards the calculated E_{rev} of a particular ion is used to identify the ion producing the current. This shift is called a " Nernstian shift " because the equilibrium

potential shifts towards the calculated E_{rev} of the major conducting ion across a membrane as determined by the Nernst Equation (Nernst 1888; Hille 2001).

The Nernst equation is calculated with the assumption that the equilibrium potential (E), varies linearly with absolute temperature (T = t °C + 273.15) in Kelvin and logarithmically with ion concentration (see equation 4.1,4.2).

$$E_{cation} = \frac{RT}{zF} \ln \frac{[cation]o}{[cation]i} \quad \textbf{(Equation 4.1)}$$

$$E_{anion} = \frac{RT}{zF} \ln \frac{[anion]i}{[anion]o} \quad \textbf{(Equation 4.2)}$$

where (R) is the ideal gas constant at 8.3145 V C mol^{-1} K^{-1}.

4.2.1. Boyle's and Avogadro's Law Define "R" the Ideal Gas Constant

The following describes the derivation and concept of the ideal gas constant (R) used in the Nernst Equation. Discussion of the Nernst equation continues in the next paragraph. The ideal gas constant (R) is defined by the ideal gas equation PV = nRT which is a summary of Boyle's law; that the volume of an ideal gas varies inversely to the pressure, if the temperature remains constant, and Avogadro's law that at a fixed temperature and pressure, the volume of a gas is directly proportional to the amount of gas. R is usually derived with reference to standard temperature and pressure, assuming that 1 mol gas = 24.789 L at 25 ° C which is equal to 1 bar = 10^5 pascal (Pa) = 10^5 newton per square meter (N m^{-2}). This is based on Boyle's results which shows that the density of mecury is13.546 gm/mL due to acceleration of gravity, g = 9.81 m s^{-2}, which is approximately equal to 1 bar. It is not based on standard temperature and pressure of 1 mol gas = 22.4 L at 0°C at 1 atm because 1 atm = 1.01325 bar, making the conversion

to voltage difficult. Given the relations 1 L = 10^{-3} m^3 and 1 bar = 10^5 Pa = 10^5 N m^{-2} and 1 N m = 1 J = 1 VC (volt coulomb) because 1 volt = 1 joule/coulomb we can define the total free energy of the ionic solution as R (Equation 4.3) (Barrow 1988; Hille 2001).

Z is defined as the valence of the ion, **n** the number of moles and **F** is Faraday's constant = 9.6485 X10^4 C mol^{-1}. This is the amount of charge required to deposit one gram atomic mass (one mole) of a single-valence element on an electrode in units of coulombs (1 coulomb is 1.602 X 10^{-19} electrons). These factors allow conversion of the energy R (which is the total free energy of the solution) to total possible voltage. The

$$R = \frac{V \quad P}{T \quad n}$$

$$= \frac{(24.789 \quad L)(1 \quad bar)}{(298.15 \quad K)(1 \quad mol)} = 0.083143 \ L \quad bar \quad K^{-1} \quad mol^{-1}$$

$$= 0.083143 \ L \quad bar \quad K^{-1} \quad mol^{-1} \ X \frac{10^{-3} \quad m^3}{1 \quad L} X \frac{10^5 \quad N \quad m^{-2}}{1 \quad bar}$$

$$= 8.3143 \ N \quad m \quad K^{-1} \quad mol^{-1}$$

$$= 8.3143 \ J \quad K^{-1} \quad mol^{-1}$$

$$= 8.3143 \ V \quad C \quad K^{-1} \quad mol^{-1}$$

(Equation 4.3)

voltage which is generated depends on the separation of the solution across the plasma membrane as determined by equations 4.1 & 4.2 (Hille 2001).

To correspond to the physiological convention, all membrane potentials are measured inside minus outside. Thus, when using a cation the denominator is the inside concentration and when using an anion the denominator is the outside concentration (Hille 2001).

However, the Nernst equation only allows an approximation of the E_{rev}, because ionic solutions are not ideal gases. One possible way to circumvent this problem is to use ion activities rather then concentrations (Altenberg 1996; Hille 2001). The ion activity is different from the free concentration. The ion activity is generally lower at physiological solute concentration because the mobility of ion in solution is restricted by ion-ion and ion-solvent interactions (Altenberg 1996). The correction factor required to convert free concentration to activity is the activity coefficient. This is based on the premise that the nonideal contribution to free energy of ions in solution can be interpreted as the difference between the energy required to create the ion in solution where there are no interionic interactions and the energy where there are such interactions. It is derived from the Debye-Huckel limiting law at 25 ^{o} C in water equation:

$$\log \gamma_{\pm} = 0.5091 Z_{+} Z_{-} \sqrt{\mu} \qquad \textbf{(Equation 4.4)}$$

where γ is the activity coefficient, Z is the valency and μ is the ionic strength. (see (Barrow 1988) for derivation). Unfortunately, the derivation does not take into account

the (multi-ionic) nature of many physiological buffers. In addition, many complex ions deviate from derived coefficients, indicating that effects other than electrostatic ones need to be taken into account (Barrow 1988). Thus, the use of such a coefficient is of limited use in a physiological buffer. Additionally, given the usual background current and leakage in most experiments, concentration calculations are usually adequate. When determining the major ionic contribution to the current, one usually looks for the shift towards the Nernst equilibrium potential rather than precisely obtaining that potential.

4.3. Pipet Junction Potentials

Liquid junction potential is the potential difference between two solutions of differing composition. Potential difference results from separation of charge that occurs when anions and cations of different mobilities diffuse across boundaries (Sakmann 1995). In the case of patch clamp, the boundary and solution difference is between the pipet and the bath solutions. When a pipet solution containing a large bulky anion such as glutamate with low mobility is used with a cation with high mobility such as potassium, a large junction potential can develop as the potassium ions move quickly into the bath solution leaving the glutamate behind, and creating a potential difference.

It is normal to use the pipette offset to compensate for this potential at the beginning of an experiment when the pipette is placed into the bath. However, on whole cell access the potential no longer exists because as the cell equilibrates with pipette solution. The plasma membrane then prevents a liquid-liquid junction effect.

However, the pipette potential is compensated for by the pipette offset when the pipette is originally placed in the bath. To determine the actual voltage placed on the

cell membrane during the experiment the original junction potential has to be measured or calculated. Computer based calculations based on ion mobility in the pClamp 8.1 software (Axon instruments, Foster City, CA) were used. Measurements were also performed. This was accomplished by placing the amplifier in current clamp mode and measuring the voltage produced after changing the bath solution from one composed of the internal pipette solution to the experimental bath solution. The reference electrode was a flowing 3 M KCl electrode to minimize junction potentials at this electrode.

4.4. Trans-Epithelial Current Measurements in the Ussing Chamber

Trans-epithelial current was assessed in a Ussing chamber. This apparatus permits measurement of the voltage or current produced across an epithelium by transepithelial ion movement (Ussing 1951; Cotton 1996). The experimental tissue is placed with apical and basolateral sides of the epithelium facing opposite and isolated baths. The two baths only communicate though an aperture which is spanned by the epithelium. The electrical properties of the epithelium are then studied using a two electrode system. One set of electrodes, one electrode in the bath on each side of the tissue, measures the transepithelial voltage. A second set of electrodes delivers a current or a voltage across the epithelium. The system is usually run either open circuit (measuring the voltage produced) or short circuit (measuring I_{sc}, which is the current required to voltage clamp at 0 mV). We generally use the open circuit condition as, in our experience, it results in a healthier tissue and better recordings.

To determine the resistance of the tissue (an indication of the integrity of the tissue examined), the tissue is pulsed to a known current (ΔI), usually 10 μA. Using the

resulting voltage change (ΔV), one can then determine the resistance of the tissue. If resistance of the tissue is known, then short circuit current of the tissue can be calculated (Equation 4.5).

$$I_{sc} = \frac{V_{measured}}{R = \frac{\Delta V_{measured}}{\Delta I_{known}}} \quad \textbf{(Equation 4.5)}$$

$$R = \frac{\Delta V_{known}}{\Delta I_{sc}} \quad \textbf{(Equation 4.6)}$$

Alternatively, the system can be run in short circuit and the tissue resistance can be determined by inducing a known voltage pulse. The resulting current is then measured and resistance is calculated (Equation 4.6).

4.6. Chloride Efflux

Efflux of $^{36}Cl^-$ gives an assessment of permeability of the cell membrane to the chloride ion. Increases or decreases in permeability are measured, but the technique does not give insight into how the chloride is released from the cell. In particular, it does not distinguish between electrogenic and electroneutral ion transport. It is also highly influenced by cell physiology, as the driving force for chloride efflux is not externally controlled in most experimental setups.

Generally, cells were loaded by incubation in an isotonic loading buffer (see specific chapters for buffers) containing 2 Ci/ml of $^{36}Cl^-$ for 2 hours. The loading buffer was created by adding added Na^+ $^{36}Cl^-$ at ~ 1 Ci /ul to the efflux buffer. $^{36}Cl^-$ is shipped as $H^{36}Cl$ at ~ 2 to 3 M. It is neutralized with NaOH to obtain Na $^{36}Cl^-$. The amount of

NaOH need to neutralize the $H^{36}Cl$ was determined from the specific activity, A (mCi/g), the radiochemical concentration, B (mCi/ml), the volume of radionucleide in mls, C, and the molecular weights Cl^- = 35.5 g/mol and NaOH = 40 g /mol.

$$\frac{\mathbf{B}\ \text{mCi / ml}}{36.5\text{g / mol X}\ \ \mathbf{A}\ \text{mCi / g}}\ \text{X}\ \mathbf{C}\ \text{ml X}\ \ 40\text{g / mol} = \mathbf{D}\ \text{g of NaOH} \qquad \textbf{(Equation 4.7)}$$

The $^{36}Cl^-$ addition to loading buffer only increases the NaCl concentration (140 mM) by ~ 2 mM. After complete equilibration with loading buffer, the cells were washed rapidly 5 times with efflux buffer. The final wash was designated the start of the efflux. One ml of efflux buffer was replaced every two minutes through the time course of the efflux. The removed buffer was placed in 1.5 ml of Beckman Redisafe scintillation cocktail and counted on a Beckman LS3800 counter. The $^{36}Cl^-$ concentration in the loading buffer was determined by measuring $^{36}Cl^-$ cpm/ml, which was divided by the number of nmol Cl^-/ml in the buffer to give cpm per nmol Cl^-. This allowed the calculation of "nmol Cl^- release" used in Chapter 5. Other measures of chloride release are specified where relevant in each chapter.

4.7. RNA Preparation and RT-PCR

RNA was harvested under the usual chaotropic conditions using guanidinium-thiocyanate to disrupt RNase and prevent RNA degradation. DNA was removed with DNAase. The phenol was acidified to prevent partitioning of the RNA from the aqueous phase into phenol. Propanol and ethanol were used to precipitate the RNA. Total RNA was used as reverse transcriptase template to generate cDNA as a template for

polymerase chain reaction (PCR). Specific reaction conditions are outlined in each chapter. All reactions cycled in the order of melting (production of single strand DNA), annealing (binding of primer) and extension (extension of primer by Taq DNA polymerase) to drive the exponential growth of the product determined by specific primers (Saiki, Gelfand et al. 1988). Primer design was computer-aided, with special efforts to avoid primer sequence that promoted non-specific template binding, hairpin and primer dimer formation. A high GC content was preferred at the 3' end of the primer to assure specific and strong annealing. Magnesium concentrations were sometimes altered from the default value in ± 0.1 mM increments to deal with difficult templates. It is presumed that magnesium ions shield charges on the phosphate backbone of the DNA, thereby reducing secondary structure.

4.8. CLCA1 Antibody Production

Antibody-epitope interaction is considered to be noncovalent bonding (not sharing of valance electrons in bond). The forces that are involved include:

1. Hydrogen bonding which is formed when a H atom bound to a highly electronegative atom is simultaneously attracted to a small highly electronegative atom of a neighboring molecule. Hydrogen bonding can occur only with H atoms because all other atoms have inner-shell electrons to shield their nuclei.
2. Ionic bonds form between charged amino acids that attract each other through electrostatic forces.

3. van der Waals interactions are weak bonds between two uncharged atoms that have developed electric dipoles due to interactions with nearby atoms.
4. Hydrophobic bonds, which are caused by the intrinsic attractions between nonpolar amino acid subunits in an aqueous environment. Hydrophobic bonding is based on maximizing thermodynamic stability by minimizing the entropy decrease needed to order water molecules around hydrophobic portions of molecules (Lehninger 1993). The hydrophobic bonds usually contribute the greatest part of the energy to the antibody-antigen interaction, which is why many of the programs used to select a preferred antigenic region are based on amino acid residue hydrophobicity.

The importance of hydrophobicity can seen in the successful application of the Hopp and Woods method that predicts the location of antigenic determinants by finding area of greatest local hydrophobicity (Hopp and Woods 1981). Along with a database of known antigenic sites, this method gives a fairly good prediction of antigenic regions of a protein (Thornton, Edwards et al. 1986). These methods were employed using computer software PCGENE to identify a small peptide which was then synthetically produced, conjugated to keyhole limpet hemocyanin and used to immunize two rabbits (Sigma-Genosys, Woodlands Texas). The predicted sequence amino acid sequence of pCLCA1 chosen for best antigenicity was CKEKNHNKEAPNDQNQK (residues 250-266). It should be noted that membrane topology predictions locate this region of the protein in an N terminal extracellular domain.

4.9. Western blot

Cellular proteins were separated by SDS PAGE, and transferred from polyacrylamide gels onto nitrocellulose blotting membrane using a high power wet cell transfer system (BioRad) to drive the protein from the gel onto the membrane. After protein transfer to the nitrocellulose the membrane was blocked with 3% skim milk powder in TTBS to prevent non-specific binding of the primary antibody to the membrane. The blocked membrane was incubated with suitable dilutions of preimmune or immune rabbit antisera. Unbound primary antibody was removed by washing, and membranes were equilibrated with TTBS containing dilutions of secondary antibody conjugated to a detecting element to visualize the location of the pCLCA1 antigenic epitope on the blot (Burnette 1981).

4.10. Flow Cytometry

Flow cytometry involves the projection of a beam of light from a diode laser through a liquid stream of cells which are labeled with fluorochromes that will fluoresce upon appropriate excitation. The emitted fluorescence can then be filtered and detected with individual photomultiplier tubes to identify the presence of individual fluorochromes on each cell. The process permits simultaneous cell and fluorochrome counting to identify population responses to particular screening procedures using dye or antibody.

The Coulter® Epics® Elite ESP (Coulter corporation, Miami FL) flow cytometer was configured with forward and side scatter parameters in linear mode PMT5 (detecting propidium iodide) and PMT2 (detecting FITC) fluorescence channels in logarithmic modes. Compensation was set with Flow-Check Fluorospheres beads (10

μm Beckman Coulter Inc., Fullerton, CA), and photomultiplier gates were set with Caco-2 cells treated with preimmune serrum. 10,000 events were acquired for each experimental condition. The data were presented as two-parameter dot plot where the two lower quadrants identify intact cells negative for propidium iodide fluorescence, while the two right hand quadrants identify cells with surface pCLCA1 epitope display that interacts with primary antibody, and FITC-conjugated secondary antibody. Hence the lower right hand quadrant contains intact cells expressing surface pCLCA1 epitope.

Chapter 5. THE CALCIUM-DEPENDENT CHLORIDE CONDUCTANCE MEDIATOR pCLCA1

5.1. Abstract

The regulatory behavior, inhibitor sensitivity, and properties of the whole cell chloride conductance observed in cells expressing the cDNA coding for a chloride conductance mediator isoform of the CLCA gene family, pCLCA1, have been studied. CommonC-kinase consensus phosphorylation sites between pCLCA1 and the closely related human isoform hCLCA1 are consistent with a role for calcium in channel activation. Both channels are activated rapidly on exposure to the calcium ionophore ionomycin. Direct involvement of calcium in the activation of pCLCA1 was supported by the finding that treatment with the intracellular calcium chelator 1,2-bis(2-aminophenoxy)ethane-N,N,N',N'-tetraacetic acid-AM reduced the rate of chloride efflux from NIH/3T3 cells expressing the pCLCA1 channel. No combination of A-kinase activators used was effective in activating chloride efflux via this channel despite the presence of a unique strong A-kinase consensus site in pCLCA1. Notable differences of pCLCA1 from the reported properties of CLCA family members include the failure of phorbol 12-myristate 13-acetate to activate chloride efflux in cells expressing pCLCA1 and a lack of inhibition of chloride efflux from these cells after treatment with DIDS or dithiothreitol. However, selected inhibitors of anionic conductance inhibited pCLCA1-dependent anion efflux. The electrogenic nature of the ionomycin-dependent efflux of

chloride from cells expressing pCLCA1 was confirmed by detection of outwardly rectifying chloride current and inhibition of this current by chloride conductance inhibitors in a whole cell patch-clamp study.

5.2. Introduction

There are a least three major types of chloride channels with the potential to act as gating molecules controlling the electrogenic release of chloride from the apical membrane of secretory epithelial tissues. The cystic fibrosis transmembrane regulator (CFTR) protein, some members of the related isoforms of the ClC protein family, and the CLCA family of calcium-dependent chloride channels are all expressed in the apical membrane of epithelial cells lining the surface of secretory tissues. There is experimental evidence supporting the roles of members of each of these channel families in transepithelial electrolyte and fluid transport (Anderson, Gregory et al. 1991; Anderson and Welsh 1991; Fuller and Benos 2000b; Mohammad-Panah, Gyomorey et al. 2001). Cystic fibrosis disease arises from mutations in the CFTR protein that directly or indirectly reduce chloride transport by the CFTR molecule (Quinton 1983; Berschneider, Knowles et al. 1988; Riordan, Rommens et al. 1989). ClC-2 is present in the apical membrane of intestinal epithelial cells and can contribute to chloride currents in these cells (Loewen, MacDonald et al. 2000; Mohammad-Panah, Gyomorey et al. 2001). Isoforms bCLCA1, mCLCA1, and hCLCA2 are expressed in trachea and lung epithelium, and hCLCA1 expression was reported in the human gut, where it is postulated to participate with CFTR in regulated chloride transport (Chow, Uribe et al.

2000) (Gruber, Elble et al. 1998; Gruber, Gandhi et al. 1998; Fuller and Benos 2000b; Fuller and Benos 2000a).

Our laboratory has reported the cloning of a porcine (pCLCA1) isoform of the CLCA gene family (Gaspar, Racette et al. 2000). Nucleotide sequence data show that the pCLCA1 channel is most similar to the hCLCA1 isoform of that family, with 78% identity in the predicted amino acid sequence. Predicted amino acid sequence data also suggest a common transmembrane topology for pCLCA1 and hCLCA1. Monobasic proteolytic cleavage sites likely to be involved in post translational processing of hCLCA1 are common to pCLCA1.

Heterologous expression of hCLCA1 and hCLCA2 as well as mCLCA1, mCLCA2, and bCLCA1 in HEK-293 cells and Xenopus oocytes is accompanied by the appearance of a calcium-sensitive anion conductance(Gandhi, Elble et al. 1998; Gruber, Elble et al. 1998; Romio, Musante et al. 1999) The calcium-dependent anion conductance is reported to be sensitive to inhibition by 4,4'-diisothiocyanostilbene-2,2'-disulfonic acid (DIDS) and by the reducing agent dithiothreitol (DTT). Weak consensus C-kinase phosphorylation sites in a predicted cytosolic loop at S535, T580, and T593 and the strong site at T600 are common to the predicted amino acid sequences of hCLCA1 and pCLCA1. CLCA channel activation by A-kinase has not been reported. The strong RRSS587 A-kinase consensus site in the predicted cytosolic loop containing four conserved C-kinase phosphorylation sites is unique to predicted pCLCA1 amino acid sequence.

As with the bCLCA1 and hCLCA1 isoforms, pCLCA1 is expressed in tracheal and small intestinal epithelium, with highest levels in association with the secretory cell

types in the tracheal submucosal glands and the small intestinal crypts of Lieberkuhn (Racette, Gabriel et al. 1996; Gaspar, Racette et al. 2000). In addition to the expression sites for pCLCA1, two other lines of evidence relate to a potential role for this protein in epithelial electrolyte and fluid secretion. The initial evidence came from the monoclonal antibody used in expression cloning of the pCLCA1 gene. Incubation of this monoclonal antibody with apical membrane vesicles prepared from porcine ileum inhibited up to 95% of electrogenic chloride uptake by these vesicles (Racette, Gabriel et al. 1996). Expression of the pCLCA1 gene in permanently transfected 3T3 mouse fibroblasts introduced a calcium-dependent chloride efflux from the fibroblasts expressing pCLCA1 (Gaspar, Racette et al. 2000).

This report outlines the sensitivity of the pCLCA1 protein to second messenger activators and to some inhibitors of anion conductance, as well as some properties of the anion currents observed in whole cell patch-clamp measurements on 3T3 cells expressing pCLCA1.

5.3. Materials and Methods

5.3.1. Materials

Tissue culture media, G418 antibiotic, and Superscript II reverse transcriptase were purchased from GIBCO Life Technologies. Taq and Pfu DNA polymerases were obtained from Stratagene, dNTPs from Pharmacia, and restriction enzymes from New England Biolabs. Molecular biology grade chemicals and anion transport inhibitors including DIDS, glibenclamide, 5-nitro-2-(3-phenylpropylamino)benzoate (NPPB), α-phenylcinnamate (α-PC), and diphenylamine carboxylate (DPC) were obtained from

Sigma-Aldrich. $^{36}Cl^-$ was purchased from New England Nuclear. Oligonucleotides were synthesized at the Core DNA Services Laboratory, University of Calgary (Calgary, Canada).

5.3.2. Production of Cell Lines.

NIH/3T3 fibroblasts were grown in DMEM medium supplemented with 10% fetal bovine serum (FBS) and glutamine (2 mM) (complete DMEM medium). Optimum settings for plasmid transfection by electroporation used voltage and capacitance conditions sufficient to kill ~20% of freshly suspended recipient cells within 48 h of receiving a single electrical discharge. NIH/3T3 cells (8×10^6 cells) were mixed with 100 μg of pcDNA3 plasmid containing pCLCA1 cDNA or pcDNA3 vector without insert and then subjected to a 250-V discharge at 250 μF in a 4-mm gap electroporation cuvette. After electroporation, cells were plated at 2×10^5 cells per well in 24-well plates. G418 (2.5 mg/ml) was added to wells 24 h later to select for successful transfectants. Cells were switched to maintenance medium (500 μg/ml G418 in complete DMEM) 7 days posttransfection.

5.3.3. RT-PCR

Total RNA was isolated by extraction in guanidiniumthiocyanate-phenol (Trizol; GIBCO) and used as a template in a reverse transcriptase PCR reaction. Total RNA (5 μg) from transfected cells was used as a template in a reverse transcriptase reaction containing dNTPs, 200 units of Superscript reverse transcriptase, and 1 pmol of primer (5'-GAGAAAGCTTGCGGCCGCTCGTGCAGAAAGTCTAAAATG-3') specific to a section of unique sequence in the 3' untranslated region of pCLCA1 and

not found in any other CLCA isoform. The reverse transcriptase reaction product (1 µl) was used as template in a nested PCR reaction with sense (5'-GTGAACACGCCACGCAGAAG-3') and antisense (5'-GTCCAACCAGAATAGCTGTC-3') primers for 24 cycles at 94°C for 45 s, 52°C for 45 s, and 72°C for 1 min to produce a 518-base pair product. PCR products were separated by electrophoresis in 0.1% agarose gels in Tris-borate-EDTA buffer and exposed to ethidium bromide, and the fluorescence of the ethidium bromide-DNA complex was recorded on a GelDoc visualizing system (Bio-Rad).

5.3.4. Chloride Efflux Measurements

Stable pCLCA1 transfectants of mouse 3T3 fibroblasts were grown in DMEM supplemented with 2 mM glutamine, 10% fetal calf serum (FCS), and G418 (500 µg/ml). Confluent 35-mm plates of these cells were loaded with $^{36}Cl^-$ by removing growth medium and incubating with loading buffer containing 4 mM KCl, 2 mM $MgCl_2$, 1 mM KH_2PO_4, 1 mM $CaCl_2$, 5 mM glucose, 10 mM HEPES, pH 7.5, and 140 mM NaCl plus 2 Ci/ml $^{36}Cl^-$ for 2 h. Extracellular $^{36}Cl^-$ was removed by rapidly washing cells five times with 1 ml of efflux buffer (loading buffer without $^{36}Cl^-$). The $^{36}Cl^-$ content of the last wash was reported as the time 0 efflux value. The rate of release of chloride from the cells was determined by repetitively adding 1 ml of efflux medium and removing the medium 2 min later. The chloride efflux values reported at each 2-min interval represent the amount of $^{36}Cl^-$ (measured by liquid scintillation counting) released from the cells during the preceding 2 min. Cells were removed from the plates at the end of the efflux by addition of 1.0 mM EDTA and mechanical agitation for the determination of total protein (Bio-Rad protein assay).

5.3.5. Agonists

Potential activators of pCLCA1 chloride conductance were added to the efflux buffer after the end of the last wash. When ionomycin (10 μM), phorbol 12-myristate 13-acetate (PMA), or 8-(4-chlorophenylthio)-AMP (CPT-cAMP; 0.5 mM), 3-isobutyl-1 methylxanthine (IBMX; 2.0 mM), and forskolin (10 μM) were added to the efflux buffer, they were also present in the buffer used for each successive 2-min efflux period.

5.3.6. Antagonists

Potential inhibitors of cell signaling including the calcium chelator 1,2-bis (2 aminophenoxy)ethane-N,N,N',N'-tetraacetic acid-acetoxymethyl ester (BAPTA-AM) and the calcium calmodulin kinase II (CaMKII) inhibitor 2-[N-(2-hydroxyethyl)-N-(4 methoxybenzenesulfonyl)]amino-N-(4-chlorocinnamyl)- N-methylbenzylamine (KN-93) were added to uptake medium during the 2-h $^{36}Cl^-$ loading period. DTT and potential chloride transport inhibitors with lipid-soluble anion properties presumed to interact with an anion channel in the conductance protein (DIDS, NPPB, etc.) were added to the wash solution during the five cell washes preceding efflux measurements and were also in the buffer during the subsequent timed $^{36}Cl^-$ efflux.

5.3.7. Whole Cell Patch Clamp

Whole cell voltage-clamp studies. The pipette solution for intracellular dialysis contained 1 mM sodium pyruvate, 40 mM Tris - HCl, 90 mM D-gluconic acid lactone, 90 mM Tris base, 5 mM N-tris(hydroxymethyl)methyl-2-aminoethanesulfonic acid

(TES), 1 mM EGTA, 2 mM $MgCl_2$, 0.1 mM $CaCl_2$, 1 mM MgATP, and 0.1 mM Na_2GTP (pH 7.4). Ca^{2+} activity was buffered to ~40 nM (1.0 mM EGTA and 0.1 mM $CaCl_2$). The routine bath solution contained 150 mM NaCl, 2 mM $MgCl_2$, 1 mM $CaCl_2$, 5 mM TES, and 30 mM sucrose (adjusted to pH 7.4 with Tris). The low-chloride solution contained 40 mM NaCl, 2 mM $MgCl_2$, 1 mM $CaCl_2$, 5 mM TES, and 250 mM sucrose. Single-cell, rapid solution changes were applied by using a gravity-fed Perfusion Fast-Step SF-77B perfusion system (Warner Instrument, Hamden, CT). Ionomycin (10 μM) was added as a single-cell bath solution change. Patch-clamp electrodes were pulled and fire-polished from borosilicate glass capillaries (outer diameter 1.5 mm; inner diameter 1.17 mm) with an inner filament (Harvard Apparatus, Edenbridge, UK) on a DMZ universal puller (Dagan, Minneapolis, MN). Patch pipettes had a tip resistance of 3-5 MΩ with these solutions. Whole cell currents were acquired with an Axopatch-1D patch-clamp amplifier (Axon Instruments, Foster City, CA) at 500 Hz, filtered at 100 Hz with Clampex 8, and analyzed with Clampfit 8 (Axon Instruments). The standard voltage-clamp protocol had a holding potential of 0 mV with voltage pulses applied for 600 ms from - 80 to +100 mV in 20-mV increments. After a (>1 G Ω) seal was obtained, capacitance compensation was carried out before whole cell access. Subsequent to whole cell access, all cells were dialyzed for 2 min before recording. Only those cells that had a membrane resistance ~100 times that of the access resistance before ionomycin activation were used. Current differences were normalized by the whole cell capacitance recorded from an integrated 10-mV hyperpolarizing pulse. All membrane potentials were corrected at the time of analysis for the measured

junction potentials of pipette to bath solution, 4.8 ± 0.2 mV in bath solutions containing 150 mM Cl^- and 0.8 ± 0.2 mV in bath solutions containing 40 mM Cl^-.

5.3.8. Statistical Methods

Two-way repeated-measures ANOVA was used to compare treatment over time or voltage effects. The Fisher least significant difference (LSD) method for pairwise multiple comparisons was used as a post-ANOVA test to determine treatment effects at individual points. Reversal potential (E_{rev}) values were compared using Student's t-test. The SigmaStat statistical software package was used to perform all these comparisons.

5.4. Results

5.4.1. Cell Lines

Untransfected NIH/3T3 fibroblasts are killed by continuous exposure to complete DMEM medium containing 500 μg/ml of G418. The expression of pCLCA1 mRNA in transfected cells resistant to G418 was verified by reverse transcriptase PCR. Amplification of a 518-base pair product from reverse transcribing 5 μg of total RNA from cells transfected with the pCLCA1-expressing construct (Figure 5.1) indicates that the construct was intact and that the transfected cells would be expected to synthesize the pCLCA1 protein.

5.4.2. Agonists

The pCLCA1 mRNA was cloned from a porcine intestinal cDNA library (Gaspar, Racette et al. 2000). Apical chloride channels from crypt cells in the intestinal

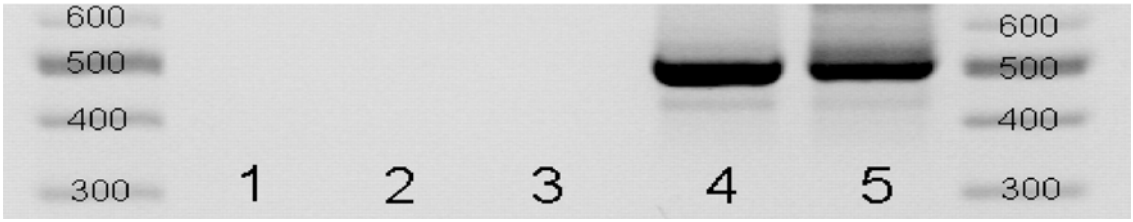

Figure 5.1. Identification of pCLCA1 mRNA expression in transfected NIH/3T3 fibroblasts. Reverse transcriptase PCR reaction was carried out with total RNA isolated from 2,500 cells. Reverse transcriptase was primed with an antisense primer complimentary to a pCLCA1-specific 3' untranslated sequence. The reverse transcriptase reaction product (1 μl) was used as template for a PCR reaction with nested primers designed to amplify a 518-base pair product. Flanking standard lanes contain a 100-base pair ladder. Lane 1, PCR no-template control; lane 2, NIH/3T3 mRNA RT template; lane 3, pcDNA3-transfected NIH/3T3 mRNA RT template; lane 4, pCLCA1-transfected NIH/3T3 mRNA RT template; lane 5, pCLCA1 cDNA control.

mucosa are activated *in situ* in response to treatment with cholera toxin, with the heat-labile and heat-stable enterotoxins produced by enteropathogenic strains of Escherichia coli. The cyclic nucleotide phosphodiesterase inhibitors theophylline and IBMX are rapid and potent activators of apical chloride conductance. Various calcium ionophores including A23187 and ricinoleic acid are also recognized as in situ activators of apical chloride channel conductance and intestinal secretion. Exogenous expression of the pCLCA1 protein in mouse 3T3 fibroblasts provides a model that can be used to test for the sensitivity of this presumptive anion channel to activation by various second messenger substances.

The presence of a strong A-kinase consensus site in pCLCA1 raises the possibility of activation of this channel by cAMP. Addition of CPT-cAMP, forskolin, and IBMX to transfected 3T3 cells expressing pCLCA1 mRNA did not affect the rate of release of $^{36}Cl^-$ from cells loaded with this isotope (Figure 5.2.; ±pCLCA1 × time, P = 0.482). This lack of response to A-kinase activation was also observed in control-transfected 3T3 cells. The conditions used in this study should be sufficient for A-kinase activation in most test systems, but significantly higher concentrations of IBMX (5-10 mM) are routinely used for *in situ* activation of secretion without any CPT-cAMP or forskolin. Exposure of pCLCA1-transfected 3T3 cells to 5 mM IBMX for 6 or 10 min before extracellular $^{36}Cl^-$ was washed significant efflux response to the cyclic nucleotide phosphodiesterase inhibitor (data not shown).

There is a strong *in situ* secretory response to calcium ionophores including ricinoleic acid, bile acids, the A-subunit of cholera toxin, and A-23187 in porcine small intestine (Maenz and Forsyth 1982; Maenz and Forsyth 1987). Addition of ionomycin

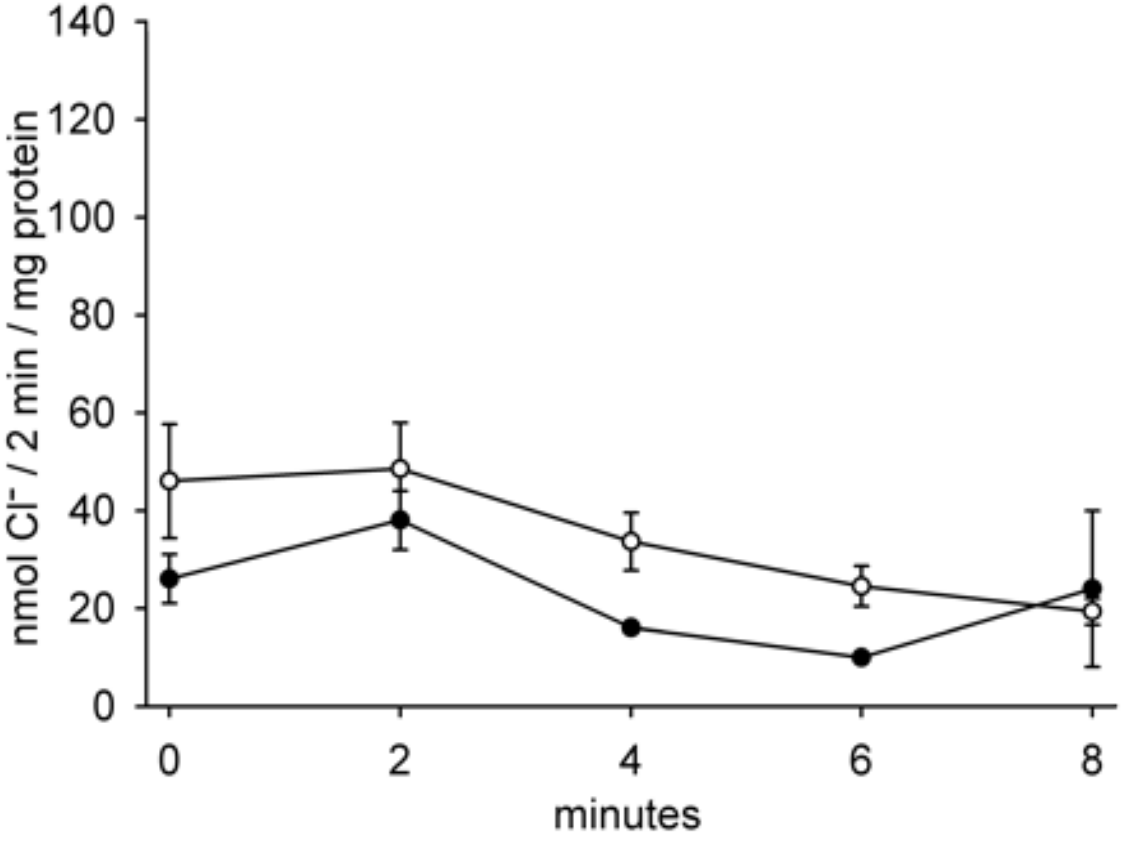

Figure 5.2. Effect of pCLCA1 transfection on chloride release by NIH/3T3 fibroblasts treated with activators of protein kinase A (PKA). Medium on confluent cells in 3.5-cm dishes was replaced with loading buffer containing 4 mM KCl, 2 mM $MgCl_2$, 1 mM KH_2PO_4, 1 mM $CaCl_2$, 5 mM glucose, 10 mM HEPES, pH 7.5, and 140 mM NaCl plus 2 μCi/ml ^{36}Cl. After 2 h, cells were washed rapidly 5 times with 1 ml of efflux buffer (loading buffer without $^{36}Cl^-$). The $^{36}Cl^-$ content of the last wash is reported as the time 0 efflux value. $^{36}Cl^-$ release was measured by changing the efflux buffer at 2-min intervals. 8-(4-Chlorophenylthio)-AMP (CPT-cAMP; 0.5 mM), 3-isobutyl-1-methylxanthine (IBMX; 2.0 mM), and forskolin (10 μM) were added to the efflux buffer at time 0 and at each subsequent buffer replacement interval to facilitate activation of PKA. ●, 3T3 cells (control) transfected with pcDNA3; ○ , 3T3 cells transfected with pcDNA3 containing pCLCA1. Values are means ± SE (n = 6

to pCLCA1-transfected 3T3 cells increased the rate of $^{36}Cl^-$ efflux from these cells. The ionomycin-dependent stimulation of $^{36}Cl^-$ efflux was not observed in control-transfected cells containing only the pcDNA3 vector (Fig 5.3.; ± pCLCA1 × time, $P < 0.001$). The calcium dependence of this ionomycin effect was investigated by adding the calcium chelator BAPTA-AM to the loading medium during the 2-h loading with ^{36}Cl. Normal loading buffer was modified for trials with BAPTA-AM by omitting 1.0 mM $CaCl_2$. There was a significant decrease in the rate of $^{36}Cl^-$ efflux from cells expressing pCLCA1 after treatment with BAPTA. (Fig 5.4.; ±BAPTA × time, $P < 0.001$). The activation of whole cell currents in Xenopus oocytes expressing a truncated form of the bCLCA1 channel by 10^{-7} M PMA was cited as evidence for channel activation by protein kinase C (PKC) (Ji, DuVall et al. 1998). The conservation of four C-kinase phosphorylation acceptor sites between hCLCA1 and pCLCA1 in the predicted cytoplasmic loop between TM3 and TM4 domains implies an importance of these sites in control of channel activity. However, there was only an insignificant effect of 1×10^{-7} M PMA on $^{36}Cl^-$ efflux from 3T3 cells transfected with pCLCA1 (Fig 5.5.; ±pCLCA1 in presence of PMA × time, $P = 0.106$).

5.4.3 Antagonist and Blockers

There are also conserved CaMKII phosphorylation sites in hCLCA1 and pCLCA1. The CaMKII inhibitor KN-93 (Sumi, Kiuchi et al. 1991) was added to pCLCA1-transfected 3T3 cells to test for any effects of this reportedly specific inhibitor on the ionomycin-dependent increase in $^{36}Cl^-$ efflux rate from these cells. Although the KN-93 inhibitor is reported to have an inhibition constant of 0.37 μM, there was no inhibitory effect on $^{36}Cl^-$ efflux when pCLCA1-transfected 3T3 cells were exposed to

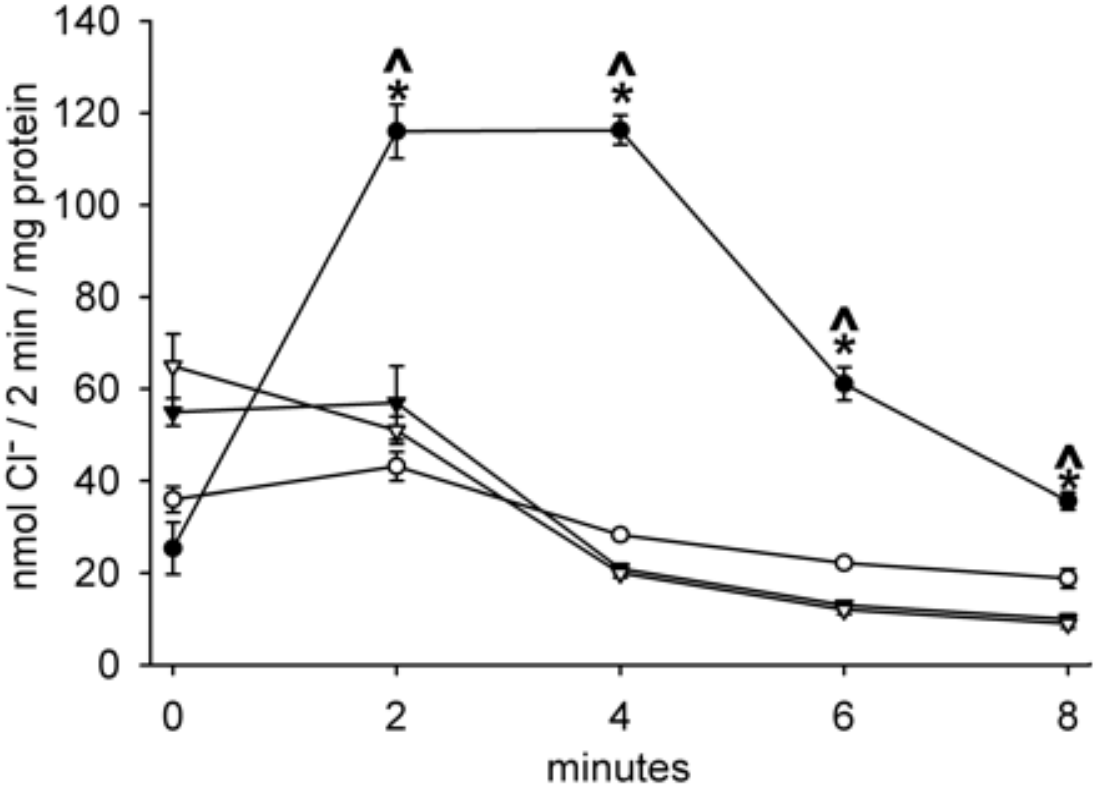

Figure 5.3. Effect of ionomycin addition on chloride efflux from pCLCA1-transfected NIH/3T3 fibroblasts. See legend to Fig. 2 for efflux conditions. ●, pCLCA1-transfected 3T3 cells with 10 μM ionomycin added at time 0; ○, pCLCA1-transfected 3T3 cells without ionomycin; ▽, pcDNA3.1 (control)-transfected 3T3 cells with 10 μM ionomycin added at time 0; ▼, pcDNA3.1 (control)-transfected 3T3 cells without 10 μM ionomycin. * Significant ionomycin effects on Cl^- efflux in pCLCA1-transfected cells. ^ Significant effect of pCLCA1 transfection on ionomycin-dependent Cl^- efflux. Values are means ± SE (n = 6).

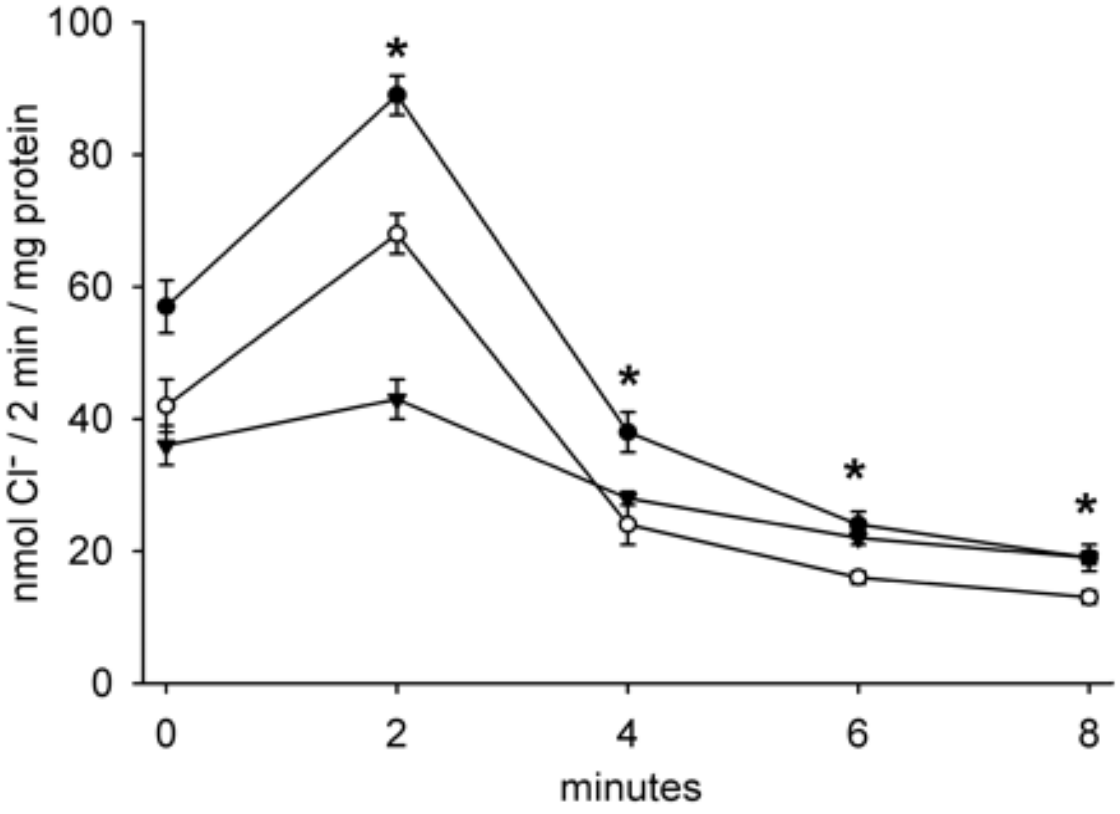

Figure 5.4. Effect of intracellular calcium chelation by 1,2-bis(2-aminophenoxy)ethane-N,N,N',N'-tetraacetic acid (BAPTA) on chloride efflux from pCLCA1-transfected 3T3 cells. BAPTA-AM (50 μM) was added to the ^{36}Cl-containing loading buffer 90 min before the effect of ionomycin addition was measured on chloride release. ●, Ionomycin (10 μM) added at time 0; ○, cells pretreated with BAPTA and then with ionomycin (10 μM) added at time 0; ▼, control, untreated cells. * Significant BAPTA effects on ionomycin-dependent Cl^- efflux. Values are means ± SE (n = 6)

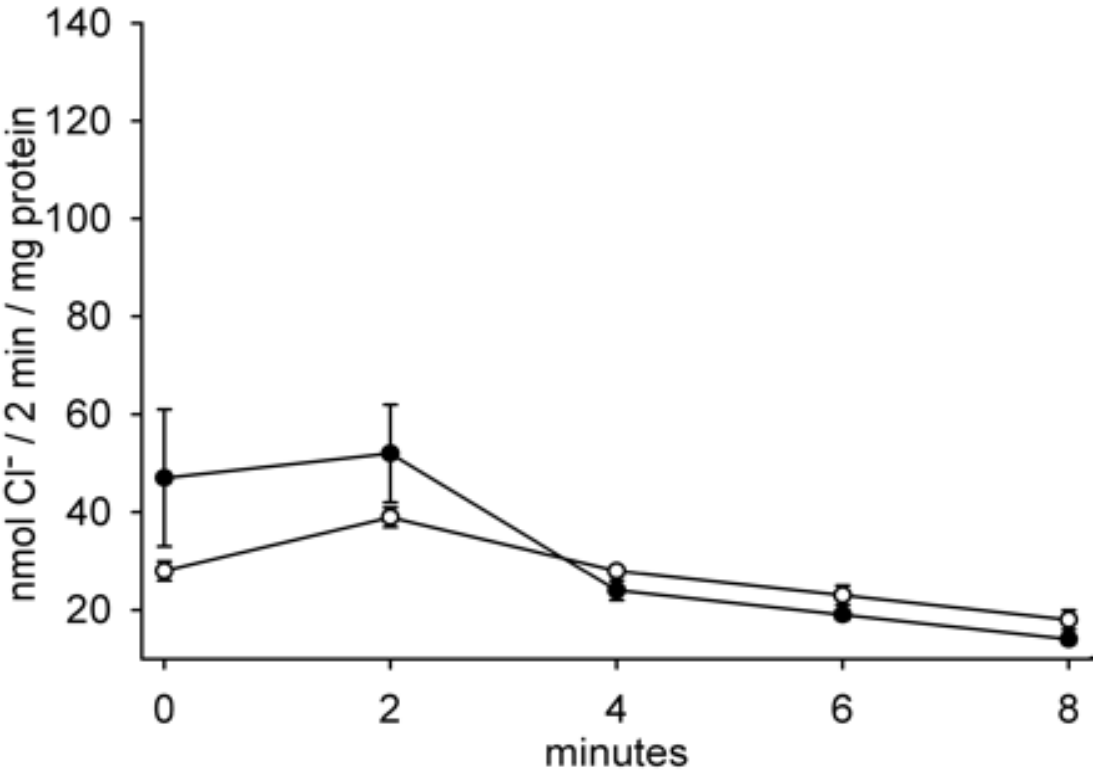

Figure 5.5. Effect of phorbol 12-myristate 13-acetate (PMA) on chloride efflux from control and pCLCA1-transfected NIH/3T3 fibroblasts. Cells were loaded and chloride efflux carried out as described in Fig. 2. PMA (100 nM) was added to efflux buffer at time 0. ○, 3T3 cells transfected with pCLCA1; ●, 3T3 cells transfected with pcDNA3.1 vector with no insert in polylinker region. Values are means ± SE (n = 8)

20 μM KN-93 for 1 h before $^{36}Cl^-$ efflux was stimulated by addition of ionomycin (Figure 5.6.). Statistical analysis of ±KN-93 in the presence of ionomycin × time gave a significant ionomycin-KN-93 interaction (P = 0.03). Post-ANOVA analysis indicated KN-93 effects approaching significance (e.g., for 2-min time, P = 0.061).

In addition to being able to distinguish chloride transporters by the second messenger signal pathways involved in their activation, it would be helpful to distinguish channels or to be able to rule out particular channels as contributors to an endogenous chloride conductance through the use of specific ion channel inhibitors. DTT was reported to inhibit chloride currents that could be due to the native form of bCLCA1 (Cunningham, Awayda et al. 1995) as well as the other isoforms that have been the efflux of ^{36}Cl- from 3T3 fibroblasts expressing pCLCA1 (data not shown) expressed for functional study. We found that the reducing agent DTT did not inhibit. DIDS is recognized as an inhibitor of whole cell and single-channel chloride currents mediated by CLCA proteins. Addition of DIDS to 3T3 cells transfected with pCLCA1 had no effect on the rate of ionomycin-dependent release from these cells. The $^{36}Cl^-$ efflux response in the presence of 500 μM DIDS (Fig. 5.7.; ±DIDS in the presence of ionomycin × time, P = 0.71) was similar to the lack of effect observed at a concentration of 100 μM DIDS (not shown).

Glibenclamide has been reported to be a relatively specific inhibitor of the chloride transport activity of CFTR. Addition of glibenclamide to the cell wash solutions and to the efflux medium at a concentration of 100 μM reduced the initial rate of ionomycin dependent $^{36}Cl^-$ efflux from pCLCA1-transfected 3T3 cells (Figure 5.8; ±glibenclamide in the presence of ionomycin × time, P = 0.044). Ionomycin-dependent

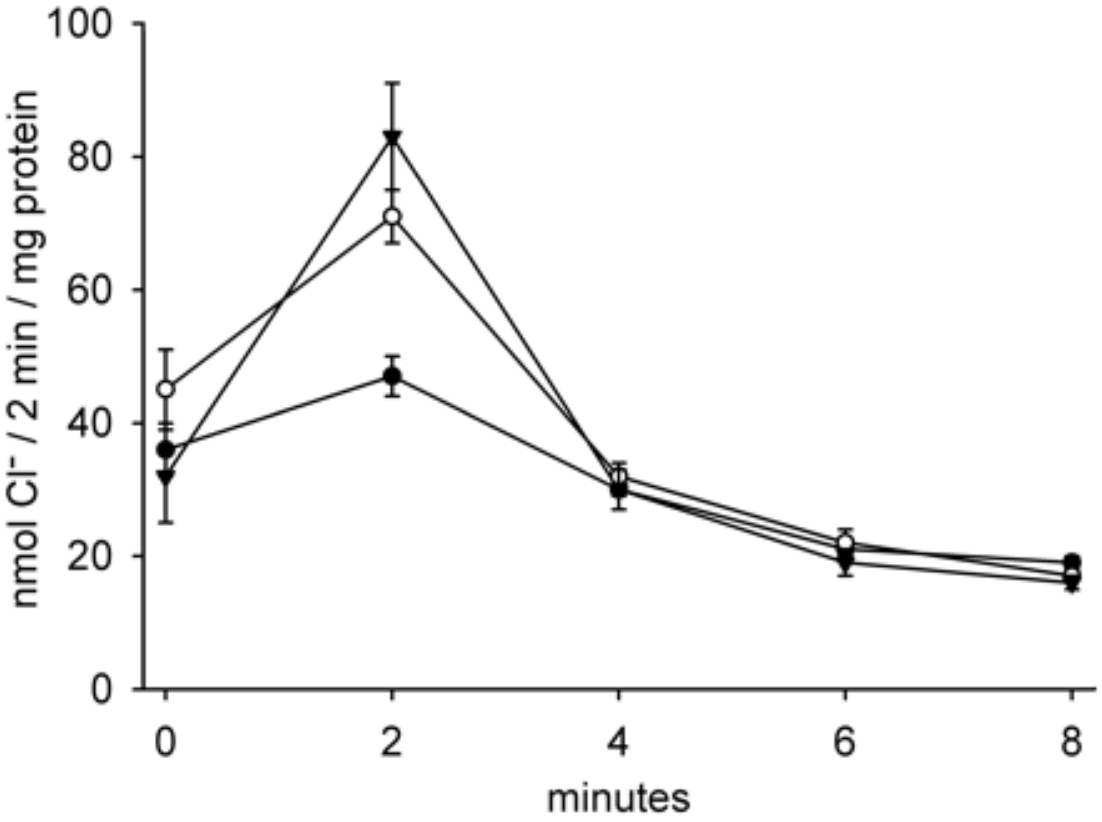

Figure 5.6 Inhibition of ionomycin-dependent chloride efflux from pCLCA1-transfected 3T3 cells by calcium-calmodulin kinase inhibitor KN-93. Loading and efflux conditions were as described for Fig. 2. Ionomycin (10 μM) was added at time 0. ○, Ionomycin alone; ▼, ionomycin plus 20 μM KN-93; ●, pCLCA1 control without ionomycin. Values are means ± SE (n = 6)

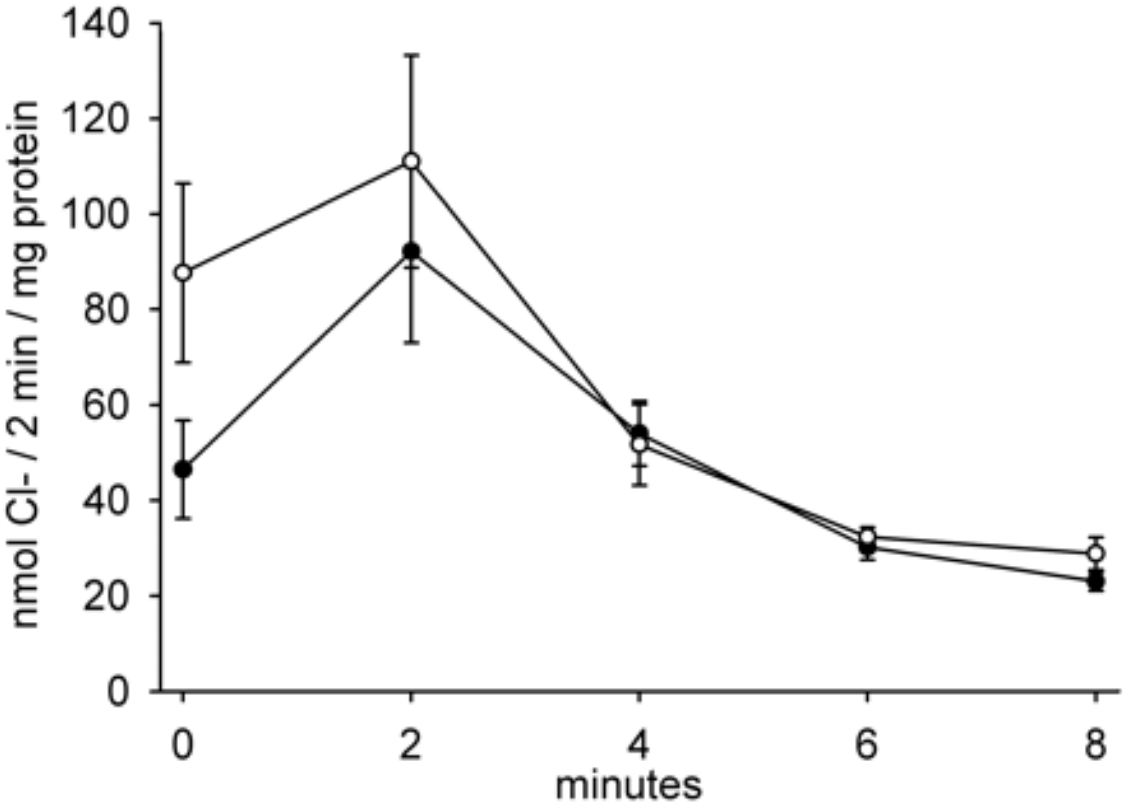

Figure 5.7. Effect of 4,4'-diisothiocyanostilbene-2,2'-disulfonic acid (DIDS) on ionomycin dependent chloride efflux from pCLCA1-transfected 3T3 cells. Loading and efflux conditions were as described for Fig. 3. Ionomycin (10 μM) was added to all cells at time 0. ●, Ionomycin alone, with no DIDS added; ○, DIDS (500 μM) present in efflux buffer during the 5 washes and for the first 8 min of the efflux, with ionomycin added at time 0. Values are means ± SE (n = 6).

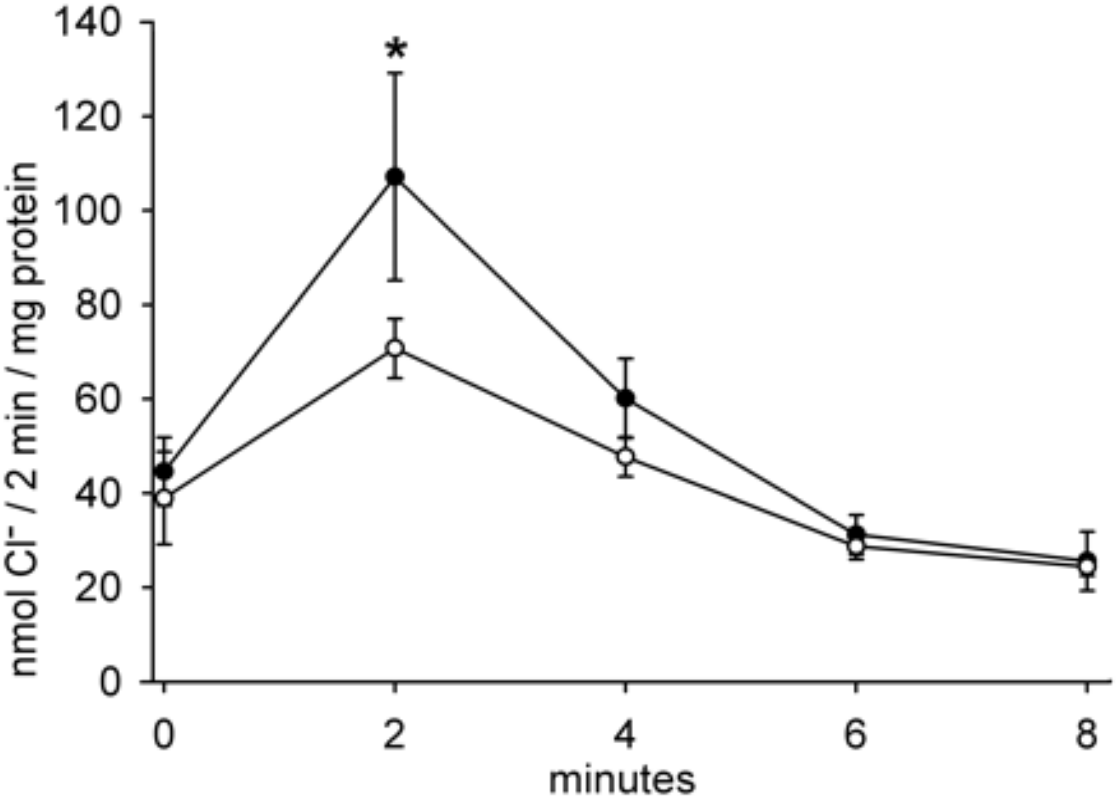

Figure 5.8. Inhibition of ionomycin-dependent chloride efflux from pCLCA1-transfected 3T3 cells by glibenclamide. Loading and efflux conditions were as described for Fig. 2. Ionomycin (10 μM) was added to all cells at time 0. ●, Ionomycin alone, with no glibenclamide added; ○, glibenclamide (100 μM) present in efflux buffer during the 5 washes and for the first 8 min of the efflux, with ionomycin added at time 0. * Significant effect of glibenclamide on ionomycin-dependent Cl^- efflux. Values are means ± SE (n = 6).

$^{36}Cl^-$ efflux from pCLCA1-transfected 3T3 cells was inhibited by other anion channel blockers that fall in the broad category of lipid-soluble anions. α-PC, DPC, and NPPB all inhibited $^{36}Cl^-$ efflux from loaded cells when used at concentrations employed by others for this purpose. Walsh et al. (Walsh, Long et al. 1999) have reported a Ki value of 130 μM for the inhibition of CFTR-mediated chloride conductance by NPPB. Preliminary investigations into the apparent affinity of DPC and NPPB for inhibition of $^{36}Cl^-$ efflux indicated that both of these inhibitors were effective at concentrations as low as 10 μM for DPC (Fig.5.9; ±10 μM DPC, $P = 0.012$) and 50 μM for NPPB (Figure. 5.10.; ±50 μM NPPB, $P < 0.001$). Hence, it appears that distinctive inhibitor affinities could be investigated as a tool for discriminating between possibly competing chloride conductance proteins until a thorough search for specific inhibitors can be completed (Hipper, Mall et al. 1995).

α-PC has been reported to inhibit conductive chloride uptake by ileal mucosal brush border vesicles (Forsyth and Gabriel 1989b). The anion conductance in this vesicle system was inhibited by the monoclonal antibody that was used to clone pCLCA1 from a porcine small intestinal cDNA library. These circumstances would lead to the prediction that α-PC may be an inhibitor of expressed pCLCA1 activity. The rate of ionomycin-dependent chloride efflux from 3T3 cells transfected with pCLCA1 was significantly reduced by the inclusion of α-PC in the efflux buffer (Figure 5.11.; ± α-PC in the presence of ionomycin × time, $P < 0.001$).

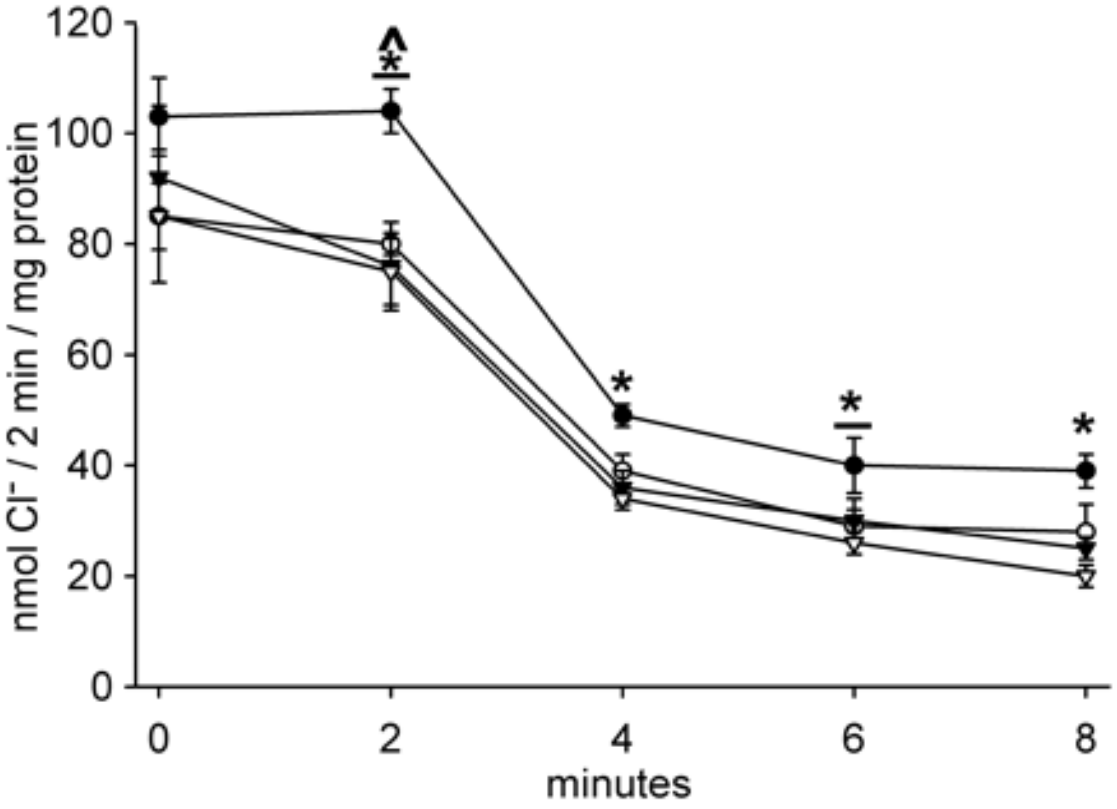

Figure 5.9. Inhibition of ionomycin-dependent chloride efflux from pCLCA1-transfected 3T3 cells by diphenylamine carboxylate (DPC). Loading and efflux conditions were as described for Fig. 2. Ionomycin (10 μM) was added to all cells at time 0. ●, Ionomycin alone, with no DPC added; ○, ionomycin plus 10 μM DPC; ▼, ionomycin plus 50 μM DPC; ▽, ionomycin plus 200 μM DPC. * Significant inhibition of Cl^- efflux by 200 μM DPC. ^ Significant inhibition of Cl^- efflux by 50 μM DPC. ⁻ Significant inhibition of Cl^- efflux by 10 μM DPC. Values are means ± SE (n = 6)

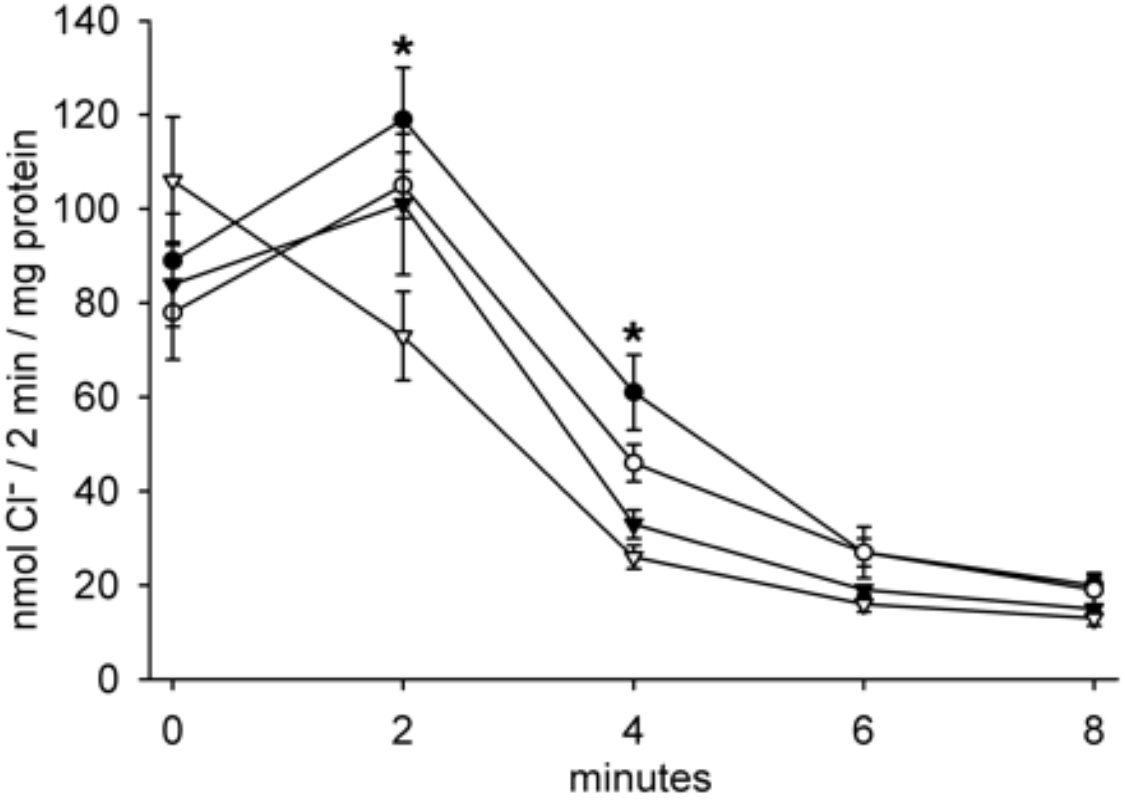

Figure 5.10. Inhibition of ionomycin-dependent chloride efflux from pCLCA1-transfected 3T3 cells by 5-nitro-2-(3-phenylpropylamino) benzoate (NPPB). Loading and efflux conditions were as described for Fig. 2. Ionomycin (10 μM) was added to all cells at time 0. ●, Ionomycin alone, with no NPPB added; ○, ionomycin plus 2 μM NPPB; ▼, ionomycin plus 10 μM NPPB; ▽, ionomycin plus 50 μM NPPB. * Significant effect of 50 μM NPPB on ionomycin-dependent Cl^- efflux.Values are means ± SE (n = 6

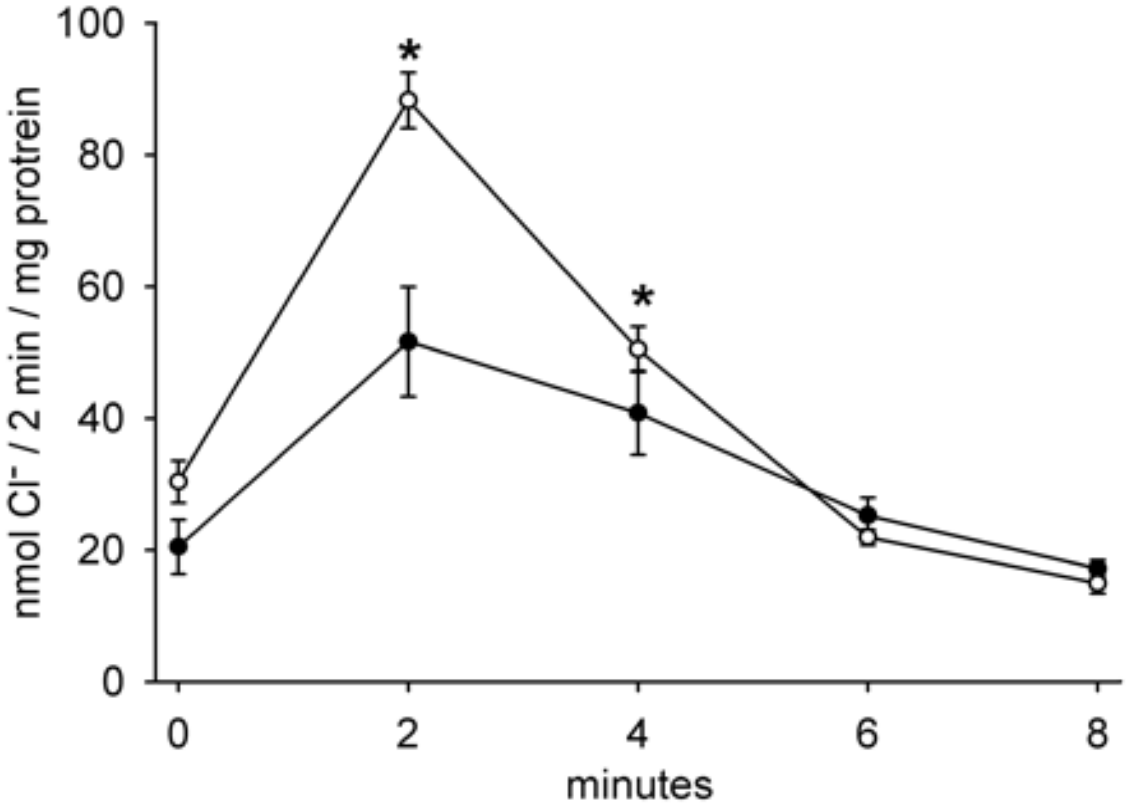

Figure 5.11. Inhibition of ionomycin-dependent chloride efflux from pCLCA1-transfected 3T3 cells by α - phenylcinnamate (α - PC). Loading and efflux conditions were as described for Fig. 2. Ionomycin (10 μM) was added to cells at time 0. ●, Ionomycin alone, with no α-PC added; ○, ionomycin plus 100 μM α-PC. * Significant effect of 100 μM α -PC on ionomycin-dependent Cl^- efflux. Values are means ± SE (n = 6).

5.4.4. Whole Cell Patch Clamp

pCLCA1 contributes to an outwardly rectifying calcium-activated chloride current when expressed in the NIH/3T3 cell line. Transfection of NIH/3T3 cells with pCLCA1 significantly increased an outwardly rectifying calcium-activated chloride current above the levels present in cells transfected with pcDNA3 vector (Figure 5.12). The current density in a high-chloride bath solution (156 mM Cl) was significantly higher than in controls at 40, 80, and 100 mV in the pCLCA1-transfected cell line (±pCLCA1 vs. voltage, $P < 0.001$, $n = 8$). The E_{rev} in the pCLCA1-transfected cell line (-10.3 ± 2.8 mV, $n = 8$) was significantly more negative than the E_{rev} measured in the vector control cell line (0.7 ± 2.6 mV, $n = 8$, $P = 0.027$).

The current density in a low-chloride bath solution (46 mM Cl) was significantly higher than in controls at 80, 60, 80, and 100 mV in the pCLCA1-transfected cell line (±pCLCA1 vs. voltage, $P < 0.001$, $n = 8$). The E_{rev} in the pCLCA1-transfected cell line shifted significantly from that seen in the high-chloride bath solution (0.7 ± 2.9 mV, $n = 8$, $P = 0.036$), fulfilling one criterion of a chloride current (Figure 5.13). However, the E_{rev} did not shift on transfer of the pcDNA3, control-transfected cell line to the bath solution containing 46 mM Cl^- (0.8 ± 2.1 mV, $n = 8$). No difference was found between the E_{rev} of the two cell lines at low chloride concentrations.

The effect of anionic current inhibitors on whole cell currents in pCLCA1-transfected and control cell lines was measured because the E_{rev} deviated from the theoretical value for a pure chloride current. Whole cell currents were studied in the presence of inhibitory concentrations of DPC, α-PC, NPPB, and DIDS. The case for the mediation of a chloride conductance by pCLCA1 was supported by inhibition of the

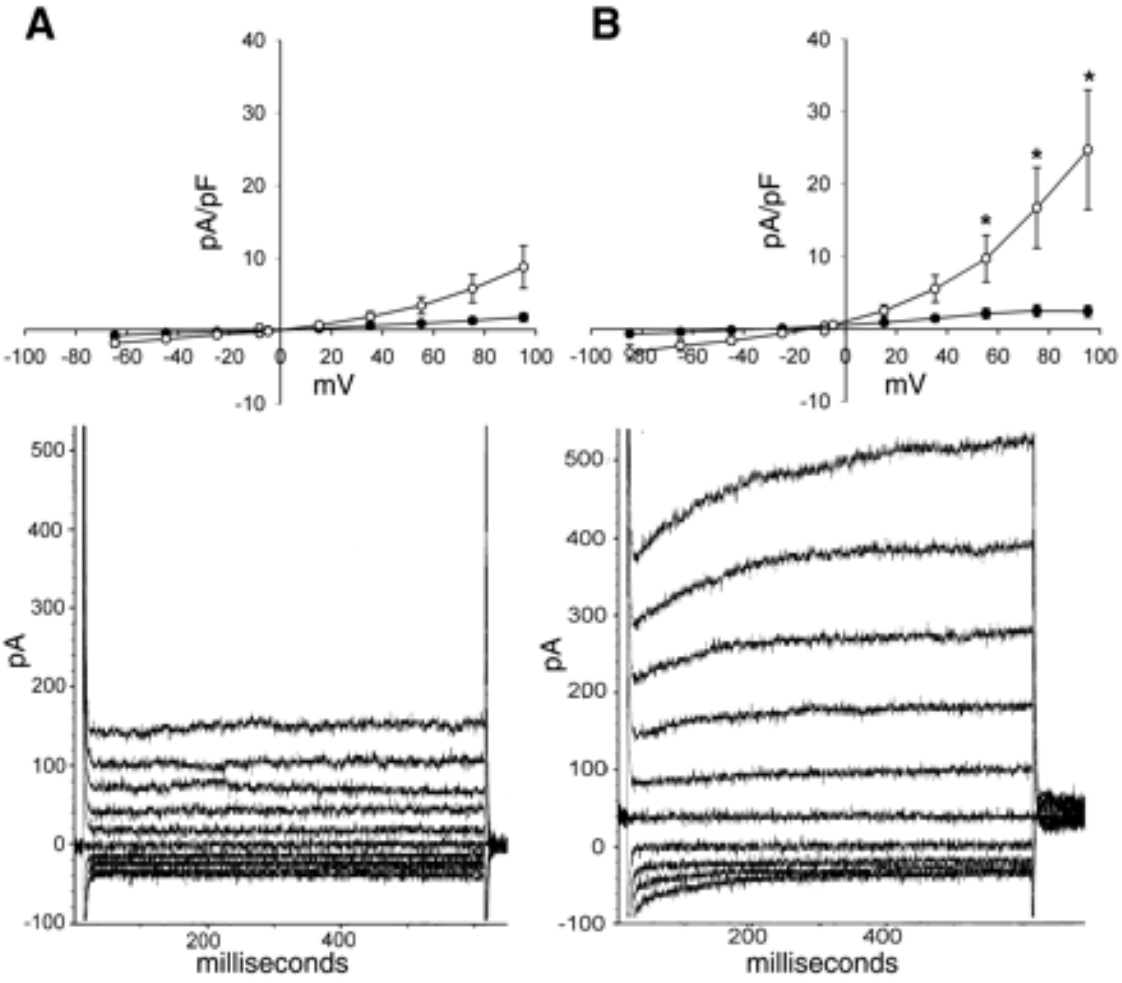

Figure 5.12. Effect of ionomycin on whole cell chloride currents in NIH/3T3 fibroblasts transfected with the pcDNA3.1 vector or with the vector containing pCLCA1 cDNA. Current (bottom) vs. 20-mV increments in transmembrane potential (top) are shown for control cells transfected with vector alone (A) and for cells transfected with pcDNA3 containing pCLCA1 cDNA (B).○ , 10 μm ionomycin added to cells at t = 0; ●, no ionomycin added. $P < 0.001$ for voltage × gene interaction (2-way repeated-measures ANOVA). * Voltages at which current is significantly higher in cells transfected with pCLCA1 (post-ANOVA multiple comparison analysis). At 42 mM internal Cl^- and 156 mM external Cl, the mean E_{rev} values were 0.74 ± 2.6 mV for control-transfected cells and -10.3 ± 2.8 mV for pCLCA1-transfected cells ($P = 0.027$). Representative current-voltage tracings are given for each cell line. Values are means ± SE (n = 8).

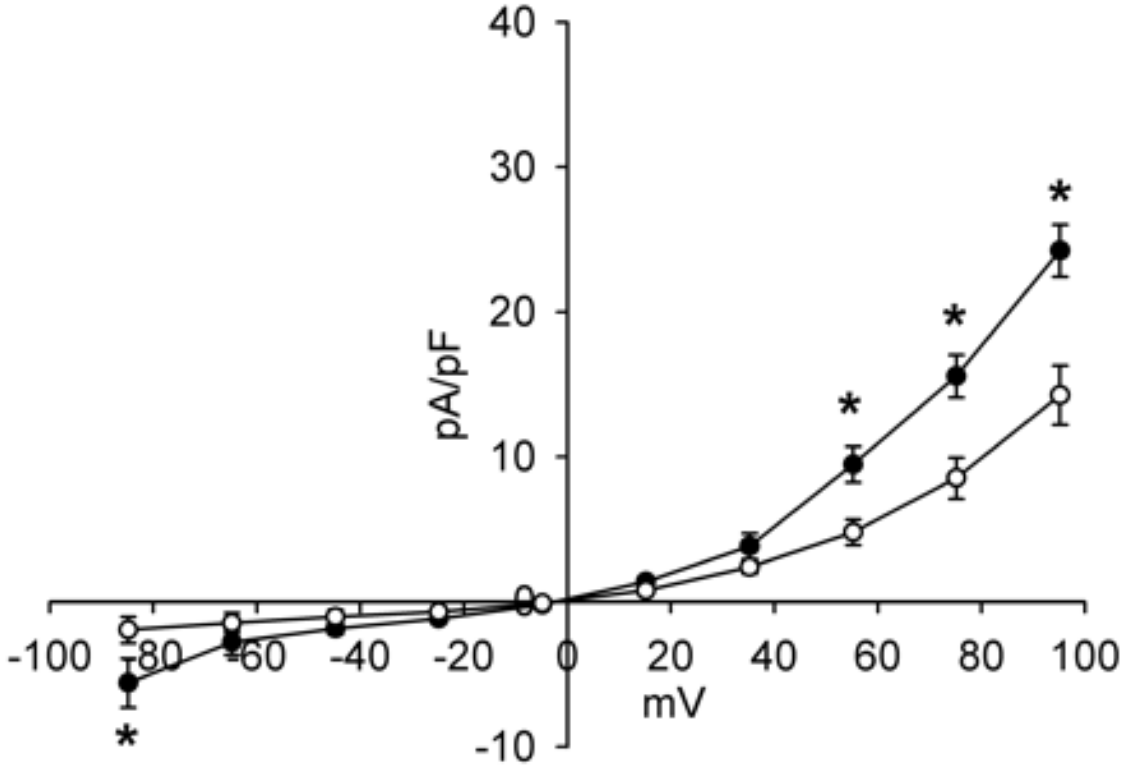

Figure 5.13. Whole cell current-voltage relationship in control- and pCLCA1-transfected NIH/3T3 fibroblasts with symmetrical chloride concentrations. E_{rev} values were 0.76 ± 2.1 mV for controls and 0.73 ± 3.0 mV for pCLCA1-transfected cells (P = 0.99) with pipette and extracellular chloride concentrations at 44 and 46 mM, respectively. ○, control-transfected cells; ●, pCLCA1-transfected cells. P < 0.001 for voltage × gene interaction (2-way repeated-measures ANOVA). * Voltages at which current is significantly higher in cells transfected with pCLCA1 (post-ANOVA multiple comparison analysis). Values are means ± SE (n = 8)

whole cell current by DPC, α-PC, and NPPB (Figure 5.14.); compared with controls, P values were 0.027, 0.009, and 0.011, respectively, for these inhibitors. There was no significant effect of inhibitors on whole cell currents from control pcDNA3-transfected cells.

5.5. Discussion

The presence of calcium-dependent electrogenic chloride currents in fibroblasts transfected with pCLCA1 cDNA is an indication of the identity of a component of the secretory apparatus in porcine small intestine. There is a significant amount of evidence pointing to a signaling role for calcium in this tissue. Ricinoleate and the bile acid deoxycholate have calcium ionophore activity and calcium-dependent secretory activity when placed in the lumen of the porcine small intestine (Maenz and Forsyth 1982). Even the secretory effects of cholera toxin have been reported to operate in this tissue through calcium ionophore activity present in the A-subunit of the enterotoxin (Maenz, Gabriel et al. 1987). This feature is particularly salient in the porcine small intestine where cholera toxin causes fluid secretion without detectable increases in cAMP concentration (Forsyth, Hamilton et al. 1978a). Though there is very little evidence for calcium-dependent chloride conductance in mouse and human small intestine, these species have calcium-dependent chloride conductance in other important secretory tissues including the tracheal epithelium (Grubb and Gabriel 1997; Gabriel, Makhlina et al. 2000). Upregulation of a calcium-dependent chloride conductance may occur as a compensatory response to a loss of CFTR function in the trachea(Gabriel, Makhlina et al. 2000). The failure to observe calcium-dependent chloride conductance in small

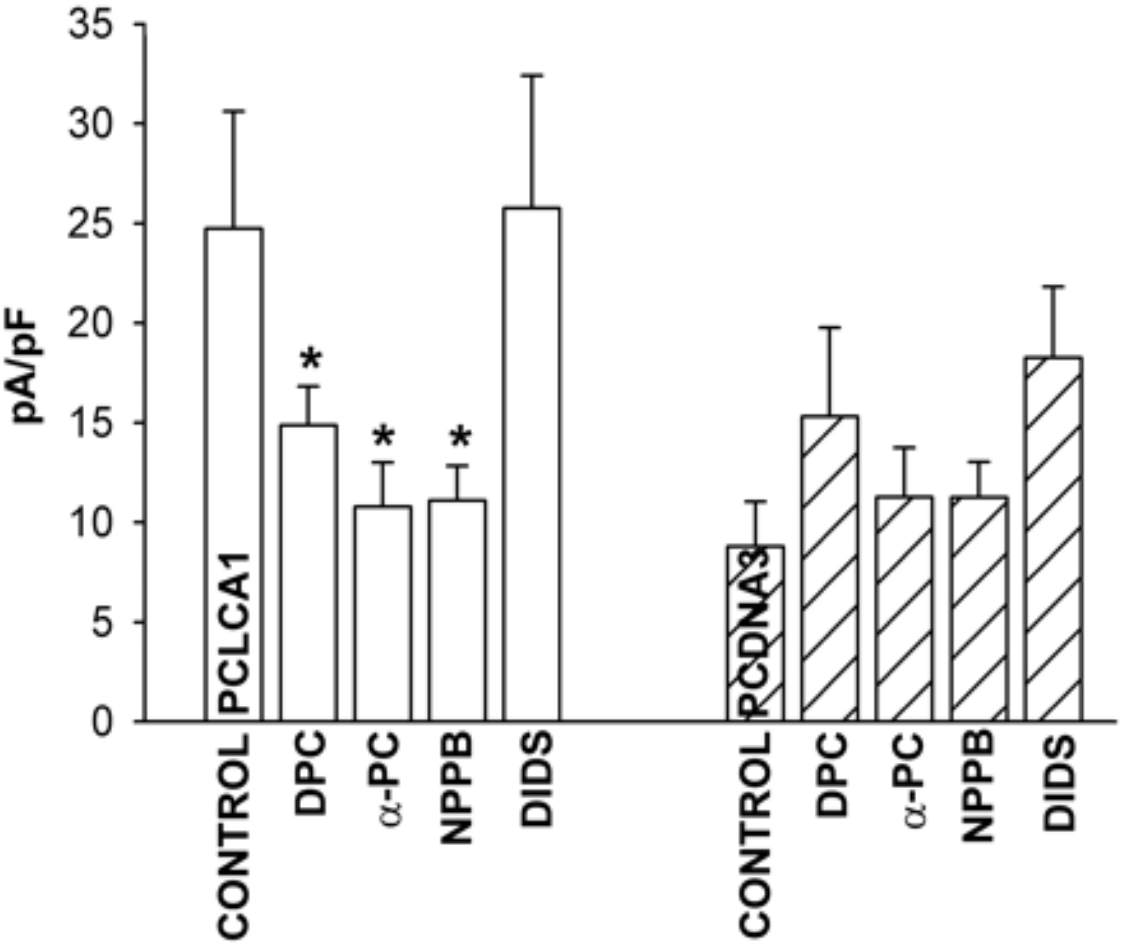

Figure 5.14. Effect of inhibitors on whole cell patch-clamp currents at +100 mV in pCLCA1- and pcDNA3 transfected 3T3 cells. Open bars, 3T3 cells expressing pCLCA1; hatched bars, 3T3 control cells. Final inhibitor concentrations were 100 μM DPC, 100 μM α-PC, 50 μM NPPB, and 300 μM DIDS. * Significant difference from whole cell current measured in uninhibited pCLCA1 cells (1-way ANOVA with post ANOVA Fisher LSD test). Values are means ± SE (n = 8).

intestine of cystic fibrosis patients (Taylor, Baxter et al. 1988) may also be a reflection of a regulatory interdependence of proteins involved in chloride conductance.

The absence of a chloride efflux response to cAMP in pCLCA1-transfected cells raises questions about the role of the strong A-kinase consensus site located on what appears to be an important cytosolic loop of this protein. More complex combinatorial experiments are required to investigate possible interactions between A- and C-kinase phosphorylation acceptor sites that could be involved in regulating the conductance activity associated with pCLCA1 transfections. The effects of simultaneous activation of two or more classes of protein kinase acceptor sites remain to be determined.

Conservation of C-kinase sites between hCLCA1 and pCLCA1 isoforms could be construed as evidence of a role for these acceptor sites in channel regulation. This proposed role is supported by evidence of activation of bCLCA1 conductance by PMA. However, the failure of treatment with PMA to increase the rate of chloride efflux from pCLCA1-transfected cells creates significant uncertainty about the role of C-kinase in the stimulation of this conductance by calcium. Activation of the A-isoform of C-kinase by PMA or epidermal growth factor is reported to inhibit tissue short-circuit currents induced by forskolin or carbamyl choline (Chow, Uribe et al. 2000; Song, Hanson et al. 2001). Although a component of these inhibitory effects could also be operating via a basal potassium conductance, it is clear that there is no necessary connection between C-kinase activation and increased calcium-dependent chloride conductance. At least the evidence in this study of the reduced rate of ionomycin-dependent $^{36}Cl^-$ efflux from cells treated with the intracellular calcium chelator BAPTA reinforces the assumption that Ca^{2+} is directly involved in the regulation of pCLCA1 activity.

The role of disulfide bonding in stabilizing CLCA channel structure and activity is somewhat controversial. Polypeptides arising from post translational cleavage of bCLCA1 may require disulfide bonding to retain conformation or aggregation properties necessary for function. However, the lack of an inhibitory DTT effect on chloride conductance activity of non glycosylated forms of bCLCA1 is not completely consistent with a role for disulfide bonding in structural stabilization (Fuller and Benos 2000b; Fuller and Benos 2000a). The predicted amino acid sequence of pCLCA1 contains conserved post translational cleavage sites found in bCLCA1 and hCLCA1, but post translational processing has not been investigated for this protein. We conclude that there is no evidence for a requirement for disulfide bonding in pCLCA1 translation products in assays measuring the rate of $^{36}Cl^-$ efflux from transfected 3T3 fibroblasts.

The chloride conductance of most endogenous calcium-activated chloride channels is inhibited by DIDS. The overall similarity of predicted amino acid sequence between hCLCA1 and pCLCA1 leads to a prediction of similar charge distribution and geometry for an anion pore involved in chloride transport. However, there are also significant differences in amino acid sequence that could affect the access of a bulky organic anion like DIDS to inhibitory sites. There is no information currently available concerning the three-dimensional structure of a possible anion pore in the CLCA proteins.

Both NPPB and DPC inhibited $^{36}Cl^-$ efflux at relatively low concentrations. There was significant inhibition at 50 μM NPPB, consistent with reports of Ki values in the range of 22 μM for blockage of calcium-activated chloride currents in Xenopus oocytes (Wu and Hamill 1992; Hipper, Mall et al. 1995). Chloride conductance by

CFTR is also reported to be inhibited by NPPB, but significantly higher concentrations of NPPB are required (Ki = 166 μM) (Hipper, Mall et al. 1995; Walsh, Long et al. 1999). Hence, this inhibitor should be useful in distinguishing between the chloride conductance of pCLCA1 and CFTR.

Inhibitory concentrations of DPC and α-PC may also permit discrimination between alternate chloride conductance proteins as mediators of a measured chloride conductance. Nishikawa et al. (Nishikawa, Ishihara et al. 1995) reported that chloride influx into porcine tracheal submucosal glands was inhibited by 10^{-9} M DPC. Maximal inhibition of $^{36}Cl^-$ efflux from pCLCA1-transfected 3T3 cells was obtained at 10 μM DPC in this study, although lower concentrations were not investigated. Much higher concentrations of DPC are necessary to inhibit CFTR (reported Ki values of 280 μM for internal application) (Zhang, Zeltwanger et al. 2000). α-PC is a potential specific inhibitor of pCLCA1, but its effects on CFTR-mediated chloride conductance have not been reported.

Previous investigations of cloned pCLCA1 function were based on net *in situ* $^{36}Cl^-$ efflux from cells grown as confluent monolayers. Whole cell chloride current measurements provide the information necessary to distinguish between anion exchange and electrogenic ion transport (Racette, Gabriel et al. 1996; Gaspar, Racette et al. 2000). The increased current density in pCLCA1-transfected cell lines over control-transfected cells and the Nernstian shift of E_{rev} on introduction to a low-chloride bath solution provide a rigorous demonstration of the electrogenic movement of chloride that cannot be supplied by $^{36}Cl^-$ efflux. However, in a bath solution with high chloride concentration, the calculated E_{rev} using the Nernst equation at 25°C is 32.4 mV. This

calculated value is significantly different from the measured E_{rev} of 10.26 ± 2.8 mV. This deviation of the measured from the calculated Erev is assumed to be caused by an undefined endogenous calcium-activated current. The contaminating endogenous current in control-transfected cells had an Erev of 0.738 ± 2.6 mV, in violation of the Nernst equilibrium potential for chloride with a bath solution concentration of 156 mM and a pipette solution at 44 mM Cl. The E_{rev} of this current was unaffected upon a shift to low chloride concentration (46 mM) in the bath solution. The identity of the conductive ion affecting the E_{rev} values for the channel is difficult to discern. The ionic compositions of bath and pipette solutions were set to permit direct identification of the ion producing the current from E_{rev} values. However, the measured Erev was not consistent with a current attributable to any single ionic species in the bathing solution.

The activation of both cationic and anionic channels, or a channel with a high permeability to both cations and anions could have produced the observed result. The calculated E_{rev} for sodium is 128.7 mV in our high-chloride bath solution. A significant increase in sodium permeability would cause a positive shift from the expected chloride E_{rev}. Cation permeability of anion channels is known, and anion channels with PNa^+/PCl^- ratios as high as 0.2 have been reported (Franciolini and Nonner 1987; Qu and Hartzell 2000; Hille 2001). In our case an endogenous chloride channel with some cation permeability could alter the E_{rev} at high bath chloride concentration without shifting the E_{rev} when both sodium and chloride concentrations were reduced.

The identity of the anionic current associated with pCLCA1 expression was confirmed by an electrogenic response distinctive from endogenous contaminating currents and by the reduction of ionomycin-induced currents to control levels by anionic

conductance inhibitors. Additional confirmation was provided by the lack of effect of anion conductance inhibitors on the basal levels of contaminating current in cells transfected only with the expression vector. The nature of the contaminating current has not been pursued beyond its insignificant response to these inhibitors.

The pathophysiological significance of a calcium-activated chloride current in the airway epithelium is well established. Expression of pCLCA1 in tracheal epithelium has been documented (Gaspar, Racette et al. 2000). The current studies support the role of pCLCA1 as a chloride conductance mediator. The extent to which this protein contributes to the *in vivo* conductance in both the presence and absence of a functional CFTR molecule is an area for future investigation.

Chapter 6. pCLCA1 BECOMES A cAMP-DEPENDENT CHLORIDE CONDUCTANCE MEDIATOR IN CACO-2 CELLS

6.1. Abstract

Members of the CLCA protein family are expressed in airway and intestinal epithelium, where they may participate in secretory activity as mediators of chloride conductance. A calcium-dependent chloride conductance has been observed upon expression of CLCA proteins in non-epithelial cell lines. The pCLCA1 gene, cloned in our laboratory, codes for a product containing a unique A-kinase consensus acceptor site not found in other CLCA proteins. Calcium-dependent, but not cAMP-dependent, chloride conductance increased when pCLCA1 was expressed in NIH/3T3 fibroblasts. We transfected the Caco-2 human colon carcinoma cell line with pCLCA1 to investigate the regulation of CLCA-associated chloride conductance in this differentiated epithelial cell line. Expression of pCLCA1 in the Caco-2 cell line enhanced cAMP-responsive $^{36}Cl^-$ efflux, short circuit current, and whole cell chloride current in these cells. This cAMP-dependent chloride conductance was localized to the apical membrane of polarized Caco-2 cells.

6.2. Introduction

The CLCA protein family was named for the appearance of a calcium-activated chloride conductance upon its expression in undifferentiated HEK293 cells. The family

includes a group of structurally related proteins with diverse functions ranging from promoting chloride transport to cellular adhesion and anti-tumor actions (Elble, Widom et al. 1997; Gruber, Elble et al. 1998; Gruber and Pauli 1999c; Gaspar, Racette et al. 2000). Chloride conductance in porcine enterocytes and net fluid secretion into the intestinal lumen can be activated by cAMP, cGMP, or by calcium ionophores (Scoot, Forsyth et al. 1980; Maenz and Forsyth 1987; Forsyth and Gabriel 1989a). A monoclonal antibody that inhibited cAMP-dependent chloride conductance in pig ileal brush border vesicles (Racette, Gabriel et al. 1996) was used to clone the pCLCA1 cDNA (Gaspar, Racette et al. 2000). There was 78% amino-acid sequence identity of pCLCA1 compared to the hCLCA1 sequence reported by Gruber et al. (Gaspar, Racette et al. 2000). Prominent differences between the two predicted protein structures included a strong A-kinase consensus site on the cytoplasmic loop between the putative TM3 and TM4 domains of pCLCA1. Expression of the pCLCA1 protein in NIH/3T3 fibroblasts induced a calcium-dependent chloride efflux and an outwardly rectified chloride current in transfected cells (Loewen, Gabriel et al. 2002). However, cAMP addition had no effect on the rate of chloride efflux from NIH/3T3 cells transfected with the pCLCA1 gene (Gaspar, Racette et al. 2000; Loewen, Gabriel et al. 2002).

We hypothesized that native physiological regulation and function of pCLCA1 may require expression in an epithelial cell line. Caco-2 cells were chosen as an expression system for their polarized, epithelial, growth characteristics. In addition to a gut epithelial origin, the lack of endogenous CLCA expression makes these cells a convenient model to study pCLCA1 function.

We report here that the expression of the pCLCA1 gene in the polarized Caco-2 intestinal epithelial cell line increased the endogenous cAMP-sensitive chloride efflux, apical short circuit current, and linear whole cell current in these cells.

6.3. Materials and Methods

6.3.1. Materials

Tissue culture media, G418 antibiotic, and Superscript II reverse transcriptase were purchased from Gibco Life Technologies, Taq and Pfu polymerases were from Stratagene, and $^{36}Cl^-$ was from New England Nuclear. Oligonucleotides were synthesized at the Core DNA Services Laboratory, University of Calgary.

6.3.2. Cell lines

Caco-2 cells were grown in DMEM as described previously (Gaspar, Racette et al. 2000). Permanent transfectants were maintained with 500 μg/ml of G418 in the growth medium. mRNA expression. RT-PCR was performed as previously described (Loewen, Bekar et al. 2002). Reverse transcriptase was primed with oligo dT. Antisense and sense primers chosen to amplify pCLCA1or hCLCA1 (5'-CAGGTTGGTCTTATCGACAG-3') and (5'-ACGATGCAAATGGTCGATACAG-3') were used to produce a common 565 base-pair product from cDNA. PCR for CFTR was primed with CF4234a (5' GCACTGGGTTCATCAAGCAG-3') and CF3578s (5'-CCAGCATAGATGTGGATAG-3') primers to amplify a 738 base-pair fragment.

6.3.3. Chloride Efflux

Caco-2 cell $^{36}Cl^-$ efflux response to addition of 10 μM forskolin and 2.0 mM isobutylmethylxanthine (IBMX) was measured as reported previously (Gaspar, Racette

et al. 2000; Loewen, Gabriel et al. 2002). Briefly, confluent monolayers of cells grown in 3 cm dishes were loaded for 2 h in isotonic medium containing $^{36}Cl^-$ (2 Ci/ml). After five rapid washings, efflux was initiated at time zero by adding and replacing isotonic efflux solution at 2 min intervals. Efflux agonist (10 M forskolin and 2 mM IBMX) was present from time zero. $^{36}Cl^-$ removed at 2-min intervals, and remaining in cells at the end of a 10-min efflux protocol, was determined by liquid scintillation counting. The rate constant for chloride release was calculated as: (0.5 (ln ((cell [Cl-]t1)/(cell[Cl-]t2)))).

6.3.4. Short Circuit Current Measurements

Differentiated monolayers of Caco-2 cells expressing pCLCA1 or control cells transfected with the pcDNA3 vector were mounted in Ussing chambers and equilibrated for 20 min in standard Krebs Bicarbonate Ringer's solution with 10 mM basal glucose and 10 mM apical mannitol prior to recording short circuit current (Isc) responses to addition of 10 μM forskolin and 2.0 mM IBMX. The response to the A-kinase agonist mixture was also measured across the apical membrane of confluent differentiated Caco-2 monolayers following permeabilization of the basal membrane by nystatin (Devor, Singh et al. 1999). Chloride gradients were established across monolayers of permeabilized cells by replacing chloride with gluconate and sodium and potassium with Tris. The high Cl- solution contained 147 mM Tris–Cl, 30 mM mannitol, 5 mM N-tris [hydroxymethyl]methyl-2-aminoethanesulfonic acid, 2 mM $CaCl_2$, and 1 mM $MgCl_2$, pH 7.4. The low Cl- solution contained 130 mM Tris–base, 130 mM -gluconic

acid, 17 mM Tris–Cl, 30 mM mannitol, 2 mM $CaCl_2$, and 1 mM $MgCl_2$, pH 7.4. A 100 mV potential was also imposed to drive chloride from the basal to apical cell surface.

6.3.5. Whole Cell Voltage–Clamp Studies

Patch clamp electrodes were pulled from borosilicate glass capillaries (outer diameter 1.5 mm; inner diameter 1.17 mm) with an inner filament (Harvard Apparatus, Edenbridge, UK) on a P-97 Flaming/Brown micropipette puller (Sutter Instrument). Patch pipettes had a tip resistance of 2–4 MΩ with solutions used in this study. Whole cell currents were acquired with an Axopatch 200B amplifier (Axon Instruments, Foster City, CA) at 10 kHz, and filtered at 2 kHz by a low pass Bessel filter with Clampex 8, and analyzed with Clampfit 8 (Axon Instruments). The standard voltage–clamp protocol had a holding potential of -80 mV, with voltage pulses applied for 800 ms from -100 to +100 in 20 mV increments. After a >1 GΩ seal was obtained, capacitance compensation was carried out before whole cell access. Subsequent to whole cell access, all cells were dialyzed for 2 min before recording. Only cells with a membrane resistance >10 times the access resistance were used. Current differences were normalized by whole cell capacitance recorded from an integrating 10 mV hyperpolarizing pulse. All membrane potentials were corrected at the time of analysis for the measured junction potential.

The pipette solution for intracellular dialysis contained 110 mM NaCl, 8 mM $MgCl_2$, 2.4 mM K_2HPO_4, 0.8 mM KH_2PO_4, 4 mM Na_2ATP, and 5 mM ethyleneglycol-bis-(-aminoethylether) N,N'-tetraacetic acid (EGTA), pH to 7.4 with NaOH. The high-chloride bath solution contained 135 NaCl, 2.4 mM K_2HPO_4, 0.8 KH_2PO_4, 3 mM $MgCl_2$, 1 mM $CaCl_2$, 10 mM glucose, and 80 mM sucrose, pH to 7.4 with NaOH. The

low-chloride bath solution contained 40 mM NaCl, 2.4 mM K_2HPO_4, 0.8 KH_2PO4, 3 mM $MgCl_2$, 1 mM $CaCl_2$, 10 mM glucose, and 270 mM sucrose, pH to 7.4 with NaOH. Single-cell, rapid solution changes were applied by using a gravity-fed Perfusion Fast-Step SF-77B perfusion system (Warner Instrument, Hamden CT).

Addition of 10 μM forskolin and 1 mM IBMX and changes in chloride concentration in the bath solution were achieved through a single-cell bath solution change.

6.3.6. Statistical Methods

Student's t-test was used to compare conductances in permeabilized cells. A two-way repeated measures ANOVA was used to compare overall and treatment by time effects. The Fisher LSD method for pairwise multiple comparisons was used as a post-ANOVA test to determine treatment effects at individual points.

6.4. Results

6.4.1. Effect of pCLCA1 on cAMP-stimulated $^{36}Cl^-$ Efflux

Caco-2 cells have an endogenous cAMP-responsive chloride conductance associated with high CFTR expression (Sood, Bear et al. 1992). Expression of pCLCA1 in Caco-2 cells caused a significant increase in the cAMP-sensitive rate of chloride efflux from these cells (Figure 6 .1., $P<0.001$). There was also a significant interaction between pCLCA1 transfection (±pCLCA1) and efflux time on Cl^- efflux rate

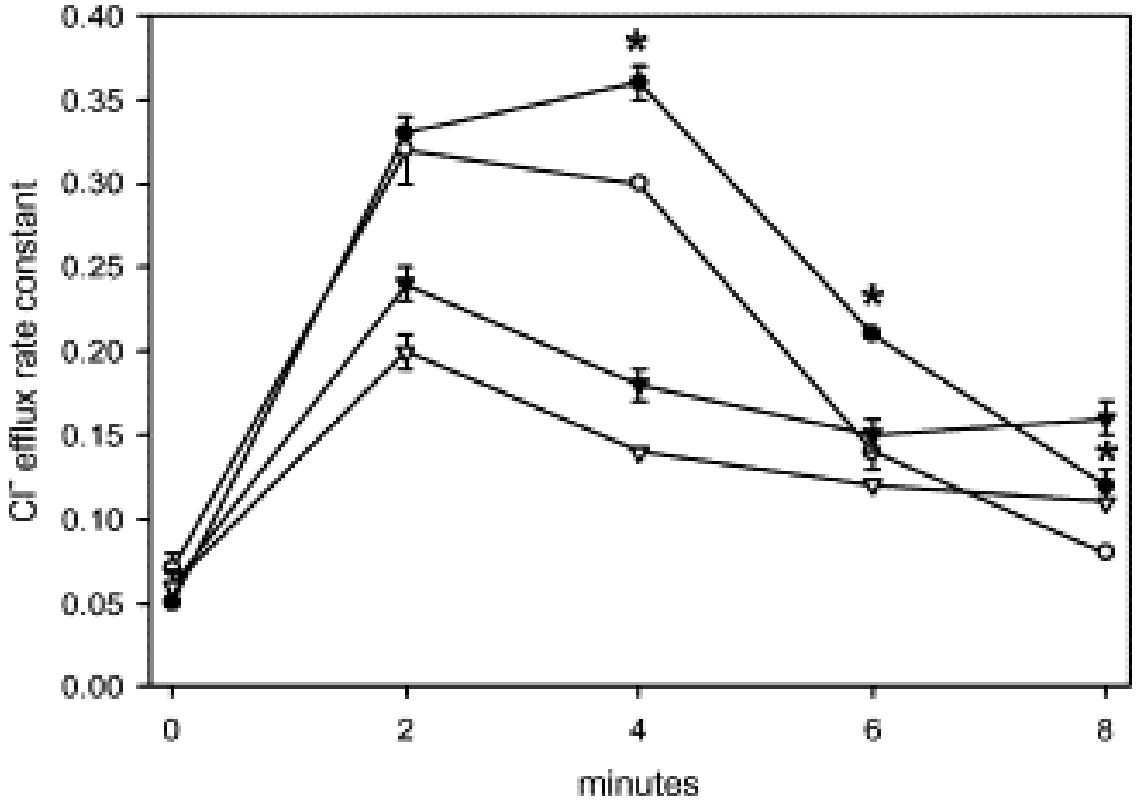

Figure 6.1. Effect of transfection of Caco-2 cells with pCLCA1 on rate of cAMP-dependent chloride efflux. pCLCA1-transfected Caco-2 cells with forskolin and IBMX ●, without A-kinase activators ▼; pcDNA3 control-transfected Caco-2 cells with forskolin and IBMX. ○; without A-kinase activators ▽ . *Significant effect of pCLCA1 on A-kinase-stimulated chloride efflux rate. n=8±SE.

(P=0.003). The overall effect of pCLCA1 transfection was significant in unactivated cells (P<0.001), but the interaction between ±pCLCA1 and efflux time was not significant (P=0.51).

The relative expression of CFTR and CLCA1 mRNA species in the control and in pCLCA1-transfected Caco-2 cells is shown in Figure 6.2. The PCR result showed much lower levels of pCLCA1 mRNA expression than CFTR mRNA expression. Unequal lane loading (15 µl pCLCA1 PCR product vs 1 µl CFTR PCR product) had to be used to give good visual comparison of the relative expression of these mRNA species in Caco-2 cells. As noted for other tumorigenic cell lines (Gruber and Pauli 1999c), we were not able to detect endogenous hCLCA1 mRNA expression in Caco-2 cells.

6.4.2. Effect of pCLCA1 on cAMP-stimulated Short Circuit Current

Changes in the rate of chloride efflux representing chloride conductance in polarized epithelial cells should be paralleled by changes in short circuit current (I_{sc}). Caco-2 cells grown on semipermeable membranes produce a polarized epithelial cell layer with tight junction formation. The effect of forskolin and IBMX addition on the I_{sc} measured across these polarized cells is shown in Figure.6.3. pCLCA1 transfection did not affect tissue resistance, but it significantly increased the increment in stimulated I_{sc} at all times after A-kinase activation. Stabilized I_{sc} values from 20 to 40 min after A-kinase activation were 12±0.015 µA/cm^2 for cells expressing pCLCA1 and 9.3±0.014 µA/cm^2 for control cells (P=0.012).

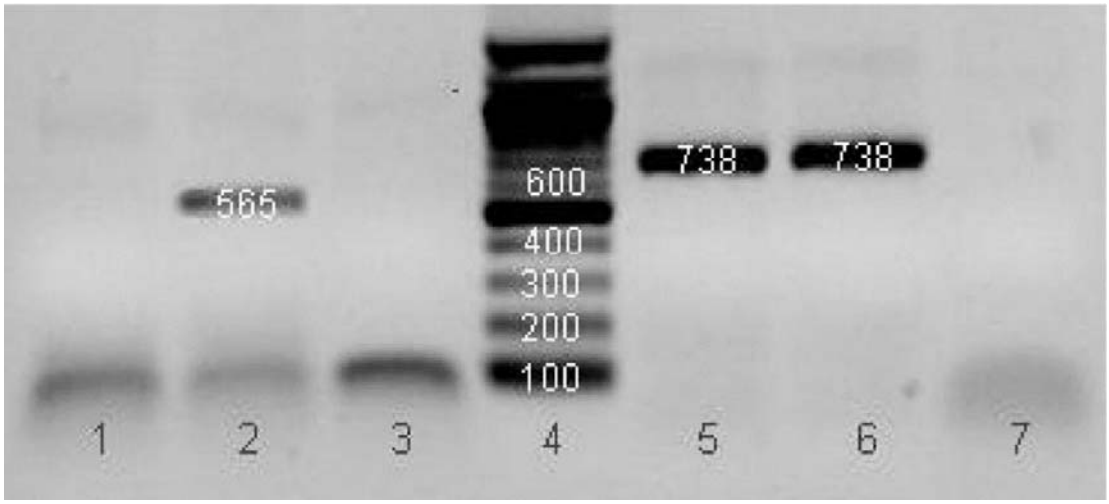

Figure 6.2. pCLCA1 mRNA in stable Caco-2 cell transfectants. Lane 1, RT-PCR primers to detect 565 base-pair fragment of CLCA1 mRNA in pcDNA3-transfected Caco-2 cells. Lane 2, RT-PCR-primers to detect 565 base-pair fragment of CLCA1 mRNA in pCLCA1-transfected Caco-2 cells. Lane 3, PCR to detect 565 base-pair fragment of CLCA1 mRNA in pCLCA1-transfected Caco-2 cells without prior RT. Lane 4, 100 base-pair ladder. Lane 5, RT-PCR-primers to detect 738 base-pair fragment of CFTR mRNA in pcDNA3-transfected Caco-2 cells. Lane 6, RT-PCR-primers to detect 738 base-pair fragment of CFTR mRNA in pCLCA1-transfected Caco-2 cells. Lane 7, PCR to detect 738 base-pair fragment of CFTR mRNA in pCLCA1-transfected Caco-2 cells without prior RT.

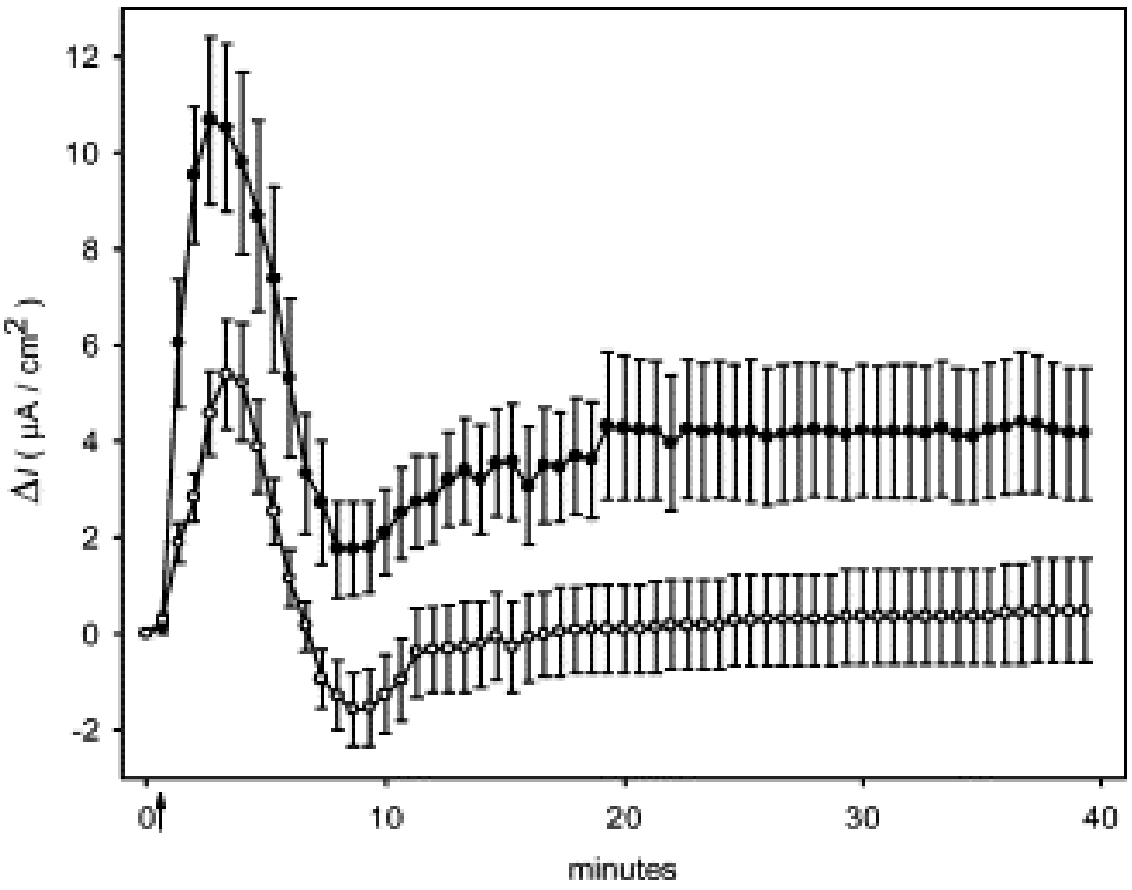

Figure 6.3. Average increments in short circuit current caused by A-kinase activation in monolayers of transfected Caco-2 cells. I_{sc} differences due to addition of forskolin and IBMX at 1 min (↑) are recorded for Caco-2 cells transfected with; ● pCLCA1 insert, o pcDNA3 without an insert. P values for all differences at individual time points after A-kinase activation were <0.05 as determined by post-ANOVA testing. n=12±SE.

6.4.3. Effect of pCLCA1 on cAMP-Stimulated Apical Short Circuit Current

Permeabilization of the basal membrane of epithelial cells to monovalent cations and anions by addition of nystatin produces an electrically isolated apical membrane (Devor, Singh et al. 1999). This condition was used to prevent contributions of membrane hyperpolarization to changes in chloride current across the apical membrane. Transepithelial conductance increased and the transepithelial potential declined to 0 mV with the equilibration of intra- and extracellular sodium and potassium after nystatin addition. Activation of A-kinase in these permeabilized pcDNA3-transfected Caco-2 cells produced a Isc that was dependent on the magnitude and the direction of the chloride ion gradient across the cell monolayer. The increment in cAMP-dependent Isc with high (150 mM) apical Cl- and 20 mM basal Cl^- was significantly increased relative to control-transfected cells (Figure 6.4., P=0.003). There was no effect of pCLCA1 expression on cAMP-dependent increments in Isc with the reverse Cl^- gradient (150 mM basal, 20 mM apical) (P=0.345). The effect of pCLCA1 on cAMP-dependent increments in I_{sc} with 150 mM basal and 20 mM apical Cl^- with a 100 mV potential difference imposed across the epithelial monolayer approached significance (P=0.06). The pCLCA1-associated I_{sc} increments in Caco-2 cells with permeabilized basal membranes indicate that an apical cAMP-dependent chloride conductance increased independent of basal K^+ conductance effects.

6.4.4. Effect of pCLCA1 on cAMP-Stimulated Whole Cell Patch Clamp Current

The characteristics of the whole cell currents associated with pCLCA1-transfection of Caco-2 cells were investigated with whole cell patch clamp. Ten

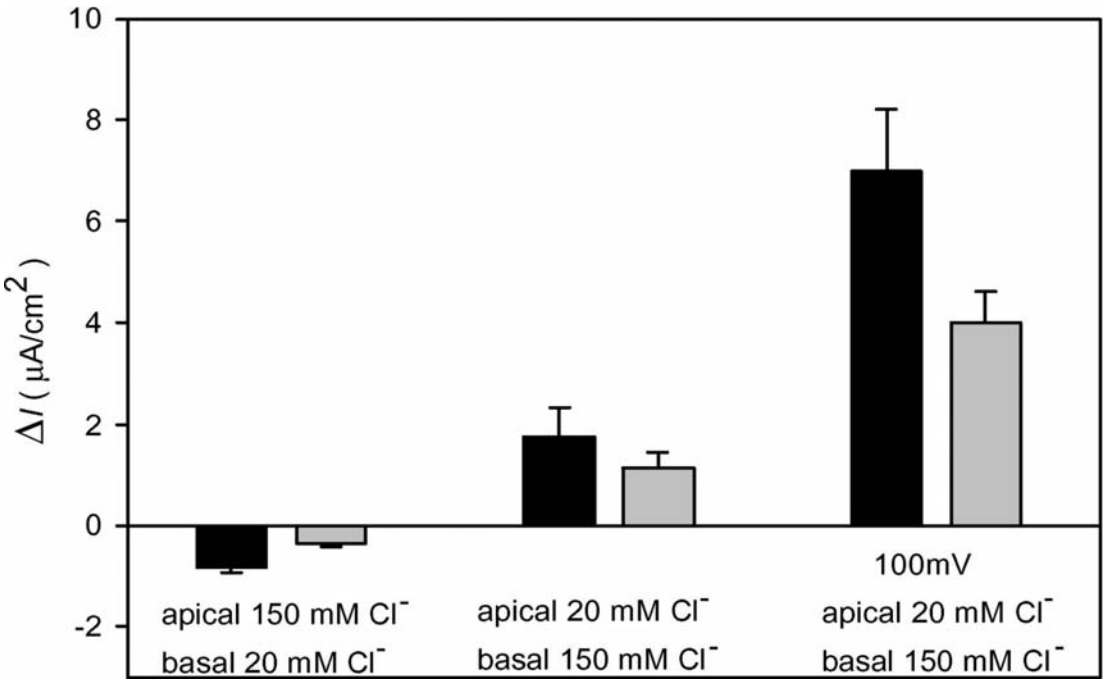

Figure 6.4. Effect of pCLCA1 transfection on short circuit current changes caused by A kinase activation in Caco-2 monolayers with permeabilized basal membranes. Average changes in I_{sc} 4 min after forskolin and IBMX addition to monolayers permeabilized by exposure to basal nystatin are reported. Electrical and chloride ion gradients responsible for generating the I_{sc} in monolayers with permeabilized basal membranes are indicated. Negative changes represent apical to basal (absorptive) increments in I_{sc}, positive increments in I_{sc} represent basal to apical current flow. Black bars, pCLCA1-transfected monolayers; grey bars, control-transfected monolayers. n=7±SE.

pClCA1-transfected cells and nine vector control cells were successfully recorded. Data from cells failing to show an E_{rev} shift on exposure to a bath solution containing low chloride concentration were not considered. A significant pCLCA1 overall gene effect on peak whole cell currents 30 s after the addition of 10 μM forskolin and 1 mM IBMX (P=0.017) is shown in Figure. 6.5A. Significant post-ANOVA differences occurred at -100 mV and -80 mV (P<0.001), -60 mV (P<0.011), 80 mV (P=0.008), and 100 mV (P<0.001). The Erev values for the pClCA1-transfected cell line (1±1.6 mV) and the vector control (-5.1±3.4 mV) with 126 mM internal, and 143 mM external Cl^- were similar (P=0.814) and neither value differed significantly from the calculated chloride E_{rev} of -3.2 mV. The overall gene effect of pClCA1 on unstimulated whole cell currents (Figure. 6.5B) approached significance (P=0.089) and the voltage × gene interaction was significant (P<0.001). Post-ANOVA analysis detected significant gene effects at -100 mV (P=0.001), -60 mV (P=0.009), and -40 mV (P=0.048). The pClCA1-transfected cell line had an E_{rev} of -2.5±1.2 mV and the vector control E_{rev} was -19.5±6.9 mV. This difference of E_{rev} under basal conditions with $[Cl^-i]$=126 mM and $[Cl^-o]$=143 mM was significant (P=0.016).

There was a significant change in Erev values (Fig. 6.5C) when cells stimulated by exposure to forskolin and IBMX were switched to a low external chloride

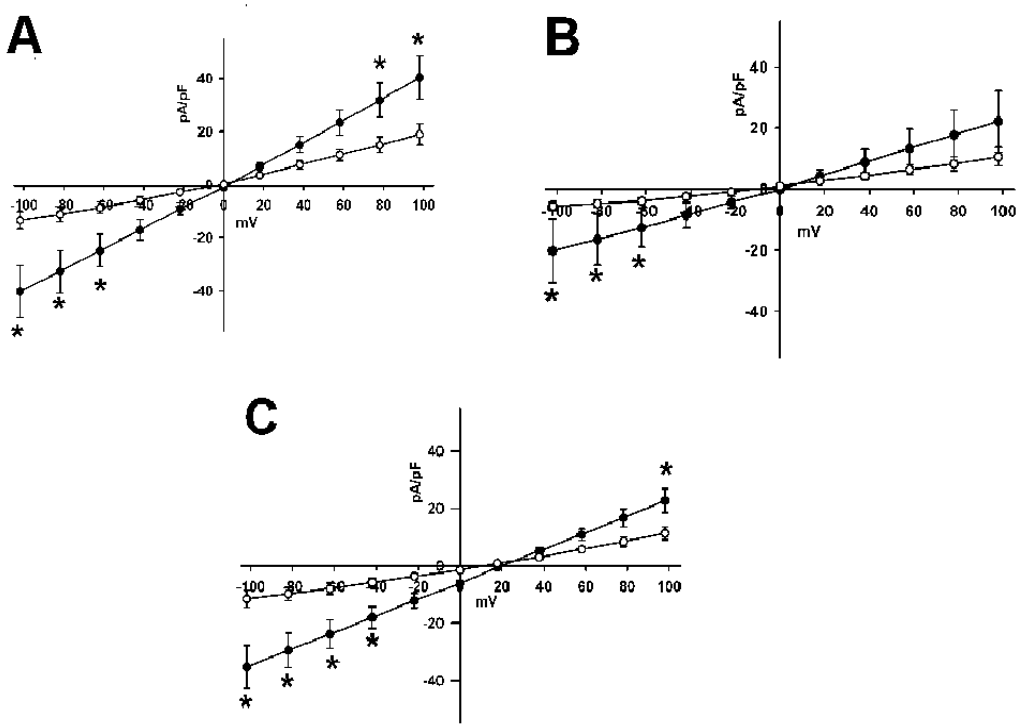

Figure 6.5. Effect of pCLCA1 expression on whole cell currents in Caco-2 cells. Caco-2 cells were transfected with pcDNA3.1 vector, o, or with the vector containing pCLCA1 cDNA,● . (A) Peak whole cell currents 30 s after the addition of 10 µM forskolin and 1 mM IBMX to cells with 126 mM internal and 143 mM external Cl^-. (B) Peak whole cell currents in unstimulated cells with 126 mM internal and 143 mM external Cl^-. (C) Peak 10 µM forskolin and 1 mM IBMX-stimulated whole cell currents in cells exposed to 126 mM internal and low (48 mM) external chloride. *Voltages at which current was significantly higher in cells transfected with pClCA1 as determined by post-ANOVA analysis. Values are means±SE (n=6)

concentration ([Cl^- o] reduced from 143 to 48 mM Cl^- in the bath, [Cl^-i]- maintained at 126 mM). Erev values of 18.83 ± 1.4 mV in pClCA1-transfected cells and 11±2.5 mV in the vector controls with 48 mM Cl^- in the bath can be compared to the calculated chloride equilibrium potential of 24.45 mV. P values were 0.029 and 0.012 for this E_{rev} shift in pClCA1-transfected and vector control cells, respectively. The pCLCA1 effect on the difference between the E_{rev} in 48 mM [Cl^-o] was not significant (P=0.607). As we observed for the high bath chloride concentration, there was a significant overall gene effect of pClCA1 to increase whole cell current in low bath chloride (P=0.007). Post-ANOVA analysis indicated significant pCLCA1 effects on elevation of current at -100 mV, -80 mV, and -60 mV (P<0.001), -40 mV (P=0.006), and 100 mV (P<0.010).

6.4.5. Discussion

The reduction or loss of a cAMP-dependent outwardly rectified chloride conductance in CF patients is thought to be the critical cellular component that is defective in CF disease (Frizzell, Rechkemmer et al. 1986) (Hayslett, Gogelein et al. 1987). Functional reconstitution of the CFTR protein and the strong association of mapped mutations in CFTR with phenotypic variants of CF disease provide convincing evidence for the importance of this protein in exocrine chloride secretion (Bear, Li et al. 1992; Clarke, Grubb et al. 1992; Tsui 1992). Defective chloride transport in CF disease is *de facto* evidence against independent chloride conductance of co-expressed CLCA or ClC proteins in the intestine. While this evidence supports the importance of the anion transport function for CFTR, it does not define the total requirements for *in vivo* chloride conductance. Other proteins could facilitate chloride conductance at several

levels. Accessory proteins may increase CFTR activity by affecting open-probability or numbers of functional CFTR channels in the apical membrane. There is also good evidence for a regulatory role of CFTR on other cAMP-dependent chloride conductance processes in exocrine tissues (Gabriel, Clarke et al. 1993; Guggino 1993). The outwardly rectified chloride conductance that is found to be defective in cystic fibrosis, and is reported to reside in a protein distinct from, but regulated by CFTR is a good example of this latter category.

Previous findings of a Ca^{2+}- dependent release of $^{36}Cl^-$ from pCLCA1-transfected NIH/3T3 cells (Gaspar, Racette et al. 2000; Loewen, Bekar et al. 2002) support the introduction of anion conductance into the cytoplasmic membrane of transfected fibroblasts, or the activation of a quiescent endogenous chloride conductance. A-kinase activation did not stimulate this chloride conductance in 3T3 cells, even though pCLCA1 contains a strong A-kinase consensus site and antibody used to clone pCLCA1 inhibited cAMP-dependent chloride conductance in jejunal brush border vesicles. In switching to the Caco-2 epithelial expression model we hypothesized that unique cell-specific accessory proteins related to the exocrine fluid secretion process may be required for cAMP-, but not for Ca^{2+} -responsiveness. Candidate accessory proteins that could be required for cAMP-responsiveness of pCLCA1, but could be under-expressed in fibroblasts, include ClC proteins, a cAMP-sensitive K^+ conductance, the Na^+ $K^+/2Cl^-$ cotransporter, and CFTR.

The elevation of both cAMP-dependent and unstimulated rates of $^{36}Cl^-$ efflux in pCLCA1-transfected Caco-2 cells in comparison to control-transfected cells was consistent with the background of the cloned pCLCA1 channel. The significant

pCLCA1 effect in the absence of a significant interaction between pCLCA1 transfection and efflux time in unstimulated cells would be expected if basal cAMP levels in these cells were responsible for a slight increase in open probability of a transfected or endogenous anion conductance. Significant group and group × time effects after addition of forskolin and IBMX were evidence for pCLCA1 effects on anion permeability that correlate with increases in the intracellular concentration of cAMP.

Reverse transcriptase-PCR data confirm that the Caco-2 cells do not express detectable levels of endogenous hCLCA1 mRNA. This finding is supported by observations of others who have shown loss of CLCA protein expression in tumorigenic cell lines (Gruber and Pauli 1999c). The data also identify significant expression of CFTR mRNA in this cell line. High CFTR expression correlates with the significant endogenous cAMP-dependent chloride conductance of Caco-2 cells. Relatively low amounts of pCLCA1 mRNA expression in the transfected Caco-2 cells were adequate to produce a significant impact on the endogenous cAMP-dependent chloride conductance of these cells.

Increased rates of chloride efflux could reflect activation of an anion exchange process. It is important to study polarized tissue in Ussing chambers to confirm that chloride efflux has an experimental counterpart in electrogenic chloride release from Caco-2 cells expressing pCLCA1 upon the activation of cAMP-sensitive anion channels. Our Ussing chamber experiments on intact polarized epithelium confirmed that the $^{36}Cl^-$ efflux response was representative of a unidirectional electrogenic chloride secretion.

Increases in chloride conductance can occur without modulating chloride channel gating. Conditions that hyperpolarize the cell will increase the driving force for chloride exit through unstimulated apical anion channels. Rendering the basal membrane of an epithelial cell layer permeable to small anions and cations eliminates the endogenous electrical driving force. In this situation it is possible that cAMP-dependent changes in the I_{sc} produced by an imposed asymmetrical chloride concentration reflect an increase in open probability of an apical anion channel associated with pCLCA1 expression.

Significant increases in cAMP-dependent absorptive chloride current observed in Caco-2 cells expressing pCLCA1 (Fig. 6.4) were consistent with earlier observations of outward rectification of whole cell currents induced in NIH/3T3 cells expressing pCLCA1(Loewen, Bekar et al. 2002). Outwardly rectifying anion currents favor anion absorption, as we observed in the electrically isolated apical membrane of pCLCA1-transfected Caco-2 cells. cAMP-dependent increments in outward (secretory) chloride currents, associated with pCLCA1 expression, only approached statistical significance in asymmetrical chloride solutions (150 mM basal, 20 mM apical) with an externally imposed 100 mV transmembrane potential difference. The combined effects of asymmetrical chloride and the imposed potential difference across the isolated apical membranes may approximate the normal forces driving chloride secretion in a cell with a significant apical transmembrane potential difference.

Whole cell patch clamp data confirm that cAMP-dependent increases in whole cell chloride current accompany pCLCA1 expression. The identity of the chloride currents was confirmed by shifts in the reversal potential as imposed chloride gradients

were changed. Deviations of the measured reversal potential from the calculated equilibrium potential for chloride were attributed to a combination of small amounts of contaminating Na^+ current or leakage in the membrane-pipette seal.

This is the first instance of CLCA protein expression in a differentiated epithelial cell line. This is also the first report of activation of a member of the CLCA gene family by cAMP. How can the second messenger system controlling channel gating, be specific to the host cell used in the expression system? Electrical properties of the cytoplasmic membrane could differ significantly between fibroblast host and a polarized epithelial cell host, inducing different gating configurations and second messenger sensitivity for controlling chloride channel activity associated with pCLCA1 expression. Current data support the hypothesis that pCLCA1 is not a chloride channel, but acts as a regulatory protein that can interact with and enhance the chloride conductance of ClC, CFTR, or ORCC chloride channels. Possible regulatory effects of pCLCA1 will be explored by expression in systems with variable levels of ClC and CFTR. Our results confirm that significant increments in cAMP-dependent chloride conductance can be induced in cells expressing pCLCA1. The novel findings from this model should be of broad interest, as they may have therapeutic applications in clinical disorders of exocrine secretion.

Chapter 7. CLCA PROTEIN AND CHLORIDE TRANSPORT IN CANINE RETINAL PIGMENT EPITHELIUM

7.1. Abstract:

Problems in ion and fluid transfer across the retinal pigment epithelium (RPE) are a probable cause of inappropriate accumulations of fluid between the photoreceptors of the retina and the RPE. The activities of chloride transporters involved in basal fluid transfer across the RPE have been compared to determine whether calcium-dependent or cAMP-dependent channels may be responsible for basal housekeeping levels of secretory activity in this tissue. The role of a candidate calcium-dependent CLCA protein in the basal RPE transport of chloride has been investigated. Low concentrations of the chloride conductance inhibitors glibenclamide and 5-nitro-2-(3-phenylpropylamino) benzoate reduced the short circuit current in dog RPE preparations mounted in Ussing chambers, and decreased the calcium-dependent chloride efflux from fibroblasts expressing the pCLCA1 chloride conductance regulator. However, these same agents did not inhibit the rate of chloride release from cultured fibroblasts expressing the cystic fibrosis transmembrane regulator (CFTR) conductive chloride channel. Addition of ionomycin to primary cultures of canine RPE cells or to fibroblasts expressing the pCLCA1 channel regulator increased the rate of release of chloride ion from both types of cultured cells. However, the presence of pCLCA1 also increased cAMP-dependent chloride ion release from fibroblasts expressing CFTR. We conclude

that Ca2+-dependent chloride transport may be more important than cAMP-dependent chloride transport for normal fluid secretion across the RPE. Further, it appears that CLCA proteins expressed in the RPE may regulate the activity of other chloride transporters, rather than functioning as primary ion transport proteins.

7.2 Introduction

Ion transport activity in isolated RPE choroid preparations has been characterized by Tsuboi and co-workers (Tsuboi, Manabe et al. 1986; Tsuboi 1987) and by others (Bialek and Miller 1994). Their findings are consistent with a model where Na^+/K^+ ATPase activity in the apical RPE membrane, adjacent to the rod and cone photoreceptors, generates a sodium ion gradient across this membrane. High extracellular levels of Na^+ are harnessed to drive uptake of chloride and potassium by the RPE via a coupled $Na^+/ K^+/2Cl^-$ cotransporter localized to the same apical membrane. Activity of this cotransporter maintains RPE intracellular $K^+$and Cl^- concentrations above their respective equilibrium potentials. Net "absorptive" fluid movement (from the vitreous to the choroid) occurs with increased opening of basal chloride conductance channels on the choroidal side of the RPE, permitting Cl^- release down its electrochemical potential. Sodium ions follow the released chloride to maintain electroneutrality, and osmotic forces draw water after the electrolytes to cause fluid to be "secreted" from the vitreous to the choriocapillaris. Disruptions in the direction or magnitude of this ion and fluid transport are one possible cause of conditions such as serous retinopathy (Hughes, Gallemore et al. 1998).

The activity of the basal chloride conductance channels that regulate this ion and fluid transport process is controlled by changes in the concentration of intracellular

second messenger molecules including 3',5'-adenosine monophosphate (cAMP)(Peterson and Miller 1995; Hughes, Gallemore et al. 1998) and intracellular Ca^{2+} (Joseph and Miller 1992; Ueda and Steinberg 1994). However, there seems to be a significant degree of uncertainty about the relative importance of cAMP-dependent versus Ca^{2+}-dependent chloride conductance in this tissue. Recent studies on human fetal RPE indicate the presence of an apical adrenergic receptor in these cells (Quinn, Quong et al. 2001). Transepithelial potentials in the human fetal RPE cells responded positively to both cAMP and ionomycin, indicating activation of chloride conductance by A-kinase and by a Ca^{2+}-dependent mechanism. Expression of the cystic fibrosis transmembrane regulator protein (CFTR) and variants of the ClC chloride channel, including ClC-3 has been reported in human RPE (Miller, Rabin et al. 1992; Wills, Weng et al. 2000).

Although there is much evidence for CFTR expression in this tissue there are no reports of serous retinopathy in cystic fibrosis patients. Based on this evidence it seems likely that calcium-dependent chloride channels may be responsible for most of the basal housekeeping levels of secretory activity in RPE.

Studies on an inherited multifocal retinopathy (Grahn, Philibert et al. 1998), and on the distribution of a member of the CLCA choride conductance channel family (Fuller and Benos 2000b; Fuller and Benos 2000a) cloned recently in our laboratory (Gaspar, Racette et al. 2000) have led us to use inhibitor sensitivity profiles to examine the relative roles of cAMP-dependent CFTR versus Ca^{2+}-dependent chloride conductance proteins in the basal housekeeping levels of secretory activity occurring in this tissue. Basal and activated short circuit current has been measured across RPE-

choroid preparations. Extension of these studies to primary cultures of canine RPE cells has permitted comparisons of the importance of CFTR and Ca^{2+}-dependent chloride channels in this process. The results of this study suggest a novel role for the canine isoform of pCLCA1 in RPE cells.

7.3 Methods

7.3.1. Ussing Chamber Electrophysiology

Guidelines of the Canadian Council on Animal Care were followed in harvesting eyes from healthy dogs that had been euthanized by others for non-medical reasons. The posterior portion of the eye was bisected to separate tapetal and non-tapetal areas. After removing the sclera and the retina the RPE-choroid preparations were mounted in Costar 5mm diameter vertical diffusion chambers. The bathing solution was Krebs Ringer bicarbonate buffer pH 7.5 containing 5.5 mM glucose and 5.0 mM K^+ ion. Tissues were maintained at 37 ^{o} C, and oxygenated with 95% O_2, 5% CO_2. Electrical measurements were made with glass barreled microelectrodes (Navicyte) using an EVC 400 Precision voltage/current clamp (World Precision Instruments). Measurements were made after stable transepithelial potentials were achieved (20 to 30 minutes after mounting tissues). Chloride conductance inhibitors were added to tissue bathing solutions from stock solutions in dimethylsulfoxide (maximum final DMSO concentration of 0.1%).

7.3.2. Conditions for Primary Culture of Dog RPE.

Enucleation was carried out under sterile conditions. Eyes were rinsed with Betadine disinfectant and dissected in a sterile environment. The anterior segment and

the vitreous were removed, a small area of retina was peeled away, creating a well that was filled with 0.5% trypsin (Gibco). After 5 minutes RPE cells were dislodged by pipetting, collected by centrifugation, washed and suspended in DMEM (Gibco) buffered with 20 mM HEPES pH 7.4 supplemented with 10% fetal bovine serum (Gibco), 10 ng/ml basic fibroblast growth factor (Gibco), and 50 μg/ml Pen-Strep. Cells were grown to confluence on 35 mm Primera plates coated with mouse laminin (2.5 μg/cm2). Identity of the RPE cells was confirmed by immunohistochemical staining for cytokeratin and vimentin (McLellan and Bedford 1997).

7.3.3. RT PCR conditions

Reverse transcriptase PCR was carried out on total RNA from confluent cultures of RPE cells at passage number 3. Cells were frozen in 0.15 M NaCl, 5 mM dithiothreitol, 10 mM Tris pH 8.0 containing 10% (v/v) RNAse inhibitor (RNA-Guard, Gibco). Total RNA from 12.5 cells was reverse transcribed with antisense primer specific to unique 3' untranslated sequence in pCLCA1 (5'-GAGAAAGCTTGCGGCCGCTCGTGCAGAAAGTCTAAAATG-3'), or to a conserved region of CFTR (5'-GCACTGGGTTCATCAAGCAG - 3'). The cDNA from the reverse-transcription reaction was used as template in a PCR reaction containing: dNTPs 200 μM, primers 25 pmol, 5% DMSO, 1.25 units of Taq and 1.25 units of *Pfu* DNA polymerases. *Pfu* was omitted from PCR reactions intended for TA cloning. Antisense primers were the same as used in the reverse transcriptase, while sense primers were CFTR 3578 (5'-CCAGCATAGATGTGGATAG-3') and pCLCA1 33 (5'-ACGATGCAAATGGTCGATACAG-3'). PCR was run for 30 cycles with annealing for 45 seconds at 52 ^{o}C, extension for 1 min at 72 ^{o}C, and denaturation at 94 ^{o}

C for 45 seconds. The identity of the amplified cDNA in the PCR of pCLCA1 was determined by TA cloning and sequencing of three independent clones (University of Calgary, Core DNA Services).

cRNA templates were produced from CFTR cDNA in Bluescript (American Type Culture Collection clone T16-4.5) and pCLCA1 cDNA cloned into the Not I site of pcDNA3 (Gaspar, Racette et al. 2000). 10 µg of DNA from each vector with insert was linearized by a single cut at the 3' end of the insert, using Xba I for pCLCA1 and Spe I for CFTR, run through a Qiagen PCR cleanup column, and used as template for cRNA synthesis. The synthesis system also contained 0.1 M dithiothreitol (DTT), 250 µM dNTPs, 1 µl of RNAguard (Gibco), and 100 units of T7 RNA polymerase in a final volume of 100 µl. The reaction was allowed to proceed for two hours at 37 ^{o}C. The cRNA product was incubated with 10 units of pancreatic DNAse for 30 minutes at 37 ^{o} C and separated from DNA digestion products using a Qiagen RNeasy column. The cRNA products were quantitated by optical absorbance at 260 and 280 nm, and known amounts of the cRNA were used in parallel RT-PCR experiments to quantitate mRNA in cell extracts.

7.3.4. Immunohistochemistry.

Polyclonal rabbit antiserum was raised to a KLH-conjugated 17-mer peptide sequence CKEKNHNKEAPNDQNQK, corresponding to deduced amino acid sequence residues 250 to 266 in pCLCA1. Immunohistochemistry was carried out with the capillary gap method (Fisher Code-On IHC stainer) and with the Venta Benchmark flatbed IHC stainer. Formalin-fixed, paraffin embedded sections from a normal dog eye were deparaffinized, treated to inactivate endogenous peroxidase, exposed to protease

(Code-On) or heat (Benchmark) for epitope retrieval, and blocked before exposing overnight to 1:1000 diluted rabbit anti-pCLCA1 17-mer peptide. Secondary antibody was biotinylated anti-rabbit IgG. Avidin-peroxidase complex was added after secondary antibody, followed by NovaRED peroxidase substrate (Vector). Slides were then counterstained with hematoxylin and prepared for viewing.

7.3.5. Chloride Efflux

Stable CFTR and pCLCA1 transfectants of mouse 3T3 fibroblasts expressed under the control of the CMV promoter were grown in DMEM with 10% fetal calf serum, and maintained by selection on G418 (500 μg/ml). These stable transfectants, or cultured canine RPE cells (P2) were grown to confluence on 35 mm plates and loaded with $^{36}Cl^-$ by removing growth media and incubating with loading buffer containing 5 mM glucose, 10 mM HEPES pH 7.5, and 120 mM NaCl plus 2 Ci/ml $^{36}Cl^-$ for 90 minutes. Release of $^{36}Cl^-$ from cells equilibrated with the loading buffer was measured after rapidly washing cells four times with one mL of efflux buffer (loading buffer without $^{36}Cl^-$) to remove extracellular chloride ion. Then the rate of release of chloride from the cells was determined by removing and replacing one ml of the efflux medium at two minute intervals with liquid scintillation counting of ^{36}Cl. The sensitivity of chloride release from loaded cells to perturbations in cell second messenger systems was studied with 10 μM ionomycin in efflux buffer of cells expressing pCLCA1, or 10 μM forskolin and 0.5 mM CPT cAMP plus 2 mM isobutylmethylxanthine (IBMX) in cells expressing CFTR. These efflux agonists were added after the fourth wash and were present in solutions during sampling for $^{36}Cl^-$

release. Inhibitor effects on chloride release were determined by including inhibitor (or vehicle) in the wash solution and during the subsequent timed $^{36}Cl^-$ efflux.

7.4. Results

7.4.1. Basal RPE Short Circuit Current

Secretory fluid transport across the RPE should transfer any accumulated serous fluid from between the retina and the RPE, through the RPE epithelial layer, into the choroidal capillary drainage. The highest frequency of focal serous retinopathy lesions has been observed in tapetal areas (Grahn, Philibert et al. 1998). This situation could be caused by the tapetal pigments acting as a physical barrier to ion and fluid transport across tapetal regions of the retina. The short circuit current and resistance measurements across canine RPE-choroid preparations from tapetum and from non-tapetal areas mounted in Ussing chambers are shown in Figure 7.1. Averaged short circuit currents in the non-tapetal area measured with the transepithelial potential reduced to zero exceeded the values in the tapetal area at each observation time. There was also a consistent trend to larger transepithelial potential differences in non-tapetal preparations (data not shown). These findings were consistent with greater ion and fluid transport activity in the RPE cell layer of the non-tapetal tissue. Tissue from this non-tapetal region of the canine eye was used for subsequent measurements of antagonist effects on short circuit current across the canine RPE.

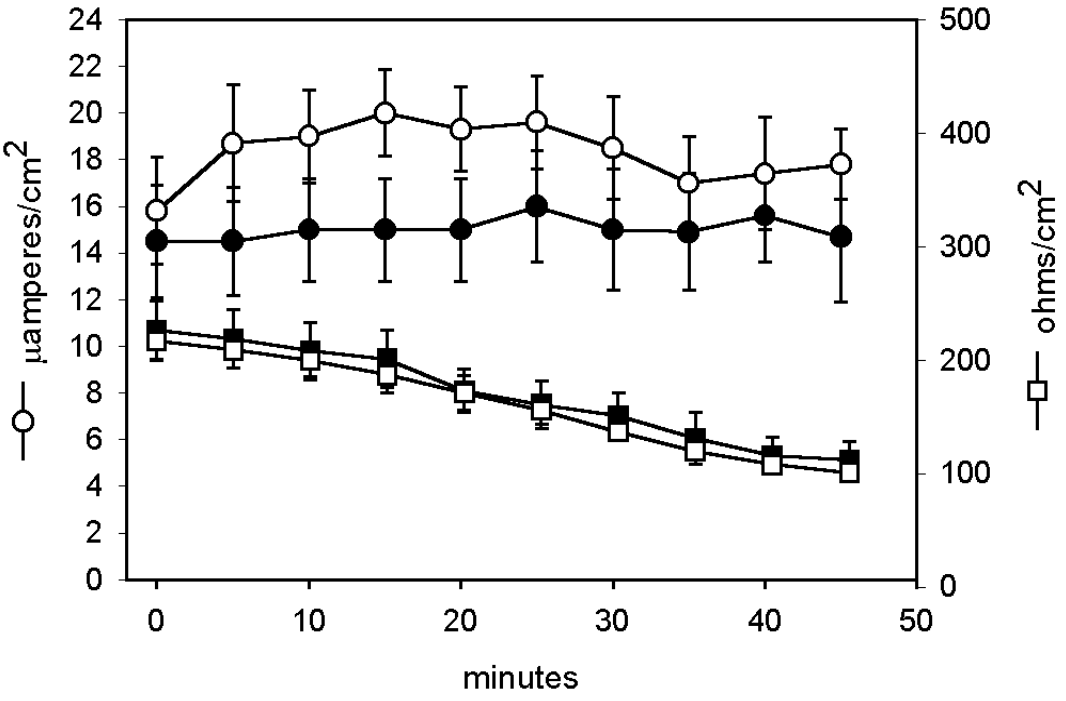

Figure 7.1. Short circuit current and resistance values in dog RPE-choroid preparations mounted in Ussing chambers. Tissues were mounted in 5 mm diameter aperture Ussing chambers and bathed in oxygenated Krebs Ringer buffer. Data collection commenced after parameters stabilized. Filled symbols, tapetum, n = 6; open symbols non-tapetal, n = 10 ± SE.

7.4.2. RPE Agonist Induced Short Circuit Current

Previous reports of cAMP and Ca^{2+}-dependent chloride conductance in RPE indicate that two regulatory processes, and possibly two ion transport processes may be present in these tissues (Hughes and Segawa 1993; Hughes, Gallemore et al. 1998). Increments in RPE short circuit current following addition of forskolin and IBMX, or the Ca^{2+}-ionophore ionomycin to non-tapetal RPE tissues mounted in Ussing chambers are shown in Figure 7.2. These results reveal that agonists operating through activation of adenylate cyclase or increases in free intracellular Ca^{2+} ion are both capable of stimulating chloride ion transfer from the retina to the choroidal vessels in this tissue.

7.4.3. Inhibitors of Basal RPE Short Circuit Current

Basal levels of ion transport processes are presumed to be responsible for housekeeping transfer of fluid from the vitreous to the choroid. The issue of which type of chloride ion transporter was responsible for this basal transport was investigated by the following studies, employing inhibitors of conductive chloride transport. The non-specific chloride channel antagonist 4-acetamido-4'-isothiocyanostilbene-2,2'-disulfonate (SITS) has been reported to inhibit active chloride transport in RPE (Hughes and Segawa 1993). Those findings were confirmed in the non-tapetal RPE-choroid preparations used in this study by a reduction of short circuit current to about 50% of the normal value on addition of 1 mM SITS (Figure 7.3.). The inhibitory action of SITS occurred immediately upon addition, but tissue integrity is shown in the constant tissue resistance

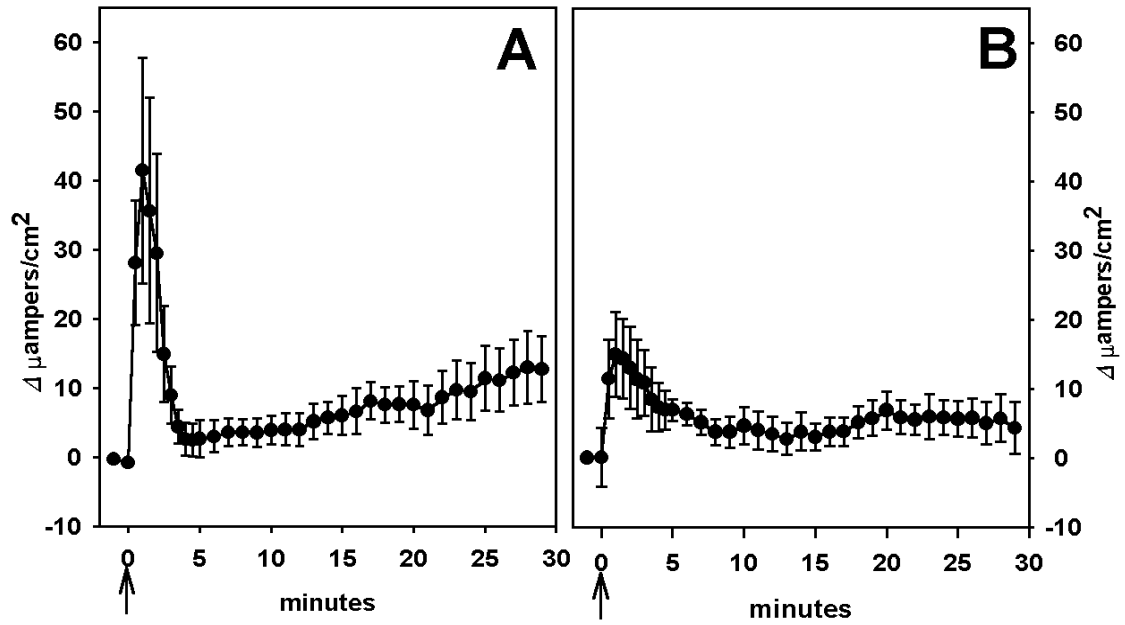

Figure 7.2. Increments in short circuit current caused by activation of chloride conductance in RPE choroid tissue preparations. Tissues were mounted in Ussing chambers as described in Fig 7.1. Activation agonists were added at zero time, and the increment in I_{sc} following agonist addition are reported. A) addition of forskolin (10μM) and IBMX (2 mM). B) addition of ionomycin (10μM) n=6 ± SE.

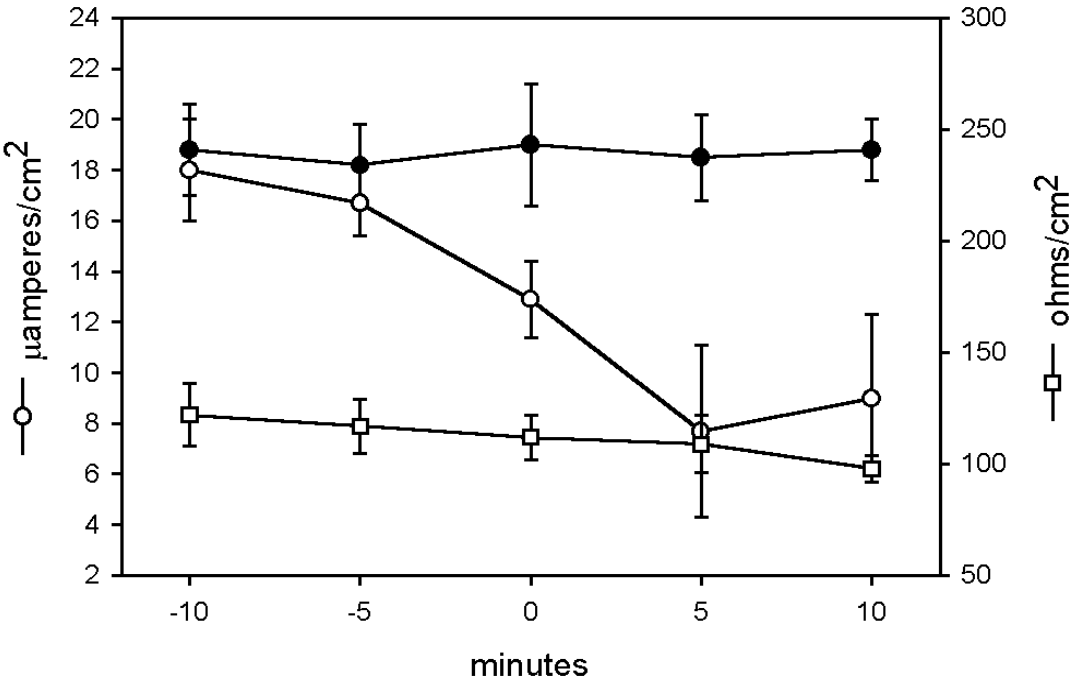

Figure 7.3. Effect of addition of SITS on the short circuit current measured in canine RPE. SITS (1.0 mM) was added at time zero to stabilized canine RPE-choroid preparations mounted in Ussing chambers. Control (●), n = 8; SITS addition short circuit current (○) and tissue resistance (□), n = 4; ± SE.

The rapid drop in short circuit current was consistent with other observations suggesting a role for anion conductance in the short circuit currents seen in this tissue. The oral hypoglycemic sulfonylurea compound glibenclamide is reported to be a relatively specific inhibitor of chloride transport occurring through the CFTR chloride conductance channel (Illek, Yankaskas et al. 1997). Addition of 50 μM glibenclamide to RPE-choroid preparations had no effect on transepithelial resistance, but the short circuit current measured across the tissue was reduced by about 40% (Figure 7.4). These are the results that would be expected if canine CFTR or some other glibenclamide-sensitive chloride conductance activity contributes to the ion and fluid transport across the canine RPE. 5-nitro-2-(3-phenylpropylamino) benzoate (NPPB) is a relatively potent inhibitor of chloride conductance activity. Addition of 10 μM NPPB to the RPE-choroid preparations caused a significant inhibition of the short circuit current (Figure 7.5.). Earlier investigations with this compound have indicated that 10 μM concentrations were not inhibitory for the chloride conductance activity of CFTR (Hipper, Mall et al. 1995). Recently Walsh and coworkers reported a Kd of 166 μM for the interaction of NPPB with CFTR (Walsh, Long et al. 1999).

7.4.4. Inhibitor of CLCA Modulated Calcium Activated Efflux vs cAMP CFTR Efflux

Short circuit current in secretory epithelium is believed to be to a large extent a measurement of chloride release through basal or apical chloride conductance channels in polarized epithelial cells. Since the concentration of NPPB that inhibited the short

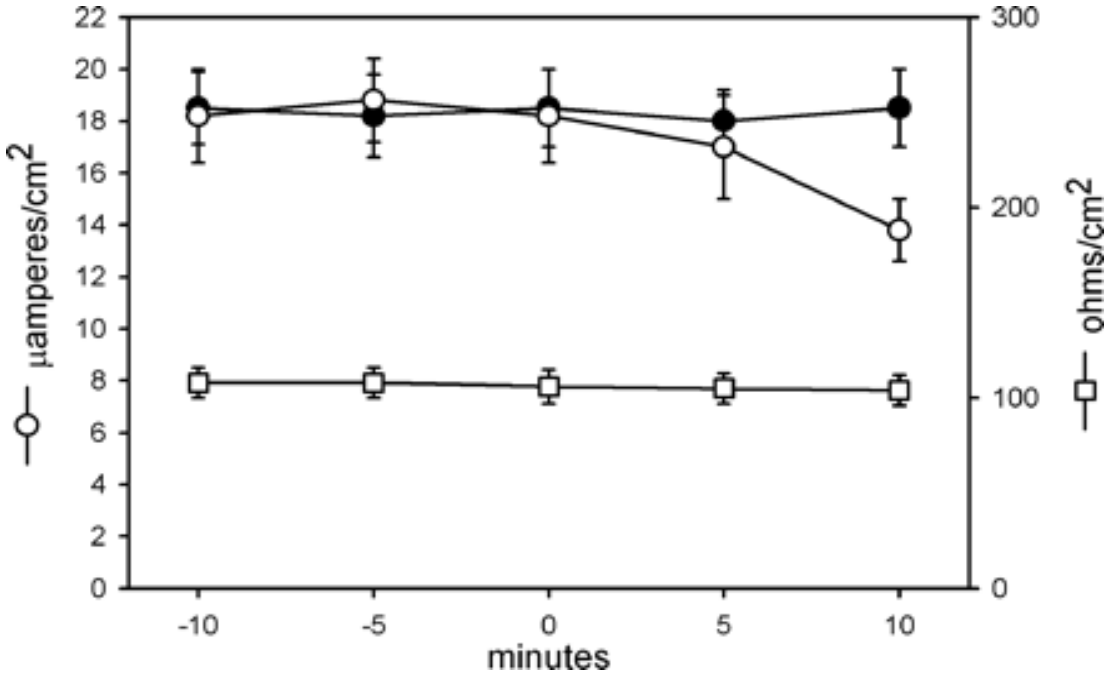

Figure 7.4. Effect of glibenclamide on short circuit current in dog RPE-choroid preparations in Ussing chambers. Vehicle (●), or glibenclamide (50 µM) were added at zero time. Short circuit current (○) and tissue resistance (□) in preparations treated with glibenclamide. n = 7 ± SE

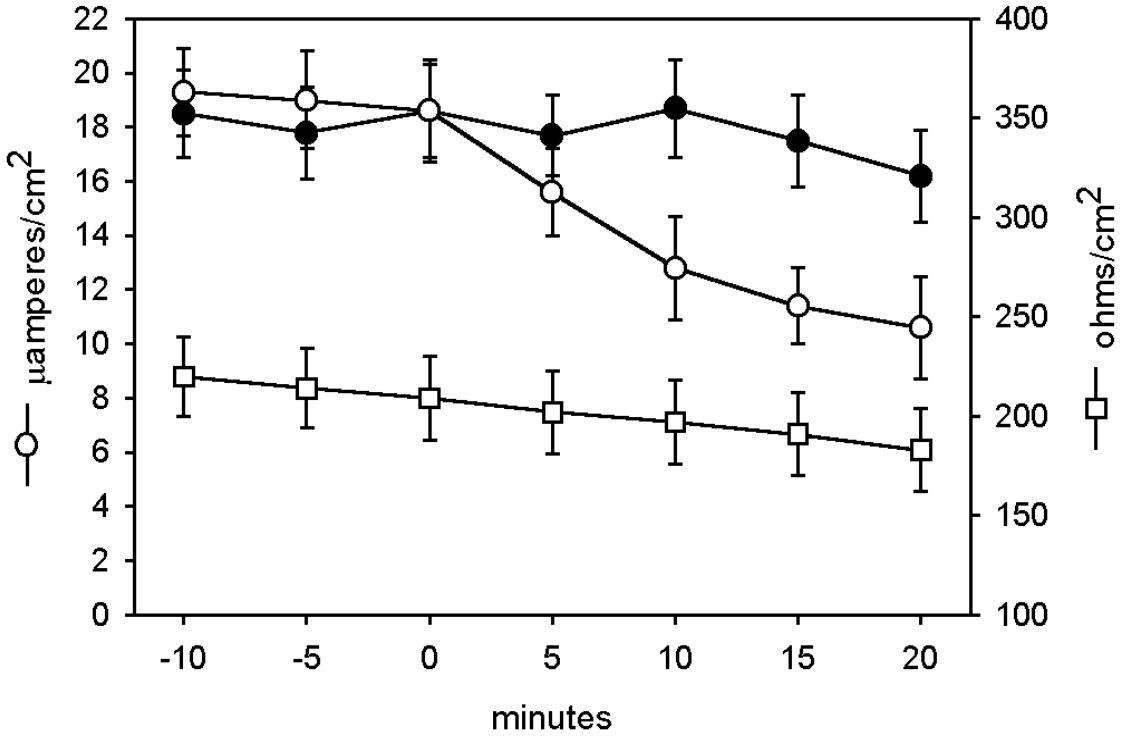

Figure 7.5. Effect of NPPB on short circuit current in dog RPE-choroid preparations in Ussing chambers. Vehicle (●), or NPPB (10 µM) were added at zero time. Short circuit current (○) and tissue resistance (□) in preparations treated with NPPB (10 µM). n = 8 ± SE

circuit current in RPE-choroid was significantly less than the levels reported to inhibit the CFTR chloride conductance we extended these studies to compare the activity of CFTR and of a calcium-activated chloride conductance channel in a cell culture system. Mouse fibroblasts expressing CFTR under the control of the CMV promotor have a significant cAMP-dependent chloride efflux when loaded with ^{36}Cl. This cAMP-dependent chloride efflux is much less prominent in control mouse fibroblasts transfected with the vector alone, without the CFTR cDNA insert (data not shown). The concentrations of glibenclamide (50 μM) and NPPB (10 μM) used in the short circuit current experiments with canine RPE-choroid preparations had no inhibitory effect on the efflux of $^{36}Cl^-$ from mouse fibroblasts transfected with and expressing the CFTR chloride conductance channel (Figure 7.6.).

The recently cloned chloride conductance regulator pCLCA1 is a member of a family of proteins named for a Ca^{2+}-dependent chloride channel activity (Gaspar, Racette et al. 2000; Loewen, Bekar et al. 2002; Loewen, Gabriel et al. 2002). We investigated the sensitivity of chloride transport activated by pCLCA1 expression to the concentrations of inhibitors shown to reduce short circuit current in canine RPE-choroid preparations. Efflux of $^{36}Cl^-$ from mouse fibroblasts transfected with the pCLCA1 channel increased significantly upon exposure of these cells to the Ca^{2+}-ionophore ionomycin (Gaspar, Racette et al. 2000; Loewen, Gabriel et al. 2002). There was no significant chloride efflux response in these cells to treatment with the cAMP agonists that activated the CFTR channel. Ionomycin- or cAMP-dependent stimulation of $^{36}Cl^-$ efflux in control, vector-transfected cells was also insignificant (results not shown).

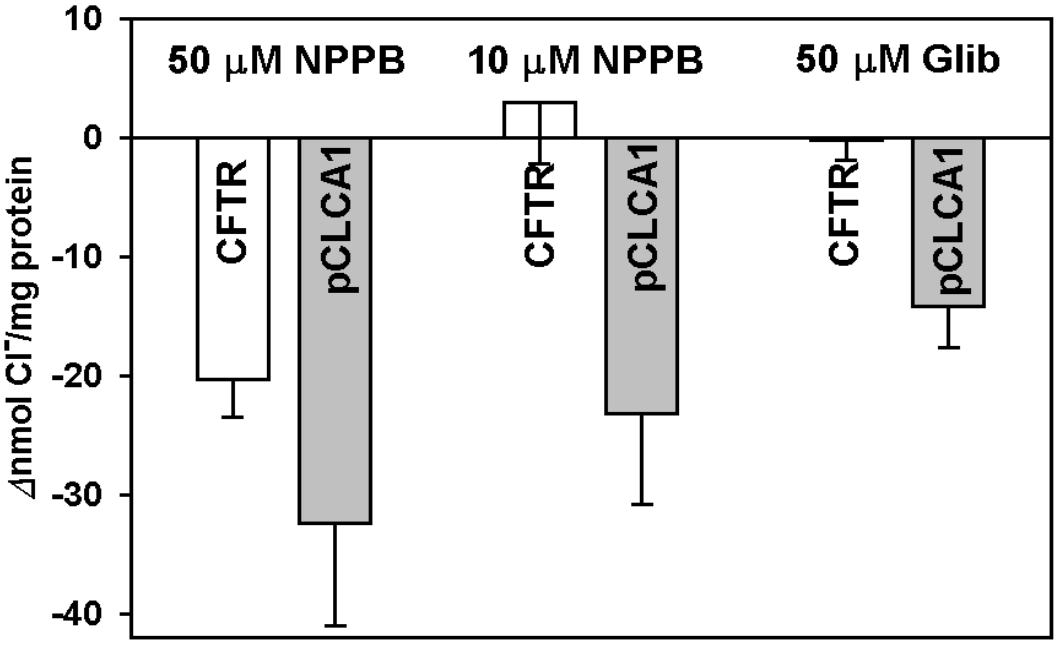

Figure 7.6. Effect of glibenclamide or NPPB on chloride efflux from mouse fibroblasts expressing CFTR or pCLCA1. Permanently transfected fibroblasts grown to confluence in 35 mm dishes, and loaded with $^{36}Cl^-$ for two hours were removed from loading medium, washed rapidly 4x in the presence of the indicated inhibitors and then used to measure the rate of chloride release. Efflux medium (1 ml) was added to plates, and replaced at two minute intervals for quantifying $^{36}Cl^-$ release. Chloride conductance was activated by zero time additions of IBMX (2 mM), 5-chlorophenyl-3',5'-cAMP (50 μM), and forskolin (10 μM) to fibroblasts expressing CFTR, or 10 μM ionomycin to fibroblasts expressing pCLCA1. Changes in the rate of chloride efflux caused by inhibitor are shown two minutes after agonist addition to cells loaded with ^{36}Cl. n = 6 ± SE.

$^{36}Cl^-$ efflux from the pCLCA1-transfected mouse fibroblast cell line was inhibited significantly by 50 μM glibenclamide and by 10 μM NPPB; concentrations that reduced short-circuit current in the intact canine RPE-choroid preparations (Figure 7.6.).

7.4.5. Detection of CLCA in RPE

The possibility that a pCLCA1 like chloride channel regulator cCLCA1 was expressed in canine RPE cells was investigated by reverse-transcriptase/PCR. With primary cultures of canine RPE cells as a source of RNA, and the reverse transcriptase reaction primed with an antisense primer located in the 3' untranslated region of the pCLCA1 cDNA sequence, the resulting cDNA was tested in PCR for the presence of pCLCA1. An 861 base pair cDNA fragment was generated in these PCR reactions. Template contamination by genomic DNA is ruled out by alignments of pCLCA1 (GenBank accession # AF095584) that indicate a minimum of two introns in the genomic sequence between the locations of the PCR primer pair. The 861 base pair PCR product was ligated directly from the PCR reaction into Invitrogen's TA cloning vector. Three independent clones isolated from the resulting transformation had 99% sequence identity to the reported pCLCA1 sequence (seven base changes out of 830 bases in the clones). These sequence changes give one conservative amino acid replacement (I845 —>V) and three non-conservative replacements (Figure 7.7.). In contrast to these minor, cross-species differences for canine and porcine pCLCA1, there are 52 different amino acids in this 252 amino acid region between hCLCA1 and pCLCA1, confirming

```
c1 : --------------AYDANGRYSVKVWALGGVNTPRRRRPPLWSGAMYIRGWIENGEIK :  45
p1 : DATKNDGIYSRYFTAYDANGRYSVKVWALGGVNTPRRRAPPLWSGAMYIRGWIENGEIK : 710
h1 : DATKDDGVYSRYFTTYDTNGRYSVKVRALGGVNAARRRVIPQQSGALYIPGWIENDEIQ : 708
                    YD DGRYSVKV ALGGVN  RRR  P  SGA YI GWIEN EI

c1 : WNPPRPDINKDDLQGKQVCFSRTASGGSFVASDVPKSPIPDLFPPCKITDLKAGIQGDNL : 105
p1 : WNPPRPDINKDDLQGKQVCFSRTASGGSFVASDVPKSPIPDLFPPCKITDLKAGIQGDNL : 770
h1 : WNPPRPEINKDDVQHKQVCFSRTSSGGSFVASDVPNAPIPDLFPPGQITDLKAEIHGGSL : 768
     WNPPRP INKDD Q KQVCFSRT SGGSFVASDVP  PIPDLFPP  ITDLKA I

c1 : INLTWTAPGDDYDHGRADRYIIRISTNILDLRDKFNDSVQVNTTDLIPKEANSEEVFVFK : 165
p1 : INLTWTAPGDDYDHGRADRYIIRISTNILDLRDKFNDSVQVNTTDLIPKEANSEEVFVFK : 830
h1 : INLTWTAPGDDYDHGTAHKYIIRISTSILDLRDKFNESLQVNTTALIPKEANSEEVFLFK : 828
     INLTWTAPGDDYDHG A  YIIRIST ILDLDRKFN S QVNTT LIPKEANSEEVF FK

c1 : PEGIPFTNGTDLFVAVQAVDKTNLESEISNIAQVSLFLPPEAPPETPPETPAPSLPRPEI : 225
p1 : PEGIPFTNGTDLFIAVQAVDKTNLKSEISNIAQVSLFLPPEAPPETPPETPAPSLPCPEI : 890
h1 : PENITFENGTDLFIAIQAVDKVDLKSEISNIARVSLFIPPQTPPETPSPD-ETSAPCPNI : 887
     PE I F NGTDLF A QAVDK  L SEISNIA VSLF PP  PPETP      S P P I

c1 : QVNSTIPGIHTLKIMVKWLGELQLSIA : 252
p1 : QVNSTIPGIHILKIMWKWLGELQLSIA : 917
h1 : HINSTIPGIHILKIMWKWIGELQLSIA : 914
       NSTIPGIHILKIM KW GELQLSIA
```

Figure 7.7. Alignment of predicted amino acid sequence from a partial clone of canine CLCA with related CLCA proteins. Predicted sequence of a partial clone of the canine isoform of pCLCA1 (c1), the porcine isoform (p1), and h1 (hCLCA1), the closest currently identified human homologue.

that canine pCLCA1 (cCLCA1) is not a species isoform of hCLCA1. The 3'-untranslated sequence contained in three dog pCLCA1 (cCLCA1) clones was identical to the reported sequence of pCLCA1.

Semi-quantitative reverse transcriptase-PCR gave an estimate of 37±7 copies of the cCLCA1 mRNA expressed in each canine RPE cell growing in tissue culture (Figure 7.8 A). CFTR mRNA was expressed in the same cells at about 5 copies per cell (Figure 7.8 B). Expression of cCLCA1 antigen in the formalin-fixed canine eye was prominent in RPE cells, using both heat and protease-induced epitope retrieval (Figure 7.9.). Antibody dilutions from 1:100 to 1:10,000 produced positive identification of the RPE (data not shown). Staining indicated that the cCLCA1 antigen was present at highest concentrations on the choroidal (basal) side of the RPE epithelial layer. There was relatively less cCLCA1 epitope evident on the apical membrane processes that interdigitate with, and feed the photoreceptor cells (note the reverse nomenclature for apical and basal relative to other secretory epithelial tissues). This polarized localization of cCLCA1 is consistent with the known direction of net fluid transport by the RPE from the vitreous to the choroid.

7.4.6. CLCA Modulates CFTR Conductance

Evidence for the coexistence of the canine isoforms of pCLCA1 (cCLCA1)and CFTR in RPE raises the possibility that these proteins could be responsible for the Ca^{2+}-

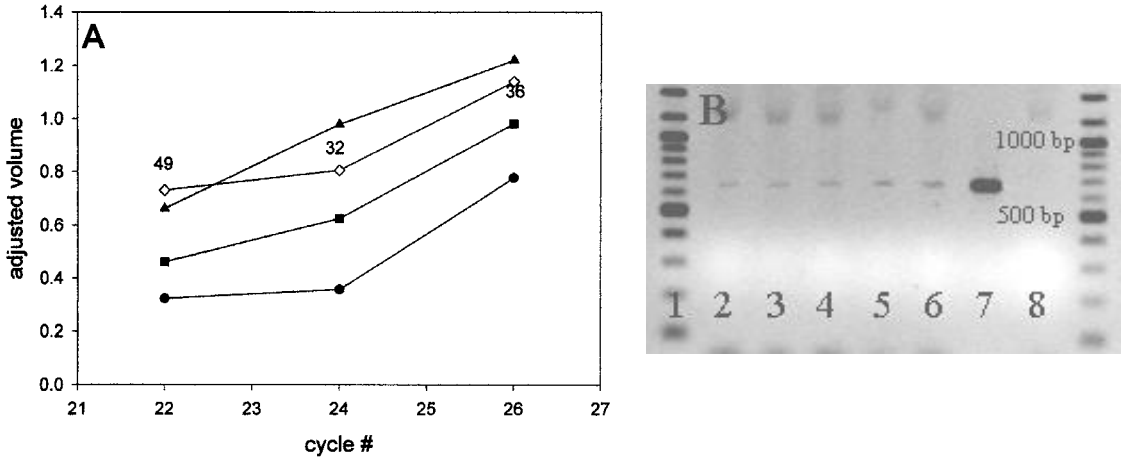

Figure 7.8. A) Reverse transcriptase- PCR quantitation of RPE mRNA species. DNA bands produced by PCR, separated by agarose gel electrophoresis and stained with ethidium bromide were quantitated by image analysis software (BioRad Discovery). A: Fluorescence intensity (adjusted volume, with background subtracted) of an 861 base pair product amplified with primers specific to pCLCA1 cDNA template. cDNA template was produced by reverse transcribing 50 (– ● –), 250 (– ■ –) or 500 (– ▲ –) molecules of pCLCA1 cRNA, or total RNA from 12 RPE cells (– ◊ –). The cDNA product of the reverse transcriptase reaction was used as a template for PCR for the indicated number of cycles. The calculated mRNA copies per RPE cell at 22, 24 and 26 cycles of PCR is shown on the figure. B) DNA banding at PCR cycle # 22. Lane 1 is 100 bp standards; PCR from cDNA templates produced by reverse transcribing 50 (lane 2), 250 (lane 3), or 500 (lane 4) molecules of pCLCA1 cRNA or RNA from 12 RPE cells (lane 5); lane 6, positive control, lane 7 no template control. B: DNA banding patterns of a 650 base pair product amplified with primers specific to canine CFTR cDNA template. Lane 1,100 base pair standards; PCR from cDNA templates produced by reverse transcribing; lane 2, total RNA from 12 RPE cells, lanes 3, 4, 5 and 6, 10, 100, 1000 and 10000 molecules of CFTR cRNA. Lane 7, positive control, lane 8, negative (no template) control

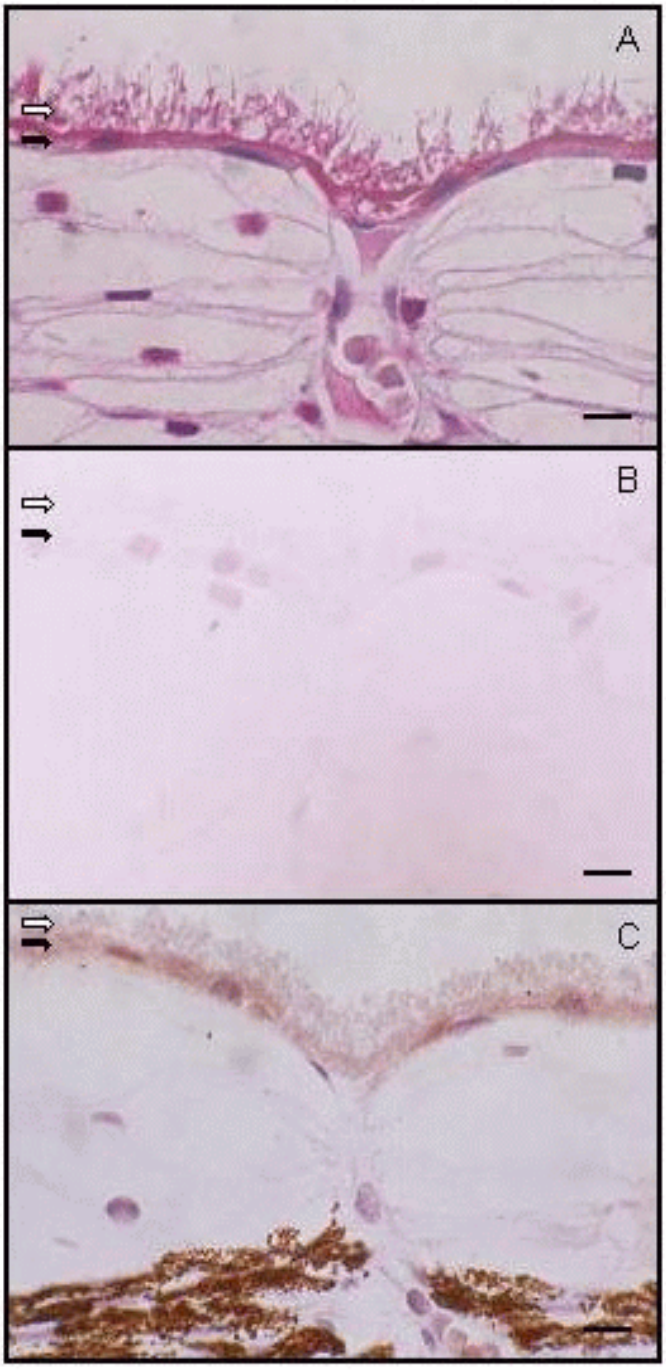

Figure 7.9. Immunohistochemical staining of pCLCA1 antigen (cCLCA1) in canine RPE. The RPE cell bodies on the choroidal side of the polarized epithelium are indicated by black arrows. The "apical" membrane processes that interdigitate with the (missing) photoreceptors are identified by white arrows. Counterstaining was with hematoxylin. Antibody binding was identified by NovaRED peroxidase substrate. Panels A and C, 1:1000 dilution of anti-pCLCA1 (cCLCA1) immune serum primary antibody. Panel A, heat-induced epitope retrieval, panels B and C, enzymatic (protease) epitope retrieval. Panel B, preimmune serum primary antibody. Bars represent 10 micron scale.

dependent, and the cAMP-dependent increases in short circuit current in the RPE reported in Figure 7.2.

This point was investigated indirectly by producing dual transfectants of NIH/3T3 fibroblasts with both CFTR and pCLCA1. When $^{36}Cl^-$ efflux from NIH/3T3 cells expressing both pCLCA1 and CFTR was examined in the presence of forskolin and IBMX, the cells expressing both proteins had a significant increase in the rate of chloride efflux relative to the parental cell line only expressing CFTR (Figure 7.10.). This finding resembles results of a previous report that pCLCA1 stimulates the cAMP-dependent chloride transport occurring when CFTR is expressed (Loewen, Bekar et al. 2002). Since other Ca^{2+}-dependent chloride conductance proteins have been reported in the canine RPE, it is possible that pCLCA1 may play a regulatory role for chloride channels, rather than functioning as a channel itself.

7.4.7. Inhibition of Calcium Activated, CLCA Modulated Efflux in RPE

The chloride efflux system in cultured canine RPE cells was investigated by the same system used to assess threshold inhibitor concentrations for transfected mouse fibroblasts. The pattern of ionomycin (Ca^{2+})-dependent $^{36}Cl^-$ efflux from the cultured RPE cells was similar to that observed with pCLCA1-transfected mouse fibroblasts, although the maximum efflux rate was greater in RPE cells. This ionomycin-dependent increase in the rate of $^{36}Cl^-$ efflux was completely blocked by addition of 10 μM NPPB. Unlike the situation observed with *in situ* RPE in Ussing chambers (Figure 7. 2.), there was no stimulation of $^{36}Cl^-$ release from primary cultures of RPE cells in response to treatment with A-kinase agonists plus IBMX (Figure 7. 11.).

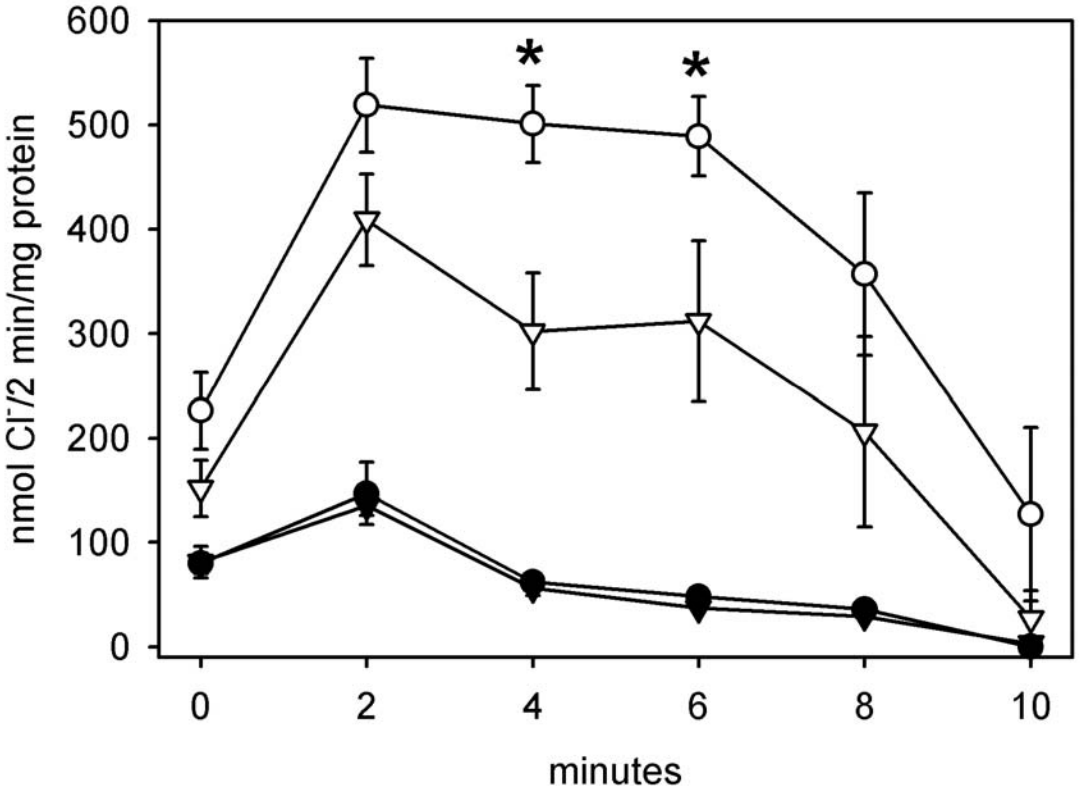

Figure 7.10. A-kinase activation in NIH/3T3 fibroblasts co-transfected with pCLCA1 and CFTR. A 3T3 cell line transfected with CFTR (pcDNA3, G418 selection) was subsequently transfected with pCLCA1 (pcDNA3.1, hygromycin selection). $^{36}Cl^-$ release from loaded cells is reported. All cells were treated with 10 μM forskolin and 2 mM IBMX from time zero. ○, cells expressing pCLCA1 and CFTR, ▽ cells expressing only CFTR, ●, cells expressing only pCLCA1, ▼ control cells transfected with pcDNA3 vector. * $P < 0.05$, $n = 8$ ± SE.

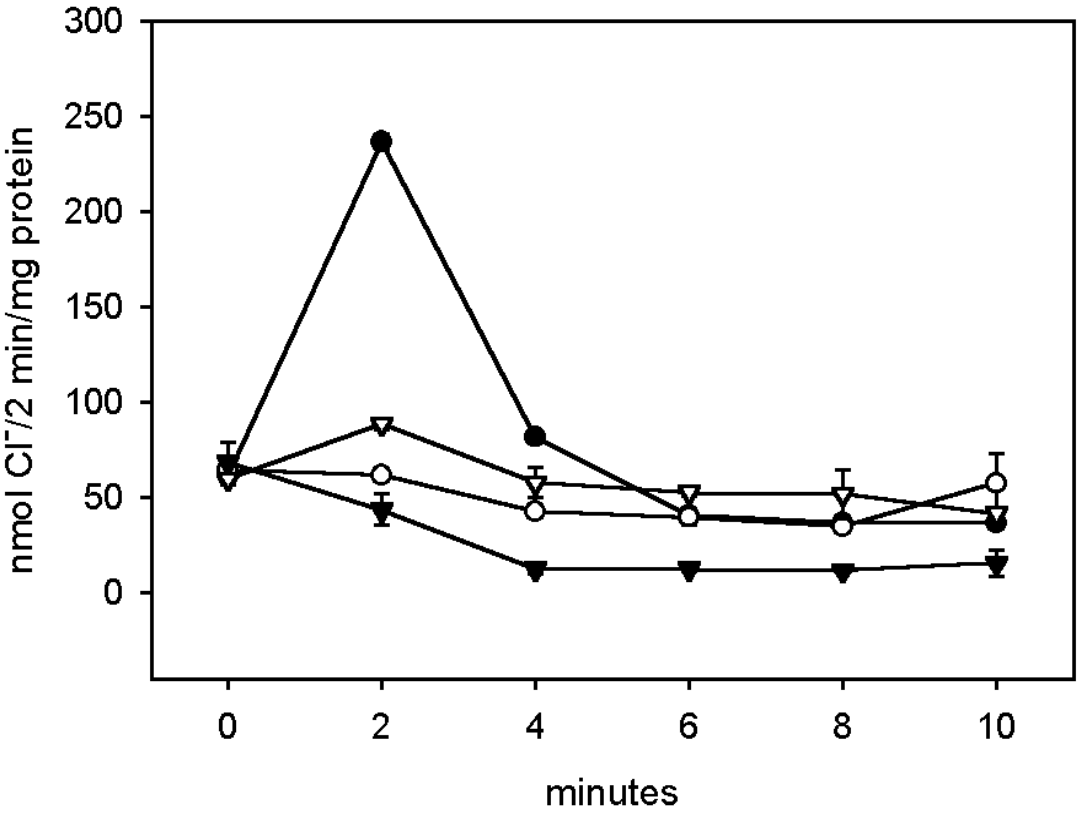

Figure 7.11. $^{36}Cl^-$ efflux from cultured canine RPE cells. RPE cells grown to confluence on laminin-coated 35 mm dishes were loaded with $^{36}Cl^-$, washed rapidly four times, and the release of $^{36}Cl^-$ was measured in media containing the following additions: 10 µM ionomycin (●), 10 µM ionomycin plus 10 µM NPPB (▽), 10 µM forskolin, 2 mM isobutylmethylxanthine, 500 µM CPT cAMP (▼), control (○). n = 6 ± SE. Missing error bars are smaller than the symbol size

7.7. Discussion

Effects of the tapetum on tissue electrical properties, including slight reductions in short circuit current and the reduced trans-RPE-choroid potential difference between tapetal and non-tapetal fundic regions have not been previously described. The significance of the tapetal pigments as a barrier to ion transport across the RPE is an interesting question, as the difference in driving force for transport observed in this study correlates with reports of a distinct tapetal sparing effect on retinal degeneration secondary to glaucoma the dog, cat and horse (B. Grahn, unpublished). We have also noted an increased incidence/severity of RPE dysplasias in the tapetal region (Grahn and Cullen 2001). The association of tapetal structure with localized differences in ion transport raises significant questions concerning a causal relationship between regional RPE transport differences and the manifestations and pathogenesis of retinal disease.

Transient changes in the rate of fluid absorption across the RPE could set up pressure gradients that increase the probability of retinal detachment from the RPE or RPE separation from the choroid. Information about the identity of the proteins responsible for chloride conductance across the RPE could be an important contribution to understanding the pathology of serous retinopathies. The cystic fibrosis transmembrane regulator protein is expressed in human, canine and bovine RPE (Miller, Rabin et al. 1992; Wills, Weng et al. 2000) and the expression site has been localized to the basal membrane (Peterson, Quong et al. 1999). However, uncertainties remain concerning the contribution of the CFTR channel to chloride conductance in the RPE. There are no reports of increased risk of serous retinopathy or retinal detachments

in cystic fibrosis patients. Hence it is possible that chloride transport through other conductance channels co-expressed with CFTR could account for the general housekeeping levels of tissue short circuit current, and intracellular chloride release from the RPE. The comparative inhibition strategy employed in this study provides evidence that, under the conditions employed, CFTR may be less important than other chloride conductance channels as a mediator of basal RPE-choroid chloride transport. However it is clear that there is a significant cAMP-dependent chloride conductance in RPE choroid preparations. Signaling cascades that might activate A kinase *in vivo* in response to increased requirements for trans-RPE fluid movement have not been reported.

The loss of cAMP-dependent chloride conductance in cultured RPE cells has been reported previously in chick and bovine RPE (Kuntz, Crook et al. 1994; Strauss, Steinhausen et al. 1999). The A-kinase agonist mixture that failed to activate chloride conductance activity in cultured canine RPE cells was able to increase the rate of $^{36}Cl^-$ release from transfected mouse fibroblasts expressing CFTR under the control of the cytomegalovirus promoter (see Figure 7. 7. A). Since we have demonstrated the presence of CFTR mRNA in cultured canine RPE cells there may be a problem with the activation of cAMP-dependent protein kinase in these cells.

Our findings of a significant calcium-dependent chloride release from cultured canine RPE cells are in agreement with a role for intracellular calcium in controlling chloride conductance, as reported by Strauss et al. (Strauss, Steinhausen et al. 1999) in cultured rat RPE cells. Expression of pCLCA1 mRNA in canine RPE cells was considered to be a probable source of a Ca^{2+}-dependent chloride conductance in this

tissue. Protein expression of CLCA and basal membrane localization was confirmed by immunohistochemistry. The basal side of the RPE that locates against the choriocapillaris is functionally equivalent to the apical membrane of secretory epithelial cells in the trachea or small intestine. Hence the basal membrane of the RPE is the site of chloride conductance proteins involved in active ion transport. Concentration of the pCLCA1 (cCLCA1) antigen on the basal side of RPE cells was consistent with a role in either chloride transport or in the regulation of chloride transport proteins (Loewen, Bekar et al. 2002; Loewen, Gabriel et al. 2002). However, the regulatory effect of pCLCA1 on cAMP-dependent chloride transport that we have reported previously in Caco-2 cells has also been observed in the fibroblast cell model used in this study. These results suggest that the primary function of the CLCA protein may involve regulation of the activity of other proteins that mediate chloride conductance.

These studies indicate that cAMP-dependent ion channels are less important than Ca^{2+}-dependent channels to basal, housekeeping levels of conductive chloride transport in canine RPE. The extension from pCLCA1 expression in RPE cell membranes to regulatory effects on chloride transport activity in 3T3 fibroblasts raises questions about the function of this protein as Ca^{2+}-dependent chloride channel in canine RPE. However, the localization of the CLCA protein at the basal RPE cell membrane is consistent with the regulatory effects of this protein on Ca^{2+} and cAMP-dependent chloride conductance reported previously in the Caco-2 human colon carcinoma cell line (Loewen, Gabriel et al. 2002).

Chapter 8. pCLCA1 LACKS INHERENT CHLORIDE CHANNEL ACTIVITY IN AN EPITHELIAL COLON CARCINOMA CELL LINE

8.1. Abstract

The effects of CLCA protein expression on the regulation of chloride conductance by intracellular Ca2+ and cyclic AMP have been studied previously in non-epithelial cell lines chosen for low backgrounds of endogenous chloride conductance. However, CLCA proteins have been cloned from, and normally function in differentiated epithelial cells. In this study, we examine the effects of differentiation of the Caco-2 epithelial colon carcinoma cell line on modulation of chloride conductance by pCLCA1 protein expression. Chloride transport was measured as $^{36}Cl^-$ efflux, as transepithelial short circuit currents, and as whole cell patch clamp current/voltage relationships. The rate of $^{36}Cl^-$ efflux and amplitude of currents in patch clamp studies after addition of the Ca^{2+}ionophore A23187 were increased significantly by pCLCA1 expression in freshly passaged Caco-2 cells. However, neither endogenous nor pCLCA1-dependent Ca^{2+}-sensitive chloride conductance could be detected in 14-day post-passage cells. Unlike Ca^{2+}-sensitive chloride conductance, endogenous cAMP-dependent chloride conductance does not disappear upon Caco-2 differentiation. cAMP-dependent chloride conductance was modulated by pCLCA1 expression in Caco-2 cells, and this modulation was observed both in freshly passaged, and in mature 14-day post-passage Caco-2 cultures. pCLCA1 mRNA expression, antigenic pCLCA1

protein epitope expression, and pCLCA1 function as a modulator of cAMP-dependent chloride conductance were retained through differentiation in Caco-2 cells, while calcium-dependent chloride conductance disappeared. We conclude that pCLCA1 expression may increase the sensitivity of preexisting endogenous chloride channels to Ca^{2+} and cAMP agonists, but apparently lacks inherent chloride channel activity under growth conditions where endogenous channels are not expressed.

8.2. Introduction

Chloride transport across the apical membrane is a defining property of secretory epithelial cells. This apical chloride conductance is activated in small intestinal and tracheal tissues by increasing local concentration of either cAMP or Ca^{2+}. The cAMP-dependent cystic fibrosis transmembrane regulator (CFTR) is thought to be the principle chloride channel responsible for this chloride conductance. The CFTR was identified by reverse genetics as the protein directly involved with the secretory defects of cystic fibrosis disease (Rommens, Iannuzzi et al. 1989). However, members of the Ca^{2+}-dependent CLCA protein family were discovered when small intestinal (Gaspar, Racette et al. 2000) and tracheal (Cunningham, Awayda et al. 1995) expression libraries were screened with monoclonal antibody that inhibited conductive chloride transport. Related murine and human CLCA proteins with reported chloride conductance activity have also been cloned (Gandhi, Elble et al. 1998; Gruber, Elble et al. 1998; Gruber, Gandhi et al. 1998; Gruber, Schreur et al. 1999; Romio, Musante et al. 1999).

The role of the CLCA proteins in the apical chloride conductance that drives intestinal fluid secretion has been investigated by heterologous expression in cell lines from non-epithelial sources that have low levels of endogenous chloride channel activity. Expression of CLCA proteins in HEK 293 and NIH/3T3 cell lines caused the appearance of an enhanced Ca^{2+}-dependent chloride channel activity in these cell lines (Gruber, Schreur et al. 1999; Gaspar, Racette et al. 2000). The chloride conductance appearing upon CLCA expression in HEK cells and 3T3 cells was activated by treating cells with Ca^{2+} ionophores, but not by A-kinase activation (Gaspar, Racette et al. 2000). If cAMP-dependent CFTR is the most significant chloride conductor in intestinal epithelium it is curious that antibody which inhibits chloride conductance should identify a Ca^{2+}-dependent chloride channel.

Functional expression of CLCA proteins in simple, undifferentiated cells may give limited information about the physiological potential of this protein (Loewen, Gabriel et al. 2002), since the protein normally functions in differentiated epithelial cells. This study was initiated to determine how pCLCA1 may affect the regulation of chloride conductance in a true secretory epithelial cell line. Caco-2 cells are of intestinal epithelial origin, and they differentiate in culture to produce enterocyte-like monolayers complete with tight junction formation and surface mucus secretion. Caco-2 cells normally express CFTR, and have an endogenous cAMP-dependent chloride conductance (Sood, Bear et al. 1992). We have previously reported the enhancement of endogenous cAMP-dependent chloride conductance in Caco-2 cells expressing pCLCA1 (Loewen, Gabriel et al. 2002). This cell type-specific, functional response to pCLCA1 transfection could reflect a need for a basal $Na^+K^+/2Cl^-$ cotransporter and

K^+conductance to demonstrate the activity of a cAMP-dependent chloride conductance mediated by pCLCA1 (Loewen, Bekar et al. 2002). However, it is also possible that chloride conductance effects attributed to pCLCA1 expression may be due to increased responsiveness of existing conductance channels to normal agonists, either Ca^{2+} or cAMP. In this study we present evidence from differentiating Caco-2 cells that distinguishes between these alternative explanations for pCLCA1 effects on chloride conductance.

Differentiation of maturing epithelial cell cultures during *in vitro* growth is accompanied by the loss of Ca^{2+}dependent chloride conductance as they polarize and form tight junctions (Anderson and Welsh 1991; Davenport, Mergey et al. 1996; Tarran, Loewen et al. 2002). We confirm that Caco-2 cells lose Ca^{2+}-dependent chloride conductance during differentiation, and we exploit this phenomenon to show that pCLCA1 may modulate the chloride conductance attributed to other ion channels, but is not sufficient, by itself, to conduct chloride.

8.3. Materials and Methods

8.3.1.Materials

Tissue culture media and G418 antibiotic were purchased from Gibco Life Technologies. Peptide synthesis, conjugation and polyclonal antibody production was carried out by Sigma Genosys. Sigma/Aldrich was the source of molecular biology grade chemicals including ionomycin, A23187, forskolin and isobutylmethylxanthine (IBMX). $^{36}Cl^-$ was purchased from New England Nuclear.

8.3.2. Cell lines

Caco-2 cells were grown in DMEM medium supplemented with 10 % fetal bovine serum, 2 mM glutamine, MEM non-essential amino acids (0.1 mM), 1 % MEM vitamin solution, and 1 mM sodium pyruvate (complete DMEM medium). Stable transfections of Caco-2 cells with pcDNA3 plasmid with, and without the pCLCA1 cDNA, were carried out as described previously (Loewen, Bekar et al. 2002). After electroporation cells were plated at 2 x 10^5 cells per well in 24 well plates. G418 (2.5 mg per ml) was added to wells 24 hours later to select for successful transfectants. Cells were switched to maintenance medium (500 μg per ml of G418 in complete DMEM) 7 days post-transfection. For pCLCA1 and pcDNA3 control transfections, cells from three separate wells showing good growth under selection pressure and randomly designated as lines 1, 2 and 3 were passaged and used subsequently to test for clonal selection effects.

8.3.3. Production of Transient Transfectants

Recipient Caco-2 cells were plated at low density (2.5 x 10^5 cells per 75 ml flask) in complete DMEM medium, grown for 24 hours, and then transfected with the pIRES2-EGFP vector (Invitrogen) containing a polycistronic construct of pCLCA1 and EGFP. For transfections, 2 μg of vector DNA was mixed with10 μL of lipofectamine 2000TM (Invitrogen) in 800 μL of DMEM 20 min prior to addition to the flask containing 5 ml of complete DMEM without antibiotic. The transfection media was replaced with fresh media after 12 hours, and cells were grown for a further 48 hours before plating on 35 mm dishes. Cells showing EGFP fluorescence were patched about 10 hours after transfer to 35 mm dishes.

8.3.4. RT-PCR

The conditions for RT-PCR have been described previously (Loewen, Bekar et al. 2004). We used an antisense primer uniquely specific for pCLCA1 in the reverse transcriptase reaction (5'-TTTAGTCGACCATATCTAGTTGTTTAGATTG-3'), with nested antisense primer (5'-CAGGTTGGTCTTATCGACAG-3') and a sense primer (5'-GTGAACACGCCACGCAGAAG-3') to generate a 518 bp cDNA in PCR. The PCR negative control was produced by omitting the antisense primer from the RT reaction.

8.3.5. Western blot

For protein comparisons by Western blotting cells were washed with phosphate buffered saline (PBS), removed from plates by adding one ml of PBS containing 10 mM EDTA, and suspended by gentle pipetting. Washed cells were collected by centrifugation and resuspended in 40 mM Tris buffer, pH 9.0 containing phenylmethylsulfonylfluoride (1 mM), pepstatin (0.1 μM), and leupeptin (10 μg/mL). Cell protein was separated by SDS PAGE electrophoresis, and transferred to nitrocellulose membranes by wet cell electrophoresis. Membranes were blocked with 5% non-fat milk dissolved in Tris-buffered saline containing 0.1% polyoxyethylenesorbitan monolaurate (TTBS). They were incubated with diluted polyclonal rabbit antiserum prepared to a KLH conjugate of the 17-mer peptide CKEKNHNKEAPNDQNQK, corresponding to deduced amino acid sequence residues 250 to 266 in pCLCA1. Secondary mouse anti-rabbit alkaline phosphatase conjugate

(Sigma) was diluted in TTBS, and equilibrated with the nitrocellulose membrane prior to exposure to alkaline phosphatase substrate.

8.3.6. Flow Cytometry

Stable pCLCA1 and control-transfected Caco-2 cells were grown in flasks for 24 hours or 14 days after passaging. Medium was removed from flasks, and replaced by phosphate-buffered saline (PBS) containing 10 mM EDTA. Cells were dislodged, filtered through 30 M nylon mesh, and suspended at a density of 10^6 cells per ml in PBS plus 3% bovine serum albumen. Diluted preimmune or anti-pCLCA1 serum was incubated with cell suspensions for 30 minutes at 4 ^{o}C. Cells were washed 3x, and suspended in diluted fluorescein-conjugated goat anti-rabbit fab secondary antibody for a second 30 minute incubation. The first of three washings contained 50 μg/ml propidium iodide. Washed cells were analyzed for fluorescence by flow cytometry using photomultiplier gates optimized for discrimination between emission of fluorescein and propidium iodide.

8.3.7. Chloride Efflux

Stable pCLCA1 and control-transfected Caco-2 cells were plated at a density of 5 x 10^5 in 35 mm culture dishes and grown in DMEM supplemented with 2 mM glutamine, 10% fetal calf serum and G418 (500 μg/ml). After 24 hours or 14 days of growth the confluent monolayers were loaded with $^{36}Cl^-$ by removing growth media, and incubating for two hours with loading buffer containing 4 mM KCl, 2 mM $MgCl_2$, 1 mM KH_2PO_4, 1 mM $CaCl_2$, 5 mM glucose, 10 mM HEPES pH 7.5, and 140 mM

NaCl plus 2 Ci/ml $^{36}Cl^-$. Extracellular $^{36}Cl^-$ was removed by rapidly washing cells five times with one ml of efflux buffer (loading buffer without ^{36}Cl) prior to time zero. Agonists (10 μM ionomycin or 10 μM forskolin plus 2 mM IBMX) were added to the efflux buffers from time zero, through to the end of the timed efflux. $^{36}Cl^-$ release from the cells was determined by consecutively adding and removing one ml of efflux medium. Residual cell $^{36}Cl^-$ at the end of the efflux was determined by washing cells from the plates with 1.0 mM EDTA, and liquid scintillation counting. The rate constant for chloride release was calculated as: (0.5 (ln ((cell [Cl-]t1) / (cell [Cl-]t2)))).

8.3.8. Short Circuit Current Measurements

Differentiated monolayers of Caco-2 cells expressing pCLCA1 or control cells transfected with the pcDNA3 vector were mounted in Ussing chambers and equilibrated for 20 min in standard Krebs Bicarbonate Ringers solution with 10 mM basal glucose and 10 mM apical mannitol prior to adding agonists. Chloride gradients were established across monolayers of permeabilized cells by replacing chloride with gluconate and Na^+ and K^+ with Tris. The high Cl^- solution contained 147 mM Tris Cl, 30 mM mannitol, 5 mM N-tris[hydroxymethyl]methyl-2-aminoethanesulfonic acid (TES), 2 mM $CaCl_2$ and 1 mM $MgCl_2$, pH 7.4. The low Cl^- solution contained 130 mM Tris base, 130 mM D-gluconic acid, 17 mM Tris Cl, 30 mM mannitol, 2 mM $CaCl_2$ and 1 mM $MgCl_2$, pH 7.4.

8.3.9. Whole Cell Patch-Clamp.

Transfected cells were identified using an Axiovert 10 inverted microscope (Zeiss) equipped with a mercury lamp and excitation and emission filters of 425 and 540 nm, respectively. Transfected cells were patched using a MP-285 computer controlled micromanipulator (Sutter Insturments) and Grass AM8 audio monitor (Grass-Telefactor West Warwick, RI). After a seal was obtained (> 1 GΩ), capacitance compensation was carried out before gaining whole cell access. Subsequent to whole cell access, all cells were dialyzed for 1 min before recording.

Whole cell currents were acquired with an Axopatch 200B amplifier (Axon Instruments, Foster City, CA) at 10 kHz and filtered at 2 kHz by a low pass Bessel filter with Clampex 8 and analyzed with Clampfit 8 (Axon Instruments). Cells were held at 0 mV with voltage pulses applied for 800 ms from - 100 to +100 mV in 20 mV increments. Current differences were normalized by whole cell capacitance recorder from an integrating 10 mV hyperpolarizing pulse. The pipette offset was adjusted upon immersion into the bath solution. A single-cell bath solution change (Perfusion Fast Step SF-77B perfusion system; Warner Instruments, Hamden CT) was used to add agonists and change bath chloride concentration.

The pipette solution for intracellular dialysis contained 110 mM CsCl, 1 mM $MgCl_2$, 3mM MgATP, 5mM TES, 1 mM EGTA, 0.38 mM $CaCl_2$. pH was adjusted to 7.4 by adding CsOH (~ 9.2 mM Cs added). The high chloride bath solution contained 135 mM CsCl, 3 mM $MgCl_2$, 5 mM TES, 2 mM $CaCl_2$, 90 mM mannitol, and ~ 2.7 mM CsOH to adjust pH to 7.4. The low chloride bath solution contained 40 mM CsCl, 3 mM $MgCl_2$, 5mM TES, 2mM $CaCl_2$, 280 mM mannitol and ~ 2.2 mM CsOH to adjust

pH to 7.4. Calculated junction potential corrections for these solutions (-2 mV) were less than the error for recorded reversal potentials, so no corrections for junction potentials were made.

Bath solution for recording with A23187 agonist contained of 135 mM N-methyl-D-glucamine HCl, 3 mM $MgCl_2$, 5 mM TES, 2 mM $CaCl_2$, and 80 mM D-mannitol (pH 7.4). The pipette solution for intracellular dialysis was 90 mM D-gluconic acid, 90 mM Tris, 40 mM Tris HCl, 5 mM TES, 1 mM sodium pyruvate 1 mM EGTA, 2 mM $MgCl_2$, 0.1 mM $CaCl_2$, 1 mM MgATP, and 0.1 mM Na_2GTP (pH 7.4). Corrections were applied for junction potentials.

8.3.10. Statistical Methods

Two way repeated measures ANOVA was used to compare overall and treatment over time or voltage interactions. The Fisher LSD method for pairwise multiple comparisons was used as a post-ANOVA test to determine statistical significance at individual points. A paired t-test was used to compare groups of paired data.

8.4. Results

We have previously reported agonist effects on chloride efflux rates from Caco-2 cells plated at a density of 5×10^5 per 3.5 cm plate, and grown for 24 hours after passaging (Loewen, Bekar et al. 2002). However, calcium-dependent chloride conductance has been shown to decrease significantly in fully differentiated epithelial cells (Anderson and Welsh 1991; Tarran, Loewen et al. 2002). For this reason, this

study compares 24 hour undifferentiated Caco-2 cultures with 14 day-old differentiated cultures for effects of pCLCA1 expression on Ca^{2+} and cAMP-dependent chloride efflux.

8.4.1. Effect of pCLCA1 on Endogenous Ca2+-Dependent Chloride Efflux in One Day-Old and Mature Cultures

pCLCA1 was found to enhances endogenous Ca2+-dependent chloride efflux in one day-old cultures, but shows no chloride conductance activity in mature cells.

The effect of pCLCA1 expression and Ca2+ ionophore addition on the rate of release of $^{36}Cl^-$ from Caco-2 cells is shown in Figure 8.1. Ca^{2+}-sensitive chloride transport was present in cells assayed 24 hours after passage. The effect of Ca^{2+} ionophore A23187 addition on the rate of $^{36}Cl^-$ efflux from these cells occurred immediately, as observed previously in NIH/3T3 cells. pCLCA1 transfection increased the rate of Ca^{2+}-sensitive chloride efflux from these freshly passaged cells. In contrast, the addition of Ca^{2+} ionophore to mature differentiated Caco-2 cells had no effect on the rate of $^{36}Cl^-$ release from these cells. Mature differentiated cells expressing pCLCA1 also failed to increase the rate of chloride release upon addition of Ca^{2+} ionophore. We conclude that heterologous pCLCA1 expression was not sufficient to confer calcium-dependent chloride efflux to mature Caco-2 cells lacking endogenous Ca^{2+}-dependent chloride efflux activity.

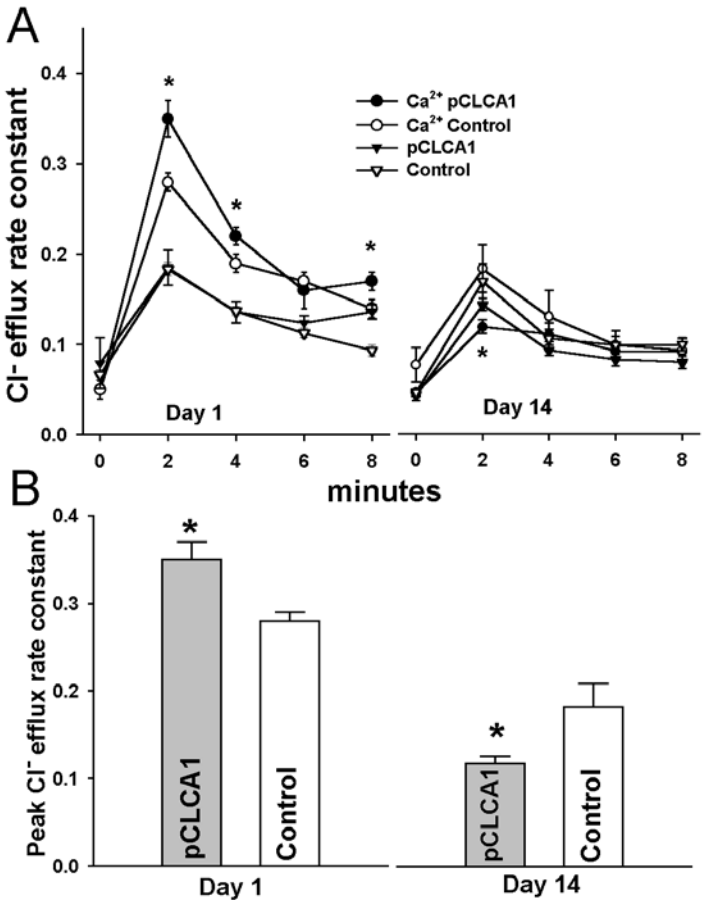

Figure 8.1. Loss of Ca2+ activated chloride efflux in 14 day old cells expressing pCLCA1. A) Efflux rates for both pCLCA1-transfected, and vector-control transfected cells, grown 1 or 14 days after passage, in response to A23187 (10 μM) added at time zero. A23187 added to pCLCA1 transfected (●); or vector-control transfected (○) cells. No additions to pCLCA1 transfected (▼), or vector-control transfected (▽) cells. (*) $P < 0.05$ compared to agonist stimulated control. For 1 day post-passage cultures; $P = 0.031$ for overall pCLCA1 effect on A23187-dependent rate of chloride efflux when compared to vector agonist control, and $P = 0.004$ for gene x time interaction. There were significant rate responses to A23187 compared to vector-control cells at 2, 4 and 8 minutes ($P = 0.009$, $P = 0.021$ and $P < 0.001$, respectively). For 14 day post-passage cultures; $P = 0.002$ for gene x time effect. By post- ANOVA analysis, A23187 and pCLCA1 transfection caused a significant decrease ($P = 0.009$) in chloride efflux rate constant 2 min after A23187 addition, compared to stimulated vector-control. $n = 9 \pm$ SE. B) Peak A23187-stimulated chloride efflux rate constant for cells grown 1 and 14 days post-passage. After A23187 addition, pCLCA1-dependent rate increase in 1 day cells ($P = 0.009$), and pCLCA1-dependent rate decrease in 14 day cells ($P = 0.009$) are shown. $n = 9 \pm$ SE

8.4.2. Effect of pCLCA1 on cAMP-dependent chloride efflux on one day old and mature cultures

pCLCA1 enhancement of endogenous cAMP-dependent chloride efflux is maintained through differentiation and polarization

The disappearance of Ca^{2+}-dependent chloride conductance from mature Caco-2 cells raised questions about the effects of differentiation and tight junction formation on other chloride conductance in these cells. We have shown previously that freshly plated Caco-2 cells conductance(Loewen, Bekar et al. 2002) or NIH/3T3 cells expressing CFTR (Loewen, Bekar et al. 2004) have a cAMP-dependent chloride efflux that is enhanced by expression of pCLCA1. This response to cAMP and pCLCA1 transfection in freshly plated cells is shown in Figure 8.2., in comparison to the rates of $^{36}Cl^-$ efflux observed in mature, confluent Caco-2 monolayers. Within the first two minutes of agonist addition there was no immediate effect of pCLCA1 transfection on the rate of PKA-dependent $^{36}Cl^-$ efflux.

However, there was a delayed effect of PKA agonists to increase the rate of chloride efflux in both freshly plated and mature Caco-2 cells expressing pCLCA1. pCLCA1-dependent increases in Cl^- efflux rates appeared at 4 minutes (freshly plated cells) or 6 minutes (mature differentiated monolayers) after forskolin and IBMX addition compared to control transfected cells. It is significant that, unlike the Ca^{2+} effect, cAMP-dependent chloride conductance was not lost from mature cells. And the ability of pCLCA1 expression to modulate that cAMP-dependent chloride conductance was present in both freshly plated and mature monolayers. These functional effects of

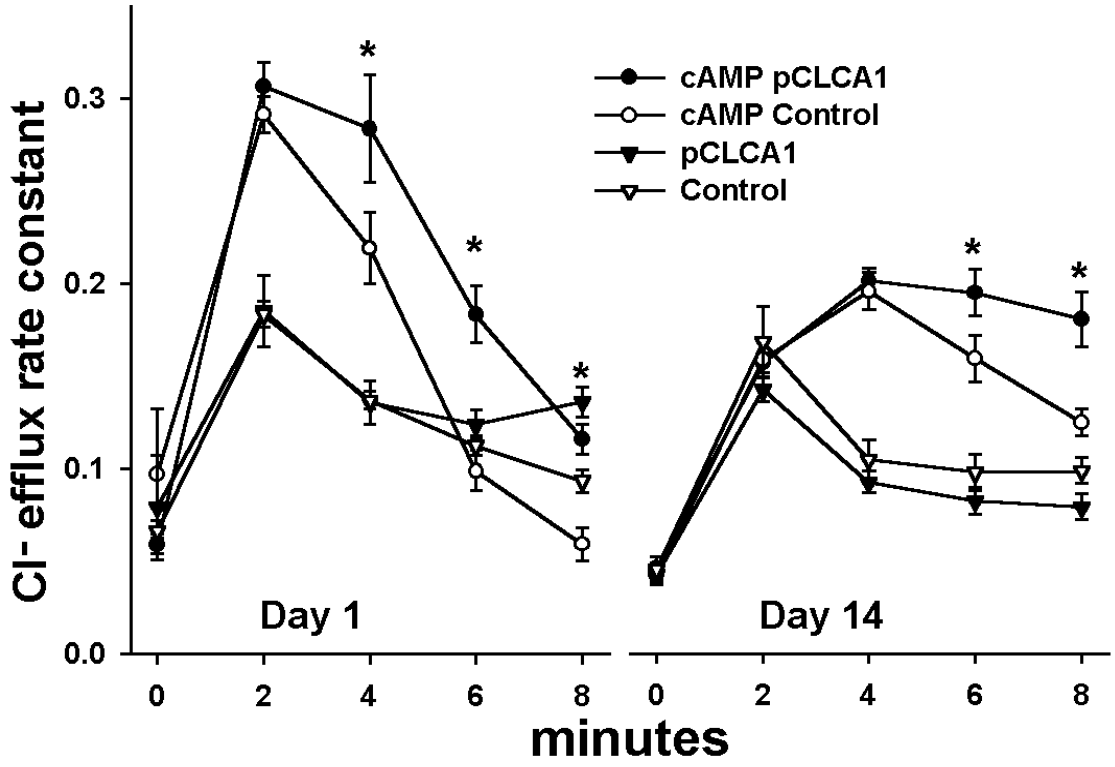

Figure 8.2. Retention of pCLCA1 modulation of cAMP stimulated efflux in 14 day old cells. Efflux rates for pCLCA1-transfected or vector-control transfected cells grown 1 or 14 days after passage in response to forskolin and IBMX added at time zero. Forskolin (10 μM) and IBMX (2 mM) added to pCLCA1 transfected (●); or vector-control transfected (○) cells. No additions to pCLCA1 transfected (▼), or vector-control transfected (▽) cells. (*) P< 0.05 compared to agonist stimulated control. For 1 day post-passage cells; P = 0.012 for overall pCLCA1 effect on forskolin-IBMX -dependent rate of chloride efflux compared to vector agonist control, and P = 0.004 for gene x time interaction. There were significant rate responses to forskolin-IBMX compared to vector-control cells at 4, 6 and 8 minutes (P = 0.012, P = 0.001 and P < 0.027, respectively). For 14 day post-passage cells; P= 0.035 for overall pCLCA1 effect on forskolin-IBMX -dependent rate of chloride efflux, and there was a significant gene x time interaction (P= 0.006). By post-ANOVA analysis forskolin-IBMX stimulated pCLCA1-transfected cells had larger rates of efflux 6 (P = 0.011) and 8 (P < 0.001) minutes after agonist addition when compared to stimulated control-transfected cells. n = 8 ± SE

pCLCA1 expression in mature Caco-2 cells are interpreted as evidence for protein expression despite the absence of a Ca^{2+}-dependent conductance.

8.4.3 Effect of pCLCA1 on Ussing chamber cAMP- and Ca2+-dependent chloride conductance.

The presence of cAMP- but not Ca2+-dependent chloride conductance in polarized Caco-2 cells in Ussing chambers

The chloride efflux rate constants reported in Figure 8.1 represent the rate of release of isotopically labeled chloride from these cells. Release rate constants should reflect permeability of the cytoplasmic membrane to chloride ion. However, release rates measured in the presence of unlabelled 140 mM extracellular chloride are not definitive measurements of a chloride uniport. Membrane leakage, KCl cotransport, and exchange of intracellular $^{36}Cl^-$ for extracellular ^{35}Cl or bicarbonate will contribute to release rates. In contrast, short circuit current (I_{sc}) measured across polarized epithelial cell layers reflects active ion transport processes that define net ion conductance. The conductive nature of the enhanced anion transport response to forskolin and IBMX in cells transfected with pCLCA1 was tested by measuring transepithelial electrical parameters in confluent Caco-2 monolayers mounted in Ussing chambers. The movement of negative ions to the lumen is expressed as a positive Isc. The addition of forskolin and IBMX caused a significantly greater increase in I_{sc} in cells transfected with pCLCA1, compared to control cells transfected only with the pcDNA3 expression vector (Figure 8.3 A). $P < 0.001$ for the overall gene effect, and for gene x time interaction. This finding confirms a conductive component in chloride

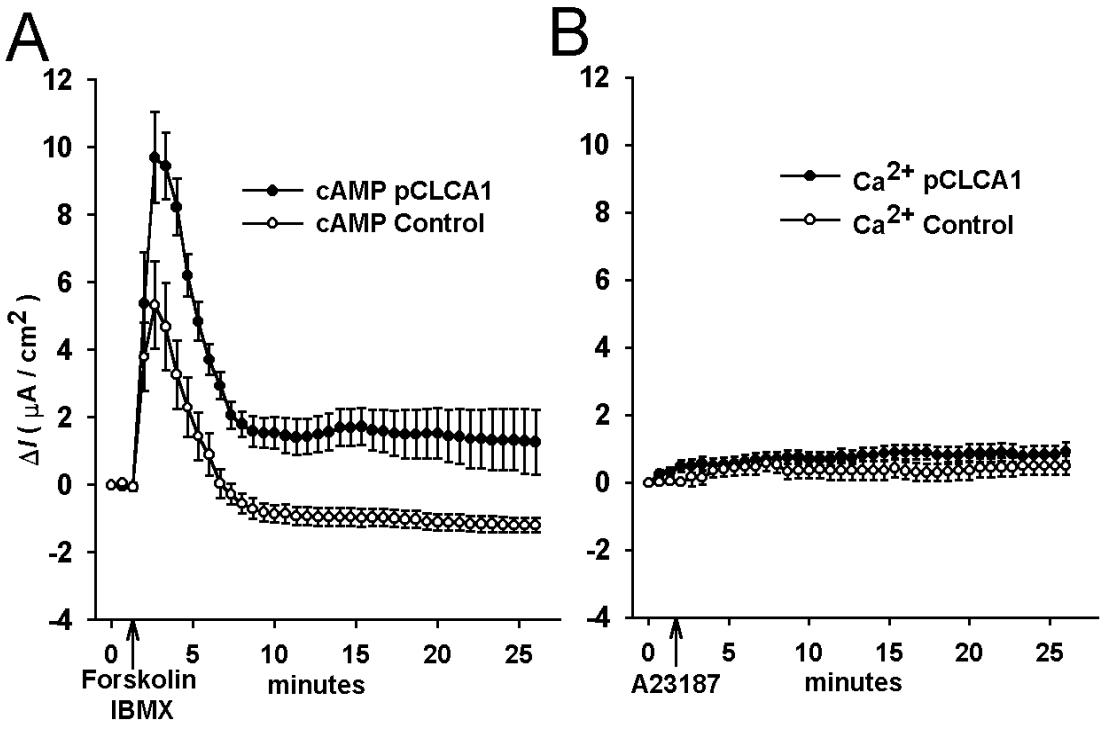

Figure 8.3. Agonist-induced short circuit current changes in transfected Caco-2 cells. pCLCA1 (●) and vector-control (○) transfected Caco-2 cells were grown 14 days on semipermeable membranes prior to mounting in Ussing chambers. Changes in I_{sc} in response to agonists A) 10 μM forskolin and 2 mM IBXM added at the indicated time. pCLCA1 transfected cells had a larger Isc response to forskolin and IBMX (overall gene effect $P < 0.001$) compared to vector control cells. B) 10 uM A23187 added at indicated time. The overall gene effect for A23187 on I_{sc} was not significant($P = 0.257$) with a power of 0.087. n = 10 ± SE.

transport rates reported in Figure 8.2.

CLCA ion channels were identified by activation of chloride conductance upon exposure to Ca^{2+} ionophores(Gandhi, Elble et al. 1998; Gruber, Elble et al. 1998; Gruber, Schreur et al. 1999; Romio, Musante et al. 1999) . Isc increments in response to treatment of Caco-2 cell monolayers with 10 μM A23187 are shown in Figure 8.3B. There was no evidence for an apical Ca2+-dependent chloride conductance in mature confluent monolayers of control pcDNA3-transfected Caco-2 cells. Transfection with pCLCA1 failed to confer Ca^{2+}-dependent chloride conductance to these mature polarized cell monolayers. P = 0.25 for overall gene effect, and 0.992 for gene x time interaction. Hence, the I_{sc} response of mature polarized cells in Ussing chamber studies confirms both the retention of the cAMP effect and the loss of Ca^{2+} effect on $^{36}Cl^-$ efflux seen in mature 14 day monolayer Caco-2 cultures.

Isc associated with chloride conductance could be elevated by an increase in the permeability of the apical membrane of the polarized cells to chloride ion, or from an increase in the driving force for chloride release (cell hyperpolarization). If pCLCA1 expression affects chloride channel activity, its primary effect should be on the former process; ie: membrane permeability to chloride. The permeability of the apical membrane to chloride was determined by measuring I_{sc} changes in response to imposed chloride gradients after the basolateral membrane of polarized cells was made permeable to Na^+ and K^+ ions (electrically isolated) by treatment with nystatin. The nature of the cAMP-dependent increase in chloride conductance in pCLCA1-transfected cells was determined by measuring I_{sc} changes in response to an imposed transmembrane chloride gradient; 153 versus 21 mM chloride. Isc changes caused by

A-kinase activation in pCLCA1, and in pcDNA3 transfected cells are shown in Figure 8.4 A. I_{sc} changes in response to A-kinase activation were significantly larger in Caco-2 cells expressing pCLCA1 than in control cells transfected with pcDNA3. These increments in chloride permeability were independent of the direction of the imposed chloride gradient, as predicted for a truly electrically-isolated apical membrane (basal to apical P = 0.001, apical to basal P = 0.023).

In contrast to the findings with A-kinase activation, there was no significant Ca^{2+}-dependent increase in apical membrane permeability (Figure 4B). Neither the control nor the pCLCA1-transfected cells responded to A23187 treatment with significant increments in I_{sc} (basal to apical P = 0.91, apical to basal P = 0.66). These findings support an effect of A-kinase activation on the apical permeability of mature differentiated Caco-2 cells. They also confirm a functional effect of expressed pCLCA1 in mature cells lacking Ca^{2+}-dependent chloride conductance.

8.4.4. pCLCA1 Expression is Maintained Throughout Differentiation/Maturation

Some CLCA gene products, including bCLCA1 and hCLCA1, are reported to code for proteins that function as chloride channels that are regulated by changes in free cytosolic Ca^{2+} concentration (Cunningham, Awayda et al. 1995; Gruber, Elble et al. 1998). The loss of a Ca^{2+}-dependent chloride conductance in mature, differentiated Caco-2 cells transfected with pCLCA1 raises questions about the effect of cell differentiation on expression of the pCLCA1 gene product. The constitutive CMV

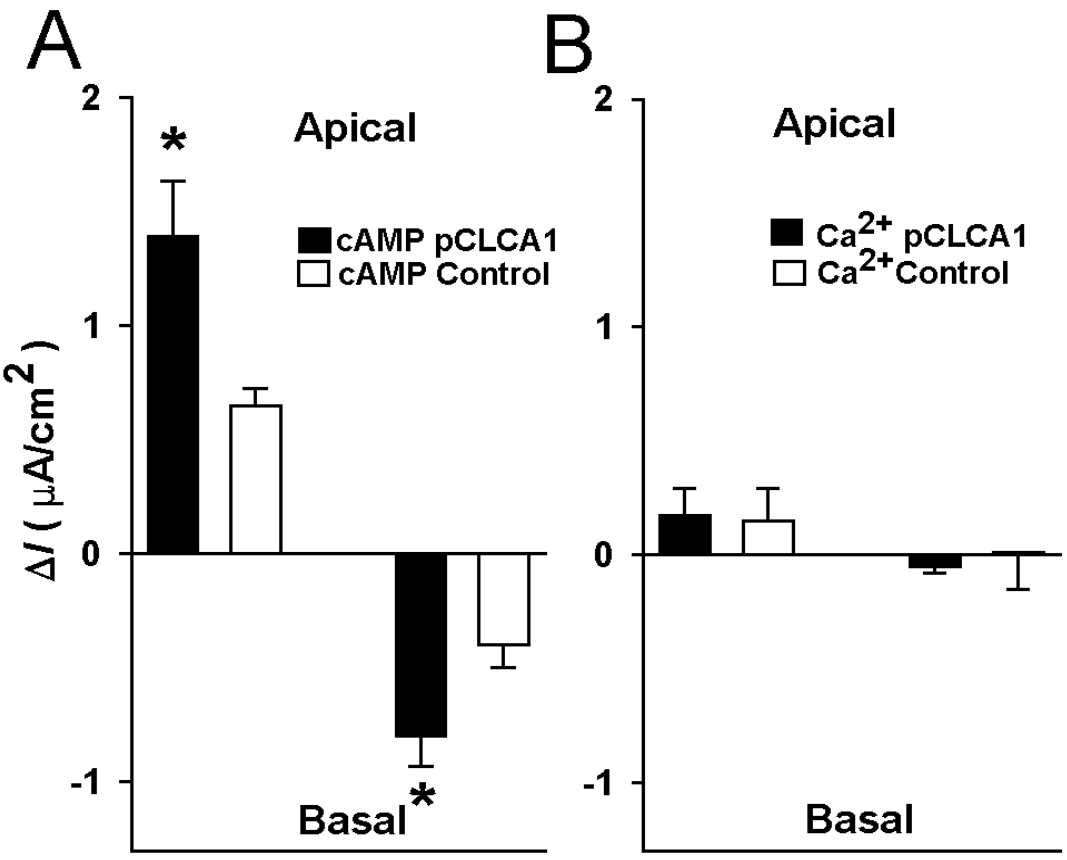

Figure 8.4. Agonist-induced short circuit changes across the electrically-isolated apical membrane of transfected Caco-2 cells. Changes in I_{sc} in response to imposed apical to basal or basal to apical chloride gradients. Black bars, permanent pCLCA1 transfectants, white bars, permanent vector- control transfectants. Panel A): changes induced by addition of 10 μM forskolin and 2 mM IBMX. Panel B): changes induced by addition of 10 μM A23187 * $P < 0.05$ (paired T-test). n = 9 ± SE.

promoter in the pcDNA3-pCLCA1 construct reduces the probability that pCLCA1 expression should be affected by cell maturation. Persistent functional effects of pCLCA1 expression on cAMP-dependent chloride efflux and short circuit current changes in transfected cells are direct evidence for the continued expression of pCLCA1 in mature, differentiated Caco-2 cells. Additional evidence can be obtained by measuring specific pCLCA1 mRNA and protein expression.

RT-PCR using primers specific for pCLCA1 confirmed expression of pCLCA1 mRNA in cells grown for one and 14 days post-passage (Figure 8.5. A). Western blotting of whole cell protein from 24 hour and 14 day old transfected Caco-2 cells showed comparable levels of a ~58 kDa processed N-terminal fragment of pCLCA1 protein present at these two growth stages (Figure 8.5. B). Alkaline phosphatase-conjugated mouse anti-rabbit IgG did not bind to duplicate blots when preimmune rabbit serum was substituted for immune antiserum as primary antibody (not shown). Persistent pCLCA1 antigen expression from 24 hours post-passage through to 14 days was consistent with the retention of pCLCA1-dependent enhancement of cAMP effects on chloride conductance, but did not correlate with age-related loss of Ca^{2+}-dependent chloride conductance.

Cell surface expression of pCLCA1 may be a significant prerequisite for interaction with ion channel proteins located in the plasma membrane. Cell surface localization of pCLCA1 epitope was investigated using rabbit anti-pCLCA1 antiserum, with detection by flow cytometry using FITC-conjugated goat anti-rabbit Fab serum.

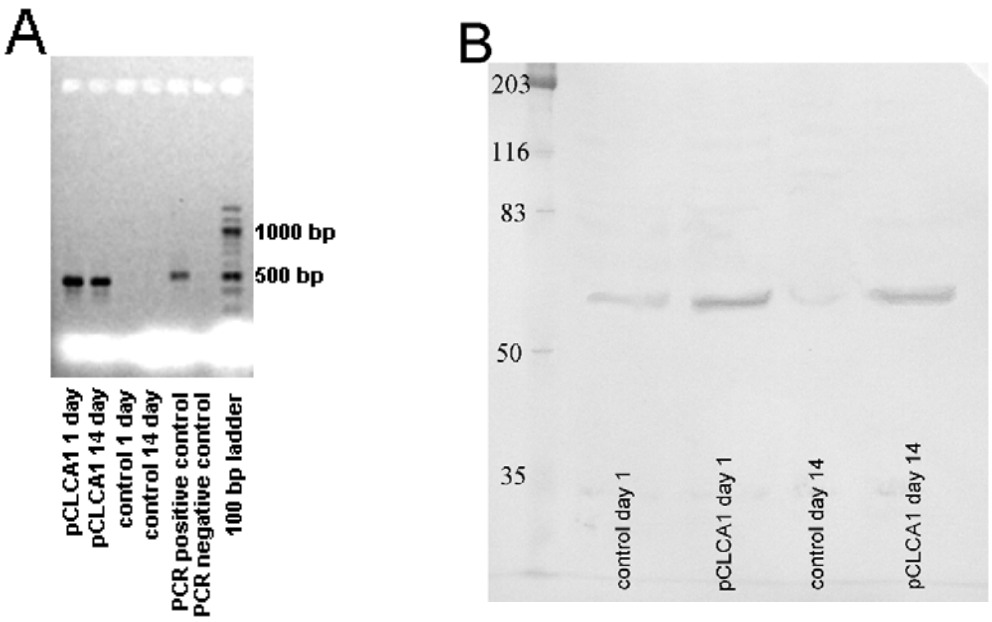

Figure 8.5. Expression of pCLCA1 in transfected Caco-2 cells at one and 14 days A) RT-PCR of pCLCA1 mRNA in transfected cells at day one and day 14 post-passage. B) Western blot of pCLCA1 protein in transfected Caco-2 cells. Sixty µg of total cell protein from tranfected Caco-2 cells grown for one or 14 days was applied per lane for SDS PAGE electrophoresis and blotting to nitrocellulose.

Freshly plated and mature monolayers of Caco-2 cells were dispersed by mechanical disruption following exposure to EDTA, and exposed to the impermeant propidium iodide marker. Trypsin treatment was avoided to protect any extracellular pCLCA1 epitope. Fluorescence energy gates on the flow cytometer were set to distinguish between emission energy of fluorescein and propidium iodide. Mechanical disruption of confluent monolayers with adherent tight junctions caused significant plasma membrane damage, as indicated by the proportion of cells with propidium iodide fluorescence (Figure 8. 6). Of the cells with intact plasma membrane (cells excluding propidium iodide), the peptide epitope corresponding to amino acids 250 to 266 of pCLCA1 was detected on 30% of intact 14 day cultured cells, versus 20% of intact 24 hr cultured cells (Table 8.1). Stable pCLCA1 transfection approximately doubled the percent of cells expressing surface CLCA epitope compared to control pcDNA3-transfected Caco-2 cells. These results confirm the presence of pCLCA1 epitope on the surface of mature differentiated cells that show cAMP-dependent effects of transfection, but have lost Ca^{2+}-dependent chloride conductance.

8.4.5. pCLCA1 Caco-2 Clones in Efflux and Whole Cell Patch Clamp

The effect of pCLCA on Cl^- Efflux and Whole Cell Current are Not Clonally Specific.

Caco-2 cell populations may not be totally uniform in chloride channel expression, activity, or susceptibility to regulatory agonists. Random clonal selection during passage of permanently transfected cells could give a pCLCA1-transfected cell line with a larger than average content of endogenous apical chloride channel targets

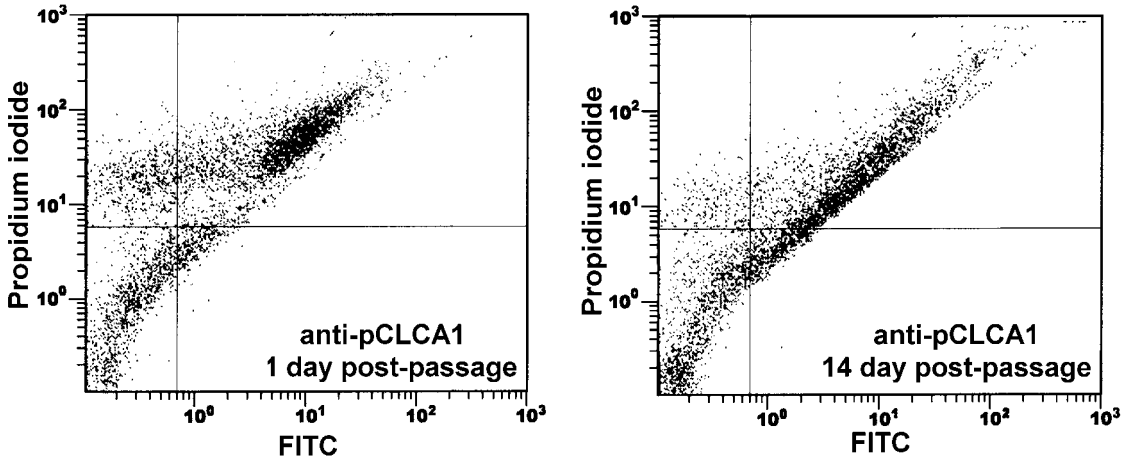

Figure 8.6. Effect of Caco-2 cell maturation on surface expression of CLCA epitope. Surface- expressed pCLCA1 epitope was protected by mechanically removing permanently pCLCA1-transfected cells from plates without trypsin. Cells were incubated with primary antiserum to a peptide with sequence of aa250-266 of pCLCA1. Secondary antibody was labeled with FITC. Photomultiplier gains for flow cytometry were set to differentiate damaged versus intact cells (exclusion of propidium iodide (50 µg/ml, 5 min) followed by three washings)) and cells with FITC fluorescence. 10,000 events were collected for analysis.

Table 8.1. Percent of intact Caco-2 cells with attached fluorescein-labeled secondary antibody to rabbit anti-pCLCA1

Transfection stats	pcDNA3		pCLCA1	
Post-passage interval	1 day	14 day	1 day	14 day
Preimmune serum	2.6% (3951)	6.4% (5417)	3.9% (2932)	6.6% (3834)
Anti-pCLCA1 serum	12.5% (3890)	17.3% (4530)	20.4% (2770)	30.1% (4146)

number of intact cells(/10,000) excluding propidium iodide are shown in parentheses for each condition

available for activation by pCLCA1 expression and agonist addition. This point was investigated by examining the effects of agonist on two additional permanently transfected Caco-2 cell lines (two more pcDNA3 controls and two more pCLCA1 test lines). The percent change in chloride efflux rate induced by pCLCA1 expression compared to a paired pcDNA control is shown in Figure 8. 7. In three independently selected cell lines plated for 24 hours, the pCLCA1-transfected cells had an enhanced rate of $^{36}Cl^-$ release in response to either C- or A-kinase agonist addition in cells. The cAMP response persisted to maturation in all three lines, but the Ca^{2+}-dependent response to pCLCA1 transfection disappeared in three of three cell lines studied.

The issue of clonal selection in permanent transfections can also be addressed by producing transient transfections. The pIRES2-EGFP vector was used to permit independent bicistronic expression of pCLCA1 and EGFP with identification of successful transfectants by fluorescence microscopy. Transient transfections were carried out on freshly passaged cells comparable to 24 hour cells at the time of patch clamp studies. Caco-2 cells expressing pCLCA1 showed an enhanced whole cell conductance response to A-kinase activation compared to cells transfected only with the pIRES2-EGFP vector (Figure 8.8. A). Reversal potential measurements confirmed the involvement of chloride ion in the observed conductance (Figure 8. 8 B). Measured E_{rev} in the 145 mM Cl- external bath solution for cells expressing pCLCA1 was -1.78 ± 0.85 mV, and - 4.43 ± 1.05 mV for control transfected cells. These measured values were close to the calculated E_{rev} of - 6.4 mV for chloride at 21^{o}C. Upon switching the bath solution to 40 mM Cl^- the measured E_{revs} of 12.22 mV ± 1.28 mV for pIRES2-

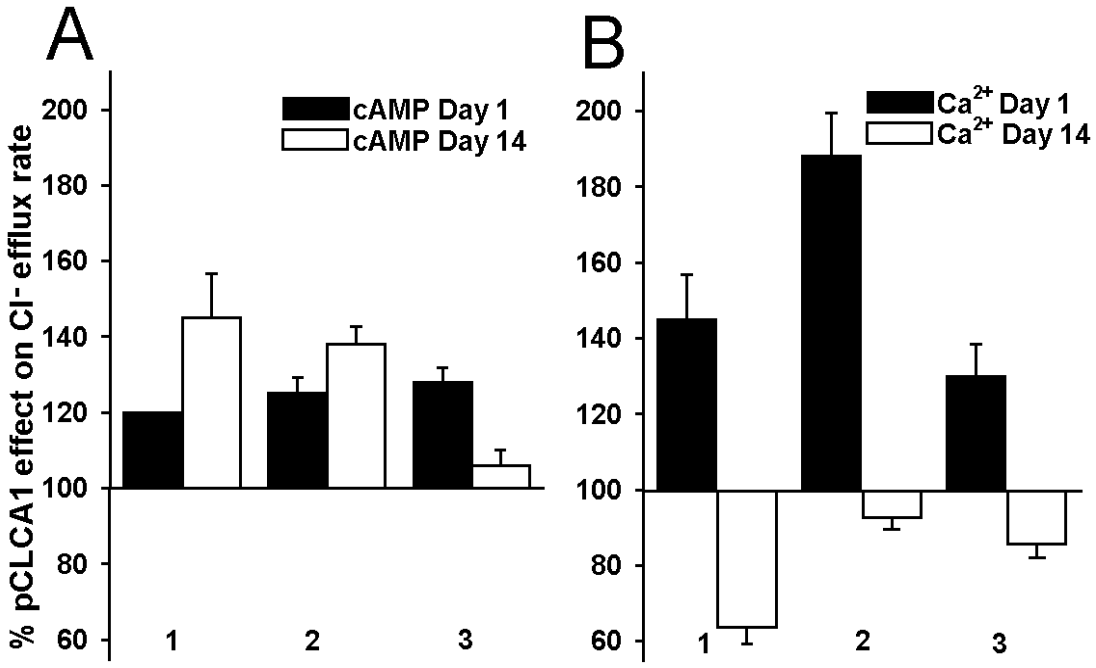

Figure 8.7. The effect of Caco-2 differentiation on Cl^- efflux response to agonist addition in independent pCLCA1-transfected cell lines. Responses were measured in three independent, randomly-identified, pCLCA1-transfected cell lines, and compared against three more randomly-identified, pcDNA3 control-transfected cell lines. A) Cl^- efflux response to forskolin / IBMX at one and 14 days in three independent pCLCA1-transfected cell lines. Chloride efflux rates are expressed as a percent of the agonist-stimulated efflux rate of three independent control cell lines (controls set as 100 %) randomly paired to the pCLCA1 expressing lines. B) Cl^- efflux response to A23187 at one and 14 days in three independent pCLCA1-transfected cell lines. Cl^- efflux rates expressed as a percent of the agonist-stimulated efflux rate as in A. Solid bars, 24 hour cultures, open bars, 14 days. n = 8 ± SE.

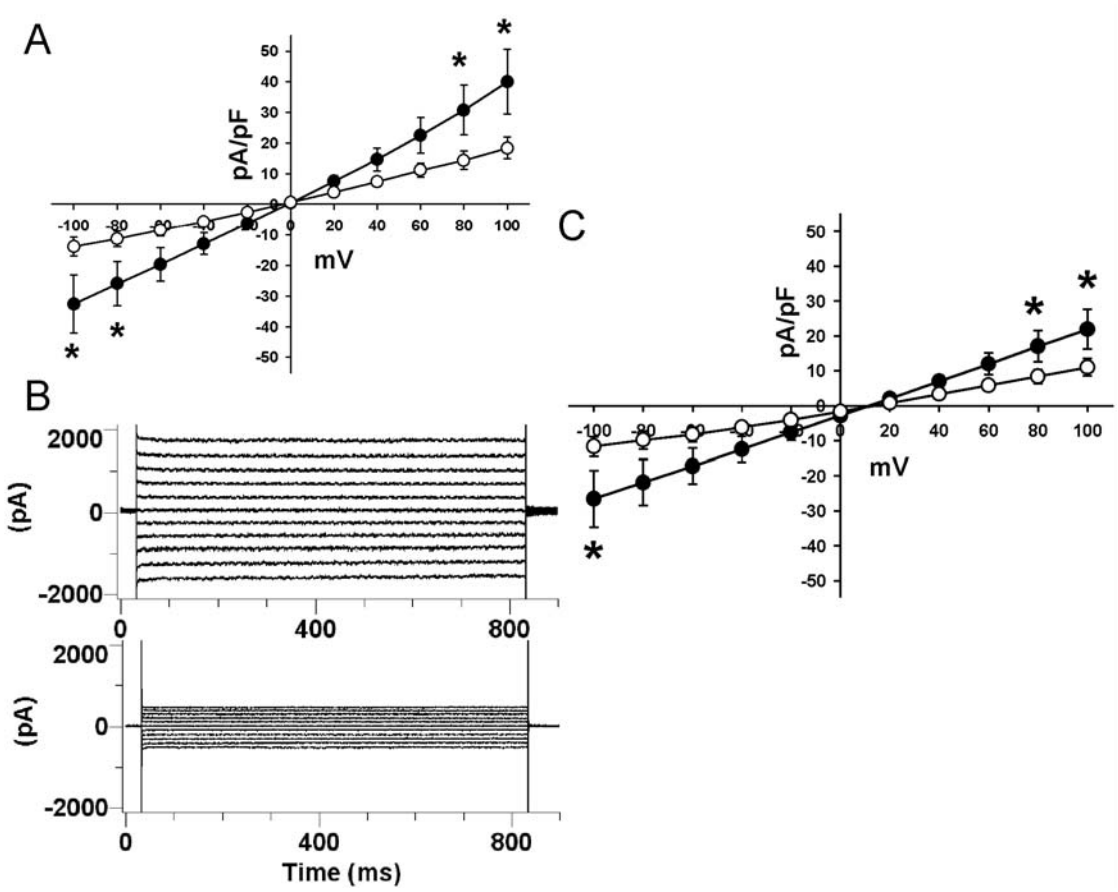

Figure 8.8. Normalized whole cell currents after addition of forskolin and IBMX to transiently-transfected Caco-2 cells. Control cells were transfected with PIRES2-EGFP vector (○), and pCLCA1 test cells with pIRES2-EGFP containing pCLCA1 (●). A) internal 112 mM Cl^- and external 145 mM Cl^-. Gene x voltage P = 0.002. B) corresponding representative tracing of A. C) Low chloride shift, 112 mM internal Cl^- and 50 mM external Cl^-. Gene x voltage P = 0.011. Voltages at which current was significantly higher in cells transfected with pCLCA1 as determined by post- ANOVA analysis (*)(P > 0.005). n = 8 ± SE.

EGFP containing pCLCA1 and 12.64mV ± 1.46 mV for control-pIRES2-EGFP shifted toward the calculated E_{rev} of 20.33 mV at 21 ^{o}C.

Stimulation of pCLCA1-transfected Caco-2 cells with A23187 produced significantly larger increments in normalized current than in control pIRES2-EGFP cells (Figure 8. 9.). Measured Erev values (-26 ± 3.1 and -24 ± 2.1 mV) did not significantly differ from each other, and were close to the calculated chloride E_{rev} value of -31 mV for the bath and pipette solutions.

These observations after transient transfection support the data collected from permanently transfected cells (Figure 8.7.), and exclude clonal selection as a basis for the enhanced chloride channel responsiveness to activation associated with pCLCA1 expression. They also confirm an increase in Ca^{2+}-dependent chloride conductance across the cytoplasmic membrane of freshly passaged Caco-2 cells expressing pCLCA1.

8.5. Discussion

The loss of Ca2+ -dependent chloride conductance in differentiated secretory epithelial tissues is relatively well recognized (Anderson and Welsh 1991; Tarran, Loewen et al. 2002). Exploitation of this phenomenon to investigate association of pCLCA1 with Ca^{2+} -dependent chloride conductance is complicated by a need for independent verification of the developmental effect by different analytical techniques. Chloride efflux studies are suited to comparing exogenous protein expression effects and agonist effects in newly passaged and in mature differentiated cell cultures, but chloride efflux from the cell need not be electrogenic. I_{sc} values from Ussing chambers

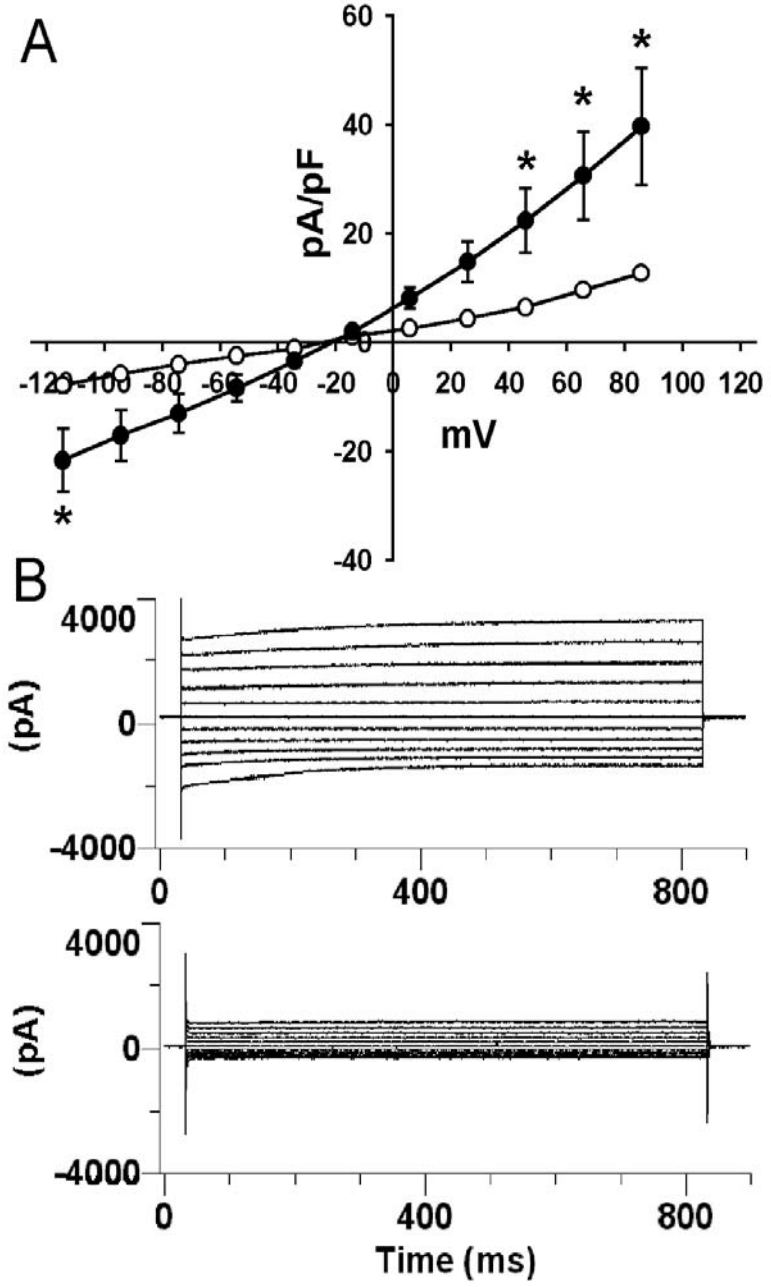

Figure 8.9. Normalized whole cell currents induced by A23187 addition in transiently-transfected Caco-2 cells. A) Control cells were transfected with pIRES-EGFP vector (○) and pCLCA1 test cells with pIRES2-EGFP containing pCLCA1 (●) P = 0.0022 for overall gene effect, gene x voltage P< 0.001. Voltages at which currents was significantly higher in cells transfected with pCLCA1 (as determined by post ANOVA analysis (*)($P < 0.05$), n = 10 ± SE.. B) Corresponding representative tracing for A

are good measurements of conductance effects, but they are not amenable to studies on freshly plated cells that have maximal levels of Ca^{2+} -dependent chloride conductance activity. The I/V dependence of whole cell conductance can be measured by patch clamp, but this technique is difficult to apply to confluent differentiated cells. Hence it seems best to use each of these techniques where it is most applicable to search for a consistent answer to the question of Ca^{2+} -dependent chloride conductance activity associated with pCLCA1 expression.

Chloride efflux and Ussing chamber measurements confirm the loss of Ca^{2+} -dependent chloride conductance from mature Caco-2 cells. Simple interpretations of the inability of pCLCA1 transfection to correct this loss could be; (1) a failure to express the pCLCA protein in mature Caco-2 cultures, (2) a failure of proper pCLCA1 insertion into the cytoplasmic membrane. (3) loss of sensitivity of differentiated Caco-2 cells to calcium ionophore effects of A23187, (4) the presence of an inhibitor of Ca2+-dependent chloride conductance in differentiated Caco-2 cells, or (5) an inability of pCLCA1 to confer Ca^{2+} -dependent chloride conductance in the absence of some accessory protein.

Parallel measurements on alternate functions, namely cAMP-dependent chloride conductance, provide chloride efflux and Ussing chamber evidence that functional, membrane-located effects of pCLCA1 expression are retained as cells differentiate and Ca^{2+} -dependent chloride conductance disappears. RT-PCR data and Western blotting confirm that Caco-2 cells maintain exogenous pCLCA1 expression while losing Ca^{2+} -dependent chloride conductance.

Quantitative extracellular pCLCA1 epitope expression measurements required dispersion of confluent monolayers for flow cytometry without protease assistance. In spite of the loss of significant numbers of cells to mechanical dispersion forces, the similarities in surface expression of the pCLCA1 epitope between freshly plated and 14-day old Caco-2 cultures suggest that pCLCA1 expression is independent of the stages of cell differentiation. There was a small endogenous background of antibody binding in control-transfected Caco-2 cells, assumed to be due to hCLCA1 expression. The 17-mer peptide antigen used for antibody production (pCLCA1 aa 250-266) has the following differences in hCLCA1; K2 –> T, K4 –>Q, and D13 –> K. The lack of coincidence of pCLCA1 epitope expression and Ca^{2+}-dependent chloride conductance supports the independence of these two processes.

Some property of well-differentiated Caco-2 cells could interfere with the access of the calcium ionophore to the cells, and prevent the calcium signaling effect from occurring. The issue of A23187 access to the membranes of mature Caco-2 cells has been addressed by others (Rutten, Cogburn et al. 1991; Wenzel, Kuntz et al. 2002). Both direct effects of A23187 on calcium flux, and indirect effects of A23187 on signaling responses to changes in intracellular calcium concentration were maintained in differentiated Caco-2 cells grown on permeable supports identical to our culture conditions.

The use of independent permanently-transfected cell lines and the measurements of whole cell current in transiently transfected Caco-2 cells confirm the presence of an increased activity of Ca^{2+}-dependent chloride conductance following pCLCA1 transfection. Disappearance of this activity upon cell differentiation was also

confirmed. Hence the combined results of measurements using a range of independent techniques are all consistent with option (4) or (5) from above; the presence of an endogenous inhibitor, or an inability of pCLCA1 to confer Ca^{2+}-dependent chloride conductance in the absence of some accessory protein.

Inhibition of Ca^{2+}-dependent chloride conductance by some substance found in mature differentiated Caco-2 cells could account for the disappearance of endogenous conductance from these cells and the inability to restore it by transfection with pCLCA1. Inositol 3,4,5,6 tetrakisphosphate is reported to inhibit Ca^{2+}-dependent chloride conductance in epithelial cells (Kachintorn, Vajanaphanich et al. 1993; Xie, Kaetzel et al. 1996) (Barrett, Smitham et al. 1998). However, sustained activation of phospholipase C is required to produce inhibitory concentrations of inositol 3,4,5,6 tetrakisphosphate (Vajanaphanich, Schultz et al. 1994). There is no agonist present in these mature cultures to constitutively activate phospholipase C. Annexin IV and epidermal growth factor may also participate in inhibition of Ca^{2+}-dependent chloride conductance (Xie, Kaetzel et al. 1996), but no manipulations have been carried out to elevate the concentrations of these substances. While known inhibitors of Ca^{2+}-dependent chloride conductance are unlikely to be responsible for the loss of the conductance response it is difficult to rule out the presence of some unknown inhibitor until the molecular identity of the endogenous channel is clarified.

It is also noteworthy that the electrical signature of chloride currents seen in pCLCA1-transfected cells are variable, depending on the cell type or the agonist involved in channel activation. The Ca^{2+}-dependent chloride currents seen in pCLCA1-transfected NIH/3T3 cells were outwardly rectifying (Loewen, Gabriel et al. 2002), but

linear current/voltage relationships of the cAMP-activated conductance channel in whole cell patch clamp of pCLCA1-transfected Caco-2 cells are consistent with current passing through a non-rectifying endogenous chloride channel (Loewen, Bekar et al. 2002).

The identity of accessory proteins that may be necessary for pCLCA1 expression to generate chloride conductance is speculative at this time. HEK293 and NIH/3T3 cell lines chosen for low backgrounds of endogenous chloride conductance have been used to functionally characterize exogenously expressed Ca^{2+}-dependenct CLCA chloride channels (Gabriel, Price et al. 1993; Gruber, Elble et al. 1998; Loewen, Gabriel et al. 2002). Low levels of endogenous chloride channel activity in these cells have not been widely acknowledged, but addition of Ca^{2+} ionophore to untransfected HEK293 and NIH/3T3 cells produced a small endogenous conductance of low cation/anion selectivity, as indicated by reversal potential measurements (Ye, Rogers et al. 1996; Loewen, Gabriel et al. 2002). Such a channel could be one possible target for activation upon expression of suitable regulatory proteins. A precedent has been reported describing interaction of a potassium channel subunit with mCLCA1 (Greenwood, Miller et al. 2002).

The recent localization of the bestrophin proteins to the basolateral plasma membrane of the retinal pigment epithelium (RPE) by Marmorstein et al. (Marmorstein, Marmorstein et al. 2000), and implication of these proteins in CaCC activity by Qu et al.(Qu, Wei et al. 2003) suggests that the molecular identity of the CaCC may reside in bestrophins. In addition to expression in secretory areas of the small intestine and the trachea, pCLCA1 expression has also been localized to the RPE where it has been

postulated to function as a regulator of CaCC activity (Loewen, Bekar et al. 2004). Taken together, these findings may be evidence against an independent chloride channel activity for pCLCA1, and increase interest in pursuing possible functional or regulatory interactions between CLCA and other ion channel proteins.

We conclude that the disappearance of calcium-dependent chloride conductance from mature Caco-2 cells due to the accumulation of some inhibitory compound cannot be excluded. However, the difference in the conductance properties associated with pCLCA1 expression in different systems increases the probability that pCLCA1 may function chiefly as a modulator of endogenous chloride conductance channels. The Ca^{2+} and cAMP-dependent chloride conductances that are modulated by pCLCA1 expression are assumed to represent the activity of distinct ion channels, indicating a possible pleiotropic effect of pCLCA1 expression on the activity of apparently unrelated chloride channels with different regulatory and I/V signatures. Young secretory cells arising from stem cell populations in the ileal crypts (Karam 1999) or tracheal submucosal glands (Borthwick, Shahbazian et al. 2001) may be the best physiological counterpart of the pCLCA1-sensitive Ca^{2+}-dependent chloride conductance present in Caco-2 cells 24 hours post-passage. Differentiated Caco-2 cells that lack endogenous Ca^{2+}-dependent chloride conductance may be better models for the mature senescent absorptive cells on the villus tip. The association of pCLCA1 with the actions of both Ca2+ and cAMP in secretory epithelial cells shows that it may be fruitful to study the role of this protein as a modulating element in normal ion transport and in pathophysiological conditions involving abnormal epithelial fluid secretion

Chapter 9. GENERAL DISCUSSION, CONCLUSIONS, AND FUTURE STUDIES

9.1 General Discussion

The work contained within this thesis provides some novel information on the molecular mechanisms behind epithelial transport. It demonstrates that pCLCA1 has a significant impact on the modulation of epithelial ion transport.

In a non-epithelial cell, the NIH 3T3 mouse fibroblast line, CLCA expression increases both the $^{36}Cl^-$ efflux and an outwardly rectifying, time-dependent chloride current. This study provided the first independent confirmation of the Pauli and Fuller's collaborative work (Gruber, Gandhi et al. 1998; Gruber, Schreur et al. 1999). However, the results also highlighted the problem of background currents which were not very well addressed in the original studies. This problem was also addressed by an Italian group studying a bovine CLCA isoform (Romio, Musante et al. 1999). They found that that protein increased chloride conductance, but they where unable to confirm intrinsic chloride conductance properties for the CLCA isoform.

Similarly, because of the small background $^{36}Cl^-$ efflux and currents observed in our studies, it was impossible to confirm intrinsic conductance for the pCLCA1. In the efflux assay, it was possible that pCLCA1 was only increasing the activity of an existing chloride channel conductance. The untransfected cells exhibited an endogenous outwardly rectifying current in whole cell patch clamp studies. However, the conductance was not anion-specific. Simultaneous lowering of both anion and cation

concentration should have altered the E_{rev} in Nernstian fashion towards the contributing conducting ion. However, no such shift was observed, indicating the background conductance was a mixed current of both anion and cation conductance. This could result from the activity of two different ion-specific conducting channels or one non-specific channel (Ye, Rogers et al. 1996; Zhu, Zhang et al. 1998). However, expression of pCLCA1 resulted in an increase in the outwardly rectifying current and an anionic Nernstian shift when external anion solution was lowered. This was strong evidence that pCLCA1 contributed to a Ca^{2+}-activated, electrogenic anion condutance. Unfortunately, the background currents made it impossible to determine if pCLCA1 was only modulating the activities of one of the endogenous channels or whether it had intrinsic channel properties. The observed effects of pCLCA1 expression could occur through pCLCA1 either increasing the conductance of an existing chloride channel, or changing a non-specific ion channel to one which is more anionic in nature.

The presence of calcium-activated chloride conductance in the human and mouse gastrointestinal tract in regions where pCLCA1 is expressed in the pig raises questions about the intrinsic Ca^{2+}-activated chloride channel properties of pCLCA1. (Taylor, Baxter et al. 1988; Hardcastle, Hardcastle et al. 1991; Grubb 1997; Mall, Bleich et al. 1998; Grubb 1999; Mall, Wissner et al. 2000). When CFTR is absent or pharmacologically inhibited only a strong mucosal to lumen potassium conductance is seen, and there is no Ca^{2+}-activated current produced upon intracellular Ca^{2+} mobilization by carbachol or ionophore(Hardcastle, Hardcastle et al. 1991; Mall, Bleich et al. 1998). However, it is possible that a small luminal Ca^{2+}-activated chloride conductance is masked by the strong potassium conductance in the human and most of

the mouse GIT. This may account in part for the strong Ca^{2+}-activated negative potential seen in distal colon in the CF mouse which is unlike the positive potential seen in other portions of the GI tract (Grubb 1999). This anatomic difference in the CF mouse is also seen in a subset of CF patients who maintain a negative lumenal response on carbachol simulation (Veeze, Sinaasappel et al. 1991). Thus, the absence of Ca^{2+}-activated chloride conductance in the gut in the face of CLCA expression may not be the best evidence for showing the lack of intrinsic chloride channel activity in CLCA.

The strongest support for a mucosal Ca^{2+}-activated chloride channel comes from comparative secretory studies between pig and rabbit. The porcine ileal response to cholera toxin, and to *E. coli* heat labile and heat stable enterotoxins has been well documented (Hamilton 1974; Hamilton, Forsyth et al. 1978; Hamilton, Johnson et al. 1978b). The response differs significantly from that seen in the lagomorph (Field 1971; Hamilton, Johnson et al. 1978a). In the rabbit, cholera toxin and heat labile enterotoxin, but not heat stable *E. coli* enterotoxin, induce intestinal secretion. However, all three enterotoxins will produce secretion in the pig. Furthermore, cholera toxin and heat labile, but not heat stable enterotoxin, elevated rabbit mucosal cAMP concentrations, while in the pig none of the enterotoxins had significant effect on mucosal cAMP concentration (Forsyth, Hamilton et al. 1978a; Hamilton, Johnson et al. 1978a). These findings support a very different mechanism by which the two species respond to enteroxin. The lagomorph response conforms to the conventional hypothesis while the porcine response differs (Evans, Chen et al. 1972; Field 1974). This difference may be due to the significantly lower levels of adenylate cyclase reported in the pig mucosa (Forsyth, Hamilton et al. 1978b). Additionally, failure to reverse cholera toxin-induced

intestinal secretion by agents which decrease mucosal cAMP supported the presence of an alternative major second messenger such as Ca^{2+} for seacretory activation (Forsyth, Hamilton et al. 1979). This hypothesis was supported by observed ionophoric properties of cholera toxin and heat labile enterotoxin (Tosteson and Tosteson 1978; Maenz and Forsyth 1986; Maenz, Gabriel et al. 1987; Krasilnikov, Muratkhodjaev et al. 1991; Krasilnikov, Sabirov et al. 1992). Support was also shown by removing Ca^{2+} from the bath solution, and significantly reducing secretory effects of enterotoxins on pig mucosal epithelium (Forsyth, Wong et al. 1985). All this evidence pointed towards Ca^{2+}-activated chloride conductance in the porcine gut.

It is very likely that pCLCA1 plays an integral role in this response as seen in its role in increasing the Ca^{2+}-activated chloride conductance of mouse NIH 3T3 fibroblast cells lines. Similarly, inhibitor profiles and expression data also support a role for pCLCA1 in the Ca^{2+}-activated chloride conductance of primary canine RPE cells. However, both pig gut epithelium and canine RPE also have a strong cAMP-activated chloride conductance. Because the role of pCLCA1 as a channel or modulator was not clear, and *in vivo* co-expression of CLCA and CFTR is known to occur, we expressed pCLCA1 in Caco-2 cell lines which express a large amount of CFTR. And we also co-expressed pCLCA1 and CFTR in NIH 3T3 cells. pCLCA1 unexpectedly increased the cAMP-activated chloride conductance in both NIH 3T3 cells expressing CFTR and Caco-2 cells which have high endogenous CFTR expression. These findings were unlike previous reports which have shown a negative correlation between increased cAMP-activated chloride and Ca^{2+}-activated chloride conductance (Kunzelmann, Mall et al. 1997). Expression of CFTR decreased the endogenous Ca^{2+}-activated channel in

Xenopus oocytes. Similar results were reported in CF mouse tracheal cells where a decrease in CFTR resulted in an increase in Ca^{2+}-activated chloride channels (Tarran, Loewen et al. 2002). Here, in these *in vitro* expression systems, we see a simultaneous increase in both activities. This finding indicates that pCLCA1 may have a modulating role rather than intrinsic channel properties. However, it is important to note that pCLCA1 is being expressed under the control of a CMV promoter in these experiments and is not under normal physiological control.

A model which lacked background chloride current was needed to expand the investigation of the channel or modulating effect of pCLCA1. We approached this problem by allowing the epithelial Caco-2 cells to polarize, differentiate and to form mature epithelial monolayers. The phenomenological developmental loss of Ca^{2+}-dependent chloride conductance has been reported previously in epithelial cells (Anderson and Welsh 1991) (Tarran, Loewen et al. 2002). All growing and dividing cells generally have some level of Ca^{2+}-activated background current. Freshly plated Caco-2 cells that are in a state of division, expansion and growth have both endogenous cAMP- and Ca^{2+}-activated chloride conductance. Although there are significant differences in the kinetics of the efflux induced each agonist, pCLCA1 expression increased responsiveness to both. Similar enhanced responses to both agonists were seen in whole cell patch clamp. pCLCA1 increased the current density of a linear non voltage-dependent cAMP-activated current as well as that of an outwardly rectifying time-dependent current activated by Ca^{2+} ionphore. However, as the cells mature endogenous Ca^{2+}-activated chloride conductance is lost along with any modulatory effect of pCLCA1 expression on Ca^{2+}-activated chloride conductance. Disappearance of

the pCLCA1 effects on Ca^{2+}-dependent chloride conductance occur despite maintained pCLCA1 expression and continued modulation of remaining cAMP-sensitive chloride currents by pCLCA1.

It would seem then that pCLCA1 modulates two apparently unrelated types of epithelial chloride conductance. The evidence indicates that pCLCA1 is unlikely to have intrinsic channel activity itself, but is more likely to interact as a subunit of yet other unidentified channels.

Overall, this thesis provides novel information pertaining to the function of a member of the CLCA gene family. Alternative interpretations of the data are possible, but the simplest conclusion is that pCLCA1 is not a channel, but is a modulator of chloride conductance. This general conclusion does not minimize the importance of this protein. Given the presence of multiple regulator consensus sequences for phosphorylation sites, the metal binding domain, and the involvement of the CLCA protein family in several correlated pathophysiological processes, there are a number of reasons why CLCA might become a valuable therapeutic target for a range of conditions involving inappropriate levels of transmembrane chloride flux.

9.2. Conclusions:

1) pCLCA1 increases Ca^{2+}-activated chloride conductance in a non-epithelial cell line.

2) pCLCA1 increases cAMP-activated chloride conductance in epithelial and non-epithelial cell lines.

3) Ca $^{2+}$-dependent chloride transport may be more important than cAMP-dependent chloride transport for normal fluid secretion across the RPE. Further, it appears that CLCA proteins expressed in the RPE may regulate the activity of other chloride transporters, rather than functioning as primary ion transport proteins.

4) When pCLCA1 is present, it enhances endogenous Ca^{2+}- and cAMP-dependent chloride currents in Caco-2 cells, but it lacks inherent Ca $^{2+}$-dependent chloride channel activity.

9.3. Future Studies

9.3.1. Channel or Modulator? More Direct Evidence.

Several independent lines of evidence support a chloride channel modulating ability of pCLCA1, and a lack of intrinsic chloride channel activity in this protein. The following studies would clarify the role of CLCA in anion conductance:

a) Single channel study study of CaCC and CFTR cell lines transfected with pCLCA1

The effect of pCLCA1 expression on the frequency/number of CFTR channels in the membrane, on the unit channel conductance and on the open probability should be assessed. These studies would clarify whether the modulation of CFTR activity was due to an increased insertion into the plasma membrane or to a direct effect on modulating the channel kinetics or conductance. Cell-attached single channel recordings would likely answer these questions.

If a channel interaction effect involving unit conductance or open probability is found, rather than an effect on channel density in the membrane, then indirect protein interactions that might be mediated via the cytoskeleton would be examined. Experiments to disrupt the cytoskeleton or prevent its assembly could begin to probe this question. A similar study should also be conducted on CaCC.

b) Protein purification and reconstitution in a defined system.

Recombinant, tagged hCLCA1 protein could be affinity purified and reconstituted into an artificial bilayer membrane for channel studies. Purified protein fragments from post-translational processing of the full length protein could be introduced into a black lipid membrane produced from isolated phospholipids and cholesterol. If chloride conductance is not associated with purified pCLCA1 addition into bilayers, gradual increase in the percentage of native cellular membrane from cells displaying channel activity after transfection with pCLCA1 according to patch clamp experiments could be added back to the artificial membrane until channel activity is obtained. If it becomes clear that pCLCA1 channel activity depends on endogenous cellular membrane components, then co-immunopreciptation and partner identification by protein sequencing via mass spectroscopy may be feasible.

c) Solve protein structure.

There is currently no hard structural data for any CLCA family member. The protein must be crystallized and its structure solved to determine the validity of

competing structural models, and whether the MIDAS domain has any role in metal ion interactions.

9.3.2. Interactions with Other Molecular Candidates

The recent studies on the Bestrophin family have identified these proteins as possible molecular candidates for the calcium-activated chloride conductance. However, as explained in the introduction, it likely that the bestrophins are only a part of CaCC. Our functional data support the possibility of an interaction between CaCC and CLCA. These two proteins should be coexpressed. Together they may expand our understanding of the molecular identity of CaCC.

9.3.3. Role in Pathophysiology

The close similarity between hCLCA1 and pCLCA1 suggests that pCLCA1 may behave like hCLCA1 in regulating mucin production. For this reason, the effect of the chloride channel regulated by interactions with pCLCA1 on mucin synthesis, condensation and exocytosis should be investigated through various methods including protein-protein interactions, fluorescence imaging and yeast two-hybrid screening. Although CaCC is involved in many of the pathophysiological processes mentioned in the literature review, its role in mucin production may have the most immediate impact on human health.

Answering, the basic question of how pCLCA1 contributes to chloride conductance should then subsequently answer how directly CLCA1 is involved in the pathophysiology of these processes.

REFERENCES:

Abdel-Ghany M, Cheng HC, Elble RC, Lin H, DiBiasio J and Pauli BU (2003). "The Interacting Binding Domains of the {beta}4 Integrin and Calcium-activated Chloride Channels (CLCAs) in Metastasis." *J Biol Chem* **278**(49): 49406-49416.

Abdel-Ghany M, Cheng HC, Elble RC and Pauli BU (2001). "The breast cancer beta 4 integrin and endothelial human CLCA2 mediate lung metastasis." *J Biol Chem* **276**(27): 25438-46.

Abdel-Ghany M, Cheng HC, Elble RC and Pauli BU (2002). "Focal adhesion kinase activated by beta(4) integrin ligation to mCLCA1 mediates early metastatic growth." *J Biol Chem* **277**(37): 34391-400.

Agnel M, Vermat T and Culouscou JM (1999). "Identification of three novel members of the calcium-dependent chloride channel (CaCC) family predominantly expressed in the digestive tract and trachea." *FEBS Lett* **455**(3): 295-301.

Alberola-Ila J and Hernandez-Hoyos G (2003). "The Ras/MAPK cascade and the control of positive selection." *Immunol Rev* **191**: 79-96.

Allikmets R, Seddon JM, Bernstein PS, Hutchinson A, Atkinson A, Sharma S, Gerrard B, Li W, Metzker ML, Wadelius C, Caskey CT, Dean M and Petrukhin K (1999). "Evaluation of the Best disease gene in patients with age-related macular degeneration and other maculopathies." *Hum Genet* **104**(6): 449-53.

Altenberg GA, Reuss L. (1996). Measurements and interpretation of cytoplasmic ion activities. *Epithelial Transport: A guide to methods and experimental analysis*. Wills NK, Ruess, L., Lewis S.A. London, Chapman&Hall**:** 146 - 163.

Amberg GC, Bonev AD, Rossow CF, Nelson MT and Santana LF (2003). "Modulation of the molecular composition of large conductance, Ca(2+) activated K(+) channels in vascular smooth muscle during hypertension." *J Clin Invest* **112**(5): 717-24.

Amberg GC and Santana LF (2003). "Downregulation of the BK channel beta1 subunit in genetic hypertension." *Circ Res* **93**(10): 965-71.

Anderson MP, Gregory RJ, Thompson S, Souza DW, Paul S, Mulligan RC, Smith AE and Welsh MJ (1991). "Demonstration that CFTR is a chloride channel by alteration of its anion selectivity." *Science* **253**(5016): 202-5.

Anderson MP and Welsh MJ (1991). "Calcium and cAMP activate different chloride channels in the apical membrane of normal and cystic fibrosis epithelia." *Proc Natl Acad Sci U S A* **88**(14): 6003-7.

Archer SL (2002). "Potassium channels and erectile dysfunction." *Vascul Pharmacol* **38**(1): 61-71.

Archer SL, Huang JM, Hampl V, Nelson DP, Shultz PJ and Weir EK (1994). "Nitric oxide and cGMP cause vasorelaxation by activation of a charybdotoxin-sensitive K channel by cGMP-dependent protein kinase." *Proc Natl Acad Sci U S A* **91**(16): 7583-7.

Arima K, Umeshita-Suyama R, Sakata Y, Akaiwa M, Mao XQ, Enomoto T, Dake Y, Shimazu S, Yamashita T, Sugawara N, Brodeur S, Geha R, Puri RK, Sayegh MH, Adra CN, Hamasaki N, Hopkin JM, Shirakawa T and Izuhara K (2002). "Upregulation of IL-13 concentration in vivo by the IL13 variant associated with bronchial asthma." *J Allergy Clin Immunol* **109**(6): 980-7.

Atherton H, Mesher J, Poll CT and Danahay H (2003). "Preliminary pharmacological characterisation of an interleukin-13-enhanced calcium-activated chloride conductance in the human airway epithelium." *Naunyn Schmiedebergs Arch Pharmacol* **367**(2): 214-7.

Atherton HC, Jones G and Danahay H (2003). "IL-13-induced changes in the goblet cell density of human bronchial epithelial cell cultures: MAP kinase and phosphatidylinositol 3-kinase regulation." *Am J Physiol Lung Cell Mol Physiol* **285**(3): L730-9.

Bakall B, Marknell T, Ingvast S, Koisti MJ, Sandgren O, Li W, Bergen AA, Andreasson S, Rosenberg T, Petrukhin K and Wadelius C (1999). "The mutation spectrum of the bestrophin protein--functional implications." *Hum Genet* **104**(5): 383-9.

Baldi A, Modina S, Cheli F, Gandolfi F, Pinotti L, Scesi LB, Fantuz F and Dell'Orto V (2002). "Bovine somatotropin administration to dairy goats in late lactation: effects on mammary gland function, composition and morphology." *J Dairy Sci* **85**(5): 1093-102.

Barrett KE, Smitham J, Traynor-Kaplan A and Uribe JM (1998). "Inhibition of Ca(2+)-dependent Cl- secretion in T84 cells: membrane target(s) of inhibition is agonist specific." *Am J Physiol* **274**(4 Pt 1): C958-65.

Barrow GM (1988). *Physical Chemistry*. New York, McGraw-Hill Book Company.

Bear CE, Li CH, Kartner N, Bridges RJ, Jensen TJ, Ramjeesingh M and Riordan JR (1992). "Purification and functional reconstitution of the cystic fibrosis transmembrane conductance regulator (CFTR)." *Cell* **68**(4): 809-818.

Benson WE, Kolker AE, Enoch JM, Van Loo JA, Jr. and Honda Y (1975). "Best's vitelliform macular dystrophy." *Am J Ophthalmol* **79**(1): 59-66.

Berschneider H, Knowles M, Azizkhan R, Boucher R, Tobey N, Orlando R and Powell D (1988). "Altered intestinal chloride transport in cystic fibrosis." *Faseb J* **2**(10): 2625-2629.

Bertrand CA, Danahay H, Poll CT, Laboisse C, Hopfer U and Bridges RJ (2003). "Niflumic acid inhibits ATP-stimulated exocytosis in a mucin-secreting epithelial cell line." *Am J Physiol* **286**: C247-55.

Bialek S and Miller SS (1994). "K+ and Cl- transport mechanisms in bovine pigment epithelium that could modulate subretinal space volume and composition." *J Physiol* **475**(3): 401-17.

Bistritzer T, Kerem E, Berkovitch M, Rapoport MJ, Evans S and Aladjem M (2002). "Erythrocyte Na+,K+-ATPase and nasal potential in pseudohypoaldosteronism." *Clin Endocrinol (Oxf)* **56**(5): 575-80.

Boese SH, Glanville M, Aziz O, Gray MA and Simmons NL (2000). "Ca2+ and cAMP-activated Cl- conductances mediate Cl- secretion in a mouse renal inner medullary collecting duct cell line." *J Physiol* **523 Pt 2**: 325-38.

Borthwick DW, Shahbazian M, Krantz QT, Dorin JR and Randell SH (2001). "Evidence for stem cell niches in the tracheal epithelium." *Am J Respir Cell Mol Biol* **24**: 662-670.

Boucher RC, Cheng EH, Paradiso AM, Stutts MJ, Knowles MR and Earp HS (1989). "Chloride secretory response of cystic fibrosis human airway epithelia. Preservation of calcium but not protein kinase C- and A-dependent mechanisms." *J Clin Invest* **84**(5): 1424-31.

Bremner SA, Carey IM, DeWilde S, Richards N, Maier WC, Hilton SR, Strachan DP and Cook DG (2003). "Early-life exposure to antibacterials and the subsequent development of hayfever in childhood in the UK: case-control studies using the General Practice Research Database and the Doctors' Independent Network." *Clin Exp Allergy* **33**(11): 1518-25.

Brenner C and Kroemer G (2000). "Apoptosis. Mitochondria--the death signal integrators." *Science* **289**(5482): 1150-1.

Brenner R, Perez GJ, Bonev AD, Eckman DM, Kosek JC, Wiler SW, Patterson AJ, Nelson MT and Aldrich RW (2000). "Vasoregulation by the beta1 subunit of the calcium-activated potassium channel." *Nature* **407**(6806): 870-6.

Breyer MD and Harris RC (2001). "Cyclooxygenase 2 and the kidney." *Curr Opin Nephrol Hypertens* **10**(1): 89-98.

Britton FC, Ohya S, Horowitz B and Greenwood IA (2002). "Comparison of the properties of CLCA1 generated currents and I(Cl(Ca)) in murine portal vein smooth muscle cells." *J Physiol* **539**(Pt 1): 107-17.

Brusselle GG, Kips JC, Tavernier JH, van der Heyden JG, Cuvelier CA, Pauwels RA and Bluethmann H (1994). "Attenuation of allergic airway inflammation in IL-4 deficient mice." *Clin Exp Allergy* **24**(1): 73-80.

Burnette WN (1981). ""Western blotting": electrophoretic transfer of proteins from sodium dodecyl sulfate-polyacrylamide gels to unmodified nitrocellulose and radiographic detection with antibody and radioiodinated protein A." *Anal Biochem* **112**(2): 195-203.

Busse WW and Lemanske RF, Jr. (2001). "Asthma." *N Engl J Med* **344**(5): 350-62.

Caldwell GM, Kakuk LE, Griesinger IB, Simpson SA, Nowak NJ, Small KW, Maumenee IH, Rosenfeld PJ, Sieving PA, Shows TB and Ayyagari R (1999). "Bestrophin gene mutations in patients with Best vitelliform macular dystrophy." *Genomics* **58**(1): 98-101.

Capuco AV, Wood DL, Baldwin R, McLeod K and Paape MJ (2001). "Mammary cell number, proliferation, and apoptosis during a bovine lactation: relation to milk production and effect of bST." *J Dairy Sci* **84**(10): 2177-87.

Cheng HF, Wang JL, Zhang MZ, Miyazaki Y, Ichikawa I, McKanna JA and Harris RC (1999). "Angiotensin II attenuates renal cortical cyclooxygenase-2 expression." *J Clin Invest* **103**(7): 953-61.

Cheng SH, Gregory RJ, Marshall J, Paul S, Souza DW, White GA, O'Riordan CR and Smith AE (1990). "Defective intracellular transport and processing of CFTR is the molecular basis of most cystic fibrosis." *Cell* **63**(4): 827-34.

Chipperfield AR and Harper AA (2000). "Chloride in smooth muscle." *Prog Biophys Mol Biol* **74**(3-5): 175-221.

Chobanian AV, Bakris GL, Black HR, Cushman WC, Green LA, Izzo JL, Jr., Jones DW, Materson BJ, Oparil S, Wright JT, Jr. and Roccella EJ (2003). "Seventh Report of the Joint National Committee on Prevention, Detection, Evaluation, and Treatment of High Blood Pressure." *Hypertension*.

Chow JYC, Uribe JM and Barrett KE (2000). "A Role for Protein Kinase Cepsilon in the Inhibitory Effect of Epidermal Growth Factor on Calcium-stimulated Chloride Secretion in Human Colonic Epithelial Cells." *J Biol Chem* **275**(28): 21169-21176.

Chung J, Bachelder RE, Lipscomb EA, Shaw LM and Mercurio AM (2002). "Integrin (alpha 6 beta 4) regulation of eIF-4E activity and VEGF translation: a survival mechanism for carcinoma cells." *J Cell Biol* **158**(1): 165-74.

Clarke LL and Boucher RC (1992). "Chloride secretory response to extracellular ATP in human normal and cystic fibrosis nasal epithelia." *Am J Physiol* **263**(2 Pt 1): C348-56.

Clarke LL, Grubb BR, Gabriel SE, Smithies O, Koller BH and Boucher RC (1992). "Defective epithelial chloride transport in a gene-targeted mouse model of cystic fibrosis." *Science* **257**(5073): 1125-1128.

Connon CJ, Yamasaki K, Kawasaki S, Quantock AJ, Koizumi N and Kinoshita S (2004). "Calcium-activated Chloride Channel-2 in Human Epithelia." *J Histochem Cytochem* **52**(3): 415-418.

Cotton CU (2000). "Basolateral potassium channels and epithelial ion transport." *Am J Resp Cell Mol Biol* **23**(3): 270-272.

Cotton CU, Russ, L. (1996). Characterization of epithelial ion transport. *Epithelial Transport: A guide to methods and experimental analysis*. Wills N.K. RL, Lewis S.A. London, Chapman & Hall**:** 70-92.

Cotton CU, Stutts MJ, Knowles MR, Gatzy JT and Boucher RC (1987). "Abnormal apical cell membrane in cystic fibrosis respiratory epithelium. An in vitro electrophysiologic analysis." *J Clin Invest* **79**(1): 80-5.

Cross HE and Bard L (1974). "Electro-oculography in Best's macular dystrophy." *Am J Ophthalmol* **77**(1): 46-50.

Cunningham SA, Awayda MS, Bubien JK, Ismailov, II, Arrate MP, Berdiev BK, Benos DJ and Fuller CM (1995). "Cloning of an epithelial chloride channel from bovine trachea." *J Biol Chem* **270**(52): 31016-26.

Danahay H, Atherton H, Jones G, Bridges RJ and Poll CT (2002). "Interleukin-13 induces a hypersecretory ion transport phenotype in human bronchial epithelial cells." *Am J Physiol* **282**(2): L226-36.

Dans M, Gagnoux-Palacios L, Blaikie P, Klein S, Mariotti A and Giancotti FG (2001). "Tyrosine phosphorylation of the beta 4 integrin cytoplasmic domain mediates Shc signaling to extracellular signal-regulated kinase and antagonizes formation of hemidesmosomes." *J Biol Chem* **276**(2): 1494-502.

Davenport SE, Mergey M, Cherqui G, Boucher RC, Gespach C and Gabriel SE (1996). "Deregulated expression and function of CFTR and Cl- secretion after activation

of the Ras and Src/PyMT pathways in Caco-2 cells." *Biochem Biophys Res Commun* **229**(2): 663-672.

Deane KHO and Mannie MD (1992). "An Alternative Pathway of B-Cell Activation - Stilbene Disulfonates Interact with a Cl- Binding Motif on Aen-Related Proteins to Stimulate Mitogenesis." *European J Immunol* **22**(5): 1165-1171.

DeCoursey TE, Chandy KG, Gupta S and Cahalan MD (1984). "Voltage-gated K+ channels in human T lymphocytes: a role in mitogenesis?" *Nature* **307**(5950): 465-8.

Devi L (1991). "Consensus sequence for processing of peptide precursors at monobasic sites." *FEBS Lett* **280**(2): 189-94.

Devor DC, Singh AK, Lambert LC, DeLuca A, Frizzell RA and Bridges RJ (1999). "Bicarbonate and chloride secretion in Calu-3 human airway epithelial cells." *J Gen Physiol* **113**(5): 743-760.

Downward J (1996). "Control of ras activation." *Cancer Surv* **27**: 87-100.

Eksandh L, Bakall B, Bauer B, Wadelius C and Andreasson S (2001). "Best's vitelliform macular dystrophy caused by a new mutation (Val89Ala) in the VMD2 gene." *Ophthalmic Genet* **22**(2): 107-15.

El Biaze M, Boniface S, Koscher V, Mamessier E, Dupuy P, Milhe F, Ramadour M, Vervloet D and Magnan A (2003). "T cell activation, from atopy to asthma: more a paradox than a paradigm." *Allergy* **58**(9): 844-53.

Elble RC, Ji G, Nehrke K, DeBiasio J, Kingsley PD, Kotlikoff MI and Pauli BU (2002). "Molecular and functional characterization of a murine calcium-activated chloride channel expressed in smooth muscle." *J Biol Chem* **277**(21): 18586-91.

Elble RC and Pauli BU (2001). "Tumor suppression by a proapoptotic calcium-activated chloride channel in mammary epithelium." *J Biol Chem* **276**(44): 40510-7.

Elble RC, Widom J, Gruber AD, Abdel-Ghany M, Levine R, Goodwin A, Cheng HC and Pauli BU (1997). "Cloning and characterization of lung-endothelial cell adhesion molecule-1 suggest it is an endothelial chloride channel." *J Biol Chem* **272**(44): 27853-61.

Emsley J, King SL, Bergelson JM and Liddington RC (1997). "Crystal structure of the I domain from integrin alpha2beta1." *J Biol Chem* **272**(45): 28512-7.

Emsley J, Knight CG, Farndale RW, Barnes MJ and Liddington RC (2000). "Structural basis of collagen recognition by integrin alpha2beta1." *Cell* **101**(1): 47-56.

Espinosa M, Noe G, Troncoso C, Ho SB and Villalon M (2002). "Acidic pH and increasing [Ca(2+)] reduce the swelling of mucins in primary cultures of human cervical cells." *Hum Reprod* **17**(8): 1964-72.

Evans DJ, Jr., Chen LC, Curlin GT and Evans DG (1972). "Stimulation of adenyl cyclase by Escherichia coli enterotoxin." *Nat New Biol* **236**(66): 137-8.

Fagard RH and Van den Enden M (2003). "Treatment and blood pressure control in isolated systolic hypertension vs diastolic hypertension in primary care." *J Hum Hypertens* **17**(10): 681-7.

Field M (1971). "Ion transport in rabbit ileal mucosa. II. Effects of cyclic 3', 5'-AMP." *Am J Physiol* **221**(4): 992-7.

Field M (1974). "Mode of action of cholera toxin: stabilization of catecholamine-sensitive adenylate cyclase in turkey erythrocytes." *Proc Natl Acad Sci U S A* **71**(8): 3299-303.

Fong P, Argent BE, Guggino WB and Gray MA (2003). "Characterization of vectorial chloride transport pathways in the human pancreatic duct adenocarcinoma cell line HPAF." *Am J Physiol* **285**(2): C433-45.

Forsyth GW and Gabriel SE (1989a). "Activation of chloride conductance in pig jejunal brush border vesicles." *J Membrane Biol* **107**(2): 137-144.

Forsyth GW and Gabriel SE (1989b). "Inhibiting conductive Cl uptake in membrane vesicles: specificity of alpha-phenylcinnamate." *Biochim Biophys Acta* **977**(1): 19-25.

Forsyth GW, Hamilton DL, Goertz KE and Johnson MR (1978a). "Cholera toxin effects on fluid secretion, adenylate cyclase, and cyclic AMP in porcine small intestine." *Infect Immun* **21**(2): 373-80.

Forsyth GW, Hamilton DL, Goertz KE and Oliphant LW (1978b). "Some comparative properties and localization of porcine jejunal adenylate cyclase." *Can J Biochem* **56**(4): 280-6.

Forsyth GW, Hamilton DL, Scoot A, Goertz KE and Kapitany RA (1979). "Failure to reverse cholera toxin induced intestinal secretion by agents which decrease mucosal cAMP." *Can J Physiol Pharmacol* **57**(9): 1004-10.

Forsyth GW, Wong PH and Maenz DD (1985). "Calcium mediation of the pig jejunal secretory response." *Can J Comp Med* **49**(2): 179-85.

Foster PS, Hogan SP, Ramsay AJ, Matthaei KI and Young IG (1996). "Interleukin 5 deficiency abolishes eosinophilia, airways hyperreactivity, and lung damage in a mouse asthma model." *J Exp Med* **183**(1): 195-201.

Franciolini F and Nonner W (1987). "Anion and cation permeability of a chloride channel in rat hippocampal neurons." *J Gen Physiol* **90**(4): 453-78.

Frangieh GT, Green WR and Fine SL (1982). "A histopathologic study of Best's macular dystrophy." *Arch Ophthalmol* **100**(7): 1115-21.

Frizzell RA, Rechkemmer G and Shoemaker RL (1986). "Altered regulation of airway epithelial cell chloride channels in cystic fibrosis." *Science* **233**(4763): 558-560.

Fuller CM and Benos DJ (2000a). "Ca(2+)-Activated Cl(-) Channels: A Newly Emerging Anion Transport Family." *News Physiol Sci* **15**: 165-171.

Fuller CM and Benos DJ (2000b). "Electrophysiological characteristics of the Ca2+-activated Cl- channel family of anion transport proteins." *Clin Exp Pharmacol Physiol* **27**(11): 906-10.

Fuller CM, Ji HL, Tousson A, Elble RC, Pauli BU and Benos DJ (2001). "Ca(2+)-activated Cl(-) channels: a newly emerging anion transport family." *Pflugers Arch* **443 Suppl 1**: S107-10.

Gabriel SE, Clarke LL, Boucher RC and Stutts MJ (1993). "CFTR and outward rectifying chloride channels are distinct proteins with a regulatory relationship." *Nature* **363**(6426): 263-268.

Gabriel SE and Forsyth GW (1991). "Candidate proteins for conductive chloride transport in porcine ileal brush-border membrane." *J Biol Chem* **266**(27): 17764-9.

Gabriel SE, Makhlina M, Martsen E, Thomas EJ, Lethem MI and Boucher RC (2000). "Permeabilization via the P2X7 purinoreceptor reveals the presence of a Ca2+-activated Cl- conductance in the apical membrane of murine tracheal epithelial cells." *J Biol Chem* **275**(45): 35028-35033.

Gabriel SE, Price EM, Boucher RC and Stutts MJ (1993). "Small linear chloride channels are endogenous to non-epithelial cells." *Am J Physiol* **263**: C708-713.

Gabriel SE, Racette KJ, Gaspar KJ and Forsyth GW (1992). "Inhibition of ileal brush-border chloride conductance by specific antibody." *J Membr Biol* **129**(3): 323-8.

Gallemore RP, Griff ER and Steinberg RH (1988). "Evidence in support of a photoreceptoral origin for the "light-peak substance"." *Invest Ophthalmol Vis Sci* **29**(4): 566-71.

Gallemore RP, Steinberg RH and Griff ER (1989). "Effects of DIDS on the chick retinal pigment epithelium. II. Mechanism of the light peak and other responses originating at the basal membrane." *J Neurosci* **9**(6): 1977-84.

Gambaletta D, Marchetti A, Benedetti L, Mercurio AM, Sacchi A and Falcioni R (2000). "Cooperative signaling between alpha(6)beta(4) integrin and ErbB-2 receptor is required to promote phosphatidylinositol 3-kinase-dependent invasion." *J Biol Chem* **275**(14): 10604-10.

Gandhi R, Elble RC, Gruber AD, Schreur KD, Ji HL, Fuller CM and Pauli BU (1998). "Molecular and functional characterization of a calcium-sensitive chloride channel from mouse lung." *J Biol Chem* **273**(48): 32096-101.

Gaspar KJ, Racette KJ, Gordon JR, Loewen ME and Forsyth GW (2000). "Cloning a chloride conductance mediator from the apical membrane of porcine ileal enterocytes." *Physiol Genomics* **3**(2): 101-11.

Ghosh S, Mendoza T, Ortiz LA, Hoyle GW, Fermin CD, Brody AR, Friedman M and Morris GF (2002). "Bleomycin sensitivity of mice expressing dominant-negative p53 in the lung epithelium." *Am J Respir Crit Care Med* **166**(6): 890-7.

Goetz DJ, el-Sabban ME, Hammer DA and Pauli BU (1996). "Lu-ECAM-1-mediated adhesion of melanoma cells to endothelium under conditions of flow." *Int J Cancer* **65**(2): 192-9.

Gottlieb RA and Dosanjh A (1996). "Mutant cystic fibrosis transmembrane conductance regulator inhibits acidification and apoptosis in C127 cells: possible relevance to cystic fibrosis." *Proc Natl Acad Sci U S A* **93**(8): 3587-91.

Grahn BH and Cullen CL (2001). "Retinopathy of Great Pyrenees dogs: fluorescein angiography, light microscopy and transmitting and scanning electron microscopy." *Vet Ophthalmol* **4**(3): 191-9.

Grahn BH, Philibert H, Cullen CL, Houston DM, Semple HA and Schmutz SM (1998). "Multifocal retinopathy of Great Pyrenees dogs." *Vet Ophthalmol* **1**(4): 211-221.

Greenberg SG, Lorenz JN, He XR, Schnermann JB and Briggs JP (1993). "Effect of prostaglandin synthesis inhibition on macula densa-stimulated renin secretion." *Am J Physiol* **265**(4 Pt 2): F578-83.

Greenwood IA, Miller LJ, Ohya S and Horowitz B (2002). "The large conductance potassium channel beta-subunit can interact with and modulate the functional properties of a calcium-activated chloride channel, CLCA1." *J Biol Chem* **277**(25): 22119-22.

Grubb BR (1997). "Ion transport across the murine intestine in the absence and presence of CFTR." *Comp Biochem Physiol A Physiol* **118**(2): 277-82.

Grubb BR (1999). "Ion transport across the normal and CF neonatal murine intestine." *Am J Physiol* **277**(1 Pt 1): G167-74.

Grubb BR and Gabriel SE (1997). "Intestinal physiology and pathology in gene-targeted mouse models of cystic fibrosis." *Am J Physiol* **273**(2): G258-266.

Grubb BR, Vick RN and Boucher RC (1994). "Hyperabsorption of Na+ and Raised Ca2+-Mediated Cl- Secretion in Nasal Epithelia of Cf Mice." *Am J Physiol* **266**(5): C1478-C1483.

Gruber AD, Elble RC, Ji HL, Schreur KD, Fuller CM and Pauli BU (1998). "Genomic cloning, molecular characterization, and functional analysis of human CLCA1, the first human member of the family of Ca2+-activated Cl- channel proteins." *Genomics* **54**(2): 200-14.

Gruber AD, Elble RC and Pauli BU (2002). Discovery and cloning of the CLCA gene family. *Calcium-Activated Chloride Channels*. **53:** 367-387.

Gruber AD, Gandhi R and Pauli BU (1998). "The murine calcium-sensitive chloride channel (mCaCC) is widely expressed in secretory epithelia and in other select tissues." *Histochem Cell Biol* **110**(1): 43-9.

Gruber AD and Pauli BU (1999a). "Clustering of the human CLCA gene family on the short arm of chromosome 1 (1p22-31)." *Genome* **42**(5): 1030-2.

Gruber AD and Pauli BU (1999b). "Molecular cloning and biochemical characterization of a truncated, secreted member of the human family of Ca2+-activated Cl- channels." *Biochim Biophys Acta* **1444**(3): 418-23.

Gruber AD and Pauli BU (1999c). "Tumorigenicity of human breast cancer is associated with loss of the Ca2+-activated chloride channel CLCA2." *Cancer Res* **59**(21): 5488-91.

Gruber AD, Schreur KD, Ji HL, Fuller CM and Pauli BU (1999). "Molecular cloning and transmembrane structure of hCLCA2 from human lung, trachea, and mammary gland." *Am J Physiol* **276**(6 Pt 1): C1261-70.

Guggino WB (1993). "Outwardly rectifying chloride channels and CF: a divorce and remarriage." *J Bioenergetics Biomembranes* **25**(1): 27-35.

Guibert C, Marthan R and Savineau JP (1997). "Oscillatory Cl- current induced by angiotensin II in rat pulmonary arterial myocytes: Ca2+ dependence and physiological implication." *Cell Calcium* **21**(6): 421-9.

Hamilton DL (1974). Net and unidirectional fluid and electrolyte flux in the small intestine of weanling swine as influenced by Echerichia coli enterotoxins. *Veterinary Physiological Sciences*. Saskatoon, University of Saskatchewan (CANADA)**:** 248.

Hamilton DL, Forsyth GW, Roe WE and Nielsen NO (1978). "Effect of heat stable and heat labile Escherichia coli enterotoxins and cholera toxin in combination with theophylline on unidirectional sodium and chloride flux in the small intestine of weanling swine." *Can J Comp Med* **42**(3): 316-21.

Hamilton DL, Johnson MR, Forsyth GW, Roe WE and Nielsen NO (1978a). "The effect of cholera toxin and heat labile and heat stable Escherichia coli enterotoxin on cyclic AMP concentrations in small intestinal mucosa of pig and rabbit." *Can J Comp Med* **42**(3): 327-31.

Hamilton DL, Johnson MR, Roe WE and Nielsen NO (1978b). "Effects of intraluminal glucose on intestinal secretion induced by heat stable and heat labile Escherichia coli enterotoxin, cholera toxin and theophylline." *Can J Comp Med* **42**(1): 89-96.

Hardcastle J, Hardcastle PT, Taylor CJ and Goldhill J (1991). "Failure of cholinergic stimulation to induce a secretory response from the rectal mucosa in cystic fibrosis." *Gut* **32**(9): 1035-9.

Harris RC and Breyer MD (2001). "Physiological regulation of cyclooxygenase-2 in the kidney." *Am J Physiol* **281**(1): F1-11.

Hauber HP, Manoukian JJ, Nguyen LH, Sobol SE, Levitt RC, Holroyd KJ, McElvaney NG, Griffin S and Hamid Q (2003). "Increased expression of interleukin-9, interleukin-9 receptor, and the calcium-activated chloride channel hCLCA1 in the upper airways of patients with cystic fibrosis." *Laryngoscope* **113**(6): 1037-42.

Hayslett JP, Gogelein H, Kunzelmann K and Greger R (1987). "Characteristics of apical chloride channels in human colon cells (HT29)." *Pflug Arch Eur J Physiol* **410**(4-5): 487-494.

Hille B (2001). *Ionic Channels of Excitable Membranes*. Sunderland, MA, Sinauer.

Hipper A, Mall M, Greger R and Kunzelmann K (1995). "Mutations in the putative pore-forming domain of CFTR do not change anion selectivity of the cAMP activated Cl- conductance." *FEBS Letters* **374**(3): 312-316.

Hirakawa Y, Gericke M, Cohen RA and Bolotina VM (1999). "Ca(2+)-dependent Cl(-) channels in mouse and rabbit aortic smooth muscle cells: regulation by intracellular Ca(2+) and NO." *Am J Physiol* **277**(5 Pt 2): H1732-44.

Hobom M, Dai S, Marais E, Lacinova L, Hofmann F and Klugbauer N (2000). "Neuronal distribution and functional characterization of the calcium channel alpha(2)delta-2 subunit." *European J Neurosci* **12**(4): 1217-1226.

Hopp TP and Woods KR (1981). "Prediction of protein antigenic determinants from amino acid sequences." *Proc Natl Acad Sci U S A* **78**(6): 3824-8.

Hoshino M, Morita S, Iwashita H, Sagiya Y, Nagi T, Nakanishi A, Ashida Y, Nishimura O, Fujisawa Y and Fujino M (2002). "Increased expression of the human Ca2+-activated Cl- channel 1 (CaCC1) gene in the asthmatic airway." *Am J Respir Crit Care Med* **165**(8): 1132-6.

Hughes AD (1995). "Calcium channels in vascular smooth muscle cells." *J Vasc Res* **32**(6): 353-70.

Hughes BA, Gallemore RP and Miller SS (1998). *Transport mechanisms in the retinal pigment epithelium.* New York, Oxford University Press.

Hughes BA and Segawa Y (1993). "cAMP-activated chloride currents in amphibian retinal pigment epithelial cells." *J Physiol* **466**: 749-66.

Humbert M, Durham SR, Ying S, Kimmitt P, Barkans J, Assoufi B, Pfister R, Menz G, Robinson DS, Kay AB and Corrigan CJ (1996). "IL-4 and IL-5 mRNA and protein in bronchial biopsies from patients with atopic and nonatopic asthma: evidence against "intrinsic" asthma being a distinct immunopathologic entity." *Am J Respir Crit Care Med* **154**(5): 1497-504.

Illek B, Yankaskas JR and Machen TE (1997). "cAMP and genistein stimulate HCO3- conductance through CFTR in human airway epithelia." *Am J Physiol* **272**(4 Pt 1): L752-61.

Jackson WF (2000). "Ion channels and vascular tone." *Hypertension* **35**(1 Pt 2): 173-8.

Jaggar JH, Porter VA, Lederer WJ and Nelson MT (2000). "Calcium sparks in smooth muscle." *Am J Physiol* **278**(2): C235-56.

Jerry DJ, Dickinson ES, Roberts AL and Said TK (2002). "Regulation of apoptosis during mammary involution by the p53 tumor suppressor gene." *J Dairy Sci* **85**(5): 1103-10.

Ji HL, DuVall MD, Patton HK, Satterfield CL, Fuller CM and Benos DJ (1998). "Functional expression of a truncated Ca2+-activated Cl- channel and activation by phorbol ester." *Am J Physiol* **274**(2 Pt 1): C455-64.

Joseph DP and Miller SS (1992). "Alpha-1-adrenergic modulation of K and Cl transport in bovine retinal pigment epithelium." *J Gen Physiol* **99**(2): 263-90.

Kachintorn U, Vajanaphanich M, Barrett KE and Traynor-Kaplan AE (1993). "Elevation of inositol tetrakisphosphate parallels inhibition of Ca(2+)-dependent Cl- secretion in T84 cells." *Am J Physiol* **264**(3 Pt 1): C671-6.

Kad NM, Rovner AS, Fagnant PM, Joel PB, Kennedy GG, Patlak JB, Warshaw DM and Trybus KM (2003). "A mutant heterodimeric myosin with one inactive head generates maximal displacement." *J Cell Biol* **162**(3): 481-8.

Karam SM (1999). "Lineage committment and maturation of epithelial cells in the gut." *Frontiers in Bioscience* **4**: D286-D298.

Karkanis T, DeYoung L, Brock GB and Sims SM (2003). "Ca2+-activated Cl- channels in corpus cavernosum smooth muscle: a novel mechanism for control of penile erection." *J Appl Physiol* **94**(1): 301-13.

Keegan LP, Haerry TE, Crotty DA, Packer AI, Wolgemuth DJ and Gehring WJ (1997). "A sequence conserved in vertebrate Hox gene introns functions as an enhancer regulated by posterior homeotic genes in Drosophila imaginal discs." *Mech Dev* **63**(2): 145-57.

Kerem B, Rommens JM, Buchanan JA, Markiewicz D, Cox TK, Chakravarti A, Buchwald M and Tsui LC (1989). "Identification of the cystic fibrosis gene: genetic analysis." *Science* **245**(4922): 1073-80.

Kerem E, Bistritzer T, Hanukoglu A, Hofmann T, Zhou Z, Bennett W, MacLaughlin E, Barker P, Nash M, Quittell L, Boucher R and Knowles MR (1999). "Pulmonary epithelial sodium-channel dysfunction and excess airway liquid in pseudohypoaldosteronism." *N Engl J Med* **341**(3): 156-62.

Kim JA, Kang YS, Lee SH, Lee EH, Yoo BH and Lee YS (1999). "Glibenclamide induces apoptosis through inhibition of cystic fibrosis transmembrane conductance regulator (CFTR) Cl(-) channels and intracellular Ca(2+) release in HepG2 human hepatoblastoma cells." *Biochem Biophys Res Commun* **261**(3): 682-8.

Kim JA, Kang YS and Lee YS (2003). "Role of Ca2+-activated Cl- channels in the mechanism of apoptosis induced by cyclosporin A in a human hepatoma cell line." *Biochem Biophys Res Commun* **309**(2): 291-7.

Kim MO, Yun SJ, Kim IS, Sohn S and Lee EH (2003). "Transforming growth factor-beta-inducible gene-h3 (beta(ig)-h3) promotes cell adhesion of human astrocytoma cells in vitro: implication of alpha6beta4 integrin." *Neurosci Lett* **336**(2): 93-6.

Kirk KL, Halm DR and Dawson DC (1980). "Active sodium transport by turtle colon via an electrogenic Na-K exchange pump." *Nature* **287**(5779): 237-9.

Klaassen CHW and Depont J (1994). "Gastric H+/K+-Atpase." *Cellular Physiology and Biochemistry* **4**(3-4): 115-134.

Knight CH, Docherty AH and Peaker M (1984). "Milk yield in rats in relation to activity and size of the mammary secretory cell population." *J Dairy Res* **51**(1): 29-35.

Knight CH and Peaker M (1984). "Mammary development and regression during lactation in goats in relation to milk secretion." *Q J Exp Physiol* **69**(2): 331-8.

Komiya T, Tanigawa Y and Hirohashi S (1999). "Cloning and identification of the gene gob-5, which is expressed in intestinal goblet cells in mice." *Biochem Biophys Res Commun* **255**(2): 347-51.

Kramer F, White K, Pauleikhoff D, Gehrig A, Passmore L, Rivera A, Rudolph G, Kellner U, Andrassi M, Lorenz B, Rohrschneider K, Blankenagel A, Jurklies B, Schilling H, Schutt F, Holz FG and Weber BH (2000). "Mutations in the VMD2 gene are associated with juvenile-onset vitelliform macular dystrophy (Best disease) and adult vitelliform macular dystrophy but not age-related macular degeneration." *Eur J Hum Genet* **8**(4): 286-92.

Krasilnikov OV, Muratkhodjaev JN, Voronov SE and Yezepchuk YV (1991). "The ionic channels formed by cholera toxin in planar bilayer lipid membranes are entirely attributable to its B-subunit." *Biochim Biophys Acta* **1067**(2): 166-70.

Krasilnikov OV, Sabirov RZ, Ternovsky VI, Merzliak PG and Muratkhodjaev JN (1992). "A simple method for the determination of the pore radius of ion channels in planar lipid bilayer membranes." *FEMS Microbiol Immunol* **5**(1-3): 93-100.

Kritikou EA, Sharkey A, Abell K, Came PJ, Anderson E, Clarkson RW and Watson CJ (2003). "A dual, non-redundant, role for LIF as a regulator of development and STAT3-mediated cell death in mammary gland." *Development* **130**(15): 3459-68.

Kubo M, Nakaya Y, Matsuoka S, Saito K and Kuroda Y (1994). "Atrial natriuretic factor and isosorbide dinitrate modulate the gating of ATP-sensitive K+ channels in cultured vascular smooth muscle cells." *Circ Res* **74**(3): 471-6.

Kuntz CA, Crook RB, Dimitriev A and Steinberg RH (1994). "Modification by cAMP of basolateral membrane chloride conductance in chick retinal pigment epithelium." *Invest Ophthalmol Vis Sci* **35**: 422-433.

Kunzelmann K, Kathofer S and Greger R (1995). "Na+ and Cl- Conductances in Airway Epithelial-Cells - Increased Na+ Conductance in Cystic-Fibrosis." *Pflugers Archiv-European Journal of Physiology* **431**(1): 1-9.

Kunzelmann K, Mall M, Briel M, Hipper A, Nitschke R, Ricken S and Greger R (1997). "The cystic fibrosis transmembrane conductance regulator attenuates the endogenous Ca2+ activated Cl- conductance of Xenopus oocytes." *Pflugers Arch* **435**(1): 178-81.

Lapis K, Paku S and Liotta LA (1988). "Endothelialization of embolized tumor cells during metastasis formation." *Clin Exp Metastasis* **6**(1): 73-89.

Lee D, Ha S, Kho Y, Kim J, Cho K, Baik M and Choi Y (1999). "Induction of mouse Ca(2+)-sensitive chloride channel 2 gene during involution of mammary gland." *Biochem Biophys Res Commun* **264**(3): 933-7.

Lehninger ALN, D.L. Cox, M.M. (1993). *Principles of Biochemistry*. New York, NY, Worth Publishers.

Leverkoehne I and Gruber AD (2000). "Assignment of the murine calcium-activated chloride channel genes Clca1 and Clca3 (alias gob-5) to chromosome 3 band H2-H3 using somatic cell hybrids." *Cytogenet Cell Genet* **88**(3-4): 208-9.

Leverkoehne I and Gruber AD (2002). "The murine mCLCA3 (alias gob-5) protein is located in the mucin granule membranes of intestinal, respiratory, and uterine goblet cells." *J Histochem Cytochem* **50**(6): 829-38.

Leverkoehne I, Horstmeier BA, von Samson-Himmelstjerna G, Scholte BJ and Gruber AD (2002). "Real-time RT-PCR quantitation of mCLCA1 and mCLCA2 reveals differentially regulated expression in pre- and postnatal murine tissues." *Histochem Cell Biol* **118**(1): 11-7.

Levy DE and Lee CK (2002). "What does Stat3 do?" *J Clin Invest* **109**(9): 1143-8.

Lewis SA (1996). Epithelial Structure and Function. *Epithelial Transport: A guide to methods and experimental analysis*. Wills N.K. RL, Lewis S.A., Chapman and Hall. **1:** 1- 20.

Li X, Cowell JK and Sossey-Alaoui K (2004). "CLCA2 tumour suppressor gene in 1p31 is epigenetically regulated in breast cancer." *Oncogene* **23**(7): 1474-80.

Li X, Low SH, Miura M and Weimbs T (2002). "SNARE expression and localization in renal epithelial cells suggest mechanism for variability of trafficking phenotypes." *Am J Physiol* **283**(5): F1111-22.

Loewen ME, Bekar LK, Gabriel SE, Walz W and Forsyth GW (2002). "pCLCA1 becomes a cAMP-dependent chloride conductance mediator in Caco-2 cells." *Biochem Biophys Res Commun* **298**(4): 531-6.

Loewen ME, Bekar LK, Walz W, Forsyth GW and Gabriel SE (2004). "Differentiated Caco-2 cells expressing pCLCA1 lose Ca^{2+}-dependent chloride conductance." *Am J Physiol GI & Liver*: in press.

Loewen ME, Gabriel SE and Forsyth GW (2002). "The calcium-dependent chloride conductance mediator pCLCA1." *Am J Physiol* **283**(2): C412-21.

Loewen ME, MacDonald DW, Gaspar KJ and Forsyth GW (2000). "Isoform-specific exon skipping in a variant form of ClC-2." *Biochim Biophys Acta - Gene Structure and Expression* **1493**(1-2): 284-288.

Loewen ME, Smith NK, Hamilton DL, Grahn BH and Forsyth GW (2003). "CLCA protein and chloride transport in canine retinal pigment epithelium." *Am J Physiol* **285**(5): C1314-21.

Lotery AJ, Munier FL, Fishman GA, Weleber RG, Jacobson SG, Affatigato LM, Nichols BE, Schorderet DF, Sheffield VC and Stone EM (2000). "Allelic variation in the VMD2 gene in best disease and age-related macular degeneration." *Invest Ophthalmol Vis Sci* **41**(6): 1291-6.

Lund LR, Romer J, Thomasset N, Solberg H, Pyke C, Bissell MJ, Dano K and Werb Z (1996). "Two distinct phases of apoptosis in mammary gland involution: proteinase-independent and -dependent pathways." *Development* **122**(1): 181-93.

Lyczak JB, Cannon CL, Pier GB, Cheng SH, Gregory RJ, Marshall J, Paul S, Souza DW, White GA, O'Riordan CR and Smith AE (2002). "Lung infections associated with cystic fibrosis
Defective intracellular transport and processing of CFTR is the molecular basis of most cystic fibrosis." *Clin Microbiol Rev* **15**(2): 194-222.

Maenz DD and Forsyth GW (1982). "Ricinoleate and deoxycholate are calcium ionophores in jejunal brush border vesicles." *J Membr Biol* **70**(2): 125-33.

Maenz DD and Forsyth GW (1986). "Cholera toxin facilitates calcium transport in jejunal brush border vesicles." *Can J Physiol Pharmacol* **64**(5): 568-74.

Maenz DD and Forsyth GW (1987). "Use of calcium depletion and chlorpromazine to study calcium dependence of secretory detergent action in the colon." *Digestion* **36**(4): 220-9.

Maenz DD, Gabriel SE and Forsyth GW (1987). "Calcium transport affinity, ion competition and cholera toxin effects on cytosolic Ca concentration." *J Membr Biol* **96**(3): 243-9.

Mainiero F, Pepe A, Wary KK, Spinardi L, Mohammadi M, Schlessinger J and Giancotti FG (1995). "Signal transduction by the alpha 6 beta 4 integrin: distinct beta 4 subunit sites mediate recruitment of Shc/Grb2 and association with the cytoskeleton of hemidesmosomes." *Embo J* **14**(18): 4470-81.

Malhi H, Irani AN, Rajvanshi P, Suadicani SO, Spray DC, McDonald TV and Gupta S (2000). "K-ATP channels regulate mitogenically induced proliferation in primary rat hepatocytes and human liver cell lines - Implications for liver growth control and potential therapeutic targeting." *J Biol Chem* **275**(34): 26050-26057.

Mall M, Bleich M, Schurlein M, Kuhr J, Seydewitz HH, Brandis M, Greger R and Kunzelmann K (1998). "Cholinergic ion secretion in human colon requires coactivation by cAMP." *Am J Physiol* **275**(6 Pt 1): G1274-81.

Mall M, Gonska T, Thomas J, Schreiber R, Seydewitz HH, Kuehr J, Brandis M and Kunzelmann K (2003). "Modulation of Ca2+-activated Cl- secretion by basolateral K+ channels in human normal and cystic fibrosis airway epithelia." *Pediatr Res* **53**(4): 608-18.

Mall M, Wissner A, Seydewitz HH, Kuehr J, Brandis M, Greger R and Kunzelmann K (2000). "Defective cholinergic Cl(-) secretion and detection of K(+) secretion in rectal biopsies from cystic fibrosis patients." *Am J Physiol* **278**(4): G617-24.

Marchant D, Gogat K, Boutboul S, Pequignot M, Sternberg C, Dureau P, Roche O, Uteza Y, Hache JC, Puech B, Puech V, Dumur V, Mouillon M, Munier FL, Schorderet DF, Marsac C, Dufier JL and Abitbol M (2001). "Identification of novel VMD2 gene mutations in patients with best vitelliform macular dystrophy." *Hum Mutat* **17**(3): 235.

Marmorstein AD, Marmorstein LY, Rayborn M, Wang X, Hollyfield JG and Petrukhin K (2000). "Bestrophin, the product of the Best vitelliform macular dystrophy gene (VMD2), localizes to the basolateral plasma membrane of the retinal pigment epithelium." *Proc Natl Acad Sci U S A* **97**(23): 12758-63.

Marmorstein LY, McLaughlin PJ, Stanton JB, Yan L, Crabb JW and Marmorstein AD (2002). "Bestrophin interacts physically and functionally with protein phosphatase 2A." *J Biol Chem* **277**(34): 30591-7.

Marquardt A, Stohr H, Passmore LA, Kramer F, Rivera A and Weber BH (1998). "Mutations in a novel gene, VMD2, encoding a protein of unknown properties cause juvenile-onset vitelliform macular dystrophy (Best's disease)." *Hum Mol Genet* **7**(9): 1517-25.

Matricardi PM, Rosmini F, Ferrigno L, Nisini R, Rapicetta M, Chionne P, Stroffolini T, Pasquini P and D'Amelio R (1997). "Cross sectional retrospective study of prevalence of atopy among Italian military students with antibodies against hepatitis A virus." *Bmj* **314**(7086): 999-1003.

Matsui H, Davis CW, Tarran R and Boucher RC (2000). "Osmotic water permeabilities of cultured, well-differentiated normal and cystic fibrosis airway epithelia." *J Clin Invest* **105**(10): 1419-1427.

Matsui H, Grubb BR, Tarran R, Randell SH, Gatzy JT, Davis CW and Boucher RC (1998). "Evidence for periciliary liquid layer depletion, not abnormal ion composition, in the pathogenesis of cystic fibrosis airways disease." *Cell* **95**(7): 1005-1015.

Mattes J and Karmaus W (1999). "The use of antibiotics in the first year of life and development of asthma: which comes first?" *Clin Exp Allergy* **29**(6): 729-32.

McLellan GJ and Bedford PG (1997). "The cytoskeletal intermediate filaments of canine retinal pigment epithelial cells in vivo and in vitro." *Res Vet Sci* **63**(3): 245-51.

McNew JA, Parlati F, Fukuda R, Johnston RJ, Paz K, Paumet F, Sollner TH and Rothman JE (2000). "Compartmental specificity of cellular membrane fusion encoded in SNARE proteins." *Nature* **407**(6801): 144-6.

Mekid H, Tounekti O, Spatz A, Cemazar M, El Kebir FZ and Mir LM (2003). "In vivo evolution of tumour cells after the generation of double-strand DNA breaks." *Br J Cancer* **88**(11): 1763-71.

Mercurio AM, Rabinovitz I and Shaw LM (2001). "The alpha 6 beta 4 integrin and epithelial cell migration." *Curr Opin Cell Biol* **13**(5): 541-5.

Miller SS, Rabin J, Strong T, Iannuzzi M, Adams AJ, Collins F, Reenstra W and McCray P, Jr. (1992). "Cystic fibrosis gene product is expressed in retina and retinal pigment epithelium." *Invest Ophthalmol Vis Sci* **33**: 1009.

Mohammad-Panah R, Gyomorey K, Rommens JM, Choudhury M, Li C, Wang YX and Bear CE (2001). "ClC-2 Contributes to Native Chloride Secretion by a Human Intestinal Cell Line, Caco-2." *J. Biol. Chem.* **276**(11): 8306-8313.

Murray AW (1994). "Cyclin-dependent kinases: regulators of the cell cycle and more." *Chem Biol* **1**(4): 191-5.

Nakamura Y, Ghaffar O, Olivenstein R, Taha RA, Soussi-Gounni A, Zhang DH, Ray A and Hamid Q (1999). "Gene expression of the GATA-3 transcription factor is increased in atopic asthma." *J Allergy Clin Immunol* **103**(2 Pt 1): 215-22.

Nakanishi A, Morita S, Iwashita H, Sagiya Y, Ashida Y, Shirafuji H, Fujisawa Y, Nishimura O and Fujino M (2001). "Role of gob-5 in mucus overproduction and airway hyperresponsiveness in asthma." *Proc Natl Acad Sci U S A* **98**(9): 5175-80.

Nandi S (1958). "Endocrine control of mammarygland development and function in the C3H/ He Crgl mouse." *J Natl Cancer Inst* **21**(6): 1039-63.

Nelson MT, Cheng H, Rubart M, Santana LF, Bonev AD, Knot HJ and Lederer WJ (1995). "Relaxation of arterial smooth muscle by calcium sparks." *Science* **270**(5236): 633-7.

Nelson MT, Conway MA, Knot HJ and Brayden JE (1997). "Chloride channel blockers inhibit myogenic tone in rat cerebral arteries." *J Physiol* **502 (Pt 2)**: 259-64.

Nelson MT, Patlak JB, Worley JF and Standen NB (1990). "Calcium channels, potassium channels, and voltage dependence of arterial smooth muscle tone." *Am J Physiol* **259**(1 Pt 1): C3-18.

Nernst W (1888). "Zur Kinetik der in Loesung befinlichen Koeper: Theorie der Diffusion." *Z. Phy. Chem*: 617 - 637.

Neville MC, McFadden TB and Forsyth I (2002). "Hormonal regulation of mammary differentiation and milk secretion." *J Mammary Gland Biol Neoplasia* **7**(1): 49-66.

Nilius B and Wohlrab W (1992). "Potassium Channels and Regulation of Proliferation of Human-Melanoma Cells." *J Physiol London* **445**: 537-548.

Nishikawa K, Ishihara H, Ozawa K and Tamura K (1995). "Chloride transport mechanism in swine tracheal submucosal gland cells." *Respiration* **62**(5): 274-9.

O'Gorman S, Flaherty WA, Fishman GA and Berson EL (1988). "Histopathologic findings in Best's vitelliform macular dystrophy." *Arch Ophthalmol* **106**(9): 1261-8.

O'Grady SM, Musch MW and Field M (1986). "Stoichiometry and ion affinities of the Na-K-Cl cotransport system in the intestine of the winter flounder (Pseudopleuronectes americanus)." *J Membr Biol* **91**(1): 33-41.

O'Grady SM, Palfrey HC, Field M and Musch MW (1987). "Characteristics and functions of Na-K-Cl cotransport in epithelial tissues." *Am J Physiol* **253**(2 Pt 1): C177-92.

Orrenius S, Zhivotovsky B and Nicotera P (2003). "Regulation of cell death: the calcium-apoptosis link." *Nat Rev Mol Cell Biol* **4**(7): 552-65.

Palomba G, Rozzo C, Angius A, Pierrottet CO, Orzalesi N and Pirastu M (2000). "A novel spontaneous missense mutation in VMD2 gene is a cause of a best macular dystrophy sporadic case." *Am J Ophthalmol* **129**(2): 260-2.

Parlati F, McNew JA, Fukuda R, Miller R, Sollner TH and Rothman JE (2000). "Topological restriction of SNARE-dependent membrane fusion." *Nature* **407**(6801): 194-8.

Pauli BU, Abdel-Ghany M, Cheng HC, Gruber AD, Archibald HA and Elble RC (2000). "Molecular characteristics and functional diversity of CLCA family members." *Clin Exp Pharmacol Physiol* **27**(11): 901-5.

Peerce BE, Seifert S and Clarke R (1991). "Partial-Purification and Reconstitution of an Anion Conductance from Rabbit Intestinal Brush-Border Membranes." *Faseb Journal* **5**(6): A1761-A1761.

Peterson WM and Miller SS (1995). "Elevation of intracellular cyclic AMP levels in bovine retinal pigment epithelium closes basolateral Cl channels." *Invest Ophthalmol Vis Sci* **36**: S216.

Peterson WM, Quong JN and Miller SS (1999). Manipulations of fluid transport in retinal pigment epithelium, Proceedings of the third great basin visual sciences symposium.

Petrukhin K, Koisti MJ, Bakall B, Li W, Xie G, Marknell T, Sandgren O, Forsman K, Holmgren G, Andreasson S, Vujic M, Bergen AA, McGarty-Dugan V, Figueroa D, Austin CP, Metzker ML, Caskey CT and Wadelius C (1998). "Identification of the gene responsible for Best macular dystrophy." *Nat Genet* **19**(3): 241-7.

Pfitzer G (2001). "Invited review: regulation of myosin phosphorylation in smooth muscle." *J Appl Physiol* **91**(1): 497-503.

Pier GB (2002). "CFTR mutations and host susceptibility to Pseudomonas aeruginosa lung infection." *Curr Opin Microbiol* **5**(1): 81-6.

Puzon-McLaughlin W and Takada Y (1996). "Critical residues for ligand binding in an I domain-like structure of the integrin beta1 subunit." *J Biol Chem* **271**(34): 20438-43.

Qu Z and Hartzell HC (2000). "Anion permeation in Ca(2+)-activated Cl(-) channels." *J Gen Physiol* **116**(6): 825-44.

Qu Z, Wei RW, Mann W and Hartzell HC (2003). "Two bestrophins cloned from Xenopus laevis oocytes express Ca(2+)-activated Cl(-) currents." *J Biol Chem* **278**(49): 49563-72.

Quinn RH, Quong JN and Miller SS (2001). "Adrenergic receptor activated ion transport in human fetal retinal pigment epithelium." *Invest Ophthalmol Vis Sci* **42**(1): 255-64.

Quinton PM (1983). "Chloride impermeability in cystic fibrosis." *Nature* **301**(5899): 421-2.

Racette KJ, Gabriel SE, Gaspar KJ and Forsyth GW (1996). "Monoclonal antibody against conductive chloride transport in pig ileal apical membrane vesicles." *Am J Physiol* **271**(2 Pt 1): C478-85.

Ran S, Fuller CM, Arrate MP, Latorre R and Benos DJ (1992). "Functional reconstitution of a chloride channel protein from bovine trachea." *J Biol Chem* **267**(29): 20630-7.

Rashid P, Leonardi-Bee J and Bath P (2003). "Blood pressure reduction and secondary prevention of stroke and other vascular events: a systematic review." *Stroke* **34**(11): 2741-8.

Riordan JR, Rommens JM, Kerem B, Alon N, Rozmahel R, Grzelczak Z, Zielenski J, Lok S, Plavsic N, Chou JL and et al. (1989). "Identification of the cystic fibrosis gene: cloning and characterization of complementary DNA." *Science* **245**(4922): 1066-73.

Robinson DS, Hamid Q, Ying S, Tsicopoulos A, Barkans J, Bentley AM, Corrigan C, Durham SR and Kay AB (1992). "Predominant TH2-like bronchoalveolar T-lymphocyte population in atopic asthma." *N Engl J Med* **326**(5): 298-304.

Romio L, Musante L, Cinti R, Seri M, Moran O, Zegarra-Moran O and Galietta LJ (1999). "Characterization of a murine gene homologous to the bovine CaCC chloride channel." *Gene* **228**(1-2): 181-8.

Rommens JM, Iannuzzi MC, Kerem B, Drumm ML, Melmer G, Dean M, Rozmahel R, Cole JL, Kennedy D, Hidaka N and et al. (1989). "Identification of the cystic fibrosis gene: chromosome walking and jumping." *Science* **245**(4922): 1059-65.

Rozakis-Adcock M, Fernley R, Wade J, Pawson T and Bowtell D (1993). "The SH2 and SH3 domains of mammalian Grb2 couple the EGF receptor to the Ras activator mSos1." *Nature* **363**(6424): 83-5.

Ruoslahti E and Rajotte D (2000). "An address system in the vasculature of normal tissues and tumors." *Annu Rev Immunol* **18**: 813-27.

Rutten MJ, Cogburn JN, Schasteen CS and Solomon T (1991). "Physiological and cytotoxic effects of Ca(2+) ionophores on Caco-2 paracellular permeability: relationship of 45Ca(2+) efflux to 51 Cr release." *Pharmacology* **42**(3): 156-68.

Saiki RK, Gelfand DH, Stoffel S, Scharf SJ, Higuchi R, Horn GT, Mullis KB and Erlich HA (1988). "Primer-directed enzymatic amplification of DNA with a thermostable DNA polymerase." *Science* **239**(4839): 487-91.

Sakmann BN, E., Ed. (1995). *Single-Channel Recording*. New York, NY, Plenum Press.

Schlaepfer DD, Hauck CR and Sieg DJ (1999). "Signaling through focal adhesion kinase." *Prog Biophys Mol Biol* **71**(3-4): 435-78.

Schlatter E, Salomonsson M, Persson AE and Greger R (1989). "Macula densa cells sense luminal NaCl concentration via furosemide sensitive Na+2Cl-K+ cotransport." *Pflugers Arch* **414**(3): 286-90.

Schwartz TW and Devi L (1986). "The processing of peptide precursors. 'Proline-directed arginyl cleavage' and other monobasic processing mechanisms: Consensus sequence for processing of peptide precursors at monobasic sites." *FEBS Lett* **200**(1): 1-10.

Scoot A, Forsyth GW, Kapitany RA and et a (1980). "Effects of isolated heat-stable enterotoxin produced by Escherichia coli on fluid secretion and cyclic nucleotide levels in the jejunum of the weanling pig." *Can J Physiol Pharmacol* **58**(7): 772-777.

Segal MS and Beem E (2001). "Effect of pH, ionic charge, and osmolality on cytochrome c-mediated caspase-3 activity." *Am J Physiol Cell Physiol* **281**(4): C1196-204.

Shaw LM, Rabinovitz I, Wang HH, Toker A and Mercurio AM (1997). "Activation of phosphoinositide 3-OH kinase by the alpha6beta4 integrin promotes carcinoma invasion." *Cell* **91**(7): 949-60.

Shirakawa T, Enomoto T, Shimazu S and Hopkin JM (1997). "The inverse association between tuberculin responses and atopic disorder." *Science* **275**(5296): 77-9.

Smalley KS (2003). "A pivotal role for ERK in the oncogenic behaviour of malignant melanoma?" *Int J Cancer* **104**(5): 527-32.

Snouwaert JN, Brigman KK, Latour AM, Malouf NN, Boucher RC, Smithies O and Koller BH (1992). "An Animal-Model for Cystic-Fibrosis Made by Gene Targeting." *Science* **257**(5073): 1083-1088.

Song JC, Hanson CM, Tsai V, Farokhzad OC, Lotz M and Matthews JB (2001). "Regulation of epithelial transport and barrier function by distinct protein kinase C isoforms." *Am J Physiol Cell Physiol* **281**(2): C649-661.

Sood R, Bear CE, Auerbach W, Reyes W, Jensen TJ, Kartner N, Riordan JR and Buchwald M (1992). "Regulation of CFTR expression and function during differentiation of intestinal epithelial cells." *Embo J* **11**: 2487-2494.

Stefanon B, Colitti M, Gabai G, Knight CH and Wilde CJ (2002). "Mammary apoptosis and lactation persistency in dairy animals." *J Dairy Res* **69**(1): 37-52.

Stohr H, Marquardt A, Nanda I, Schmid M and Weber BH (2002). "Three novel human VMD2-like genes are members of the evolutionary highly conserved RFP-TM family." *Eur J Hum Genet* **10**(4): 281-4.

Strachan DP (1989). "Hay fever, hygiene, and household size." *Bmj* **299**(6710): 1259-60.

Strauss O, Steinhausen K, Mergler S, Stumpff F and Wiederholt M (1999). "Involvement of protein tyrosine kinase in the InsP3-induced activation of Ca2+-dependent Cl- currents in cultured cells of the rat retinal pigment epithelium." *J Membr Biol* **169**(3): 141-53.

Stutts MJ, Canessa CM, Olsen JC, Hamrick M, Cohn JA, Rossier BC and Boucher RC (1995). "CFTR as a cAMP-dependent regulator of sodium-channels." *Science* **269**(5225): 847-850.

Sumi M, Kiuchi K, Ishikawa T, Ishii A, Hagiwara M, Nagatsu T and Hidaka H (1991). "The newly synthesized selective Ca2+/calmodulin dependent protein kinase II inhibitor KN-93 reduces dopamine contents in PC12h cells." *Biochem Biophys Res Commun* **181**(3): 968-75.

Sun H, Tsunenari T, Yau KW and Nathans J (2002). "The vitelliform macular dystrophy protein defines a new family of chloride channels." *Proc Natl Acad Sci U S A* **99**(6): 4008-13.

Szabo I, Lepple-Wienhues A, Kaba KN, Zoratti M, Gulbins E and Lang F (1998). "Tyrosine kinase-dependent activation of a chloride channel in CD95-induced apoptosis in T lymphocytes." *Proc Natl Acad Sci U S A* **95**(11): 6169-74.

Takagi J, Kamata T, Meredith J, Puzon-McLaughlin W and Takada Y (1997). "Changing ligand specificities of alphavbeta1 and alphavbeta3 integrins by swapping a short diverse sequence of the beta subunit." *J Biol Chem* **272**(32): 19794-800.

Tang K, Nie D, Cai Y and Honn KV (1999). "The beta4 integrin subunit rescues A431 cells from apoptosis through a PI3K/Akt kinase signaling pathway." *Biochem Biophys Res Commun* **264**(1): 127-32.

Tarran R, Loewen ME, Paradiso AM, Olsen JC, Gray MA, Argent BE, Boucher RC and Gabriel SE (2002). "Regulation of murine airway surface liquid volume by CFTR and Ca2+-activated Cl- conductances." *J Gen Physiol* **120**(3): 407-418.

Taylor C, Baxter P, Hardcastle J and Hardcastle P (1988). "Failure to induce secretion in jejunal biopsies from children with cystic fibrosis." *Gut* **29**(7): 957-962.

Thevenod F (2002). "Ion channels in secretory granules of the pancreas and their role in exocytosis and release of secretory proteins." *Am J Physiol Cell Physiol* **283**(3): C651-72.

Thevenod F, Roussa E, Benos DJ and Fuller CM (2003). "Relationship between a HCO3- -permeable conductance and a CLCA protein from rat pancreatic zymogen granules." *Biochem Biophys Res Commun* **300**(2): 546-54.

Thomas EJ, Gabriel SE, Makhlina M, Hardy SP and Lethem MI (2000). "Expression of nucleotide-regulated Cl- currents in CF and normal mouse tracheal epithelial cell lines." *Am J Physiol* **279**(5): C1578-C1586.

Thornton JM, Edwards MS, Taylor WR and Barlow DJ (1986). "Location of 'continuous' antigenic determinants in the protruding regions of proteins." *Embo J* **5**(2): 409-13.

Toda M, Tulic MK, Levitt RC and Hamid Q (2002). "A calcium-activated chloride channel (HCLCA1) is strongly related to IL-9 expression and mucus production in bronchial epithelium of patients with asthma." *J Allergy Clin Immunol* **109**(2): 246-50.

Tosteson MT and Tosteson DC (1978). "Bilayers containing gangliosides develop channels when exposed to cholera toxin." *Nature* **275**(5676): 142-4.

Trusolino L, Bertotti A and Comoglio PM (2001). "A signaling adapter function for alpha6beta4 integrin in the control of HGF-dependent invasive growth." *Cell* **107**(5): 643-54.

Tsuboi S (1987). "Measurement of the volume flow and hydraulic conductivity across the isolated dog retinal pigment epithelium." *Invest Ophthalmol Vis Sci* **28**(11): 1776-82.

Tsuboi S, Manabe R and Iizuka S (1986). "Aspects of electrolyte transport across isolated dog retinal pigment epithelium." *Am J Physiol* **250**(5 Pt 2): F781-4.

Tsui LC (1992). "Mutations and sequence variations detected in the cystic fibrosis transmembrane conductance regulator (CFTR) gene: a report from the Cystic Fibrosis Genetic Analysis Consortium." *Human Mutation* **1**(3): 197-203.

Tsunenari T, Sun H, Williams J, Cahill H, Smallwood P, Yau KW and Nathans J (2003). "Structure-function analysis of the bestrophin family of anion channels." *J Biol Chem* **278**(42): 41114-25.

Tsuruta D, Hopkinson SB, Lane KD, Werner ME, Cryns VL and Jones JC (2003). "Crucial role of the specificity-determining loop of the integrin beta4 subunit in the binding of cells to laminin-5 and outside-in signal transduction." *J Biol Chem* **278**(40): 38707-14.

Tyska MJ, Dupuis DE, Guilford WH, Patlak JB, Waller GS, Trybus KM, Warshaw DM and Lowey S (1999). "Two heads of myosin are better than one for generating force and motion." *Proc Natl Acad Sci U S A* **96**(8): 4402-7.

Ueda Y and Steinberg RH (1994). "Chloride currents in freshly isolated rat retinal pigment epithelial cells." *Exp Eye Res* **58**(3): 331-42.

Ullrich N and Sontheimer H (1997). "Cell cycle-dependent expression of a glioma-specific chloride current: proposed link to cytoskeletal changes." *Am J Physiol* **42**(4): C1290-C1297.

Ussing HH, Zerahn, K. (1951). "Active transprot of sodium as the source of electric current in the short-cuircuited isolated frog skin." *Acta Physiol Scand* **23**: 110-127.

Vaage J and Harlos JP (1987). "Spontaneous metastasis from primary C3H mouse mammary tumors." *Cancer Res* **47**(2): 547-50.

Vajanaphanich M, Schultz C, Rudolf MT, Wasserman M, Enyedi P, Craxton A, Shears SB, Tsien RY, Barrett KE and Traynor-Kaplan A (1994). "Long-term uncoupling of chloride secretion from intracellular calcium levels by Ins(3,4,5,6)P4." *Nature* **371**(6499): 711-4.

Veeze HJ, Sinaasappel M, Bijman J, Bouquet J and de Jonge HR (1991). "Ion transport abnormalities in rectal suction biopsies from children with cystic fibrosis." *Gastroenterology* **101**(2): 398-403.

Verdugo P (1991). "Mucin exocytosis." *Am Rev Respir Dis* **144**(3 Pt 2): S33-7.

Villaz M, Cinniger JC and Moody WJ (1995). "A Voltage-Gated Chloride Channel in Ascidian Embryos Modulated by Both the Cell-Cycle Clock and Cell-Volume." *J Physiol London* **488**(3): 689-699.

Walker C, Bauer W, Braun RK, Menz G, Braun P, Schwarz F, Hansel TT and Villiger B (1994). "Activated T cells and cytokines in bronchoalveolar lavages from patients with various lung diseases associated with eosinophilia." *Am J Respir Crit Care Med* **150**(4): 1038-48.

Walsh KB, Long KJ and Shen X (1999). "Structural and ionic determinants of 5-nitro-2-(3-phenylprophyl-amino)-benzoic acid block of the CFTR chloride channel." *Br J Pharmacol* **127**(2): 369-76.

Walz W, Ed. (2002). *Patch-Clamp Analysis; Advanced Techniques*. Neuromethods. Totowa, New Jersey, Humana Press.

Wang SY, Melkoumian Z, Woodfork KA, Cather C, Davidson AG, Wonderlin WF and Strobl JS (1998). "Evidence for an early G1 ionic event necessary for cell cycle progression and survival in the MCF-7 human breast carcinoma cell line." *J Cell Physiol* **176**(3): 456-464.

Wang YX and Kotlikoff MI (1997). "Inactivation of calcium-activated chloride channels in smooth muscle by calcium/calmodulin-dependent protein kinase." *Proc Natl Acad Sci USA* **94**(26): 14918-23.

Watson B, Jr. (2003). "Genetics of the kidney and hypertension." *Curr Hypertens Rep* **5**(3): 273-6.

Weimbs T, Low SH, Li X and Kreitzer G (2003). "SNAREs and epithelial cells." *Methods* **30**(3): 191-7.

Weingeist TA, Kobrin JL and Watzke RC (1982). "Histopathology of Best's macular dystrophy." *Arch Ophthalmol* **100**(7): 1108-14.

Wenzel U, Kuntz S, Diestel S and Daniel H (2002). "PEPT1-mediated cefixime uptake into human intestinal epithelial cells is increased by Ca2+ channel blockers." *Antimicrob Agents Chemother* **46**(5): 1375-80.

Whittaker CA and Hynes RO (2002). "Distribution and evolution of von Willebrand/integrin A domains: widely dispersed domains with roles in cell adhesion and elsewhere." *Mol Biol Cell* **13**(10): 3369-87.

WHO (1999). "1999 World Health Organization-International Society of Hypertension Guidelines for the Management of Hypertension. Guidelines Subcommittee." *J Hypertens* **17**(2): 151-83.

Wills NK, Weng T, Mo L, Hellmich HL, Yu A, Wang T, Buchheit S and Godley BF (2000). "Chloride channel expression in cultured human fetal RPE cells: response to oxidative stress." *Invest Ophthalmol Vis Sci* **41**(13): 4247-55.

Willumsen NJ and Boucher RC (1989). "Activation of an apical Cl- conductance by Ca2+ ionophores in cystic fibrosis airway epithelia." *Am J Physiol* **256**(2 Pt 1): C226-33.

Willumsen NJ, Boucher RC and Davis CW (1989). "Shunt resistance and ion permeabilities in normal and cystic fibrosis airway epithelia." *Am J Physiol* **256**(5 Pt 1): C1054-63.

Wilson GF and Chiu SY (1993). "Mitogenic Factors Regulate Ion Channels in Schwann-Cells Cultured from Newborn Rat Sciatic-Nerve." *Journal of Physiology-London* **470**: 501-520.

Winpenny JP, Lavery WL, Watson N and Chazot PL (2002). "Biochemical and electrophysiological characterisation of the GOB5 (mCLCA3) chloride ion channel protein after expression in HEK293 cells." *J Physiol London* **539**: 2P-2P.

Wohlrab D and Markwardt F (1999). "Influence of ion channel blockers on proliferation and free intracellular Ca2+ concentration of human keratinocytes." *Skin Pharmacology and Applied Skin Physiology* **12**(5): 257-265.

Woodfork KA, Wonderlin WF, Peterson VA and Strobl JS (1995). "Inhibition of ATP-sensitive potassium channels causes reversible cell-cycle arrest of human breast-cancer cells in tissue-culture." *J Cell Physiol* **162**(2): 163-171.

Wu G and Hamill OP (1992). "NPPB block of Ca(++)-activated Cl- currents in Xenopus oocytes." *Pflugers Arch* **420**(2): 227-9.

Xie W, Kaetzel MA, Bruzik KS, Dedman JR, Shears SB and Nelson DJ (1996). "Inositol 3,4,5,6-tetrakisphosphate inhibits the calmodulin-dependent protein kinase II-activated chloride conductance in T84 colonic epithelial cells." *J Biol Chem* **271**(24): 14092-7.

Ye C, Rogers K, Bai M, Quinn SJ, Brown EM and Vassilev PM (1996). "Agonists of the Ca(2+)-sensing receptor (CaR) activate nonselective cation channels in HEK293 cells stably transfected with the human CaR." *Biochem Biophys Res Commun* **226**(2): 572-9.

Yerxa BR, Sabater JR, Davis CW, Stutts MJ, Lang-Furr M, Picher M, Jones AC, Cowlen M, Dougherty R, Boyer J, Abraham WM and Boucher RC (2002). "Pharmacology of INS37217 P-1-(uridine 5 ')-P-4-(2 '-deoxycytidine 5 ')tetraphosphate, tetrasodium salt , a next-generation P2Y(2) receptor agonist for the treatment of cystic fibrosis." *J Pharmacol Exp Therapeutics* **302**(3): 871-880.

Zhang LF, Ding JH, Yang BZ, He GC and Roe C (2003). "Characterization of the bidirectional promoter region between the human genes encoding VLCAD and PSD-95." *Genomics* **82**(6): 660-8.

Zhang ZR, Zeltwanger S and McCarty NA (2000). "Direct comparison of NPPB and DPC as probes of CFTR expressed in Xenopus oocytes." *J Membr Biol* **175**(1): 35-52.

Zhao JH and Guan JL (2000). "Role of focal adhesion kinase in signaling by the extracellular matrix." *Prog Mol Subcell Biol* **25**: 37-55.

Zhao YJ, Wang J, Rubin LJ and Yuan XJ (1997). "Inhibition of K(V) and K(Ca) channels antagonizes NO-induced relaxation in pulmonary artery." *Am J Physiol* **272**(2 Pt 2): H904-12.

Zhou Y, Dong Q, Louahed J, Dragwa C, Savio D, Huang M, Weiss C, Tomer Y, McLane MP, Nicolaides NC and Levitt RC (2001). "Characterization of a calcium-activated chloride channel as a shared target of Th2 cytokine pathways and its potential involvement in asthma." *Am J Respir Cell Mol Biol* **25**(4): 486-91.

Zhou Y, Shapiro M, Dong Q, Louahed J, Weiss C, Wan S, Chen Q, Dragwa C, Savio D, Huang M, Fuller C, Tomer Y, Nicolaides NC, McLane M and Levitt RC (2002). "A calcium-activated chloride channel blocker inhibits goblet cell metaplasia and mucus overproduction." *Novartis Found Symp* **248**: 150-65; discussion 165-70, 277-82.

Zhu D, Cheng CF and Pauli BU (1992). "Blocking of lung endothelial cell adhesion molecule-1 (Lu-ECAM-1) inhibits murine melanoma lung metastasis." *J Clin Invest* **89**(6): 1718-24.

Zhu D and Pauli BU (1993). "Correlation between the lung distribution patterns of Lu-ECAM-1 and melanoma experimental metastases." *Int J Cancer* **53**(4): 628-33.

Zhu DZ, Cheng CF and Pauli BU (1991). "Mediation of lung metastasis of murine melanomas by a lung-specific endothelial cell adhesion molecule." *Proc Natl Acad Sci U S A* **88**(21): 9568-72.

Zhu DZ and Pauli BU (1991). "Generation of monoclonal antibodies directed against organ-specific endothelial cell surface determinants." *J Histochem Cytochem* **39**(8): 1137-42.

Zhu GY, Zhang Y, Xu HX and Jiang C (1998). "Identification of endogenous outward currents in the human embryonic kidney (HEK 293) cell line." *J Neurosci Methods* **81**(1-2): 73-83.

VITAE / AUTOBIOGRAPHY/ PUBLICATIONS

The author's family originally immigrated to Canada in 1845, helping to create the German Mennonite agricultural community of Steinbach Manitoba. He was born in Winnipeg Manitoba Canada in 1974 making him a 5th generation Canadian in his family. He received both his elementary, junior and high school education from the Fort Garry School Division No. 5, graduating high school from Fort Richmond Collegiate in Winnipeg Manitoba Canada.

He then under took studies in the Faculty of Science at University of Manitoba where he completed the majority of his studies for a Bachelor of Science with Distinction. After his studies at the U of M, he undertook studies at the University of Saskatchewan in Western College of Veterinary Medicine and graduated with a Doctorate of Veterinary Medicine.

Education

2004 - **Doctor of Philosophy at the University of Saskatchewan, pertaining to Physiology and Biochemistry** in the department of Veterinary Biomedical Sciences under the supervision of Dr. George W. Forsyth.

2001 - **Visiting scientist - University of North Carolina**, CF Center, training in molecular electrophysiology and epithelial ion transport.

1999 - **Doctor of Veterinary Medicine** from the Western College of Veterinary Medicine at the University of Saskatchewan.

1995 - **Bachelor of Science** with Distinction from the University of Manitoba (convocated Oct. 1999).

Publications

Loewen ME, Bekar LK, Walz W, Forsyth GW, Gabriel SE. (2004) pCLCA1 lacks inherent chloride channel activity in an epithelial colon carcinoma cell line. *Am J Physiol Gastrointest Liver Physiol*. 2004 Feb 26 [Epub ahead of print]

Hanik HLJ, **Loewen ME**, Appleyard GD, Grahn BH, Forsyth GW. (2004) Differences between expression of mRNA in retinal pigment epithelium of normal dogs. *Canadian Journal of Veterinary Research:* in press

Loewen ME, Smith NK, Hamilton DL, Grahn BH, Forsyth GW. (2003) CLCA protein and chloride transport in canine retinal pigment epithelium *Am J Physiol Cell Physiol*. Nov; 285(5):C1314-21. Epub 2003 Jul 16

Loewen ME, Bekar LK, Gabriel SE, Walz W, Forsyth GW. (2002) pCLCA1 becomes a cAMP-dependent chloride conductance mediator in Caco-2 cells. *Biochem Biophys Res Commun*. Nov 8; 298(4):531-6

Loewen ME, Gabriel SE, Forsyth GW. (2002) The calcium-dependent chloride conductance mediator pCLCA1. *Am J Physiol Cell Physiol* Aug;283(2):C412-21

Tarran R, **Loewen ME**, Paradiso AM., Olsen JC, Gray MA, Argent BE, Boucher RC, Gabriel SE. (2002) Regulation of Murine Airway Surface Liquid Volume by CFTR and Ca(2+)-activated Cl(-) Conductances. *J Gen Physiol*. Sep;120(3):407-18

Loewen ME, MacDonald DE, Gaspar KJ, Forsyth GW. (2000) Isoform - Specific exon skipping in a variant of ClC-2. *Biochim Biophys Acta* Sep 7;1493(1-2):284-8 2

Gaspar KJ, Racette KJ, Gordon JR, **Loewen ME**, Forsyth GW. (2000) Cloning a chloride conductance mediator from the apical membrane of porcine ileal enterocytes. *Physiol Genomics*. Aug 9; 3(2):101-11

Meeting Abstracts:

Loewen ME, Bekar LK, Walz W, Gabriel SE, Forsyth GW. (2003) A role for cAMP and Ca2+ in CLCA1- dependent regulation of chloride transport *Journal General Physiology* July; 122 (1): 92 **(Society of General Physiologists 2003 - Woods Hole, Massachusetts, USA)**

Loewen ME, Gabriel SE, Forsyth GW. (2003) pCLCA1 is central to the pathophysiology of secretory diarrhea in pigs. *Canadian Journal of Animal Science*

Sept; 83 (3): 634 **(Canadian Society of Animal Science, 2003 - Saskatoon, Saskachewan, Canada)**

Loewen ME, Forsyth GW, Gabriel SE. (2003) pCLCA1 modulates chloride conductance in Caco-2 cells. *FASEB Journal* March 17; 17 (5): A1224-A1224 Part 2 Suppl. **(EB 2003 - San Diego, California, USA).**

Gabriel SE, **Loewen ME,** Tarran R, Martsen E, Boucher RC.(2002) Enhanced activity of the airway epithelial calcium-activated CT channel is dependent on membrane polarization. *FASEB Journal* March 22;16 (5): A795-A795 Part 2 Suppl. (**EB 2002 - New Orleans, Louisiana, USA)**

Professional Memberships

1999 - 2004 - Canadian Veterinary Medical Association

1999 - 2004 - General Member of the Saskatchewan Veterinary Medical Association

2004 - 2004 - Society of General Physiologists

Professional Licenses

1999 - 2004 - Saskatchewan Veterinary Medical Association General Practice License

Academic Awards

2000 - 2004 - Inter - Provincial Graduate Student Fellowship

1997 -1998 - Inter - Provincial Summer Student Research Scholarship

1993 -1995 - John Bankier Award Western College of Veterinary Medicine (U of S)
- Dean's Honor list (U of M) x 2
- N. E. Stanger Prize in Pre Veterinary Studies (U of M)
- University of Manitoba Entrance Scholarship

Personal Skills and Interests

In addition to Science and Veterinary Medicine the author has a keen interest in skiing, windsurfing, photography and personal fitness when time permits. He also greatly enjoys arc welding and carpentry.